

**ANALYSIS OF LEAF MORPHOLOGY
AND PHOTOSYNTHESIS IN
DELETION MUTANTS OF RICE
(*Oryza sativa* L.)**

IAN R.A. SMILLIE, BSc. (Hons.)

**Thesis submitted to the University of Nottingham for the
degree of Doctor of Philosophy**

**University of Nottingham
Sutton Bonington Campus
Loughborough
Leicestershire
LE12 5RD**

JUNE 2012

ABSTRACT

Analysis of leaf morphology and photosynthesis in deletion mutants of rice (*Oryza sativa* L.)

I. Smillie

As a plant operating the C₃ photosynthetic pathway and commonly grown under tropical conditions of high light intensity and temperature, rice (*Oryza sativa*) displays high levels of photorespiration, to the detriment of photosynthetic efficiency. For this reason it is thought that improvements to net photosynthesis via an increased photosynthetic efficiency could provide significant gains in terms of grain yield. There is great interest in 1. Introducing CO₂ concentrating mechanisms into C₃ crop plants such as the C₄ photosynthetic pathway in order to facilitate enhanced photosynthetic efficiency. This requires an understanding of C₃ and C₄ leaf development and establishing whether there is sufficient plasticity in the rice genome to produce plants with C₄-like properties. 2. Improving existing C₃ photosynthesis by means of increasing leaf thickness, vein density and investigation of the impacts of mesophyll cell size.

It is in this context that a forward screen of approximately 100 mutant lines of the *indica* rice variety IR64 was developed at Nottingham to search for relevant changes in leaf morphology. Mutant seed produced using chemical mutagenesis (diepoxybutane and ethylmethanesulfonate) and irradiation (gamma and fast neutron) was supplied by the International Rice Research Institute (IRRI) in the Philippines. A rapid low resolution screen was devised using light microscopy of fresh, untreated hand cut leaf sections of plants at the leaf six stage. Seven mutant lines were identified as showing altered leaf morphologies and were termed *alm* mutants.

alm1, *alm5* and *alm6* displayed a reduced interveinal distance between neighbouring veins, a common feature of C₄ plants with Kranz anatomy, whilst *alm1* and *alm5* also displayed a reduction in the size of minor veins. *alm3* and *alm4* produced significantly thicker leaves than wild type plants, whilst the leaves of *alm7* were significantly thinner.

A detailed anatomical characterisation of leaf structure revealed that *alm3*, *alm4* and *alm5* plants all displayed a significant reduction in the size of mesophyll cells and that for all the mutant lines, the distance between veins was strongly correlated with mesophyll cell size rather than the number of mesophyll cells spanning the interveinal regions.

Physiological properties of the *alm* lines were investigated using infra-red gas analysis (IRGA) measurements of gas exchange and chlorophyll fluorescence. It was shown that none of the mutant lines displayed an increase in photosynthetic capacity when compared to wild type plants, even in lines which were shown to possess what was thought to be a favourable leaf anatomy, quite possibly a result of widespread effects of the mutation process. The *alm1* line was shown to display interesting physiological responses, with almost no transpiration and a severely reduced photosynthetic capacity, yet functioning stomata and an unimpaired stomatal conductance.

In conclusion, the future success of photosynthetic improvement in rice will rely on the screen of much larger numbers of mutant lines of rice and C₄ plants in order to identify the genes determining key conserved morphological features such as interveinal cell number, cell size and the degree to which rice mesophyll cells are lobed.

ACKNOWLEDGEMENTS

I would like to thank my supervisors, Dr Erik Murchie and Dr Kevin Pyke, for giving me the opportunity to carry out this work, and their huge efforts, enthusiasm and support throughout the duration of the project.

I would also like the various people who helped me throughout this project, with special thanks to Stella Hubbard, Fiona Wilkinson, Duncan Scholefield, Gema Vizcay-Barrena and Olubukola Ajigboye for all their assistance with various experiments.

Thanks also to the various members of Dr. Murchie's lab and office 321 over the past four years. There are too many to name individually, but thank you all for your support, friendship, many fond memories and many holiday sweets shared!

Finally I would like to thank my family, those with us and those sadly departed. You provided fantastic support and inspiration throughout the duration of this project, and without you all this would never have been possible.

TABLE OF CONTENTS

	Page
Abstract	i
Acknowledgements	iii
Table of Contents	iv
List of Figures	vii
List of Tables	xii
Abbreviations	xiii
CHAPTER 1: INTRODUCTION AND LITERATURE REVIEW	1
1.1 Rice as a crop	3
1.2 Improving production	3
1.3 Physiological traits determining yield potential	4
1.3.1 Harvest index	5
1.3.2 Remobilisation of stem reserves	7
1.3.3 Prolonged grain filling and green leaf area duration	7
1.3.4 PAR	8
1.3.5 Increased sink size	8
1.4 Photosynthesis as a limiting factor	9
1.5 Potential improvements to rice photosynthesis	10
1.6 Characteristics of C ₄ photosynthesis	13
1.6.1 The C ₄ pathway	13
1.6.2 Anatomical adaptations for C ₄ photosynthesis	16
1.6.3 Physiological consequences of C ₄ photosynthesis	19
1.7 Leaf development	21
1.8 Previous work	24
1.9 Screening for indicators of C ₄ photosynthesis	28
Chapter 2: METHODS	32
2.1 Seeds used	33
2.2 Growth of plants	33
2.2.1 Seed germination	33
2.2.2 Plant establishment	34
2.3 Screening	38
2.3.1 Leaf numbering	38
2.3.2 SPAD measurements	38
2.3.3 Gross morphology	38
2.3.4 Microscopy	38
2.3.5 Tissue storage	41
2.4 Detailed anatomical methods	41
2.4.1 Tissue fixation, resin embedding and staining	41
2.4.2 Leaf surface impressions	42
2.4.3 Cleared hand cut sections	43
2.4.4 Cell separations and chloroplast counting	44
2.4.5 Confocal microscopy	44
2.5 Gas exchange and chlorophyll fluorescence	45
2.5.1 Response to ambient CO ₂ concentration	45
2.5.2 Response to light intensity in terms of gas exchange and chlorophyll fluorescence	45

2.6 Statistical analyses	46
Chapter 3: SCREENING THE MUTANT POPULATION	48
3.1 Introduction	49
3.1.1 Genetic background of lines used	50
3.1.2 Anatomical traits related to C ₄ photosynthesis	50
3.2 Methodology	51
3.2.1 Vein distribution	51
3.2.2 Vein spacing and size	51
3.2.3 Leaf thickness	52
3.3 Leaf morphology of rice	52
3.4 Screening the mutant population	57
3.4.1 Vein arrangement	57
3.4.2 Veins mm ⁻¹ leaf width	63
3.4.3 Vein spacing	65
3.4.4 Vein size	69
3.4.5 Leaf thickness	71
3.5 Altered leaf morphology mutants	74
3.5.1 <i>alm1</i> (83-18-1-7G)	75
3.5.2 <i>alm2</i> (111-16-1-1G)	76
3.5.3 <i>alm3</i> (233-7-1-1D)	77
3.5.4 <i>alm4</i> (1536-6-1-6D)	78
3.5.5 <i>alm5</i> (3965-1-1-6G)	79
3.5.6 <i>alm6</i> (3965-1-1-7G)	80
3.5.7 <i>alm7</i> (7820-1-1-3G)	81
3.6 Discussion	82
Chapter 4: DETAILED MORPHOLOGY OF CANDIDATE LINES	84
4.1 Introduction	85
4.2 Methodology	85
4.2.1 Fixed and stained leaf sections	85
4.2.2 Confocal microscopy	86
4.2.3 Cleared and stained hand cut sections	86
4.2.4 Separated cell preparations	87
4.2.5 Leaf surface impressions	87
4.3 Detailed leaf sections	87
4.3.1 Fixed and resin embedded tissue	87
4.3.2 Confocal microscopy	89
4.3.3 Cleared and stained hand cut sections	90
4.3.4 Separated cell preparations	92
4.4 Interveinal Spacing	93
4.4.1 Distance	93
4.4.2 Cell number	95
4.4.3 Cell size	98
4.4.4 Mesophyll cell morphology and chloroplast distribution	105
4.4.5 Stomata	110
4.5 Discussion	113
4.5.1 Interveinal distance and cell number	113
4.5.2 Genetics	114
4.5.3 Chloroplast number and cell size	114
4.5.4 Stomata	115

Chapter 5: PHYSIOLOGICAL RESPONSES OF CANDIDATE LINES	117
5.1 Introduction	118
5.1.1 Response to carbon dioxide	118
5.1.2 Light response	119
5.1.3 Fluorescence	120
5.2 Methods	121
5.2.1 CO ₂ response measurement	121
5.2.2 Light response measurements	122
5.3 Plant response to CO ₂	123
5.4 Response to PAR	130
5.4.1 Gas exchange response to varying PAR	133
5.4.2 Electron transport in photosynthesis	138
5.4.3 Photoprotection	140
5.5 Discussion	142
Chapter 6: GENERAL DISCUSSION	146
6.1 Introduction	147
6.2 Conserved anatomical features of the rice leaf	147
6.2.1 Photorespiratory scavenging	148
6.2.2 Mesophyll conductance to CO ₂	148
6.2.3 Implications of the conserved nature of cell size, lobing and chloroplast distribution	149
6.3 Alterations displayed by the <i>alm</i> lines	151
6.3.1 <i>alm1</i>	151
6.3.1.1 Possible limitations in hydraulic conductance in <i>alm1</i> plants	153
6.3.1.2 Possible inhibitors of PSII in <i>alm1</i> rice plants	154
6.3.2 <i>alm2</i>	157
6.3.3 <i>alm3</i> and <i>alm4</i>	157
6.3.4 <i>alm5</i> and <i>alm6</i>	160
6.4 Potential alterations in leaf development	162
6.5 Implications for the integration of C ₄ pathway into rice	163
6.6 Future Work	164
Chapter 7: Bibliography	168

LIST OF FIGURES

	Page
Chapter 1: INTRODUCTION AND LITERATURE REVIEW	
1.1 Trends in area harvested of Asian rice (source: FAOSTAT database, 2011).	4
1.2 Trend in rice global grain production (source: FAOSTAT database, 2011).	6
1.3 Trend in global rice average yield (source: FAOSTAT database, 2011).	7
1.4 Schematic showing the photorespiratory cycle. Taken from von Caemmerer and Evans (2010).	10
1.5 Histochemical staining of GUS activity showing blue appearance in cells expressing PEP carboxylase in the C ₄ plant <i>Flaveria bidentis</i> . Taken from Stockhaus <i>et al.</i> (1997).	14
1.6 Simplified schematic of the C ₄ pathway demonstrating the fixation of atmospheric CO ₂ in the mesophyll cell chloroplasts by PEP carboxylase before transfer of the 4 carbon compound to the bundle sheath chloroplasts. Decarboxylation occurs and CO ₂ enters into the Calvin cycle, whilst PEP is returned to the mesophyll cells.	16
1.7 Representation of differences between C ₃ and C ₄ plant anatomy. Taken from Leegood <i>et al.</i> (2000). A) Demonstrates the increase in vein density in C ₄ plants compared to C ₃ , B) shows the close arrangement of mesophyll and bundle sheath cells in C ₄ leaves, and C) demonstrates the centrifugal positioning and increase in number of chloroplasts within the C ₄ bundle sheath.	17
1.8 Typical A/C _i curve for C ₃ and C ₄ plants showing the three major points of variance outlined above. Taken from Sage and Pearcy (2000). 1) demonstrates the lower CO ₂ compensation point displayed by C ₄ plants, 2) shows the sharp increase in A as [CO ₂] rises and 3) shows the elevated maximum A (A _{max}) demonstrated by C ₃ plants at high [CO ₂].	20
1.9 A) young rice plant. The leaf sheath forms around the culm, with the leaf blade emerging at the collar. B) li, ligule; au, auricle of a rice plant at 70 days post germination, taken from Lee <i>et al.</i> (2007).	22
1.10 A) The emerging leaf primordium (P1) forming from the shoot apical meristem (SA) as the P2 primordium forms a hood over the SAM. B) Extending P1 primordium forming a crescent shape. C) Cross section of P2 showing early procambial strand (PS) (Itoh <i>et al.</i> , 2005)	23
1.11 A) SAM enclosed within P3 leaf margins. Arrow denotes the blade – sheath boundary. B , C) Cross section at blade – sheath boundary showing formation of the ligule primordium (LP).	23
1.12 Transverse sections of A) wild type B) and <i>tan-1</i> adult maize leaves. m, mesophyll cell; v, vascular bundle; bs, bundle sheath cell. Adapted from Smith <i>et al.</i> (1996).	27
1.13 Transverse sections through A) wild type and B) <i>ral1</i> leaves adapted from Scarpella <i>et al.</i> (2003).	28

Chapter 2: METHODS

- 2.1** **A** Young rice seedlings floating in a polystyrene rack. **B** An open bottomed centrifuge tube. The lid and base removed used to support seedlings in the rack. **36**
- 2.2** **A** Wild type and mutant plants growing in hydroponic tanks. **B** WT plant in the lightproof support held with foam. **37**
- 2.3** Examples of hand-cut leaf sections from the mutant screen **40**

Chapter 3: SCREENING THE MUTANT POPULATION

- 3.1** Untreated hand cut transverse section of a wild type rice plant showing the full width of a wild type leaf imaged at 10x magnification. **54**
- 3.2** Enlarged transverse section of the wild type leaf showing the region between the two adjacent major veins. **54**
- 3.3** Typical wild type plant produced under hydroponic growth conditions. **56**
- 3.4** Diagram of the vein arrangement in the 6th leaf of wild type and mutant rice lines. **58**
- 3.5** Mean total number of veins present transverse section of the widest part of leaf 6 in rice plants. Bars denote standard error of the mean ($n>3$). **60**
- 3.6** Mean width of leaf 6 of rice plants at the widest part of the leaf. Bars denote standard error of the mean ($n>3$). **61**
- 3.7** Mean number of veins per mm leaf width across the whole leaf width of leaf 6 in rice plants. Bars denote standard error of the mean ($n>3$). **63**
- 3.8** The relationship between the mean width of the 6th leaf of rice plants at the widest point and the number of veins it contains. **64**
- 3.9** Average distance between neighbouring major veins in the 6th leaf of rice. Bars denote standard error of the mean ($n>3$). **66**
- 3.10** Average distance between adjacent minor and major veins of the mean ($n>3$). **67**
- 3.11** Average distance between adjacent minor veins of the mean ($n>3$). **68**
- 3.12** Mean major vein diameter as observed in transverse sections of leaf 6 of rice plants. Bars denote standard error of the mean ($n>3$). **69**
- 3.13** Mean minor vein diameter as observed in transverse sections of leaf 6 of rice plants. Bars denote standard error of the mean ($n>3$). **70**
- 3.14** Leaf thicknesses at the major vein. Bars denote standard error of the mean ($n>3$). **71**
- 3.15** Leaf thickness at the minor vein. Bars denote standard error of the mean ($n>3$). **72**
- 3.16** Leaf thickness at the bulliform cells. Bars denote standard error of the mean ($n>3$). **73**
- 3.17** Plants of the *alm1* mutant line of rice, schematic map of vein arrangement and corresponding leaf section taken from the fully expanded leaf 6th leaf. **75**

3.18	Plants of the <i>alm2</i> line, along with the relevant section of the vein map for those plants, showing that the leaves display a rough symmetry in vein distribution about the midrib.	76
3.19	Plants of the <i>alm3</i> mutant line of rice, schematic map of vein arrangement and corresponding leaf section taken from the fully expanded leaf 6 th leaf.	77
3.20	Plants of the <i>alm4</i> mutant line of rice, schematic map of vein arrangement and corresponding leaf section taken from the fully expanded leaf 6 th leaf.	78
3.21	Whole plants of the <i>alm5</i> mutant line of rice, schematic map of vein arrangement and corresponding leaf section taken from the fully expanded leaf 6 th leaf.	79
3.22	Plants of the <i>alm6</i> mutant line of rice, schematic map of vein arrangement and corresponding leaf section taken from the fully expanded leaf 6 th leaf.	80
3.23	Plants of the <i>alm7</i> mutant line of rice, schematic map of vein arrangement and corresponding leaf section taken from the fully expanded leaf 6 th leaf.	81

Chapter 4: DETAILED MORPHOLOGY OF CANDIDATE LINES

4.1	Fixed and stained section of leaf 5 of an <i>alm3</i> rice mutant, stained with toluidine blue.	88
4.2	Confocal micrograph of tissue taken from leaf 5 of a wild type rice plant. Cell walls are coloured green, and chlorophyll is coloured red.	89
4.3	Cleared and stained transverse sections of leaf 5 of wild type rice and <i>alm</i> lines 1-6.	91
4.4	Isolated mesophyll cells from leaf 5 of wild type IR64 rice plants. Individual groups of chloroplasts are highlighted with red broken line.	93
4.5	Mean distance between two adjacent minor veins in the fully extended fifth leaf. Each bar represents the mean distance for one plant.	94
4.6	Mean number of mesophyll cells present between two adjacent minor veins in the fully extended fifth leaf. Each bar represents the mean number for one plant.	96
4.7	Longitudinal section of wild type rice leaf showing intercellular airspaces (IC); mesophyll cells (M) and the junctions between mesophyll cells (arrowheads). Bar = 10µm. Taken from Sage and Sage (2009).	98
4.8	Comparison of A wild type IR64 rice mesophyll cell and B <i>Arabidopsis thaliana</i> . Note that plan area of rice mesophyll cells are typically 20 -30% of those of <i>Arabidopsis</i> . The high degree of lobing displayed by the rice mesophyll cell is also apparent.	99
4.9	Average plan area of mesophyll cells present between two adjacent minor veins in the fully extended fifth leaf. Each bar represents the mean plan area of cells of one individual plant.	99
4.10	The relationship between mesophyll cell area and mean interveinal distance in the fully expanded leaf 5 of rice plants.	100

- 4.11** Schematic showing the position of the major groups of individual plants for mean cross sectional cell area versus interveinal distance for each *alm* line. **101**
- 4.12** The relationship between the number of cells present and the interveinal distance in the fully expanded leaf 5 of rice plants. **102**
- 4.13** Interveinal cell number versus interveinal distance in individual plants demonstrating an interveinal distance of 90 μ m or less. **103**
- 4.14** Cross sectional cell area versus interveinal distance in individual plants demonstrating an interveinal distance of less than 90 μ m **104**
- 4.15** Comparison of separated mesophyll cells of the *alm* mutant lines and wild type (WT) rice plants. Note the consistent degree of lobing displayed by each line. **106**
- 4.16** The mean number of lobes per mesophyll cell. Bars denote standard error of the means. **107**
- 4.17** Mean number of chloroplasts per mesophyll cell. Bars denote standard error of the means. **108**
- 4.18** Relationship between the mean number of chloroplasts per mesophyll cell and the mean number of lobes per mesophyll cell in the fully expanded 5th leaf of rice plants. **109**
- 4.19** Leaf surface impressions taken from **A)** *alm3* adaxial surface, **B)** wild type rice adaxial surface, **C)** *alm3* abaxial surface and **D)** wild type abaxial surface. **111**
- 4.20** The relative stomatal density across different sections of the abaxial surface of 5th leaf of rice plants. A represents the field of view nearest to the midrib, moving out through successive fields of view out to D at the leaf margin. **112**
- 4.21** The relative stomatal density across different sections of the adaxial surface of 5th leaf of rice plants. A represents the field of view nearest to the midrib, moving out through successive fields of view out to D at the leaf margin. **113**

Chapter 5: PHYSIOLOGICAL RESPONSES OF CANDIDATE LINES

- 5.1** Schematic showing the pathways of energy release from the excited chlorophyll molecule following capture of a photon of light. (LiCor 6400 XT user manual v6.4) **120**
- 5.2** **A)** LiCor 6400 XT IRGA with cuvette open. **B)** Rice leaf in LiCor cuvette for gas analysis. **122**
- 5.3** Example A/C_i curve. Net assimilation (A) versus substomatal carbon dioxide concentration (C_i) in a wild type IR64 rice plant. **124**
- 5.4** Sample output from the curve fitting tool. Blue circles (Aobs) denote the observed values of A at a known C_c . The red line represents the portion of photosynthesis described by the Rubisco-limited state, the green line the RuBP-regeneration state and the yellow line the TPU state. **A,** WT; **B,** *alm1*; **C,** *alm2*; **D,** *alm3*; **E,** *alm4*; **F,** *alm5*; **G,** *alm6*. **125**

5.5	Values determined from fitted $A C_i$ curves, measured at leaf temperature (T_{leaf}). A , Maximum rate of carboxylation (VC_{max}); B , Triose phosphate utilisation (TPU); C , Rate of electron transport (J); D , Dark respiration rate (R_d); E , Mesophyll cell conductance (g_m). Bars denote standard error of the mean (n=5).	126
5.6	Values determined from fitted $A C_i$ curves, normalised to a leaf temperature of 25°C. A , Maximum rate of carboxylation (VC_{max}); B , Triose phosphate utilisation (TPU); C , Rate of electron transport (J); D , Dark respiration rate (R_d); E , Mesophyll conductance (g_m). Bars denote standard error of the mean (n=5).	128
5.7	Quantum yield (F_v/F_m) of <i>alm</i> mutants of rice. Bars denote standard error of the mean (n=5).	131
5.8	Net photosynthesis (A) in response to varying photosynthetically active radiation (PAR). Bars denote standard error of the mean (n=5)	132
5.9	Levels of transpiration (E), in response to varying PAR. Bars denote standard error of the mean (n=5).	134
5.10	Substomatal CO ₂ concentration (C_i) versus PAR. Bars denote standard error of the mean (n=5).	136
5.11	Stomatal conductance (g_s) versus PAR. Bars denote standard error of the mean (n=5).	137
5.12	Quantum yield of photosystem II ($\Phi PSII$) in response to varying PAR. Bars denote standard error of the mean.	138
5.13	Electron transport rate (ETR) in response to varying PAR. Bars denote standard error of the mean (n=5).	139
5.14	Response in photochemical quenching (q_p) in varying levels of PAR. Bars denote standard error of the mean (n=5).	140
5.15	Response in non-photochemical quenching (NPQ) in varying levels of PAR. Bars denote standard error of the mean (n=5).	141
5.16	Schematic diagram of the major protein complexes of the thylakoid membrane. Taken from Pyke (2009).	145

Chapter 6: GENERAL DISCUSSION

6.1	Comparison of A) rice mesophyll cell with B) mesophyll cell <i>Borszczowia aralocaspica</i> employing single celled C_4 photosynthesis. <i>Borszczowia aralocaspica</i> confocal image reproduced from Edwards <i>et al.</i> (2004).	151
6.2	Schematic of the thylakoid membrane proteins.	155
6.3	Partially separated tissue from the fully expanded 6 th leaf of wild type rice showing mesophyll cells in perpendicular arrangement to the bundle sheath.	166

LIST OF TABLES

	Page
Chapter 1: INTRODUCTION AND LITERATURE REVIEW	
1.1 Comparison of CO ₂ assimilation rates (A) between species (von Caemmerer, 2003).	12
1.2 Radiation Use Efficiency (RUE) for above ground biomass production in crop plants (adapted from Kiniry <i>et al.</i> 1989).	13
1.3 Morphological characteristics of <i>P. maximum</i> compared with wildtype (mean \pm S.E) adapted from Fladung (1994).	25
1.4 The frequency of visible mutations of IR64 produced by different mutagens (Wu <i>et al.</i> 2005).	30
Chapter 2: METHODS	
2.1 Ingredients of the hydroponic medium.	35
Chapter 3: SCREENING THE MUTANT POPULATION	
3.1 Anatomical characteristics of the 5 th leaf of wild type IR64.	56
3.2 Summary of mutant lines possessing a significantly reduced mean total number of veins observed in the sixth leaf and / or a significantly reduced mean width of leaf six when compared to wild type IR64 plants (n>3).	62
Chapter 5: PHYSIOLOGICAL RESPONSES OF CANDIDATE LINES	
5.1 Range and order of CO ₂ concentrations used in the production of CO ₂ response curves.	122
5.2 Range and order of light intensities used in the determination of light CO ₂ responses.	123
Chapter 6: GENERAL DISCUSSION	
6.1 Significantly altered physiological and anatomical characteristics displayed by plants of the <i>alm1</i> mutant line of rice compared to wild type rice plants.	152
6.2 Significantly altered physiological and anatomical characteristics displayed by plants of the <i>alm2</i> mutant line of rice compared to wild type rice plants.	157
6.3 Significantly altered physiological and anatomical characteristics displayed by plants of the <i>alm3</i> mutant line of rice compared to wild type rice plants.	158
6.4 Significantly altered physiological and anatomical characteristics displayed by plants of the <i>alm4</i> mutant line of rice compared to wild type rice plants.	158
6.5 Significantly altered physiological and anatomical characteristics displayed by plants of the <i>alm5</i> mutant line of rice compared to wild type rice plants.	160
6.6 Significantly altered physiological and anatomical characteristics displayed by plants of the <i>alm6</i> mutant line of rice compared to wild type rice plants.	160

ABBREVIATIONS

A	Net carbon dioxide assimilation
ABA	Abscisic acid
<i>alm</i>	Altered leaf morphology mutant
AT	Adenine-thymine
ADP	Adenosine diphosphate
ANOVA	Analysis of variance
ATP	Adenosine triphosphate
BF	Bulliform cells
BS	Bundle sheath cell
CAM	Crassulacean acid metabolism
C_a	Atmospheric carbon dioxide concentration
C_c	Chloroplast carbon dioxide concentration
C_i	Substomatal carbon dioxide concentration
CO ₂	Carbon dioxide
Cyt	Cytochrome
DEB	Diepoxybutane
E	Transpiration rate
EMS	Ethyl methanesulphonate
ETR	Electron transport rate
<i>F</i>	Fluorescence
GALP	Glycerate 3-phosphate
GC	Guanine-Cytosine
g_m	Mesophyll conductance
g_s	Stomatal conductance
<i>H</i>	Heat
Ha	Hectare
HCl	Hydrochloric acid
HI	Harvest index
IRGA	Infra-red gas analyser
IRRI	International Rice Research Institute
J	Rate of electron transport
M	Mesophyll cell

NADH	Nicotinamide adenine dinucleotide
NAD-ME	Nicotinamide adenine dinucleotide malic enzyme
NADP	Nicotinamide adenine dinucleotide phosphate
NADPH	Nicotinamide adenine dinucleotide phosphate (reduced)
NADP-ME	Nicotinamide adenine dinucleotide phosphate malic enzyme
NaEDTA	Disodium ethylene diamine tetra acetate
NPQ	Non-photochemical quenching
OAA	Oxaloacetic acid
<i>P</i>	Photochemical reaction
PAR	Photosynthetically active radiation
PBS	Phosphate Buffer Solution
PCK	Phosphoenolpyruvate carboxykinase
PEP	Phosphoenolpyruvate
PSI	Photosystem I
PSII	Photosystem II
q_p	Photochemical quenching
R	Resistance
R_d	Dark respiration rate
ROS	Reactive oxygen species
Rubisco	Ribulose-1,5-bisphosphate carboxylase oxygenase
RUBP	Ribulose bisphosphate
RUE	Radiation use efficiency
SA	Salicylic acid
SAM	Shoot apical meristem
TPU	Triose phosphate utilisation
VC_{max}	Maximum rate of carboxylation
V_{max}	Maximum rate of enzyme activity
WT	Wild type
Φ PSII	Quantum yield of photosystem II

Chapter 1
INTRODUCTION AND
LITERATURE REVIEW

Chapter 1: INTRODUCTION AND LITERATURE REVIEW

It is thought that Asian rice (*Oryza sativa* L.) was first cultivated as early as the year 10,000 BC, with relics suggesting it was grown in Eastern India, China, northern Thailand and Burma. Rice cultivation spread along the Ganges and Indus rivers between 2,500- 1,500 and was introduced through the Near East and into Europe on a small scale before Christ, although the drier climate present there favoured wheat and barley production. It was introduced into East Africa and Madagascar around the 5th century, before arriving in South America in 16th century. Rice cultivation began in North America and Australia in the 20th century (Hoshikawa, 1989). African rice (*Oryza glaberrima* Steud.) has been grown since early times, although cultivation of *O. sativa* has become more common as although generally hardier, productivity of the *glaberrima* species is low. More recently *O. sativa* and *O. glaberrima* have been crossed to produce NERICA (New Rice for Africa) varieties, which aim to give Asian rice yields in a plant which is better adapted to the harsher African conditions.

There are five subspecies of *Oryza sativa* L.; *indica* (commonly known as long grain rice) and *japonica* (short grain rice) are the major subspecies, but the *aus*, *tropical japonica*, *temperate japonica* and *aromatic* groups have also been discovered (Garris *et al.*, 2005). Of the major subspecies, *japonica* produces short plants with many tillers and short, round grains which are glutinous when cooked. Plants of the *indica* subspecies are taller, though the introduction of semi-dwarf varieties has reduced plant height. They too produce many tillers, with long thin grains which are less glutinous when cooked. There are both upland and paddy rice cultivars of both major subspecies, and also floating cultivars of *indica* have been produced (Hoshikawa, 1989).

1.1 Rice as a crop

In terms of economic value, rice is one of the world's most important crops. Paddy rice is grown on approximately 161 million ha of land worldwide (FAOSTAT, 2009), primarily in Asia in a band flanked by Pakistan to the east and Japan to the west, and provides the primary source of calories for a large proportion of the population residing in this area. Rice forms over 70% of caloric uptake in Myanmar and Bangladesh, dropping to approximately 50% in relatively wealthy countries such as Thailand (Dawe, 2000). The most recent United Nations (UN) figures suggest that, as of 2010, the Asian population stands at 4.2 billion people. Given current rates of population growth, this figure is predicted to rise to almost 6.5 billion by the year 2050, although, allowing for current trends in decreasing fertility levels, the UN perceives a figure of around 5.2 billion to be more likely (UN data, 2008). Due to the rapid rate of increase in the population of Asia, it has been suggested that a 50% increase in Asian rice yields is required by 2050 in order to avoid "misery for hundreds of millions" (Cantrell 2000). Current annual global rice production is almost 679 million tonnes and average yield is 4.2 tonnes ha⁻¹ (FAOSTAT, 2009).

1.2 Improving Production

There are numerous possible strategies that may be taken in order to improve food production from crops, including the reduction of pre- and post-harvest losses, increasing the area of land under cultivation and, perhaps most challengingly, increasing crop yield per hectare. Increases in workable arable land area provided the basis of increases in production as the world population rose toward the three billion mark around 1960 (Evans, 1998). However, currently the area of cultivated land is fairly stationary (Figure 1.1) due to increasing urbanisation so this no longer represents a strategy permissible to further agricultural production. Increasing levels of erosion and competition for land from biofuels may

also contribute to a reduction in available agricultural land (Hibberd *et al.*, 2008).

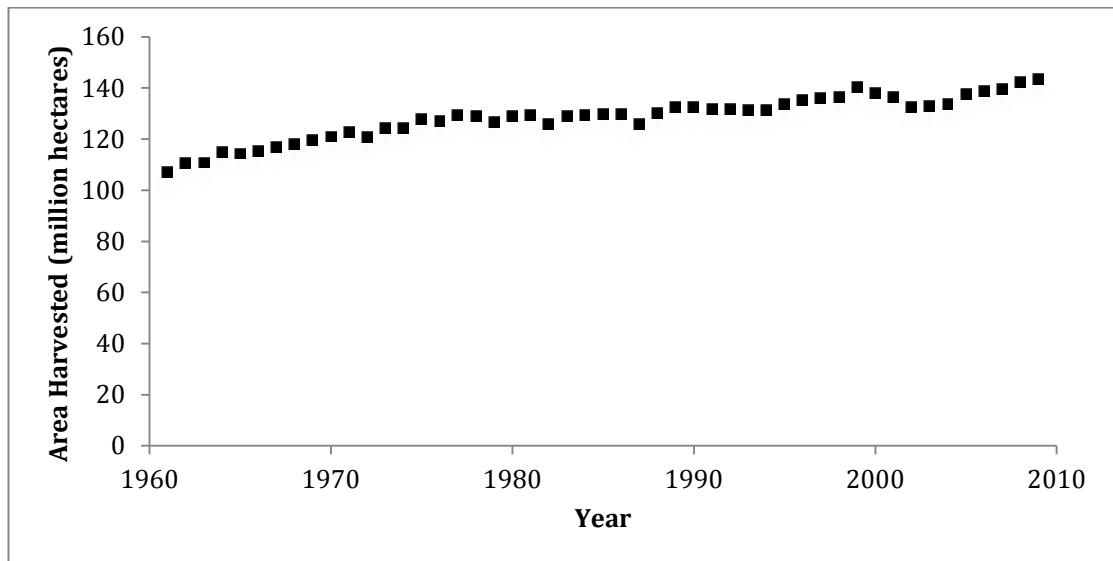


Figure 1.1 Trends in area harvested for Asian rice (source: FAOSTAT database, 2011)

Post-harvest losses also account for a significant loss in potential usable yield. Current data are sparse, but it was estimated that post-harvest losses can be as high as 26%, primarily during the drying and storage processes (Ren-Yong *et al.* 1990). However, if post-harvest losses were to be completely eliminated, current levels of rice production are still not large enough to sustain projected population increases. This leaves increasing the yield potential of rice by increasing harvested yield per hectare as the only realistic route for improving rice production.

1.3 Physiological traits determining yield potential

The harvested yield of a crop is determined by the proportion of the total plant biomass that is directed towards the harvested structures i.e. the grain when considering rice. This proportion is termed the harvest index. Biomass accumulation is facilitated by the capture of photosynthetically

active radiation (PAR, 400-700nm), which is then used in photosynthesis. The effectiveness of the use of radiation is quantified as the radiation use efficiency (RUE), the amount of dry matter produced per unit of PAR intercepted (Monteith, 1977). Summarizing this, Mitchell and Sheehy, (2006) produced the following equation:

Equation 1.1

$$Y = HI \varepsilon \sum_{i=1}^n Q_i f_i$$

where Y the grain yield (g m^{-2}), HI is the harvest index, ε is RUE (g MJ^{-1}), n is the duration of growth (days), Q_i is the PAR on the crop on the i th day (MJ m^{-2}) and f_i is the fraction of incident PAR intercepted on the i th day. Increasing any of the terms in this equation can increase harvestable yield.

1.3.1 Harvest index

During the 20th century, major advances in the production of crops with high yield potentials were brought about with the production of semi-dwarf varieties, which had reduced plant height and increased harvest index (HI) i.e. the ratio of above ground dry matter to grain yield. This period of crop improvement during 1960s and 1970s became known as the 'Green Revolution', and the cultivars produced during this period have come to dominate Asian rice production. The Green Revolution allowed rapid increases in production and yield throughout the late 20th century (Figures 1.2 and 1.3). However it is now thought that harvest index in rice is approaching an optimal level, and Green Revolution related gains have all but ceased (Kropff *et al.*, 1994, Mitchell and Sheehy, 2006, Hibberd *et al.*, 2008), or may even have to decrease a

little from its current level of 0.5 in order to give greater resistance to lodging (Mitchell and Sheehy, 2006).

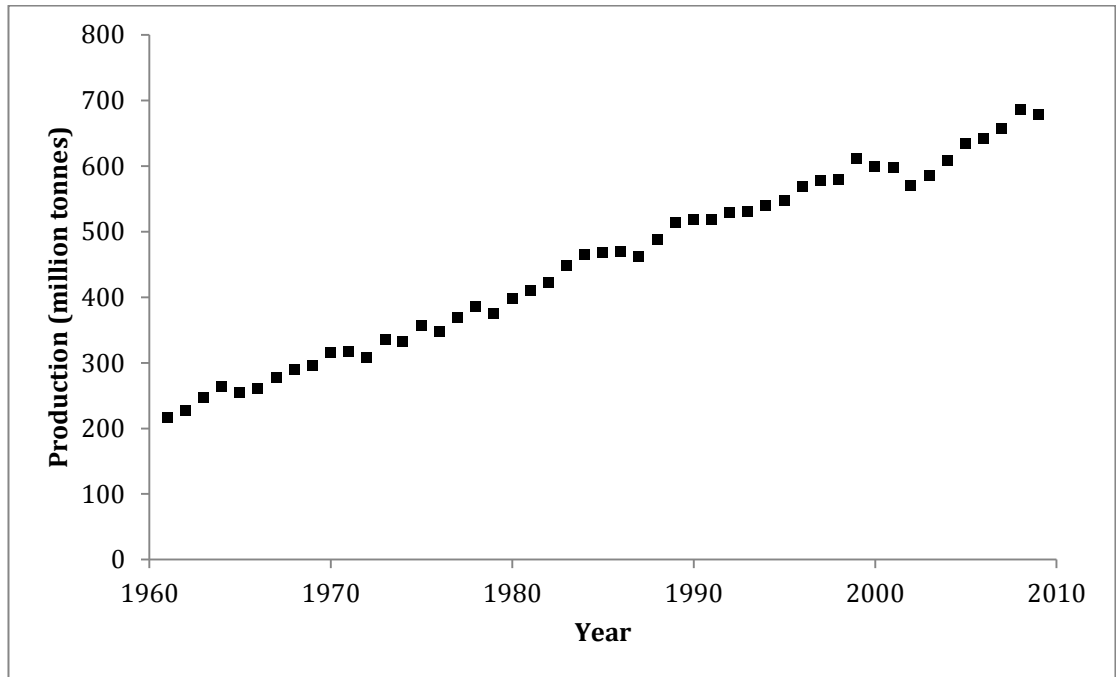


Figure 1.2 Trend in rice global grain production (source: FAOSTAT database, 2011).

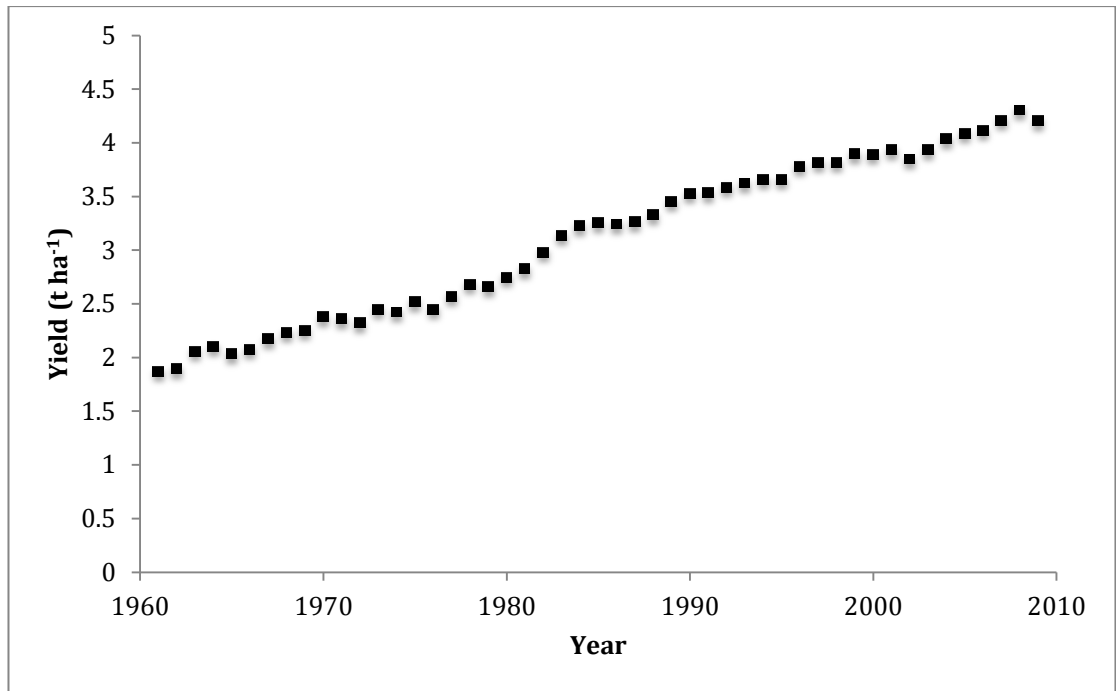


Figure 1.3 Trend in global rice average yield (source: FAOSTAT database, 2011).

1.3.2 Remobilisation of stem reserves

It was initially suggested that large gains in yield potential could be achieved by increasing assimilate partitioning from leaves to stems (Dingkuhn *et al.*, 1991). However, in the model suggested by Dingkuhn *et al.* (1991), the allocation of dry matter was expected to cease at panicle initiation, which has been shown not to be correct, as the flag leaf has yet to emerge and expand. It is likely that this incorrect assumption led to an overestimation of leaf area development during early growth which caused the model to predict a large gain in yield (Kropff *et al.*, 1994). It was therefore suggested that a small increase in yield potential may be possible as a result of increased remobilisation of stem carbohydrate reserves; however this is not of the scale needed in order to support population growth (Kropff *et al.*, 1994).

1.3.3 Prolonged grain filling and green leaf area duration

The ORYZA1 model (Kropff *et al.*, 1994b) predicts that gains in yield potential are possible if the grain-filling period is increased; however this relies on a significant proportion of the green leaf area remaining

photosynthetically active throughout this stage, a situation that does not naturally occur. Senescence would need to be considerably delayed and leaf nitrogen status maintained throughout this period to be effective (Kropff *et al.*, 1994). Further to this, and perhaps more importantly, there is generally little interest in increasing the growth duration as current durations are timed to coincide with suitable weather conditions or to allow multiple crops per year (Mitchell and Sheehy, 2006).

1.3.4 PAR

Increasing the incident PAR is obviously not possible without selecting sunnier locations or growing seasons or reliance on artificial lighting (which is impractical and most often impossible). It is also thought that intensively grown rice is as close to intercepting as large a fraction of the incident PAR as is possible, given the constraints of being an annual crop and so establishing from bare ground (Mitchell and Sheehy, 2006).

1.3.5 Increased sink size

Using both new plant types of the *japonica* germplasm of rice and current high yielding rice varieties, Sheehy *et al.* (2001) investigated the effects of increasing sink size on yield in rice. In both cases, the model predicted that if all juvenile spikelets had been converted to filled grains a yield potential more than double the observed yield would be reached. However, many juvenile spikelets were lost and grains were not filled. This reduction in observed yield compared to yield potential was still demonstrated even in well fertilised crops grown at current atmospheric CO₂ concentrations, therefore suggesting that grain yield is limited by the supply of resources necessary for its production, rather than any lack of sink capacity. As well fertilised plants showed the same effect, it seems reasonable that photosynthesis is the limiting factor in resource supply.

1.4 Photosynthesis as a limiting factor

In C₃ species such as rice, carbon fixation occurs in a cyclical process known as the Calvin cycle. The primary fixation of carbon dioxide in the Calvin cycle occurs when CO₂ is conjugated with the five carbon sugar ribulose biphosphate (RUBP), forming a highly unstable six carbon intermediate, which undergoes almost immediate spontaneous decomposition to form two molecules of phosphoglycerate, which in turn are converted to glycerate 3-phosphate (GALP). GALP is reduced using NADH and ATP to regenerate RUBP, and thus the Calvin cycle continues. This conjugation of CO₂ and RUBP is catalysed by the enzyme Rubisco (ribulose 1,5, biphosphate carboxylase / oxygenase), and it is the inefficiency of this enzyme that has promoted the evolution of C₄ photosynthesis within plants.

Rubisco is one of the great enigmas of evolutionary biology. Firstly, it is a very slow acting enzyme, which means that Rubisco is present in extremely high concentrations in the chloroplast stroma at approximately 1.68g m⁻² leaf tissue (Jin *et al.*, 2006). Secondly, Rubisco also has the ability to fix oxygen, as well as carbon dioxide; thus Rubisco is regarded as an oxygenase as well as a carboxylase. Oxygenase activity is favoured over carboxylase activity at higher temperatures and oxygen concentrations. The fixation of oxygen results in the production of phosphoglycolate, an apparently functionless substance that is entered into the photorespiration cycle to recover some of the carbon wasted within the molecule (Muhaidat *et al.*, 2007).

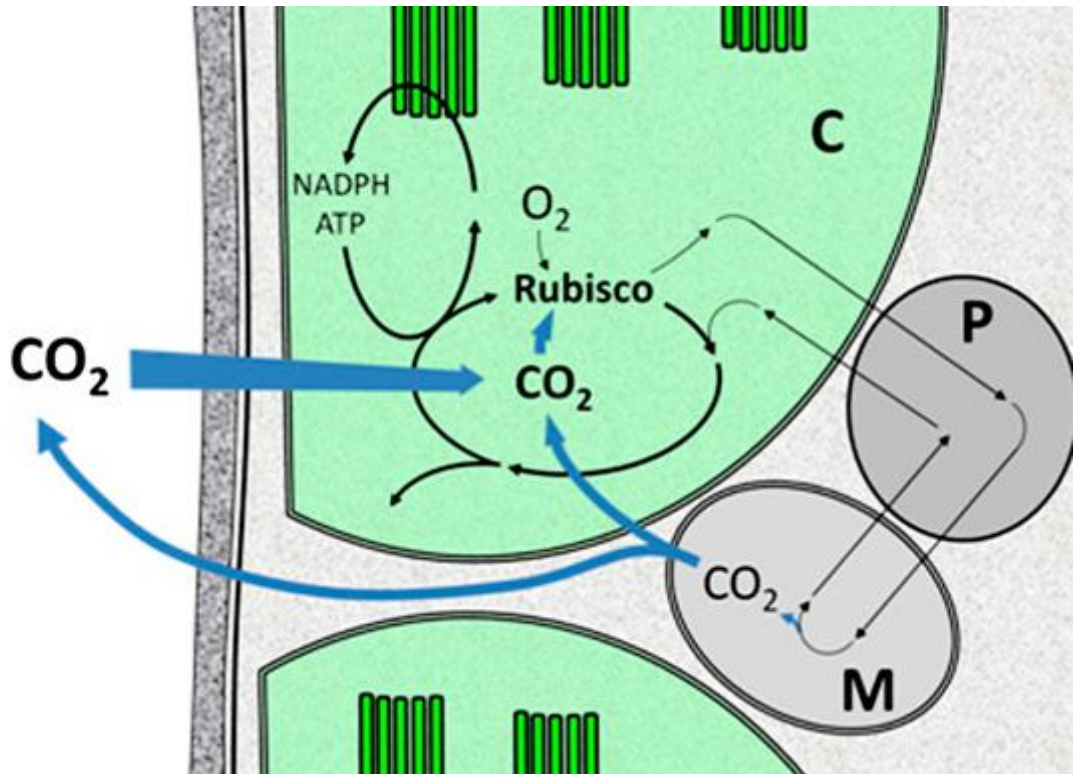


Figure 1.4 Schematic showing the photorespiratory cycle. C, chloroplast; M, mitochondrion; P, peroxisome. Taken from von Caemmerer and Evans (2010).

As a C₃ plant grown under tropical conditions, Asian rice has significant level of photorespiration due to the high temperatures at which it grows. Given current atmospheric CO₂ concentrations, at a temperature of 30°C, approximately 33% of the total level of Rubisco within a photosynthesising rice plant may be functioning as an oxygenase, thus representing a significant loss of CO₂ fixation to the plant and major limiting factor of photosynthesis (Evans and von Caemmerer, 2000). This correlates to an estimated reduction in the productivity of C₃ crops by over 30% (Ogren, 1984; Zhu *et al.* 2004).

1.5 Potential Improvements to Rice Photosynthesis

As Rubisco appears to be a major limiting factor to photosynthesis in C₃ plants grown under tropical conditions, and there is no known alternative

to this enzyme in the fixation of CO₂ in the Calvin cycle (Sage, 2004), the options for the improvement of photosynthesis appear somewhat limited.

Increasing the level of Rubisco in leaves could provide a method for increasing photosynthetic capacity; however this would not represent any gain in efficiency so improvements would still be severely limited by photorespiration. Also given that Rubisco already accounts for up to 50% of the soluble protein within leaves, further increases would require greater inputs of soil nitrogen. As improvements to rice yield would be of benefit to some of the world's poorest people, yield improvements requiring large amounts of nitrogen fertiliser would be inappropriate in terms of both economic and environmental sustainability (Mitchell and Sheehy, 2006). Further to this, leaves may be lacking the physical capacity for increased levels of Rubisco without some redesigning of leaf anatomy, as it has been shown in wheat that chloroplast number is closely correlated to cell size (Pyke and Leech, 1987).

There are species of red algae that produce a Rubisco which displays a much greater specificity for CO₂ relative to O₂. Unfortunately this improvement in specificity comes at a cost to the maximum rate of Rubisco activity (V_{max}), thus limiting the effect that expressing foreign Rubisco may have on C₃ plants (Zhu *et al.*, 2004).

In an attempt to combat the problem of photorespiration, the C₄ photosynthetic pathway has evolved many times, with at least 45 independent cases known, with over 30 lineages displayed by dicots and 15 in monocots (Sage, 2004).

C₄ photosynthesis functions by concentrating CO₂ around the active sites of Rubisco, thus almost eliminating photorespiration by competitive exclusion of O₂ (Muhaidat *et al.*, 2007). Some systems are known whereby a modified version of C₄ photosynthesis takes place within single cells such as *Hydrilla verticillata* (Reiskind *et al.*, 1997) and *Egeria densa* (Casati *et al.*, 2000). However, the low assimilation rate displayed by such species (Table 1.1) has been highlighted as a cause for concern (von Caemmerer, 2003). It is therefore suggested that single-celled C₄ photosynthesis is capable of permitting some photosynthetic gain under conditions of extreme favourability towards photorespiration; however, it appears unsuitable as a system for improving C₃ crop productivity.

Table 1.1 Comparison of CO₂ assimilation rates (*A*) between species, taken from von Caemmerer (2003)

Species	Photosynthetic type	<i>A</i> (μmol g chl ⁻¹ s ⁻¹)	Conditions	Reference
<i>Hydrilla verticillata</i>	Aquatic single cell C ₄	4	320 μL L ⁻¹ CO ₂ , 30 °C, 1000 μmol quanta m ⁻² s ⁻¹	Salvucci & Bowes (1981)
<i>Bienertia cycloptera</i>	Single cell C ₄	8	320 μL L ⁻¹ CO ₂ , 25 °C, 1300 μmol quanta m ⁻² s ⁻¹	Voznesenskaya <i>et al.</i> (2002)
<i>Borszczowia aralocaspica</i>	Single cell C ₄	17	320 μL L ⁻¹ CO ₂ , 25 °C, 1200 μmol quanta m ⁻² s ⁻¹	Voznesenskaya <i>et al.</i> (2001)
<i>Nicotiana tabacum</i>	C ₃	47–49	320 μL L ⁻¹ CO ₂ , 25 °C, 1000 μmol quanta m ⁻² s ⁻¹	Evans <i>et al.</i> (1994)
<i>Oryza sativa</i>	C ₃	36	300 μL L ⁻¹ CO ₂ , 25 °C, 1400 μmol quanta m ⁻² s ⁻¹	Makino <i>et al.</i> (1983)
<i>Triticum aestivum</i>	C ₃	54	350 μL L ⁻¹ CO ₂ , 25 °C, 2000 μmol quanta m ⁻² s ⁻¹	Watanabe <i>et al.</i> (1994)
<i>Gossypium hirsutum</i>	C ₃	77	320 μL L ⁻¹ CO ₂ , 30 °C, 2000 μmol quanta m ⁻² s ⁻¹	Wong (1979)
<i>Zea mays</i>	C ₄	118	320 μL L ⁻¹ CO ₂ , 30 °C, 2000 μmol quanta m ⁻² s ⁻¹	Wong (1979)
<i>Amaranthus edulis</i>	C ₄	134	320 μL L ⁻¹ CO ₂ , 30 °C, 1600 μmol quanta m ⁻² s ⁻¹	Leegood & von Caemmerer (1988)

Thus incorporating C₄ photosynthesis with a traditional Kranz leaf anatomy (Section 1.6) into rice appears the most attractive option for the improvement of rice potential yield. This option becomes even more attractive given that C₄ species often display a highly economic usage of water and nitrogen. The addition of an entirely new leaf anatomy into rice represents an enormous challenge; however, it is thought that the risks of such a project are well outweighed by the possible rewards (Mitchell and Sheehy, 2007). Table 1.2 shows the radiation use efficiency (RUE) of rice compared to C₃ (wheat) and C₄ (maize, sorghum) crops. This highlights the poor RUE of rice, and the potential gains that could be achieved if a C₄ system similar to that in maize was to be introduced into rice leaves.

Table 1.2 Radiation Use Efficiency (RUE) for above ground biomass production in crop plants (adapted from Kiniry *et al.* 1989).

Crop	RUE (g MJ⁻¹)	RUE/ RUE_{rice}
Maize	3.5	1.59
Sorghum	2.8	1.27
Wheat	2.8	1.27
Rice	2.2	

1.6 Characteristics of C₄ Photosynthesis

1.6.1 The C₄ pathway

The bundle sheath is a layer of parenchyma tissue surrounding the vascular bundles, which acts as a conduit between the mesophyll cells and the vasculature system of a plant (Leegood, 2008). Amongst their many functions, the bundle sheath cells are required to maintain hydraulic integrity in order to prevent air entering the xylem, as well as regulating the fluxes of compounds into and out of the leaf.

In C₃ plants, despite the bundle sheath cells typically containing fewer and smaller chloroplasts (Kinsman and Pyke, 1998), both mesophyll and bundle sheath cells are equivalent in terms of photosynthetic pathway, in that atmospheric CO₂ is assimilated using Rubisco and reduced within the Calvin cycle (Dengler and Taylor, 2000). It is this exposure of the Rubisco to atmospheric oxygen that provides opportunity for photorespiration. By spatially separating C₃ activity into the bundle sheath cells using the mesophyll cells to provide CO₂ via the C₄ pathway, a ten-fold rise in [CO₂] over atmospheric [CO₂] can be produced in the bundle sheath cell chloroplasts (Figure 1.5, 1.6), providing an effective method of suppressing photorespiration (Edwards and Walker, 1983).

C₄ photosynthesis is thought to have evolved independently more than 45 times in 19 families of angiosperms (Sage, 2004), and therefore there is some variation in the pathway from species to species, although in all cases the primary fixation of inorganic carbon involves

carboxylation of phosphoenolpyruvate (PEP) by the enzyme PEP carboxylase in the mesophyll cells. PEP carboxylase is expressed in all plants, but levels in C_4 plants may be twenty-fold those observed in C_3 species. Further to this, Stockhaus *et al.* (1997) were able to show that this increase in expression is localised only to the mesophyll cells by use of transgenic plants containing the β -glucuronidase reporter gene (Figure 1.5). In C_3 species PEP carboxylase is known to be involved in a variety of different functions, including stomatal opening, seed maturation and fruit ripening (Miyao and Fukayama, 2003).

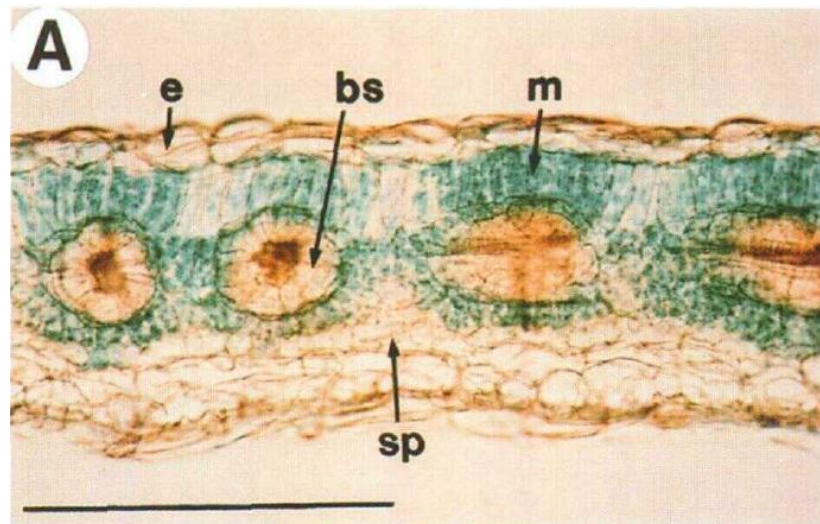


Figure 1.5 Histochemical staining of GUS activity showing the blue appearance of cells expressing PEP carboxylase in the C_4 plant *Flaveria bidentis*. e, epidermis; bs, bundle sheath; m, mesophyll; sp, spongy parenchyma. Bar denotes 500 μ m. Taken from Stockhaus *et al.* (1997).

Following carboxylation of PEP, oxaloacetic acid (OAA) is formed. OAA is highly unstable and therefore does not usually accumulate in significant quantities, so for this reason is converted to other substances for transport to the bundle sheath cells. Three variants of this transport system have evolved, although all are similar in concept:

1. Nicotinamide adenine dinucleotide phosphate malic enzyme (NADP – ME), where OAA is converted to malate, which undergoes decarboxylation by NADP – ME in the bundle sheath chloroplasts.
2. Nicotinamide adenine dinucleotide malic enzyme (NAD – ME), where malate undergoes decarboxylation by NAD – ME in the bundle sheath mitochondria
3. Phosphoenolpyruvate carboxykinase (PCK), where decarboxylation occurs in the bundle sheath cytosol (as well as some NAD – ME activity in the mitochondria).

In all cases, C₄ acids freely diffuse from the mesophyll cells where they are produced into the bundle sheath cells (via the plasmodesmata) where they undergo decarboxylation. The released CO₂ is reassimilated by Rubisco and entered into the Calvin cycle. Pyruvate (in the NADP-ME subtype) or alanine (in the NAD-ME subtype) produced following decarboxylation of the C₄ acids diffuses back to the mesophyll cells where they are converted back to PEP and recycled.

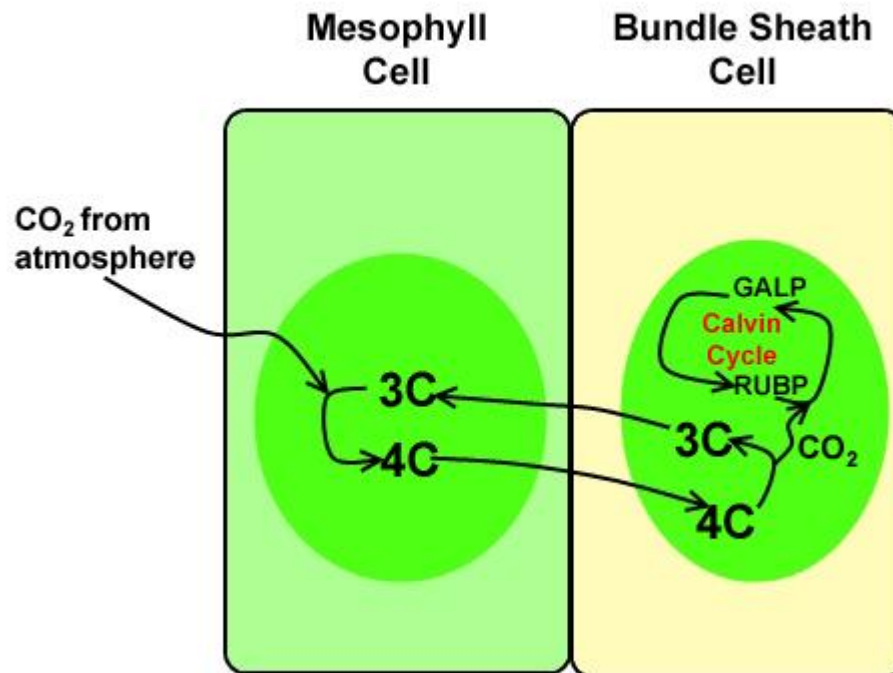


Figure 1.6 Simplified schematic of the C₄ pathway demonstrating the fixation of atmospheric CO₂ in the mesophyll cell chloroplasts by PEP carboxylase before transfer of the 4 carbon compound to the bundle sheath chloroplasts. Decarboxylation occurs and CO₂ enters into the Calvin cycle, whilst PEP is returned to the mesophyll cells.

1.6.2 Anatomical adaptations for C₄ photosynthesis

Although single celled C₄ photosynthetic systems do exist, as stated in Section 1.5, these does not appear to be of much benefit within a crop system, so for this reason this section will focus on the more typical Kranz anatomy (Hatch, 1987). There is significant variation in basic Kranz leaf architecture between various C₄ plant families, although there are a number of features that can be considered essential to the process of C₄ photosynthesis and are invariably present in C₄ species (Sage, 2004). These are the structural specialisation of two separate photosynthetic cell types (bundle sheath cells and mesophyll cells), maximised contact between these two cell types, and limited CO₂ leakage from the bundle sheath cells. In C₄ plants, the bundle sheath is typically enlarged compared to C₃ plants and contains a greater number of chloroplasts. Chloroplasts are centrifugally positioned, as shown in Figure

1.7C (Dengler and Taylor, 2000). This increase in the number of chloroplasts present in the bundle sheath (and hence the increase in size of the cells as a whole) is required to facilitate the increased levels of photosynthesis taking place within the tissue. An asymmetric distribution of chloroplasts throughout the cytosol ensures that chloroplasts are located where the CO_2 concentration is highest (i.e. next to the mesophyll cells), helping to further minimise photorespiration and speed up CO_2 uptake by minimising the distance that it is required to diffuse across (Kobayashi *et al.*, 2009)

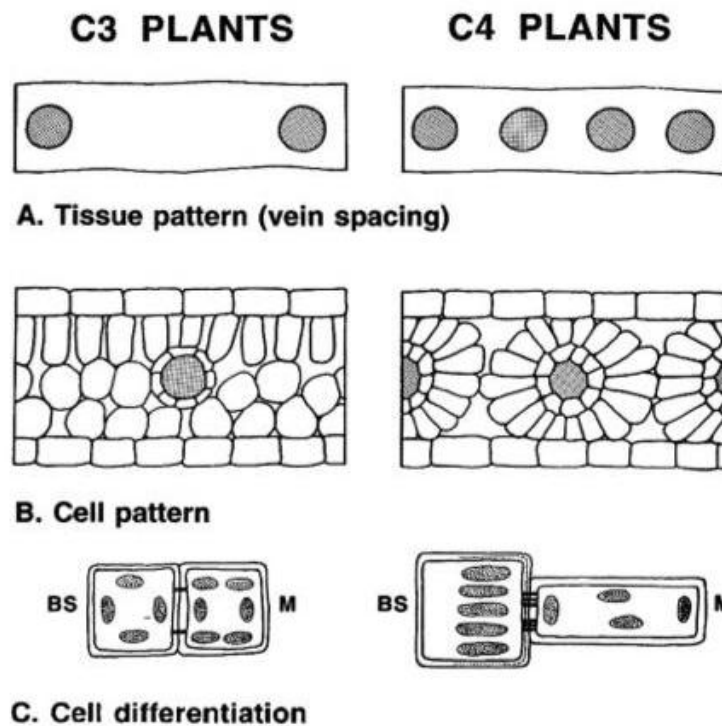


Figure 1.7 Representation of differences between C_3 and C_4 plant anatomy. Taken from Leegood *et al.* (2000). **A**) Demonstrates the increase in vein density in C_4 plants compared to C_3 , **B**) shows the close arrangement of mesophyll and bundle sheath cells in C_4 leaves, and **C**) demonstrates the centrifugal positioning and increase in number of chloroplasts within the C_4 bundle sheath.

In order to maximise the rate of diffusion of C₄ acids between mesophyll and bundle sheath cells, contact between the two cell types is maximised. Mesophyll cells are often in a radial arrangement around the bundle sheath, typically allowing each mesophyll cell to be in contact with a bundle sheath cell. There are also large numbers of plasmodesmata crossing the bundle sheath / mesophyll cell wall, providing an easy route for the diffusion of metabolites. As each mesophyll cell is in contact with a bundle sheath cell, and bundle sheath cells are located around the vascular tissue, there are typically very few mesophyll cells between each vascular bundle and veins are closer together in C₄ species (Leegood *et al.*, 2000).

In order to prevent a drop in [CO₂] within the bundle sheath cell, and thus potentially risk elevated levels of photorespiration, carbon dioxide leakage from the bundle sheath is minimised. Many C₄ species have a layer of suberin in the lamella of the bundle sheath cell wall, which is thought to make it impermeable to CO₂. Although often observed, this cannot be considered a requirement of C₄ leaf structure, as this suberinised layer is not present in all C₄ species (Sage, 2004). The total volume of intercellular airspace is also reduced in C₄ plants, as is the exposure of the bundle sheath to the intercellular airspace. This minimises the risk of diffusion of CO₂ out through the cell walls of the bundle sheath, as a reduced cellular [CO₂] compared to the surrounding cells is maintained by consuming it in the Calvin cycle (Dengler *et al.* 1994).

1.6.3 Physiological consequences of C₄ photosynthesis

There is such a different response to varying concentration of CO₂ between C₃ and C₄ species that it is a useful indicator when trying to identify C₄ photosynthesis (Downton and Tregunna, 1968). There are three major points where C₃ and C₄ responses differ (Edwards and Walker, 1983):

1. CO₂ compensation point. This is defined as the [CO₂] where gross photosynthesis is equal to respiration, thus net photosynthesis is zero. In C₄ plants the CO₂ compensation point is almost zero across all temperatures, as the C₄ mechanism is able to concentrate even low levels of atmospheric CO₂ to such an extent that photosynthesis can continue. However the compensation point for C₃ species is typically around 50 μmol CO₂ mol⁻¹ air at moderate temperatures, rising to 70 μmol mol⁻¹ at 35°C as the effects of photorespiration become more pronounced (Sage *et al.*, 1990).
2. As [CO₂] increases, the rate of increase in assimilation initially increases more sharply in C₄ plants than C₃, due to the higher activity of PEP carboxylase at cellular pH than Rubisco (Edwards and Walker, 1983)
3. At temperatures around 15°C or higher, CO₂ saturation of Rubisco occurs at much lower concentrations in C₄ plants than C₃, and is sharply delineated, whereas in C₃ it is not. This is due to limitations in either the activity of Rubisco or PEP carboxylase, the regeneration of these enzymes or any combination of these factors. Examples of all four have been described (von Caemmerer and Furbank, 1999). This response is also shown by plants grown in CO₂ rich environments, such as during the initial evolution of higher plants, which favoured C₃ species at a time when atmospheric [CO₂] was significantly greater than the present (Sage, 2004).

These responses are demonstrated in the form of an A/C_i curve in Figure 1.8, which plots net CO_2 assimilation (A) versus sub-stomatal CO_2 concentration (C_i).

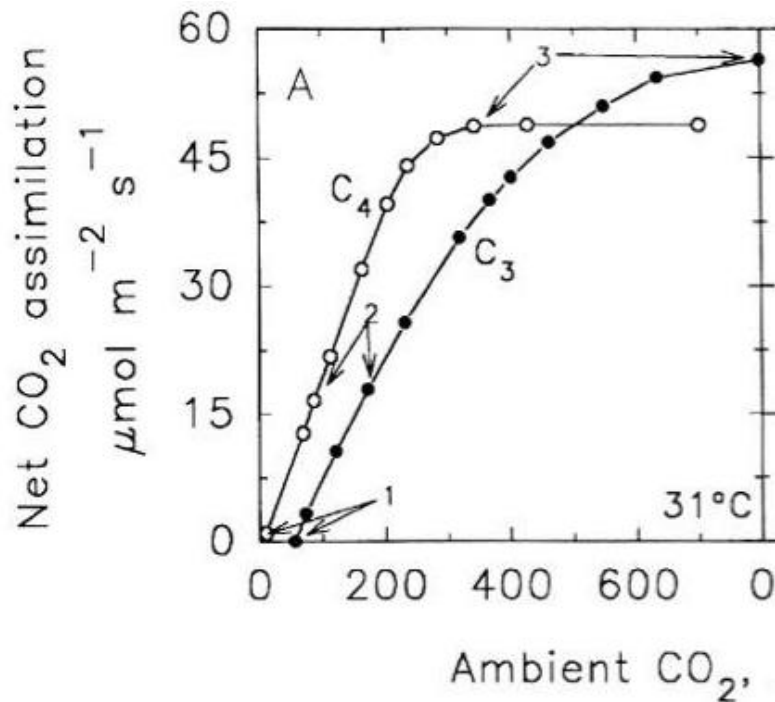


Figure 1.8 Typical A/C_i curve for C_3 and C_4 plants showing the three major points of variance outlined above. Taken from Sage and Pearcy (2000). **1**) demonstrates the lower CO_2 compensation point displayed by C_4 plants, **2**) shows the sharp increase in A as $[\text{CO}_2]$ rises and **3**) shows the elevated maximum A (A_{max}) demonstrated by C_3 plants at high $[\text{CO}_2]$.

There are also large differences in quantum yield between C_3 and C_4 species. Quantum yield is the ratio of fixed CO_2 to absorbed photons. Maximum quantum yield is generally measured because it allows direct comparison of the energy costs of C_3 and C_4 photosynthetic systems. In the absence of oxygen, when photorespiration is eliminated, the quantum yield of C_4 plants is 20 – 30% of the level in their C_3 counterparts due to the extra ATP cost of regenerating PEP. However, under normal atmospheric conditions, quantum yield is approximately equal between 25-30°C. Above 30°C the oxygenase activity of Rubisco is increased

further and photorespiration becomes significant, meaning that C₄ plants demonstrate a higher yield. However, below 25°C when levels of photorespiration are less significant C₃ photosynthesis becomes more efficient.

1.7 Leaf Development

Leaves are initially formed in the shoot apical meristem (SAM), a population of stem cells which maintain a high rate of cell proliferation (Veit, 2004). Cells on the flanks of the SAM differentiate to form the leaf and stem tissue, whilst some of the daughter cells generated retain their function as stem cells and remain within the SAM. The balance of the total number of cells produced versus the cells integrated into the emerging leaf and stem determine the size of the SAM (Fleming, 2005). In the SAM of rice, leaves are initiated on opposing sides of the SAM, which results its alternate phyllotaxy.

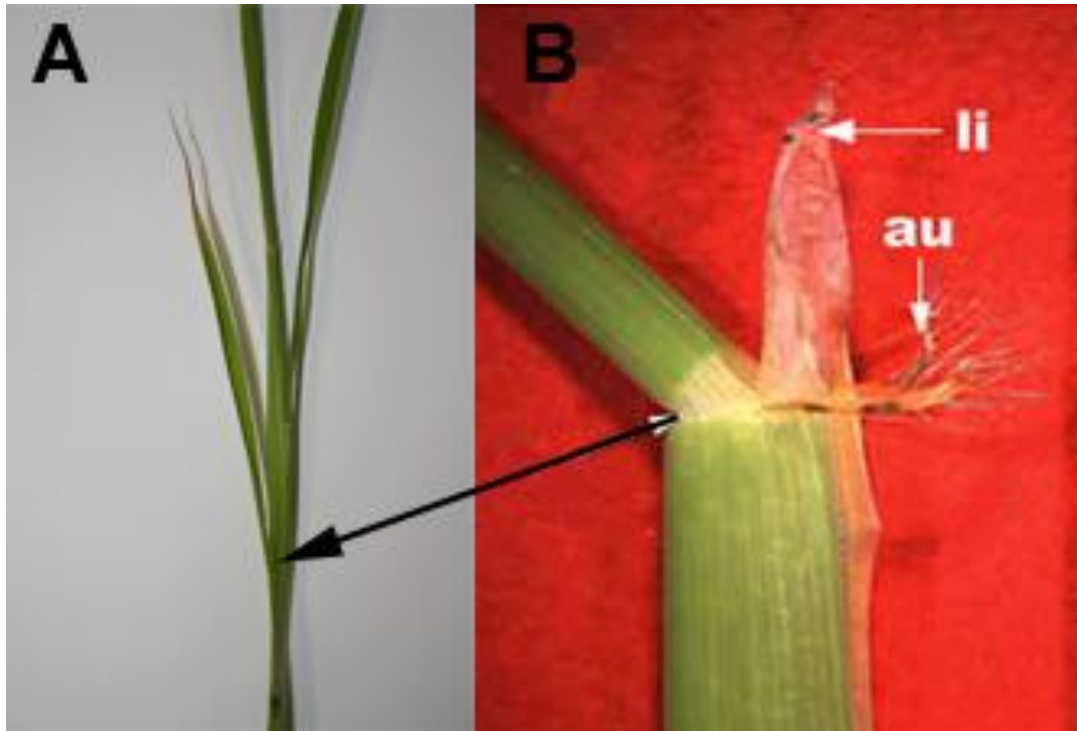


Figure 1.9 **A)** young rice plant. The leaf sheath forms around the culm, with the leaf blade emerging at the collar. **B)** li, ligule; au, auricle of a rice plant at 70 days post germination, taken from Lee *et al.* (2007)

The production of leaves in rice was described by Itoh *et al.*, (2005) and is summarised here. In rice, the emerging leaf primordium is first observed as a small bulge on the flank of the SAM and then extends above the apex of the SAM and around the side of it, giving the primordium a crescent shaped appearance. As cells of the primordium proliferate, it forms a hood over the SAM, and it is at this stage that the procambial strand is formed (Figure 1.10).

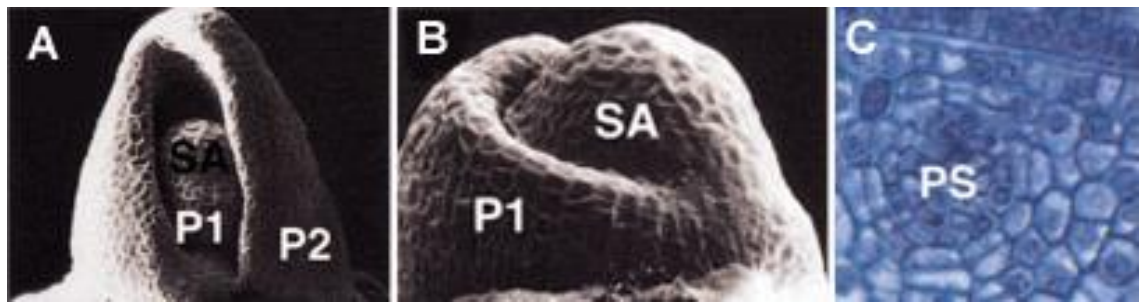


Figure 1.10 **A)** The emerging leaf primordium (P1) forming from the shoot apical meristem (SA) as the P2 primordium forms a hood over the SAM. **B)** Extending P1 primordium forming a crescent shape. **C)** Cross section of P2 showing early procambial strand (PS) (Itoh *et al.*, 2005).

As the leaf primordium expands laterally around the SAM, the leaf margins overlap and the SAM becomes enclosed as the leaf blade – sheath boundary is established.

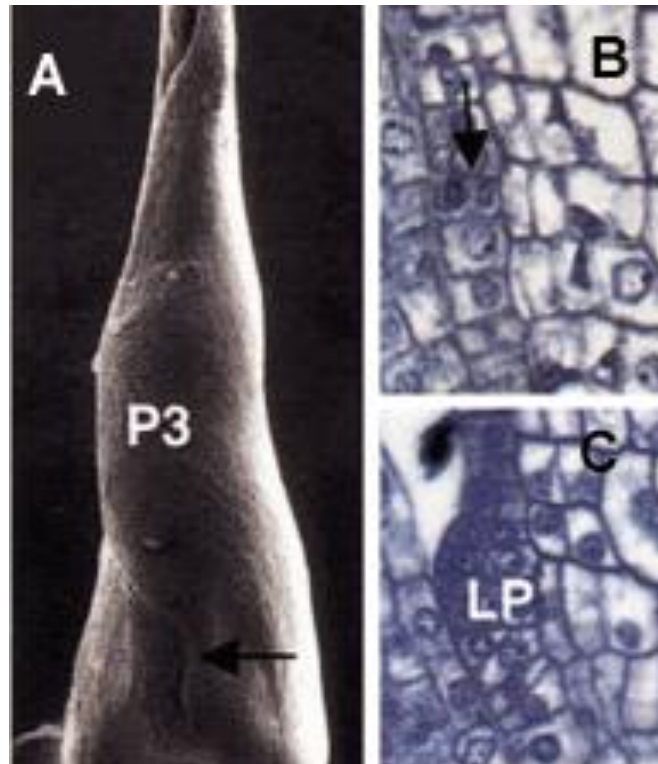


Figure 1.11 **A)** SAM enclosed within P3 leaf margins. Arrow denotes the blade – sheath boundary. **B, C)** Cross section at blade – sheath boundary showing formation of the ligule primordium (LP). (Itoh *et al.*, 2005).

Periclinal division of epidermal cells within the blade – sheath boundary gives rise to the ligule primordium, and at this stage the vascular tissue begins to form. Xylem and phloem become recognisable within the midrib, as large and small vascular bundles develop across the leaf width. It is also at this stage that stomata begin to be formed basipetally from the distal region of the leaf.

Following differentiation of the ligule primordium, the leaf blade quickly reaches its maximum length as a result of rapid elongation, at which point the leaf sheath also rapidly elongates, a process which is suppressed until leaf blade elongation has been completed. As the leaf sheath elongates, differentiated bulliform and stomatal cells are visible from the leaf apex and vascular bundles mature, to the point where the internal structures of the leaf are almost complete as the leaf emerges from the sheath of the preceding leaf. Once emerged, the leaf bends at the collar as a result of uneven elongation of the cells to give the leaf angle.

1.8 Previous Work

A limited number of studies have shown that plants displaying alterations to vein patterning and spacing can be produced, however such work has primarily been carried out using C_4 species. Fladung (1994) exposed seed of the C_4 plant *Panicum maximum* (Jacq.) to the mutagen EMS in order to isolate variants in the progeny by basis of visual inspection.

Table 1.3 Morphological characters of *P. maximum* compared with wildtype (mean \pm S.E). Adapted from Fladung (1994).

Anatomical characteristic	Genotype					
	Wild type	Midribless (<i>mbf</i>)	Large interveinal space (<i>lis1</i>)	Abnormal bundle sheath (<i>abs</i>)	High number of small veins (<i>hsv1</i>)	Variegated (<i>var1</i>)
Leaf width (4th leaf)	1.9 \pm 0.1	2.0 \pm 0.2	1.0 \pm 0.1	1.3 \pm 0.1	1.5 \pm 0.1	1.8 \pm 0.1
Interveinal distance (μm)	110 \pm 9	112 \pm 12	160 \pm 10	139 \pm 5	106 \pm 12	112 \pm 11
Number of small veins between lateral veins	4.3 \pm 0.4	6.3 \pm 0.8	5.6 \pm 0.4	5.5 \pm 1.2	6.8 \pm 1.9	4.8 \pm 1.5
Number of cells between small veins	2	2	6-7	2	2	2

Table 1.3 shows that it is possible for a chemical mutagen to induce changes in leaf structures directly involved with C₄ photosynthesis, with effects being shown in a number of different phenotypes. *P. maximum* mutants showed variation in midrib size, interveinal distance, leaf width and interveinal cell number. However, as all variants show alteration in the distribution of the midrib, small and lateral veins, it is clear from the data that, in *P. Maximum*, the establishment and arrangement of the vascular system is under highly complex genetic control, and that the alteration of one structure may have unpredictable effects on another.

While investigating the relationship between plant shape and cell division pattern, Smith *et al.* (1996) noted that the *tangled (tan-1)* mutant of maize display an altered vein distribution, with veins appearing tangled rather than uniformly distributed. Figure 1.12 shows the alteration from the typical double mesophyll cell inter-veinal space displayed in wild type maize to a much more random arrangement. This is due to alterations in longitudinal cell divisions during leaf widening as a result of the production of the inactive microtubule binding protein TAN1. However, while of potential interest relating to the production of rice with an altered vascular arrangement, it has been highlighted that the mutation affects all cells of the leaf primordium, and not specifically those of the vascular lineage, meaning that effects throughout the whole leaf can be somewhat unpredictable (Scarpella and Meijer, 2004).

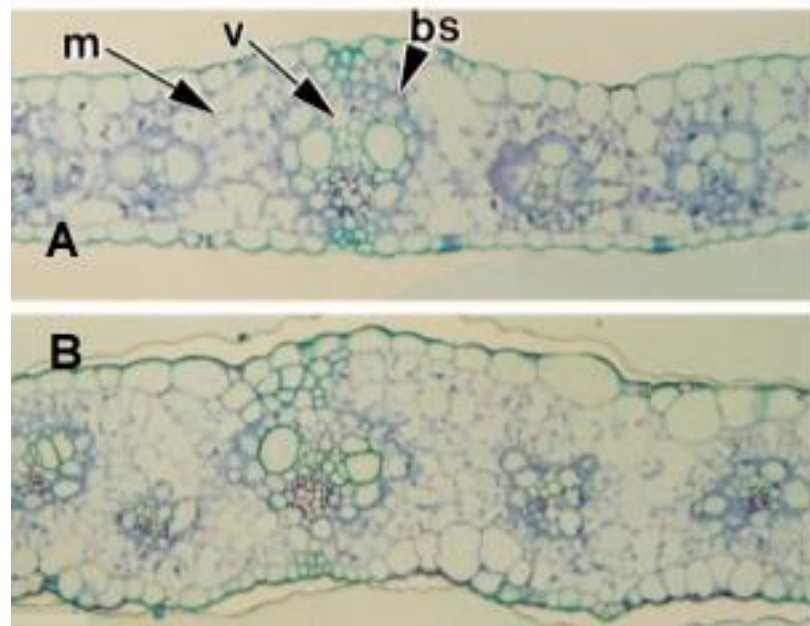


Figure 1.12 Transverse sections of **A**) wild type **B**) and *tan-1* adult maize leaves. m, mesophyll cell; v, vascular bundle; bs, bundle sheath cell. Adapted from Smith *et al.* (1996).

In monocots there are very few mutations known to produce specific vascular pattern defects (Scarpella and Meijer, 2004); however, of the few found, one has been identified in rice. Scarpella *et al.* (2003) described the *radicleless1 (ral1)* mutant as displaying a defective auxin response with an enhanced cytokinin sensitivity. This causes defects in the procambium and results in a reduced distance between veins (Figure 1.13). However, the number of large veins, and the continuity and frequency of transverse veins is reduced, the effects of which are not stated.

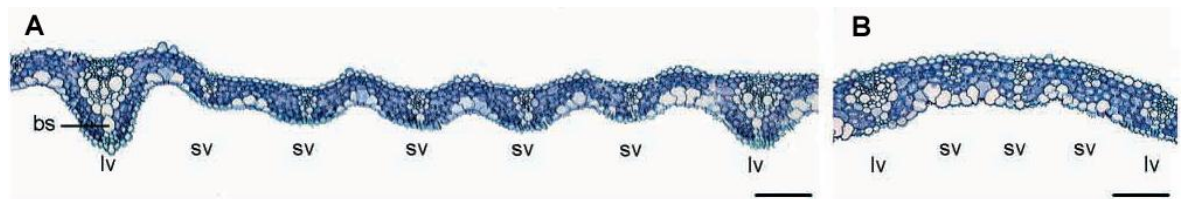


Figure 1.13 Transverse sections through **A)** wild type and **B)** *ral1* leaves adapted from Scarpella *et al.* (2003). bs, bundle sheath cell; lv, large vascular bundle; sv, small vascular bundle. Scale bars represent 50µm.

1.9 Screening for Indicators of C₄ Photosynthesis

As mentioned earlier, the creation of C₄ rice represents a huge challenge. The initial studies described in this thesis involve searching for small changes to the rice leaf anatomy which may be utilised in the creation of a typical Kranz anatomy. Rice shows great potential as a model organism for monocotyledonous plants, especially given the publication of the draft rice genome sequence (Yu *et al.*, 2002). As a species, it has a small genome compared to other cereals of approximately 430Mb and it is relatively easy to transform, both classic indicators of a model species (Hirochika *et al.*, 2004). Coupled with this, the huge economic importance of rice make it an ideal species to work with. Also, the rice genome seems particularly able to withstand large numbers of genetic lesions without proving fatal for the plant, thus allowing genome wide saturation of mutations in a relatively small number of lines (Wu *et al.*, 2005).

This study aimed to identify mutant lines of the *indica* rice IR64 which display characteristics tending towards a typical Kranz anatomy in a forward screen to identify anatomical and physiological mutations after which molecular approaches can be employed to search for the altered

genes causing the new phenotype. IR64 represents an ideal model rice line to work with as it is one of the most widely grown cultivars in South and South East Asia, owing mainly to its many positive agronomic qualities such as high yield potential, good eating quality and disease resistance. The mutant lines were produced as described in Wu *et al.* (2005) by the use of four mutational agents selected on the basis of producing a spectrum of genetic lesions. Gamma ray radiation induced mutation was used to produce lines displaying small deletions and point mutations, fast neutron radiation produced large deletions and chromosomal rearrangements, diepoxybutane (DEB) gave small deletions and point mutations and ethyl methanesulphonate (EMS) – GC to AT transitions.

Initially 60,000 mutant lines were produced, of which 38,000 mutant lines were advanced to the M₄ generation. Evaluation of some quantitative traits has taken place through repeated trials (Wu *et al.*, 2005). These are described in Table 1.4.

Table 1.4 The frequency of visible mutations of IR64 produced by different mutagens (Wu *et al.*, 2005)

Phenotypic category ^a	EMS (0.8%)		EMS (1.6%)		DEB (0.006%)		Fast neutron (33 GY)		Gamma ray (250 GY)	
	M ₂	M ₃	M ₂	M ₃	M ₂	M ₃	M ₂	M ₃	M ₂	M ₃
Albino	6.37	3.15	8.74	na	4.47	1.13	8.57	6.25	5.03	3.96
Xantha	0.41	na	1.56	na	0.60	na	0.28	0.10	0.54	0.40
Lethal	1.44	1.40	4.51	1.18	0.80	0.07	1.11	1.51	0.60	0.53
Dwarfism ^b	1.44	4.81	0.55	0.74	1.53	2.79	0.98	2.50	0.40	2.50
White leaf stripe	0.82	1.16	2.02	0.71	1.27	0.14	0.98	1.11	0.40	1.59
Pale green leaf	0.31	0.33	0.86	0.12	0.40	0.34	0.07	0.91	0.13	0.40
Pale green leaf stripe	0.31	0.39	0.37	0.12	0.07	0.14	na	0.07	na	0.07
White leaf spot	0.47	na	0.15	0.06	0.20	na	0.14	na	na	na
Broad leaf	0.10	0.49	0.06	0.12	0.07	0.07	0.07	na	0.27	0.67
Narrow leaf	0.21	2.16	0.83	0.97	0.27	0.48	0.56	2.87	0.20	2.53
Erect leaf	na	0.17	na	0.06	na	0.07	na	0.07	na	0
Chlorotic upper half	na	na	na	0.06	0.13	0.07	0.14	0	na	0.53
Dark green leaf	0.10	0.19	0.06	0.24	0.07	0.07	0.07	0.20	0.27	na
Semi-rolled leaf	0.10	0.17	0.61	0.41	0.07	0.27	0.07	0.40	0.07	0.33
Zebra	na	na	0.03	0.03	na	0.07	na	0.07	na	0.33
Chlorina	0.41	1.40	0.86	0.21	1.47	0.07	1.95	0.07	na	0.20
Spotted leaf (<i>spl</i>)	0.10	0.66	0.12	0.74	0.20	0.48	0.28	0.93	0.07	1.33
Twisted leaf	0	0	0.18	0	0.07	na	0.14	na	0.20	na
Uniculum	na	0.17	0.15	0.18	na	0.07	na	0.33	na	0.13
Reduced culm number	na	1.49	0.06	0.27	na	0.55	na	2.02	na	0.53
Increased culm number	na	0.17	0.03	0.15	na	0.14	na	0.07	na	0.13
Early heading	na	0.20	0.12	0.03	na	na	na	0.10	na	na
Late heading	na	0.49	0.12	0.77	na	na	na	0.67	na	0.26
Open hull	na	0.19	0.03	0.03	na	na	na	0.30	na	0.07
Golden hull	0	0.17	0	0	na	na	na	0.20	na	na
Purple hull	0	0.17	0	0.06	na	na	na	na	na	0.10
Broad grain	0	0.33	0	0	na	na	na	0.07	na	0.13
Awned	na	0.33	0.03	0.12	na	0.20	na	0.50	na	0.13
Low density spikelet	0.41	0.17	0.03	0.03	na	na	na	na	na	na

na = Data not available.

^a Each trait is based on observation of 750–3400 independent mutant lines.^b Dwarfism includes dwarf and semi-dwarf.

The seed used in this study was taken from plants identified in the pre-screening process as possessing either broad or narrow leaves. The rationale behind this was that lines displaying an altered leaf type such as broad or narrow leaves have undergone some obvious change in the leaf structure and may be more likely to reveal novel vein patterns than other phenotypic groups, for example the low density spikelet group (Erik Murchie, personal communication).

As suggested earlier, the typical Kranz anatomy is very complex, so it would be unlikely to find a mutant line displaying it in full. For this reason, and coupled with the need to screen as many different lines as

possible in the time available, screening was done on the basis of the most visible characteristics of C₄ photosynthesis – primarily vein spacing. By taking simple hand cut sections and visualising them under a microscope it was possible to rapidly process large numbers of mutant lines and compare them in terms of vein spacing to characterised wild type plants (Chapter 3). Those showing significant variation in vein spacing and notable morphological features were then regrown and studied at a later date to characterise the morphological variation at the cellular level (Chapter 4) and the functional consequences of these changes (Chapter 5).

Typically, the procambium can be recognised within a developing leaf primordium very shortly after initiation (Esau, 1965). These then extend toward the leaf apex so as to form the major and larger minor veins, whilst the smaller veins (initially discontinuous from the surrounding vascular tissue) form later (Nelson and Dengler, 1992). As major vein positioning is set very early in leaf development, it seems likely that this factor is under a strong genetic control, and that any alteration of venation patterning may arise as a result of mutation of these genes. Specific hypotheses to be tested were that lines within the mutant population display statistically significant variation in vein spacing and in the number of veins per mm leaf width, and that this is correlated with a significant alteration in the number of mesophyll cells making up the interveinal space.

The objectives of this study were to identify mutant lines of rice which displayed an alteration in vascular spacing and arrangement and identify the role of the mesophyll cells in determining the observed vascular anatomy. These lines were then to undergo physiological characterisation in order to determine the implications of this altered anatomy. The final aim was to assess the conserved and readily altered features of rice leaves in order to assess the implications of the potential introduction of a C₄ photosynthetic system into rice plants.

Chapter 2

METHODS

Chapter 2: METHODS

2.1 Seeds used

M₄ seeds of mutant lines of the IR64 indica rice cultivar were supplied by Hei Leung of IRRI and their production is described by Wu *et al.* (2005). Prior to dispatch from IRRI, seeds were treated with a post-harvest seed dressing to prevent fungal infection. Upon arrival at Nottingham seeds were stored in a cool, darkened room in air-tight containers. Details of the genetic background of the lines used and the reasons they were selected are given in Section 3.1.1.

2.2 Growth of plants

All stages of plant growth took place in a growth room maintained at an air temperature of 27°C with a 12/12 hour dark / light cycle. Day temperatures reached 35°C under the light source. 400W metal halide lamps (lamps Siemens, UK; bulbs Osram, Germany) were used to provide lighting. Prior to each experiment, the growth room was divided into a grid and quantum sensor (SKP 200, Skye Instruments, UK) measurements were taken to identify and minimise variation in irradiance. The position of each container of plants was altered on a daily basis to minimise the effects of uneven light distribution, with those at the edge of the room where irradiance was lowest being moved to the centre, and *vice versa*.

2.2.1 Seed germination

Seeds were thoroughly washed in distilled water to remove the post-harvest seed treatments and germinated in 60mm tissue culture dishes (Greiner Bio-One, UK) on damp filter paper in the growth room under the above conditions. Tissue culture dishes were sealed with paraffin film (Parafilm M, Alcan Packaging, UK) in order to prevent fungal contamination of the seeds and to reduce water loss.

2.2.2 Plant establishment

Previous preliminary studies had shown that rice plants grown in various potting media are prone to display significant variation in growth and rates of development, as well as displaying a greatly increased rate of seedling mortality (E. Murchie, personal communication). For this reason, plants were grown hydroponically in 20l plastic containers (pH of approximately 5.5 adjusted with 8% HCl) using a hydroponic solution adapted from Murchie *et al.*, (2005). The nutrient solution is shown in Table 2.1. Stock solutions of nutrients used in the hydroponic mixture were first prepared from the raw compounds, and were then combined to make three separate concentrated nutrient solutions. The three separate solutions were added to the 20l containers as required, but were kept separate until this point to minimise precipitation of the nutrient compounds. Concentrated solutions were created rather than simply adding the stock solutions to the containers to aid with the ease of measuring, as the amounts of some stock solutions added would be minute (as little as 0.09ml per 20l).

Table 2.1 Ingredients of the hydroponic medium. Solutions were stored separately until required in order to avoid precipitation of the minerals. All hydroponic chemicals were supplied by Fisher Scientific, UK, with the exception of $\text{MnCl}_2 \cdot 4\text{H}_2\text{O}$ and Fe-EDTA, which were supplied by Sigma-Aldrich, UK

Element Required	Compound Used	[Stock Solution] Mol	Concentrated Nutrient Solution (ml Stock solution per l)	ml concentrated nutrient solution per 20l hydroponic container
N	NH_4NO_3	4.28536	80	
P	$\text{NaH}_2\text{PO}_4 \cdot 2\text{H}_2\text{O}$	0.85571	166	
K	K_2SO_4	0.38377	312	
Mg, S	MgSO_4	1.20497	160	
Mn	$\text{MnCl}_2 \cdot 4\text{H}_2\text{O}$	0.05457	40	75
Mo, N	$(\text{NH}_4)_6\text{Mo}_7\text{O}_{24} \cdot 4\text{H}_2\text{O}$	0.00045	54	
B	H_3BO_3	0.55636	16	
Cu, S	$\text{CuSO}_4 \cdot 5\text{H}_2\text{O}$	0.00192	40	
Zn	$\text{ZnSO}_4 \cdot 7\text{H}_2\text{O}$	0.00900	20	
Ca	$\text{CaCl}_2 \cdot 6\text{H}_2\text{O}$	1.50000		8
Fe	Fe-EDTA	0.17488		8

Seeds were incubated in tissue culture dishes until they germinated and were then transferred to the hydroponic system. In order to establish seedlings in the hydroponic system, they were first transferred to a polystyrene rack floating on the hydroponic solution, suspended in an open bottomed 1.5ml microcentrifuge tube (Sarstedt, Germany) as shown in Figure 2.1. This system provides support for the young seedling whilst an established root system was produced.

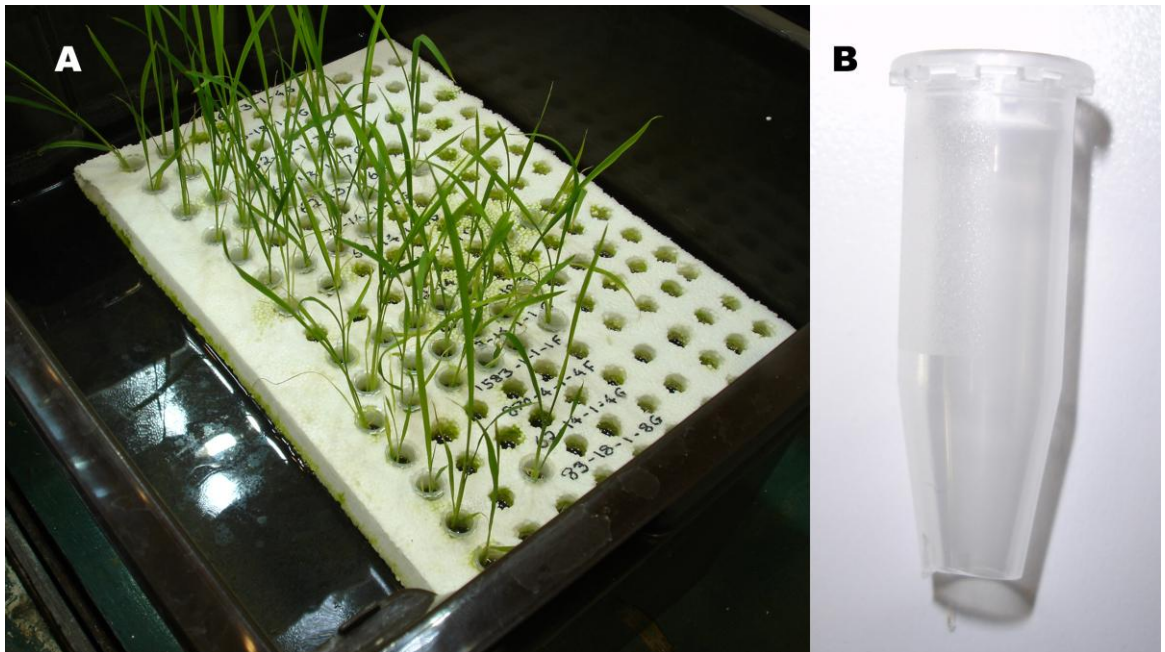


Figure 2.1 **A** Young rice seedlings floating in a polystyrene rack. **B** An open bottomed centrifuge tube with the lid and base removed used to support seedlings in the rack.

Once a sufficient root system had been established, plants were transferred to the final stage of the growth process. A sufficient root system was considered to be greater than 4cm to ensure the roots could reach the hydroponic solution.

Holes 2cm in diameter were drilled in a lightproof plastic support, and this was rested directly above the hydroponic solution (adapted from Murchie *et al.*, 2005). A small piece of foam was then wrapped around the stem of each seedling just above the root in order to hold it in place within the hole in the plastic support (Figure 2.2).



Figure 2.2 **A** Wild type and mutant plants growing in hydroponic tanks. **B** WT plant in the lightproof support supported with foam.

Each day containers were refilled to their 20l capacity to replace liquid lost. The amount of solution replaced varied according to the size of the plants.

Plants were not treated with chemical sprays; however, previous experiments indicated a slight risk to plants from red spider mite (*Tetranychus urticae*). *Phytoseiulus persimilis* (Syngenta, UK) were routinely applied as a natural predator to eliminate the red spider mites. *P. persimilis* treatment was applied at approximately 4 mites per m⁻² in

accordance with the retailer's instructions, which was sufficient to ensure that no red spider mites were observed.

2.3 Screening

2.3.1 Leaf numbering

Leaf 6 was used for all measurements. This is the sixth leaf to emerge on the primary tiller, ignoring the seed leaf. Preliminary studies identified this as a suitable leaf for measurements as it was produced relatively quickly after germination, is of a suitable width for sampling and rarely displays chlorotic lesions, unlike leaf 5, which is a likely stress effect as a result of being transplanted from tissue culture dish to hydroponic solution.

2.3.2 SPAD measurements

Upon full elongation of leaf 6, SPAD measurements were taken in the growth room using a SPAD-502 chlorophyll meter (Konica Minolta, UK). The recorded value was taken as the average of four SPAD measurements made along the leaf taking care to avoid the midrib. SPAD is a device which measures absorption of the leaf at wavelengths corresponding to chlorophyll and is referred to as a chlorophyll meter.

2.3.3 Gross morphology

Observations based upon the whole plant morphology were made, including the degree of tillering exhibited, leaf size and leaf shape. The whole plant was photographed and leaf 6 was harvested and scanned using a flatbed scanner (PCLine, UK) to provide a record of leaf area and shape.

2.3.4 Microscopy

Fresh transverse sections of rice leaf were cut by hand from the widest part of the freshly excised sixth leaf in distilled water using a sharp one-sided razor blade. The leaf was first cut across the widest part in order to create a clean edge and leaf width at this point was recorded. The cut

leaf was then held in place with the thumb of one hand and submerged in a shallow covering of distilled water. Holding a fresh one-sided razor blade in the other hand, transverse sections were then taken as thinly as possible from the cut end of the leaf, using the thumb nail as a guide but ensuring to keep the blade clear of the thumb itself. Blades were replaced regularly as contact with the water quickly caused them to tarnish.

The cut sections were then placed on a glass slide, mounted in a drop of distilled water and covered with a cover slip. Once mounted sections were examined using a light microscope at 10x magnification (Vickers Instruments, UK) and imaged using an Infinity2 digital camera (Lumenera Corporation, Canada). Images were stored as JPEG files and analyzed using the computer programme Infinity Analyze (Lumenera Corporation, Canada).

From the transverse sections the numbers of minor and major veins were counted and their arrangement was recorded. The distinction between major and minor vein was predominantly based on size, with major veins appearing significantly larger than minor veins (Figure 2.3 C). After calibration of the Infinity Analyze software using an image of a graticule, the vein spacing was measured in the region between the two major veins closest to the midrib. This region was chosen to allow direct comparison of vascular spacing in the different mutant lines as a compromise between throughput of the mutant screen and resolution. Preliminary work revealed taking measurements across the whole leaf width to be extremely time consuming, and had the full width of leaves been sampled it would not have been possible to sample as many different lines. Leaf thickness was also measured in this region, taking average measurements across bulliform cells, minor veins and major veins to give three measurements of leaf thickness.

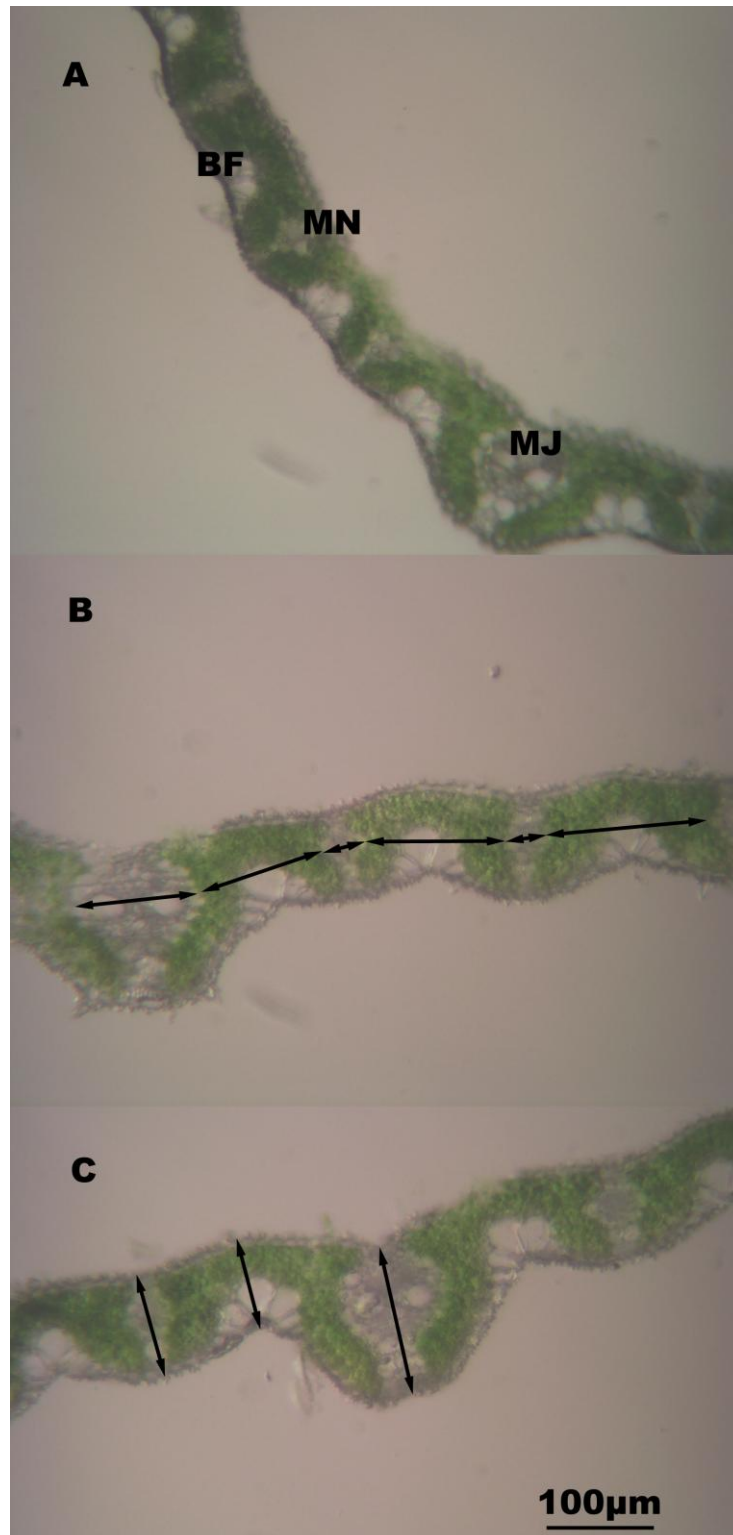


Figure 2.3 Examples of hand-cut leaf sections from the mutant screen. **A** Wild type rice leaf transverse section showing gross anatomy. BF, bulliform cells; MN, minor vascular bundle; MJ, major vascular bundle. **B** Arrows denote measurements of interveinal distance and vascular bundle size. **C** Arrows denote measurements taken of leaf thickness, at the major vascular bundle, minor vascular bundle and bulliform cells.

2.3.5 Tissue storage

Leaf samples of approximately 1cm in length were stored in 2.5% (w/v) gluteraldehyde solution (Sigma-Aldrich, UK) and kept at 4°C in microcentrifuge tubes, thus preserving the tissue for future reference.

2.4 Detailed anatomical methods

Following the identification of several interesting mutant rice lines in the screening portion of the study, it was important for them to undergo a more detailed characterisation than was permitted initially, to quantify the changes undergone in each line. This was done using a number of methods.

2.4.1 Tissue fixation, resin embedding and staining

Tissue was taken from the widest portion of the fully expanded 5th leaf of rice plants cut into strips roughly 10mm long and 5mm wide. Tissue was then fixed using 4% paraformaldehyde (Sigma-Aldrich, UK) in 100ml of phosphate buffer solution (PBS). The PBS consisted of 7.4g NaCl, 0.994g Na₂HPO₄ and 0.414g NaH₂PO₄ per l distilled water (chemicals supplied by Fisher Scientific, UK). For ease PBS was stored as a 10x concentrated solution, i.e. a 10-fold increase in the concentration of each compound, and then diluted prior to mixture with the fixative. A small quantity (0.1% w/v) of each of the detergents Triton X-100 and Tween 20 (supplied by Sigma-Aldrich, UK) was also added to the fixative in order to ensure full permeation of the fixative into the leaf tissue. Fixation was initially for a period of 30 minutes under vacuum infiltration. The fixative was then replaced with fresh fixative solution and the samples left overnight at 4°C on a rotator at 30rpm (Weiss-Gallenkamp, UK).

The following day, samples were brought back to room temperature before being washed twice in PBS for a period of 30 minutes each. The fixed tissue was then dehydrated in an ethanol series (30%, 50%, 70%,

90%, 100%, 100%) for at least 1 hour at each concentration before resin infiltration.

The resin embedding technique was adapted from personal communication with Gema Vizcay-Barrena, University of Nottingham. Tissue was embedded in TAAB Technovit 7100 (TAAB Laboratories, UK), which was prepared in accordance with the manufacturer's instructions. Leaf samples were placed into a gelatine capsule mould (TAAB Laboratories, UK), which were then filled with the resin and allowed to harden overnight. Once hardened the gelatine mould was dissolved by placing the resin capsule in warm water for several hours on a magnetic stirrer. The resin block was then attached to a plastic block using Technovit 3040 adhesive (TAAB Laboratories, UK) prior to microtome cutting using a Bright 5040 microtome (Bright Instruments, UK).

5µm thick sections were cut after careful orientation of the block to ensure that the tissue was cut perpendicular to the leaf surface. Cut sections were dried onto slides at 30°C and stained using 1% toluidine blue in 1% disodium tetraborate solution (both supplied by Sigma-Aldrich, UK) as described by Jellings and Leech (1982) for a period of 15 seconds. Stained sections were then observed at 25x magnification using a light microscope (Nikon, UK) and imaged using a Leica DFC 320 digital camera (Leica Microsystems, Germany) using the computer programme Im50 (Leica Microsystems, Germany). These images were stored as JPEG files and analyzed using Infinity Analyze as described in Section 2.3.4.

2.4.2 Leaf surface impressions

Leaf surface impressions were taken using the silicon-based impression resin Coltene President Plus Jet (Coltene Whaledent, Switzerland). Impressions were taken from the adaxial and abaxial surface of the 5th leaf at the widest point.

The two components of the resin were mixed in a Petri dish, applied smoothly to the leaf surface using a spatula and allowed to set completely before removal. Setting time was approximately 10 minutes

at room temperature. The resin impressions were then painted with a layer of clear nail varnish (Rimmel, UK), which once dry, was peeled off to reveal a replica of the leaf surface. Stomatal density was then calculated by placing the leaf impression onto a glass slide and observing it under a light microscope at 20x magnification (Nikon, UK).

The midrib was first located and positioned at the edge of the field of view. The number of stomata and the number of stomatal rows were then counted in four adjacent fields of view, starting at the midrib, and moving out to the leaf margin. Using a graticule, the area of the field of view was calculated, and the number of stomata per field of view was converted to stomatal density.

2.4.3 Cleared hand cut sections

In order to observe more detail of leaf structure than was present in the initial hand cut sections it became apparent that leaf clearing was required to enable the measurement and quantification of individual mesophyll or bundle sheath cells. This was because the highly lobed structure and very dense arrangement of the rice mesophyll cells gave a continuous green appearance whereby individual cell walls could not be easily visualised.

Sections were cut by hand as previously described and placed on a microscope slide in a drop of water. The water was then partially absorbed by tissue paper and a clearing solution of 85% lactic acid solution saturated with chloral hydrate (both supplied by Sigma-Aldrich) was added to the section (Lux *et al.*, 2005). The slide was then heated in a water bath at 70°C in a covered Petri dish for approximately 45 minutes before being removed and allowed to return to room temperature in a fume hood so as to allow dissipation of chloral hydrate fumes. The clearing solution was then removed using a pipette and the section washed several times with distilled water.

The cleared sections were then stained using 1% toluidine blue in 1% sodium tetraborate solution for 15 seconds and washed thoroughly in

distilled water. Stained sections were then viewed under a light microscope and imaged and analyzed as described in Section 2.4.1.

2.4.4 Cell separations and chloroplast counting

Cell separations were produced using a method adapted from Pyke and Leech (1987). Leaf tissue was taken from the widest section of the 5th leaf of rice mutant plants, and cut into strips approximately 1cm long. The tissue was then fixed in 4% paraformaldehyde overnight at 4°C. The fixative was removed and 0.1M NaEDTA (pH 9) added and the tissue was heated at 60°C for a minimum of 6 hours in a heating block. A reduced time of 2 hours was used for Arabidopsis samples to avoid causing complete disintegration of the tissue. Once heated, the pieces of leaf tissue were placed onto a microscope slide and mounted in the NaEDTA solution before being mechanically broken up using a pair of forceps until separation of the tissue was visible. The tissue was imaged using a light microscope with a Nomarski prism (Nikon, UK) at x40 magnification. Images were captured as described previously.

Images were analysed using the computer program Infinity Analyze (Lumenera Corporation, Canada). The software was first calibrated for measurement using an image taken of a graticule, and then cell circumference and plan area were calculated by tracing the cell outline within the software.

2.4.5 Confocal microscopy

Tissue was collected from the widest part of fully expanded 5th leaf of rice plants and cut into sections approximately 15mm in length. These were then fixed overnight in 4% paraformaldehyde (Sigma-Aldrich) at 4°C. Once fixed, tissue was treated with NaEDTA and separated cell preparations were produced as described previously. Once separated, cells were imaged using an argon laser and Leica SP2 confocal microscope (Leica Microsystems, Germany). Excitation was performed at 405nm and fluorescence was detected at 510-525nm and 645-655 to show autofluorescence of the cell wall and of chlorophyll respectively

(Furbank *et al.*, 2009). Images were captured using the computer program Leica Confocal Software (Leica Microsystems, Germany).

2.5 Gas exchange and chlorophyll fluorescence

2.5.1 Response to ambient CO₂ concentration

The effects of alteration in atmospheric [CO₂] on rice leaf photosynthesis were measured using a LiCor 6400 XT Infra Red Gas Analyser (IRGA) (LiCor Biosciences, USA). Photosynthetically active radiation (PAR) was supplied at 1000 μmol m⁻². Blue light was provided at 10% of the total PAR so as to avoid stomatal closure. Block temperature within the LiCor unit was set at 30°C, and the flow rate of gases was set to 500 μm s⁻¹. The chamber fan was set at "Fast". CO₂ was initially supplied at near atmospheric concentration (400 μmol) before a reduction to low levels and then rapid elevation. This was done to minimise stomatal responses during the period of measurement. Measurements were taken in controlled environment room conditions to avoid causing effects by moving the plants to the laboratory. Leaves were exposed to each CO₂ concentration for a minimum period of one minute and maximum of three minutes to allow the rate of photosynthesis to stabilise. Reference and analysis gases from the IRGA were equilibrated (matched) prior to the recording being taken.

Measurements were taken from the widest section of the fully expanded 6th leaf of rice plants, and the width of the leaf was noted so that the area of leaf contained within the cuvette could be calculated at a later date. More details of the measurement principles and the atmospheric CO₂ concentrations used are provided in Section 5.2.1.

2.5.2 Response to PPFD in terms of gas exchange and chlorophyll fluorescence

Measurements were taken from the widest section of the fully expanded 6th leaf of rice plants, and the width of the leaf was noted so

that the area of leaf contained within the cuvette could be calculated. Before photosynthetic measurements commenced, the leaves were first dark adapted. This was done by carefully wrapping catering foil (Terinex, UK) around the leaf to be sampled to exclude light for a period of one hour. Measurements of gas exchange and leaf fluorescence were taken simultaneously using a LiCor 6400 XT (LiCor Biosciences, USA) with leaf chamber fluorometer attachment. Plants were dark adapted to ensure that chlorophyll molecules within photosystem II are fully oxidised.

After one hour had elapsed, the leaf was then placed into the cuvette of the LiCor 6400 XT and the foil cover slipped off the leaf. The leaf was kept in darkness for a further 15 minutes within the cuvette. CO₂ was supplied to the leaf at 400µmol (near atmospheric levels), block temperature was set at 30°C, and the flow rate of gases was set to 500µm s⁻¹. The chamber fan was set at "Fast".

Following dark adaption, the leaf was exposed to a strong pulse of light to allow calculation of quantum yield, before the leaf was exposed to a range of PPFD (Table 5.2). Blue light was provided at 10%. Measurements were taken in controlled environment room conditions to avoid causing effects by moving the plants to the laboratory. Leaves were exposed to each PPFD for a minimum period of one minute and maximum of three minutes in order to allow photosynthetic rates to stabilise. Reference and analysis gasses from the IRGA were equilibrated (matched) prior to the recording being taken. More details of the measurement principles and light intensities used are provided in Section 5.2.2.

2.6 Statistical analysis

Statistical analyses were primarily carried out using analysis of variance (ANOVA) using the computer program GenStat 12th Edition (VSN International, UK). In order to check for normality of distribution of the raw data, residual plots were created and the assumption of normality

was retained if the plot appeared scattered, with no relationship between fitted values and residuals. Significance of the difference between means of groups was reported by the *F* statistic of the ANOVA test, and P values of <0.05 were taken as significant.

Where the assumption of normality failed, GenStat was used to perform regression analysis to compare mutant lines with plants of the wild type and produce values for mean and standard error of the difference between means (SED). Dunnett's test was then performed using this data to compare each mutant line with the wild type.

Chapter 3
SCREENING THE MUTANT
POPULATION

Chapter 3: SCREENING THE MUTANT POPULATION

3.1 Introduction

The dicotyledonous plant *Arabidopsis thaliana* has provided a useful model for plant biologists. This arose as a model species as there is a large collection of accumulated mutants and genes can be isolated with relative ease, especially since the publication of its genome sequence (The Arabidopsis Genome Initiative, 2000). However, the majority of our staple foods come from cereals – i.e. monocotyledonous plants, which are significantly different in many aspects of development, and for this reason a monocotyledonous model plant is highly desirable (Izawa and Shimamoto, 1996).

As the first crop species with a complete genome sequence (Yu *et al.*, 2002), rice represents an ideal model plant. Much work has been done to determine gene function by producing rice mutants using T-DNA and transposons as these allow relatively easy identification of the target gene, while chemical and irradiation based mutagenesis have typically been avoided (Wu *et al.* 2005). The reason for this is that mutations are not physically tagged, meaning that once a phenotype has been identified the effort to isolate the affecting gene(s) has traditionally been considerable. However high throughput genotyping such as the use of oligonucleotide arrays has greatly helped to improve the detection of polymorphisms (Winzeler *et al.*, 2003) and helped to improve the viability of using deletion mutants in a forward genetic screen. Chemical or irradiation based mutagenesis can provide genome-wide saturation of mutations using a relatively small population (Henikoff and Comai, 2003). Further to this, the relative ease with which deletion mutants can be produced allowed for greater availability of seed, allowing the possibility of a high throughput forward screen. It is in this context that the forward screen described in this chapter was conceived.

3.1.1 Genetic background of lines used

Mutant lines of the IR64 indica rice cultivar were supplied by Hei Leung of IRRI. IR64 was chosen for the creation of an *indica* rice mutant collection as it is the most widely grown cultivar in Southeast Asia and possesses a large number of agronomic traits including high yield potential and durable disease resistance, along with a large degree of adaptability (Wu *et al.*, 2005). Mutagenesis was performed using four mutational agents; gamma ray radiation, fast neutron radiation, diepoxybutane (DEB) and ethyl methanesulphonate (EMS). Details of the mutagens can be found in Section 1.7. As outlined in Chapter 1, the mutant collection numbered approximately 60,000 lines which were pre-screened at IRRI. Of the entire mutant collection, lines displaying pale, broad or narrow leaves were selected to work with. The reason for this was that lines displaying an obvious alteration to leaf structure may be more likely to reveal novel leaf cellular morphologies than other classes of mutant lines, such as the low density spikelet group, or those producing broad grain.

When referring to the mutants, numbers are used to represent the plant number of each generation used to produce the seed, while a letter is used as a suffix to denote the mutagen used in its production. The letter D represents DEB, G for gamma ray, F for fast neutron and E for EMS. For example, the line 233-7-1-1D is seed from plant 1 of the M₃ family, which in turn is seed from plant 1 of the M₂ family, which was taken from a plant designated to be number 233 of the M₁ family produced by DEB mutagenesis.

3.1.2 Anatomical traits related to C₄ photosynthesis

As previously mentioned, single celled C₄ photosynthetic systems have been identified in plant species such as *Borszczowia aralocaspica* (Voznesenskaya *et al.*, 2001); however, these are associated with the survival of plants grown under extreme photorespiratory pressures, rather than the high productivity displayed by crops, which utilise a traditional Kranz-type anatomy (von Caemmerer, 2003).

The primary adaptations seen in a leaf displaying Kranz anatomy are an increased vein density, increased level of contact between the mesophyll and bundle sheath cells, with few mesophyll cells present between adjacent vascular bundles, and an increase in the number of bundle sheath chloroplasts, which are centrifugally positioned away from the vascular bundle (Leegood *et al.*, 2000). It was suggested by Sage (2004) that general anatomical preconditioning such as the reduction of interveinal distance was one of the earliest phases in the evolution of the C₄ photosynthetic system. As vascular arrangement appears to be one of the key determinants in the viability of a C₄ system, this characteristic was used as a focus of the screening process.

3.2 Methodology

The production and growth conditions of the plants up to sampling date are discussed in detail in Chapter 2. Specific methodologies related to the screening of the mutant population are described below.

3.2.1 Vein distribution

Transverse sections of the rice leaves were hand cut from the widest section of the 6th leaf of each plant and the width of the leaf at this point was recorded. The leaf sections were observed using a light microscope at 10x magnification and veins were categorised as minor, major or the midrib (Figure 3.2). This information was stored in a schematic diagram (Figure 3.4) in order to investigate the relative positions of veins in the wild type rice plants and observe whether there was variation in vascular patterning between the different mutant lines.

3.2.2 Vein spacing and size

Transverse sections were taken from the 6th leaf of rice plants at the widest point. These were imaged under a light microscope at 20x magnification using the software program Infinity Capture (Lumenera

Corporation, Canada). The software program Infinity Analyze (Lumenera Corporation, Canada) was then calibrated using a graticule and measurements of the interveinal distance were taken. In order to quantify relative changes in interveinal distance in the different regions of the leaf, the spacing between adjacent minor veins, adjacent major veins and adjacent minor and major veins was measured.

3.2.3 Leaf thickness

Leaf thickness was also measured using transverse sections of the 6th leaf of rice plants imaged and analysed using Infinity Capture and Infinity Analyze. As the surface of the rice leaf undulates according to which structures are directly present under the surface (Figure 3.2), three separate measurement of leaf thickness were taken. These were the thickness at the bulliform cells, thickness at the minor vein and thickness at the major vein. Thickness at the midrib was not measured as the sectioning process often resulted in the midrib collapsing and reliable data could not be obtained.

3.3 Leaf morphology of rice

Transverse sectioning of the rice leaves reveals four primary types of tissue – the vascular tissue, chlorenchyma, bulliform cells and epidermis; of these the vascular tissue and chlorenchyma are of particular interest to this study (Figure 3.2).

The vascular bundles can be categorised into three distinct types, the midrib, major veins and minor veins (Figure 3.1, 3.2). The distinction between each group is essentially one of size, with the midrib typically being the largest vascular bundle by far, then the major and minor veins which are in turn smaller than the midrib. In wild type leaves the midrib is present in the centre of the leaf, and a pattern of minor and major veins parallel to the midrib can be observed extending towards both leaf margins (Figure 3.3).

In wild type rice plants, the relative pattern of minor and major veins is mostly symmetrical about the midrib and well conserved with deviation away from this pattern generally only observed at the leaf margins. Typically two minor veins are present adjacent to and on either side of the midrib, after which the first major vein may be observed (Figure 3.3). There then follows a repeating pattern of four minor veins between each major vein until the final major vein is reached close to the leaf margin, after which a varying number of minor veins may be observed before reaching the leaf margin.

The chlorenchyma cells are defined as parenchyma cells containing chloroplasts, and make up part of the mesophyll of the leaves. Chlorenchyma cells are the primary sites of photosynthesis. In rice, the chlorenchyma cells are small compared to other grass species, approximately half the size of those in wheat, and are extensively lobed in the transverse orientation. Chlorenchyma cells have a length to width ratio of approximately 2:1 and are orientated so that the long axis of the cell is perpendicular to the vascular tissue. When observed transversally, they are present in rows between the vascular bundles and are somewhat densely packed, with few visible airspaces. The bulliform cells are present at the adaxial side of the leaf, interrupting the rows of chlorenchyma cells between each pair of veins. This leaf morphology was also described by Hoshikawa (1989).



Figure 3.1 Untreated hand cut transverse section of a wild type rice plant showing the full width of a wild type leaf imaged at 10x magnification. Note the midrib in this image is fractured. This is common in hand cut sections due to its large size and inflexible structure; and for this reason measurements of midrib size were not routinely taken.



Figure 3.2 Enlarged transverse section of the wild type leaf showing the region between two adjacent major veins. **MR**, midrib; **MJ**, major vascular bundle; **MN**, minor vascular bundle; **B**, bulliform cells; **E**, epidermis; **C**, chlorenchyma.

Table 3.1 Anatomical characteristics of the 5th leaf of wild type IR64.

N=5

Characteristic	Mean	Standard Error
Leaf thickness (major vein, μm)	133.5	8.77
Leaf thickness (minor vein, μm)	87.3	4.79
Leaf thickness (bulliform cells, μm)	84.8	1.75
Total veins per unit width (veins mm^{-1})	4.8	0.35
Minor vein width (μm)	41.8	1.79
Major vein width (μm)	104.5	8.77
Interveinal distance (adjacent minor veins, μm)	152.3	7.67
Interveinal distance (adjacent major and minor veins, μm)	146.0	13.82
Interveinal distance (adjacent major veins, μm)	850.6	43.96

**Figure 3.3** Typical wild type plant produced under hydroponic growth conditions.

3.4 Screening the mutant population

3.4.1 Vein arrangement

By observing the organisation of veins on either side of the midrib, it is easy to see the large variation in vein development present in rice leaves within the population of mutant lines, and this may help to identify interesting mutant lines. In wild type plants, the leaves are broadly symmetrical with approximately the same number of minor and major veins present on either side of the midrib arranged in almost identical patterns. However, vein arrangement within the mutant population shows great diversity, both between and within individual mutant lines. A schematic diagram of this variation is given in Figure 3.4, and displaying the vein arrangement data in this way helps to make quick visual comparisons of wild type and mutant lines.

Whilst wild type plants typically produce two minor veins directly adjacent to the midrib before any major veins are observed, some mutant lines such as 64-14-1-2G and 83-18-1-1G produce major veins adjacent to the midrib and the intervening minor veins are absent. Some lines possessed an altered ratio of minor to major veins. For example 3315-1-1-3F produced only two major veins for every 15 minor veins, whereas the wildtype plants possessed a ratio of 13:3. Many lines displayed an increased asymmetry of vascular patterning about the midrib and in some mutant lines the midrib was not located in the centre of the leaf.

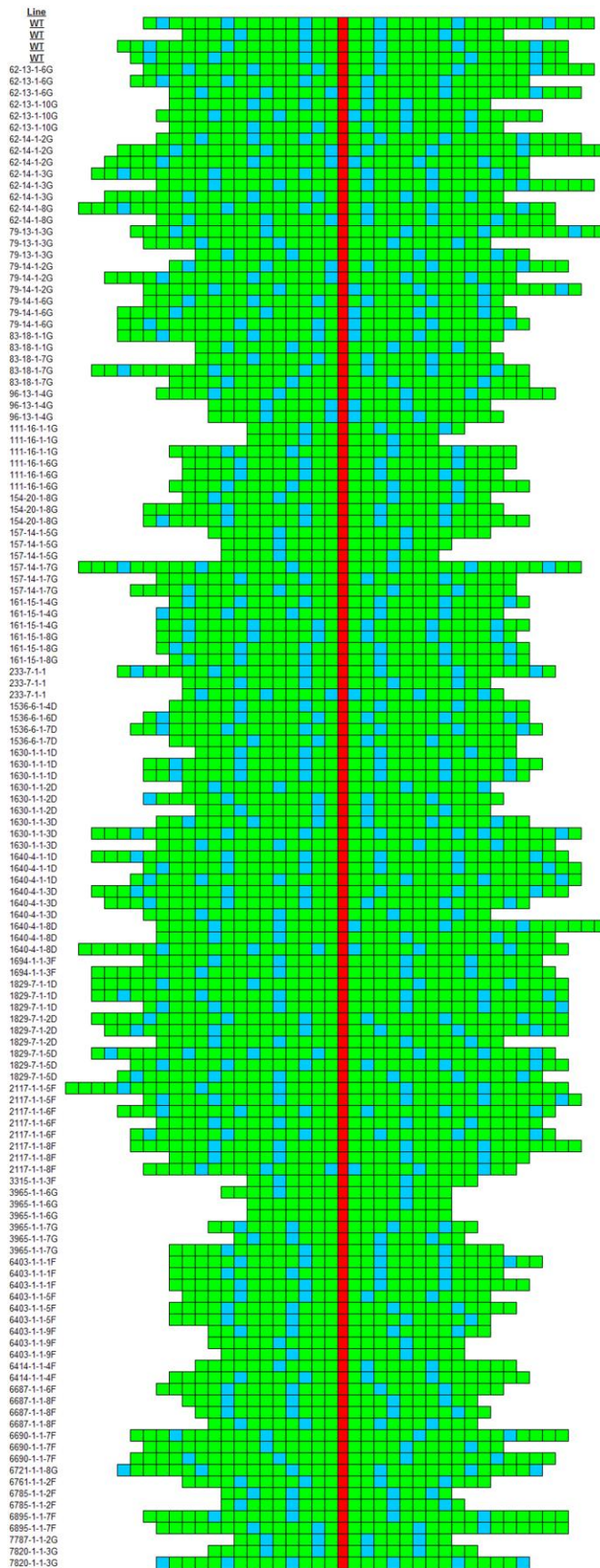


Figure 3.4 Diagram of the vein arrangement in the leaf 6 of wild type and mutant rice lines. Red squares denote the midrib, blue squares the major veins and green squares the minor veins.

There was also variation in the total number of veins present in the leaf (Figure 3.5). This ranged from an average of approximately 17 veins in the line 7787-1-1-2G to 36 veins in the 1829-7-1-1D line. The wild type mean was 29. Analysis of variance (ANOVA) showed that the data was normally distributed and that six lines produced a significantly reduced number of veins in leaf 6 when compared with the wild type plants. 111-16-6G produced a mean number of 26.3 veins ($P<0.05$), 157-14-1-5G produced a mean total of 19.0 veins per leaf ($P<0.01$) and 3965-1-1-6G produced a mean number of 17.0 veins per leaf ($P<0.01$). The sister line of 3965-1-1-6G, 3965-1-1-7G also displayed a significantly reduced vein number with 21.67 ($P<0.05$), along with the lines 6403-1-1-9F and 6761-1-1-7F with 20.3 and 22.3 veins per leaf respectively ($P<0.01$ and $P<0.05$). No lines displayed a total veins per leaf six that was significantly greater than the value demonstrated by the wild type plants.

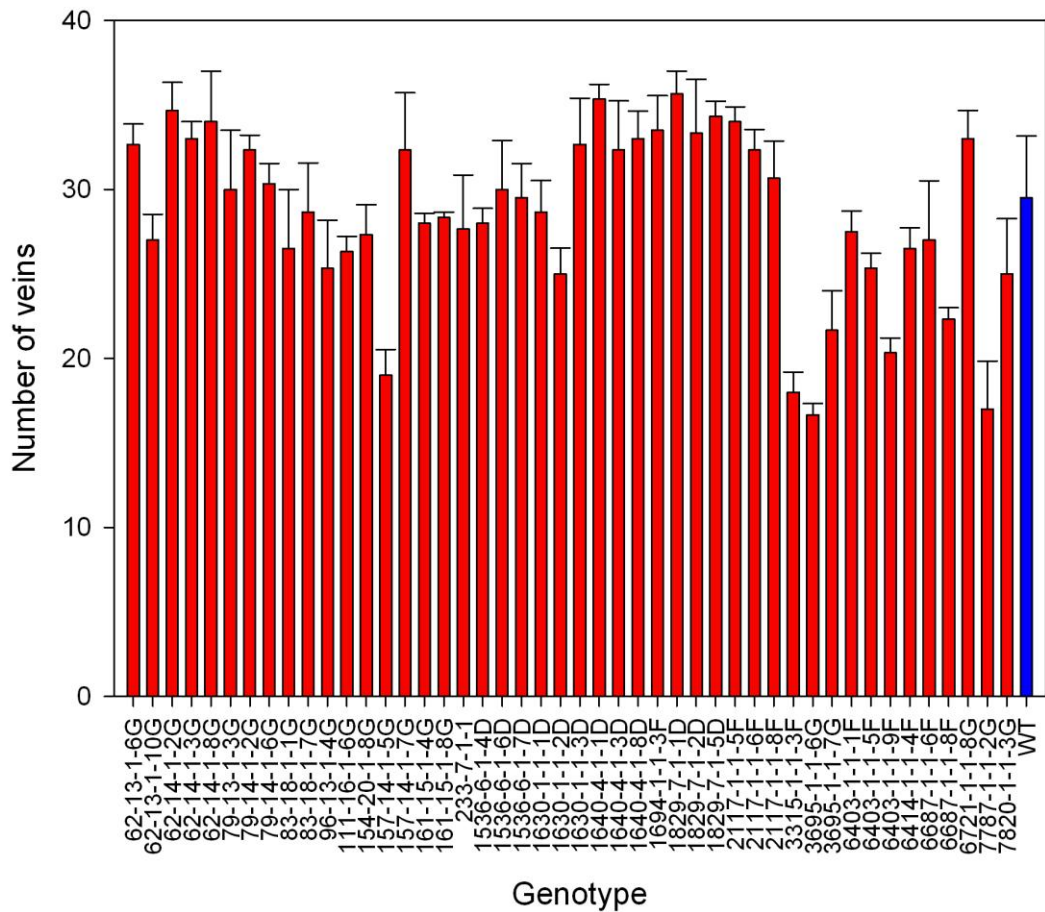


Figure 3.5 Mean total number of veins present in transverse sections of the widest part of leaf 6 in rice plants. Bars denote single standard error of the mean ($n > 3$). Plants of the wild type are shown in blue.

Leaf width also showed variation (Figure 3.6), ranging from an average of 3mm in 3965-1-1-6G to 8mm in 1536-6-1-6D, compared to a wild type mean of 6.5mm. When analysed using ANOVA, a total of nine lines displayed a significant reduction in the mean width of leaf 6. It is worth noting that all six of the lines identified as producing a significantly reduced total number of veins in the leaf 6 also had significantly narrower leaves than wild type plants (see Table 3.2 for summary).

A further five mutant lines also produced a significantly narrower sixth leaf than the wild type IR64 plants with no significant reduction in total vein number. However it is perhaps unsurprising that a number of lines would produce leaves which are significantly narrower than the wild type given that mutant lines were pre-selected for this study on the basis of altered leaf shape (see Section 3.1.1).

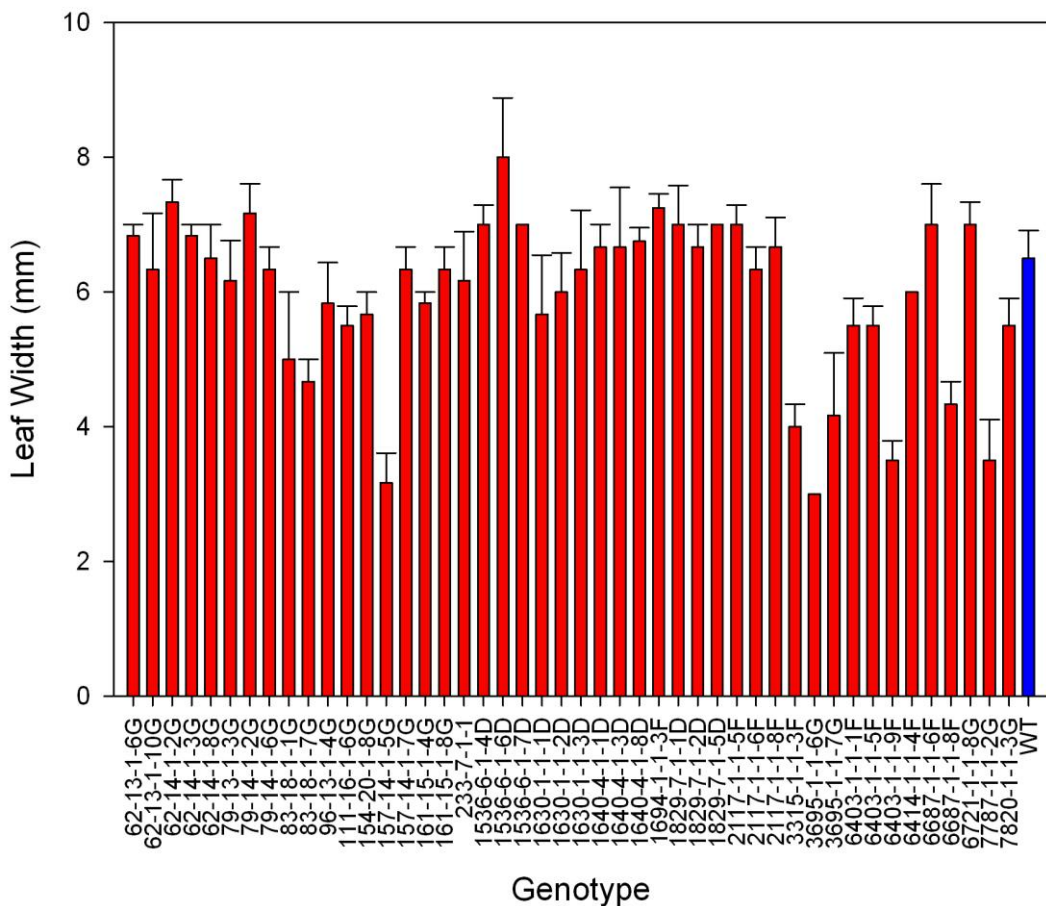


Figure 3.6 Mean width of leaf 6 of rice plants at the widest part of the leaf. Bars denote single standard error of the mean ($n > 3$). Plants of the wild type are shown in blue.

Table 3.2 Summary of mutant lines possessing a significantly reduced mean total number of veins and / or a significantly reduced mean width in leaf 6 compared with wild type IR64 plants ($n>3$). NS denotes no significance.

Line	Mean number of veins	Significance	Mean leaf width (mm)	Significance	Both width and vein number significant
Wild type	29.0	N/A	6.5	N/A	N/A
83-18-1-7G	28.7	NS	4.7	$P<0.01$	No
111-16-1-6G	26.3	$P<0.05$	5.5	$P<0.05$	Yes
157-14-1-5G	19.0	$P<0.01$	3.2	$P<0.001$	Yes
3965-1-1-6G	16.7	$P<0.01$	3.0	$P<0.001$	Yes
3965-1-1-7G	21.7	$P<0.05$	4.2	$P<0.05$	Yes
6403-1-1-1F	27.5	NS	5.5	$P<0.05$	No
6403-1-1-5F	25.3	NS	5.5	$P<0.05$	No
6403-1-1-9F	20.3	$P<0.01$	3.5	$P<0.001$	Yes
6687-1-1-8F	22.3	$P<0.05$	4.3	$P<0.01$	Yes

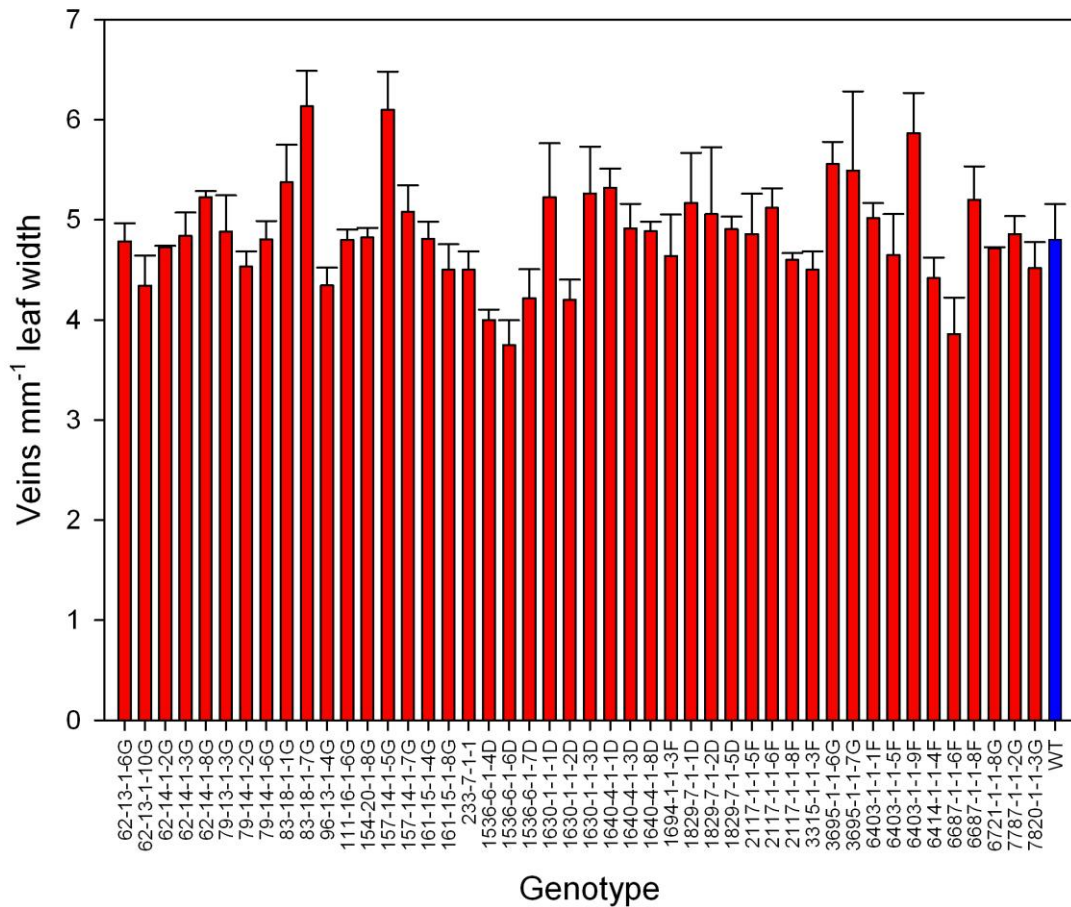
3.4.2 Veins mm⁻¹ leaf width

Figure 3.7 Mean number of veins mm⁻¹ leaf width in leaf 6 of rice plants. Bars denote single standard error of the mean (n>3). Plants of the wild type are shown in blue.

Variation in both leaf width and the total number of veins present were used to calculate total vein density in leaf 6, expressed as veins mm⁻¹ leaf width (Figure 3.7). Total vein density varied from 3.75±0.24 veins mm⁻¹ leaf width in the mutant line 1536-6-1-6D to 6.1±0.38 veins mm⁻¹ in mutant 157-14-1-5G, compared to a density of 4.8±0.3 veins mm⁻¹ in wild type plants. However, although variation in total vein density was observed, it was not large enough to prove statistically significant. This is reflected by the fact that a strong correlation between the total number of veins observed and leaf width was calculated ($R^2=0.76$) (Figure 3.8).

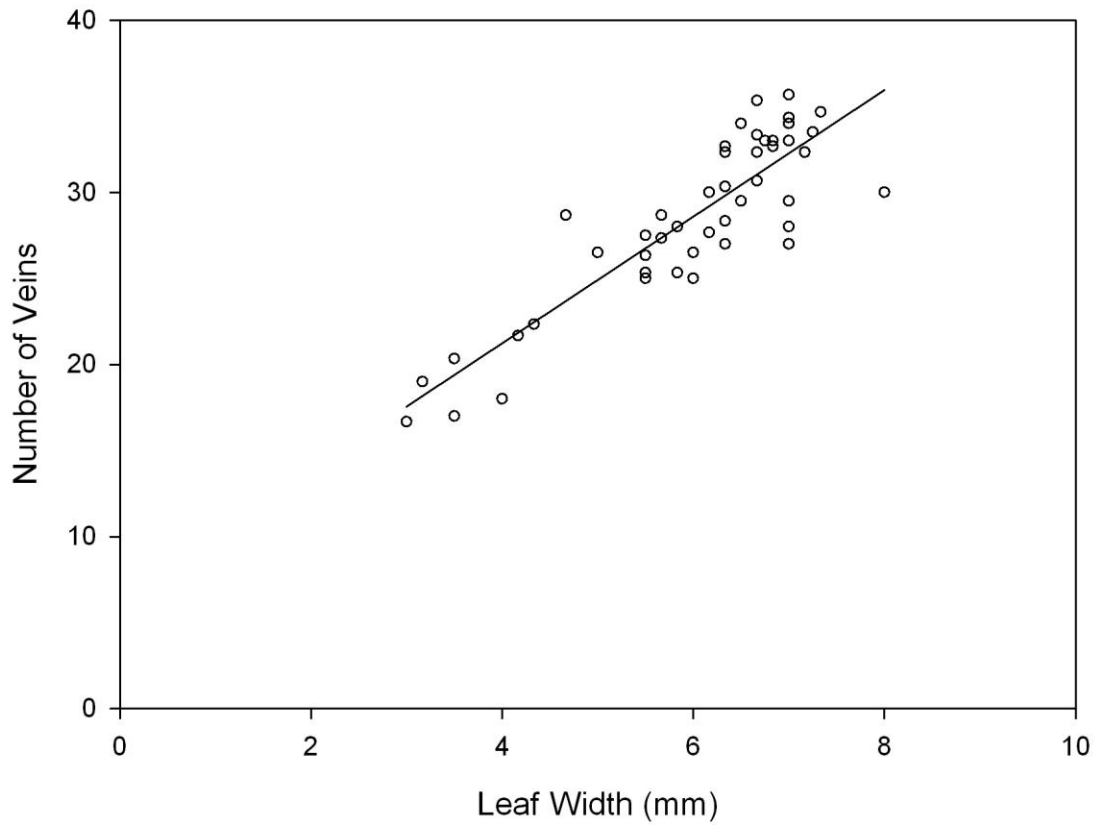


Figure 3.8 Relationship between the mean width of leaf 6 of rice plants at the widest point and the number of veins present.

The strong correlation between the total number of veins present in leaf 6 and its width, coupled with the fact that all lines displaying an altered number of veins also possessed an altered leaf width suggests that vein number mm^{-1} is predominantly a function of leaf width.

3.4.3 Vein spacing

As outlined previously, one of the features of a C₄ leaf is that there is a very small number of cells between adjacent veins. Preliminary work showed that it was not possible to section the leaves to visualise individual mesophyll cells in a way that was quick and viable as part of a high throughput screening regime. For this reason, distance between adjacent veins was measured as an indicator of vein density.

As distinct classes of veins are present within the leaf (Figure 3.2), the measurements of interveinal distance were divided into different classes, i.e. the distance between adjacent minor and major veins, the distance between adjacent minor veins, and the distance between adjacent major veins, in order to produce a greater understanding of how the veins were arranged within the leaf.

No mutant lines were found to show a significantly altered distance between neighbouring major veins compared to wild type IR64 rice plants. Figure 3.9 shows that, although there was inter-genotypic variation, there was also large intra-genotypic variation. ANOVA tests were conducted to compare the mean interveinal distance between adjacent major veins for each mutant line with the wild type. None of these gave P values <0.05, a possible explanation for which is the intra-genotypic variation. This large variation caused an increase in standard error values (see standard error bars shown in Figure 3.9) and impacts on the ability to show statistically significant results.

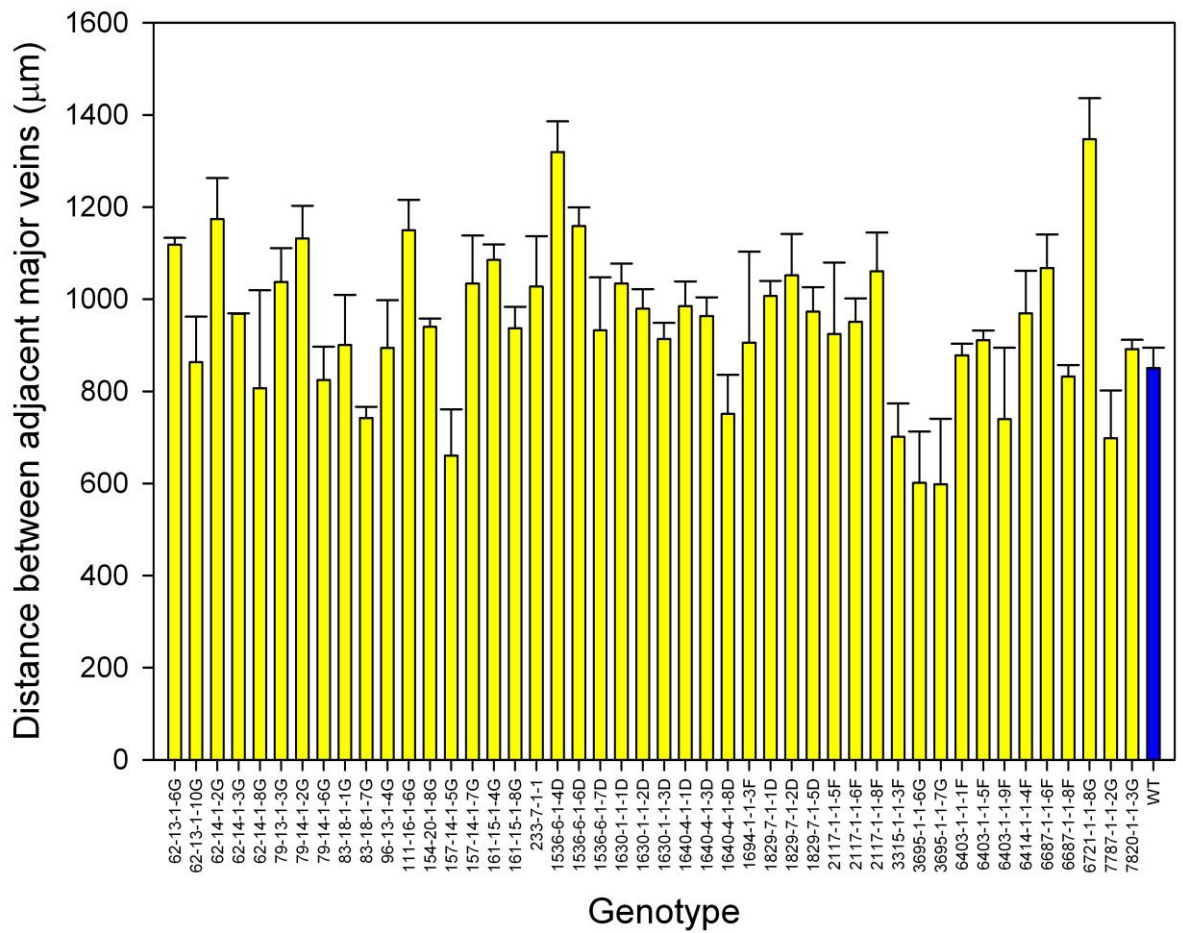


Figure 3.9 Average distance between neighbouring major veins in the leaf 6 of rice. Bars denote standard error of the mean ($n>3$). Plants of the wild type are shown in blue.

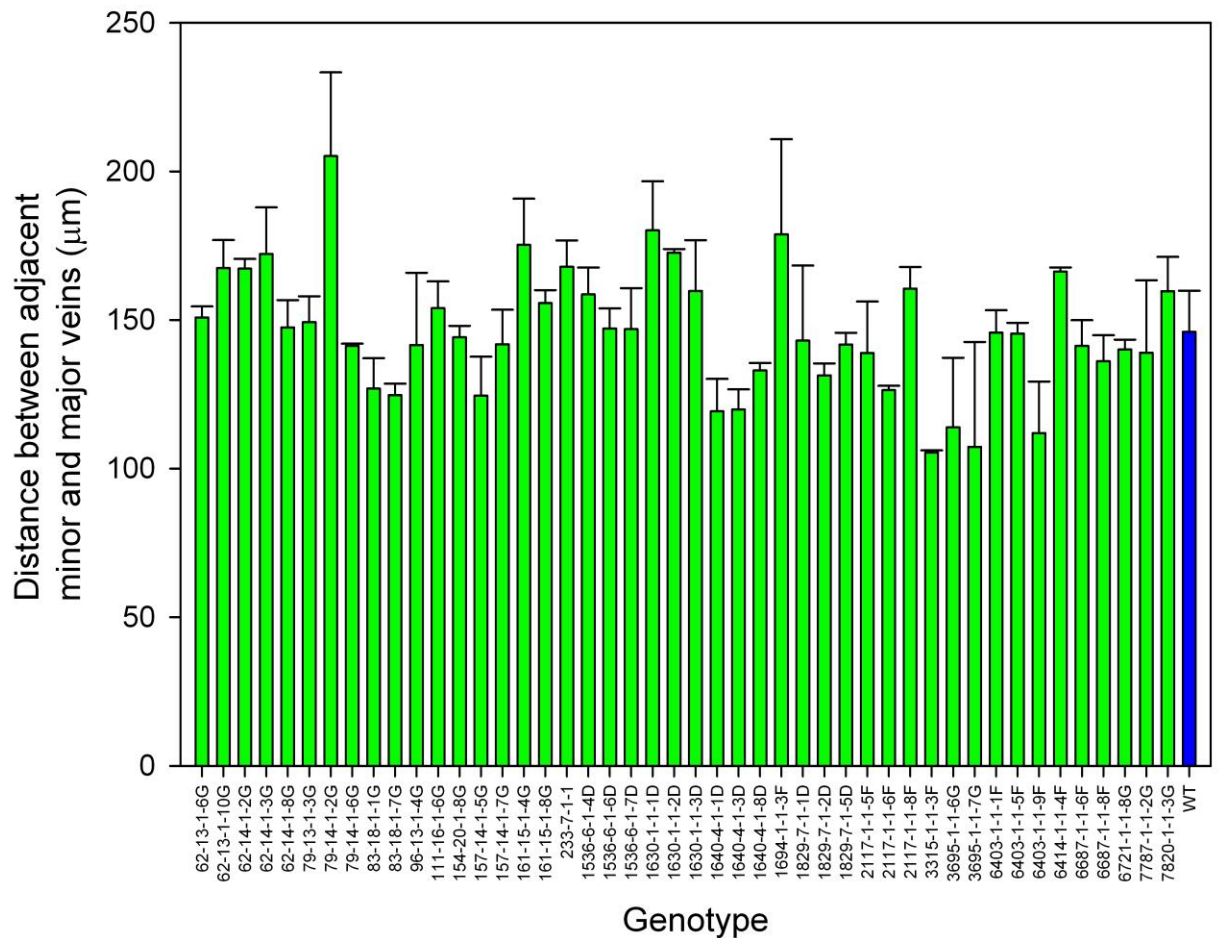


Figure 3.10 Average distance between adjacent minor and major veins in the leaf 6 of rice. Bars denote standard error of the mean ($n>3$). Plants of the wild type are shown in blue.

When analysed using ANOVA, none of the mutant lines displayed a significantly altered mean distance between adjacent minor and major veins compared with wild type IR64 plants (Figure 3.10). The line 3315-1-1-3F displayed the smallest minor to major distance with $105.4\mu\text{m}$ compared to a wild type mean of $146.0\mu\text{m}$. The largest interveinal distance was $205.1\mu\text{m}$ demonstrated by the line 79-14-1-2G.

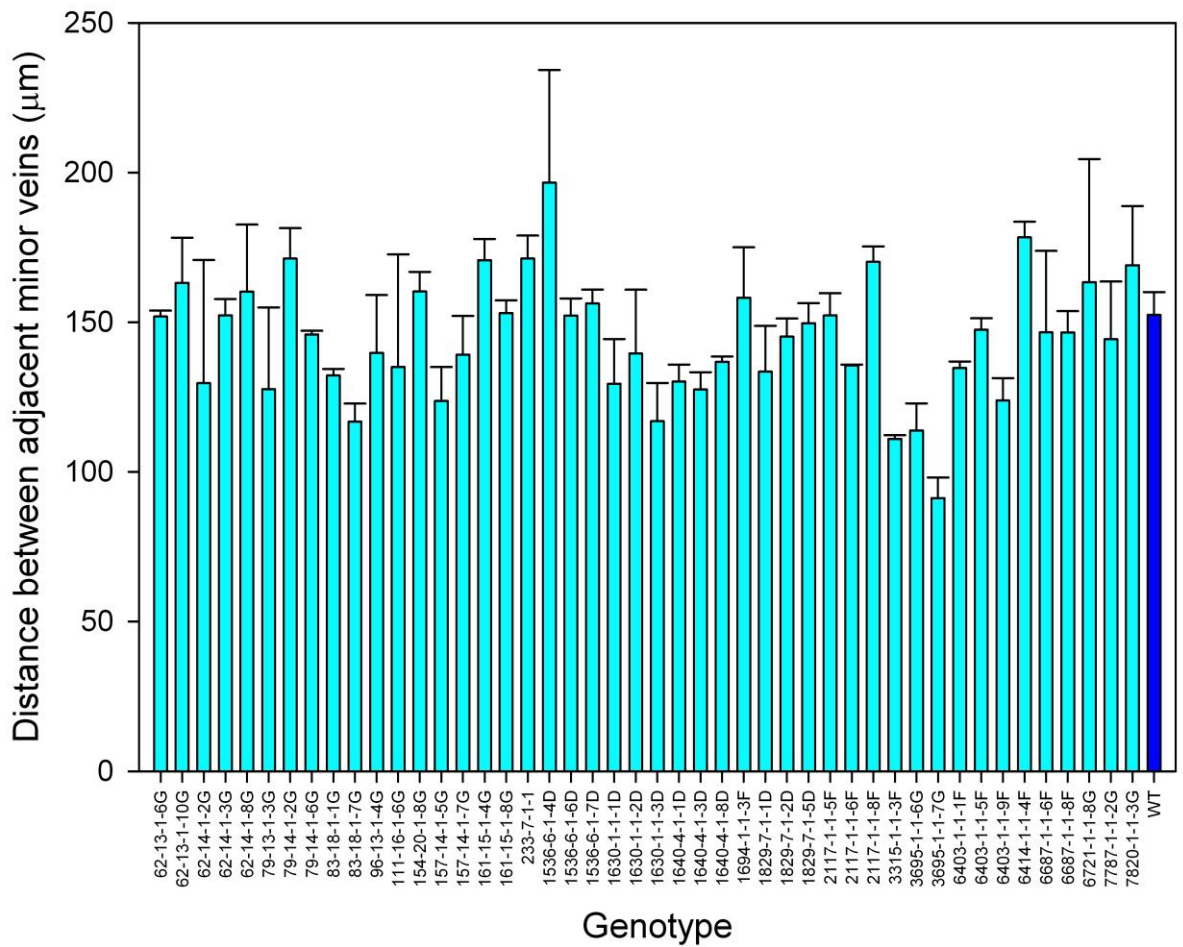


Figure 3.11 Average distance between adjacent minor veins in the leaf 6 of rice. Bars denote standard error of the mean ($n>3$). Plants of the wild type are shown in dark blue.

Figure 3.11 shows that there was extensive variation in terms of average spacing between two adjacent minor veins. Three lines have been shown to exhibit a significantly altered vein spacing - 83-18-7G ($P<0.05$), 3965-1-1-6G ($P<0.05$) and 3965-1-1-7G ($P<0.01$). Significance was shown using ANOVA tests comparing the mean distance between adjacent veins for each line against the mean distance demonstrated by wild type plants.

3.4.4 Vein Size

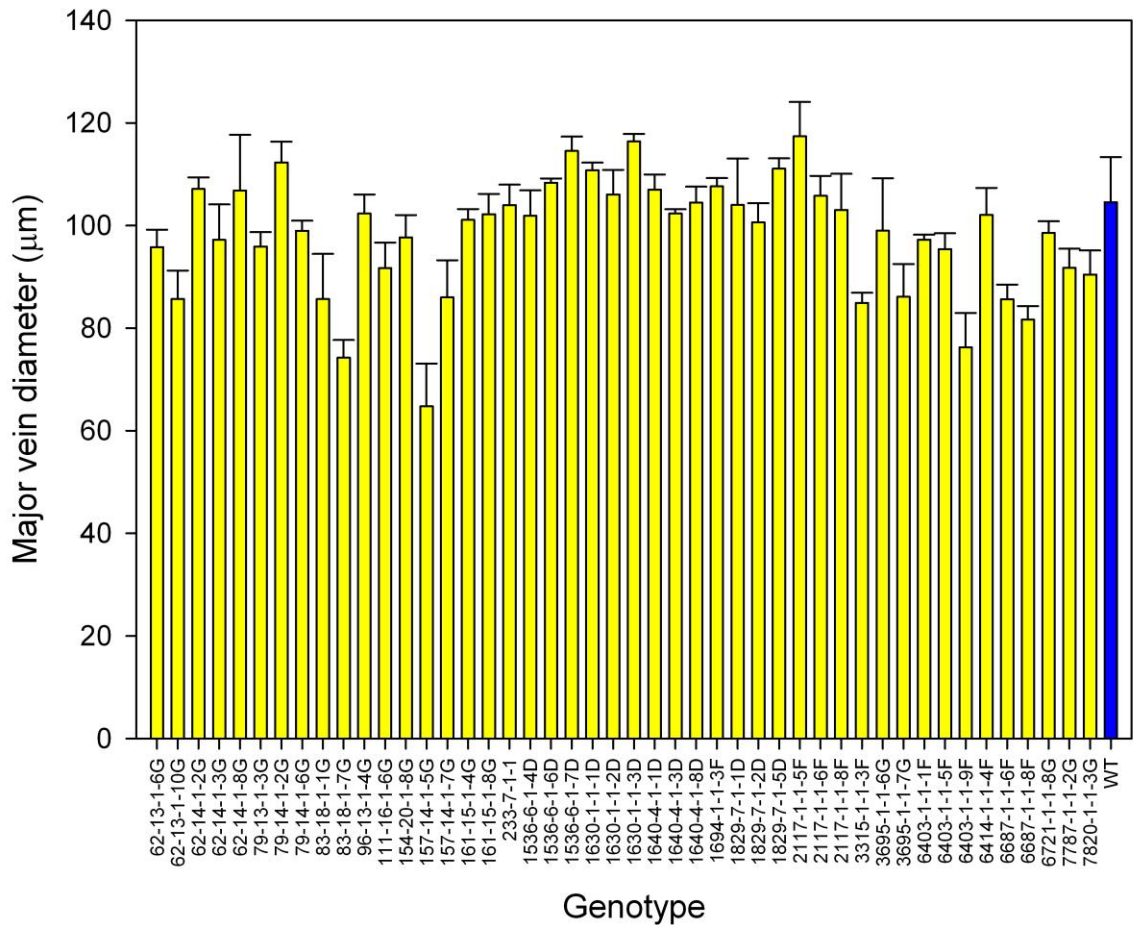


Figure 3.12 Mean major vein diameter as observed in transverse sections of leaf 6 of rice plants. Bars denote standard error of the mean ($n>3$). Plants of the wild type are shown in blue.

No significant variation between the size of the major veins displayed by the mutant lines and the wild type IR64 plants was observed (Figure 3.12). There was a large range of values observed, with the line 157-14-1-5G producing the smallest major veins with a mean diameter of $64.8\mu\text{m}$, and 2117-1-1-5F the largest at $117.4\mu\text{m}$ diameter. The wild type IR64 mean was $104.6\mu\text{m}$. Whilst ANOVA testing showed there was a significant difference between those lines displaying the largest and smallest major veins ($P<0.05$), this was of little importance as the aim of the screen was to identify those lines which are significantly altered compared to wild type plants.

In contrast much greater variation was observed in minor vein diameter (Figure 3.13). Again, intra-genotypic variation was large providing some very large standard errors (62-14-1-2G, 96-13-1-4G, 6271-1-1-8G). However, ANOVA showed that 83-18-1-7G produced narrower minor veins than the wild plants whilst 3965-1-1-6G produced minor veins that were statistically significantly wider ($P < 0.05$).

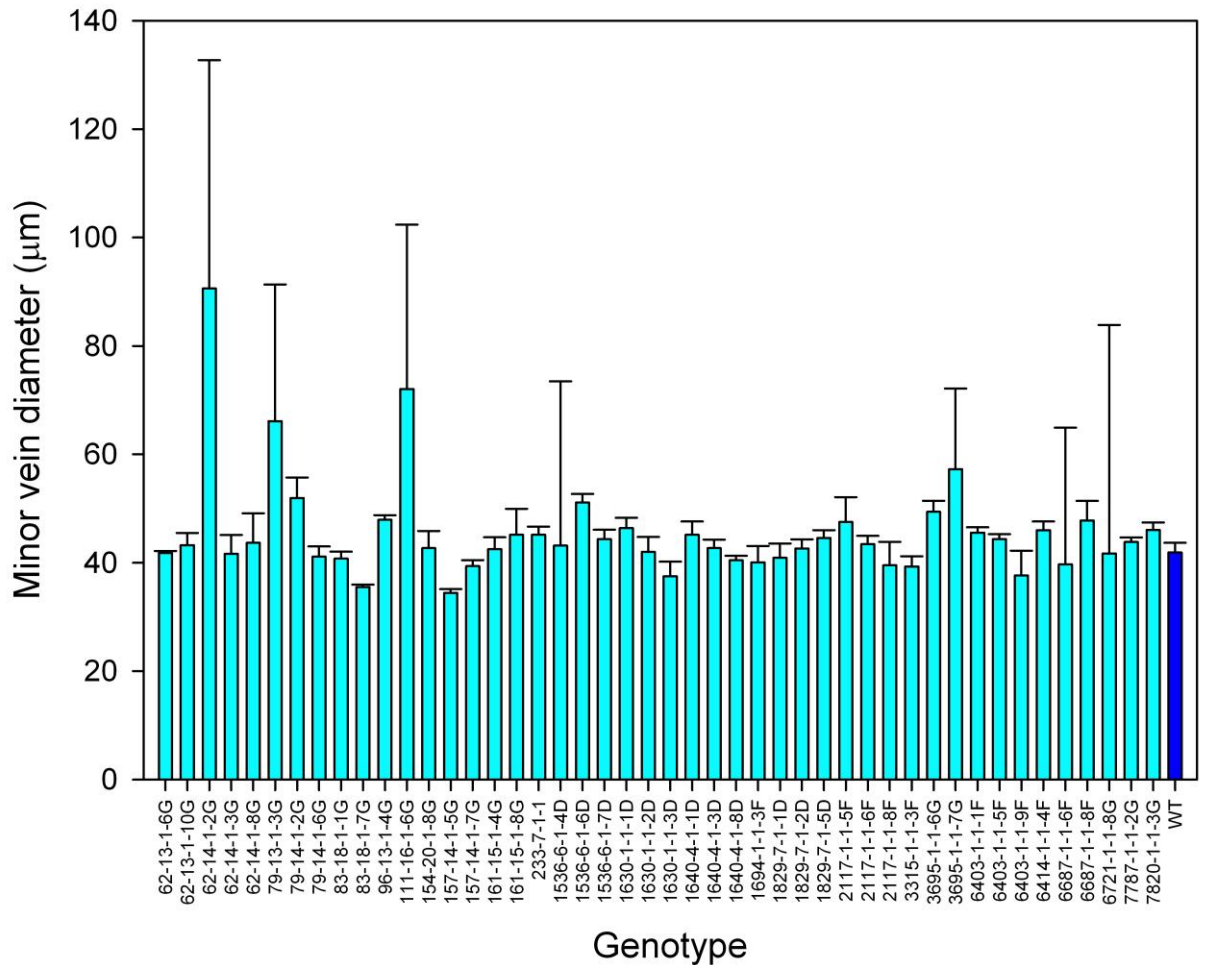


Figure 3.13 Mean minor vein diameter as observed in transverse sections of leaf 6 of rice plants. Bars denote standard error of the mean ($n > 3$). Plants of the wild type are shown in dark blue.

3.4.5 Leaf thickness

Although not primarily related to C_4 photosynthesis, leaf thickness was also measured to give a greater understanding of the impact of alterations in mesophyll thickness and vein size. As the rice leaf does not have a level surface (Figure 3.2), measurements of leaf thickness were taken in different distinct regions of the leaf, i.e. major veins, minor veins and across the bulliform cells.

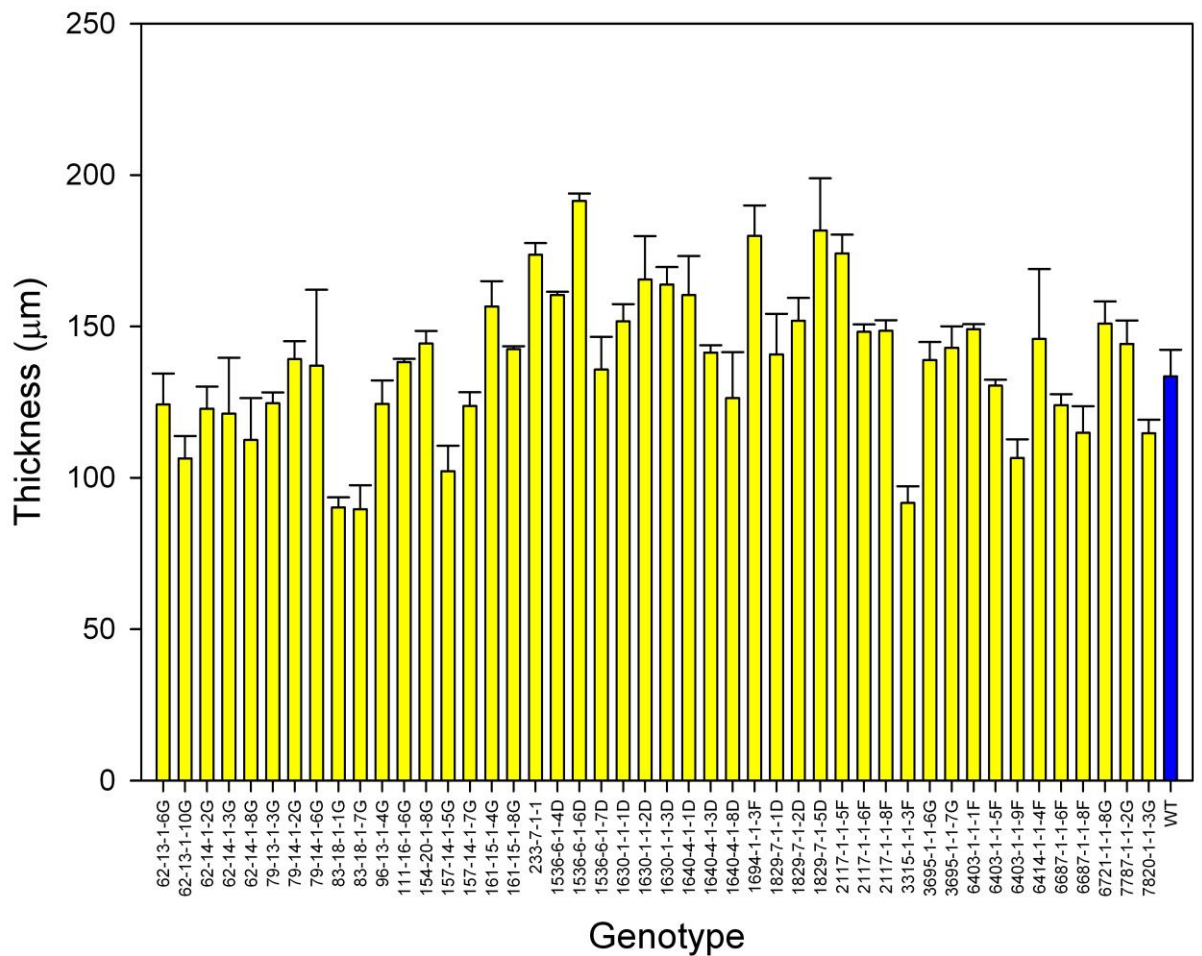


Figure 3.14 Leaf thickness at major veins. Bars denote standard error of the mean ($n > 3$). Plants of the wild type are shown in blue.

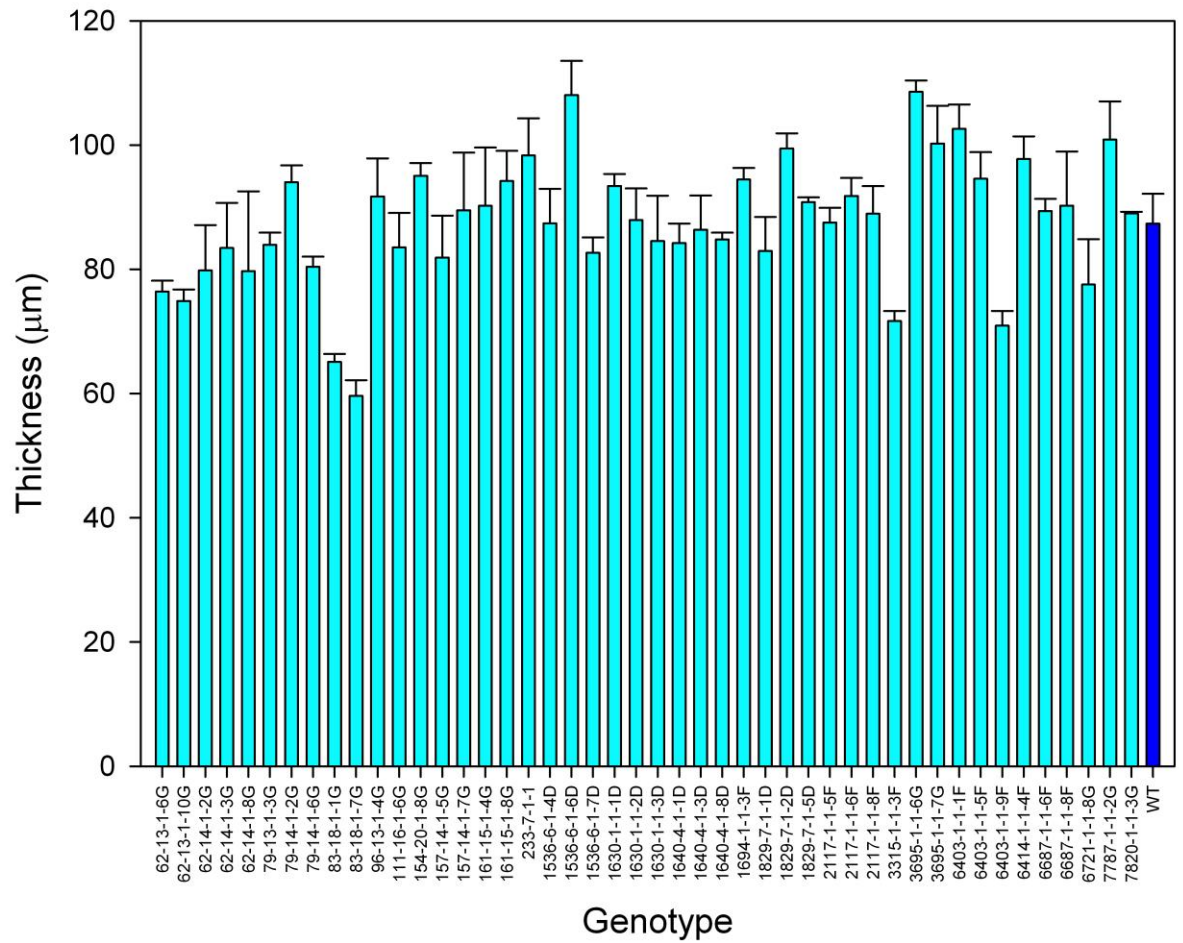


Figure 3.15 Leaf thickness at minor veins. Bars denote standard error of the mean ($n > 3$). Plants of the wild type are shown in dark blue.

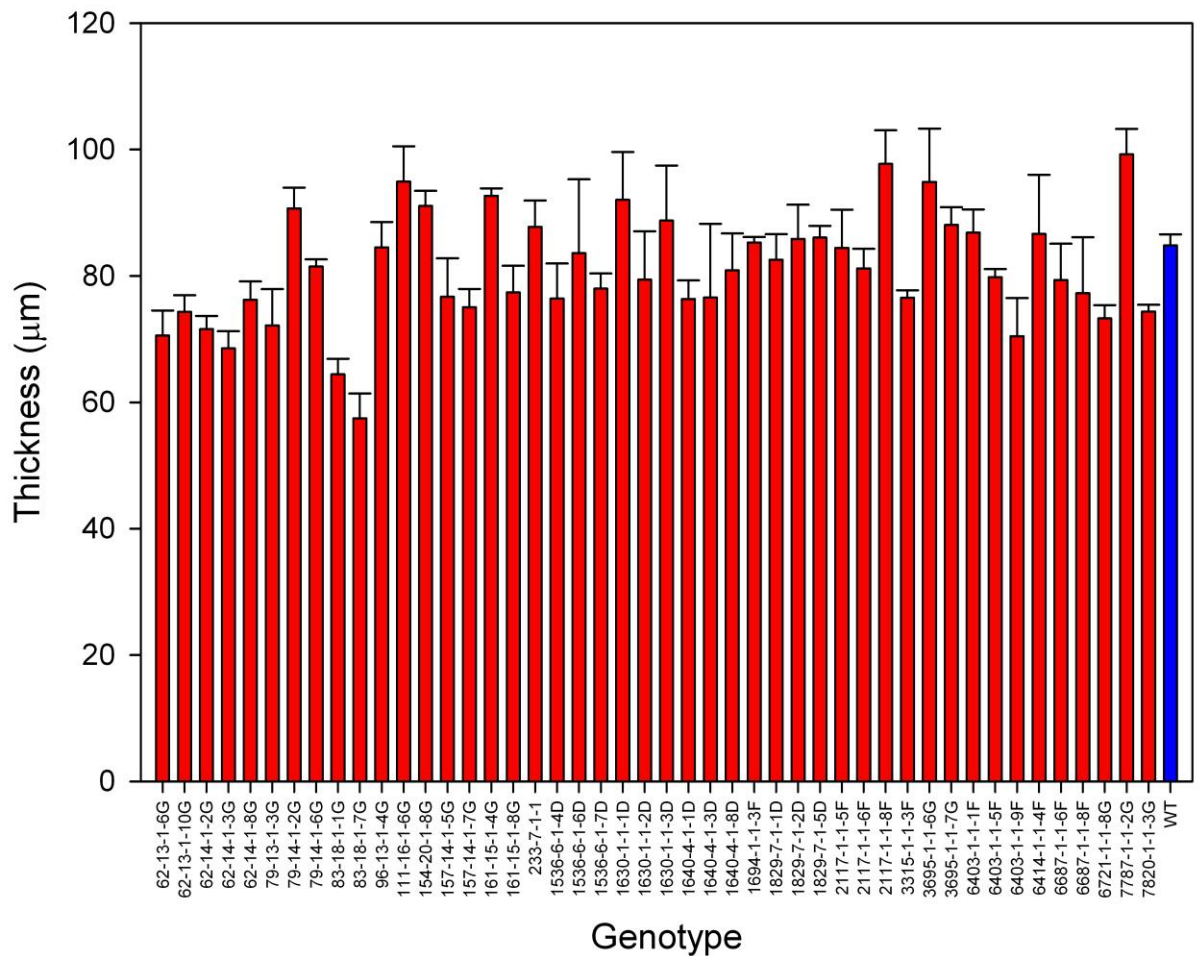


Figure 3.16 Leaf thickness at the position of the bulliform cells. Bars denote standard error of the mean ($n > 3$). Plants of the wild type are shown in blue.

There is little significant variation in leaf thickness, with the exception of three lines - 83-18-1-7G (minor vein thickness, $P < 0.05$, Figure 3.15), 233-7-1-1D (major vein thickness, $P < 0.01$, Figure 3.14) and 7820-1-1-3G (bulliform cell thickness, $P < 0.05$, Figure 3.16). It is worth noting that whilst variation is clearly present between mutant lines and wild type plants, large variation within individual mutant lines reduces the statistical significance of this data.

3.5 Altered leaf morphology mutants

Individual mutant lines showing the greatest consistent variation in leaf morphology compared to the wild type were retained for further study. These individual lines were renamed as *altered leaf morphology (alm)* mutants, and are categorised as *alm1* – *alm7*. ANOVA tests were used to compare data for each individual parameter (minor vein thickness, major to major vein distance etc.) for each line with those of the wild type, and lines showing significant differences were classed as being of interest. Further to this, a small number of lines were chosen on the basis of being anatomically interesting in that they displayed characteristics which are generally not seen in wild type plants, even though these characteristics may not be quantifiable (such as an altered gross morphology) or shown to be statistically significant.

The following sections describe the general leaf morphology displayed by the *alm* lines taken from the fresh sections used in the screening process. Subsequent Chapters will characterise these lines physiologically and anatomically in greater detail.

3.5.1 *alm1* (83-18-1-7G)

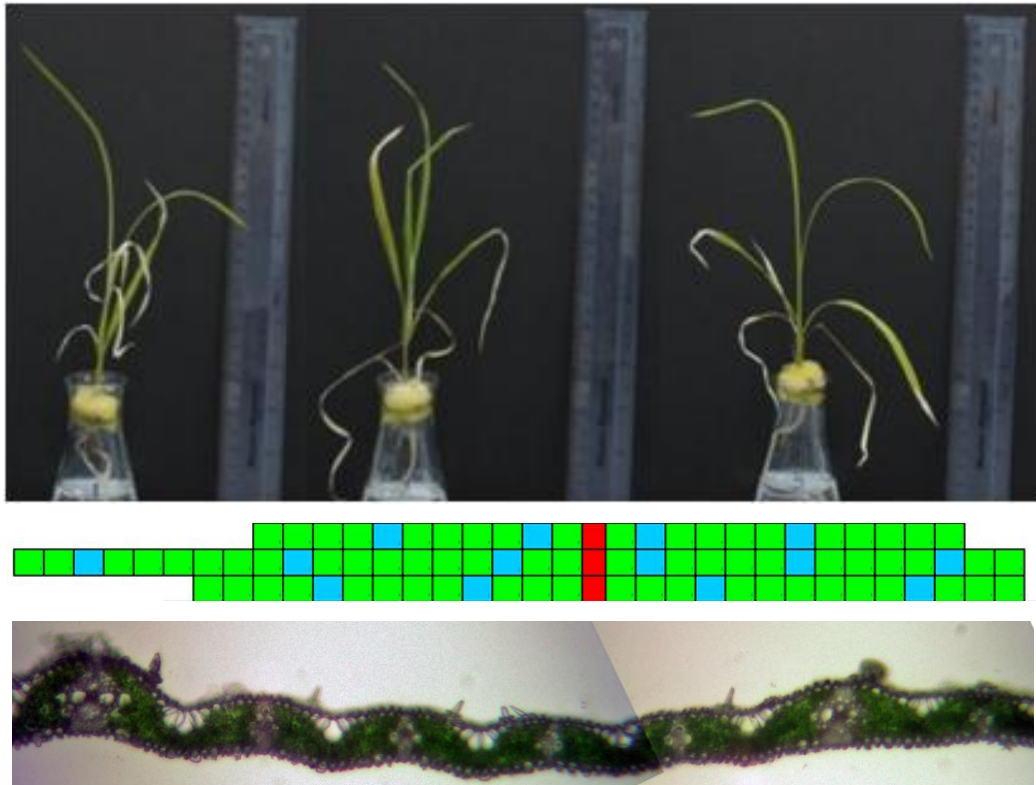


Figure 3.17 Plants of the *alm1* mutant line of rice, schematic map of vein arrangement and corresponding leaf section taken from the fully expanded leaf 6. In the vein map, red squares denote the midrib, blue the major veins and green the minor veins.

The *alm1* line demonstrates several features that make it of significant interest. The first is that the average distance between each minor vein was $116.8\mu\text{m}$ compared to $152.4\mu\text{m}$ for wild type plants ($P < 0.05$). Secondly the minor veins were significantly narrower ($P < 0.05$) than the wild type plants, with a value of $35.5\mu\text{m}$ compared with $41.9\mu\text{m}$. Finally, the general morphology of the plants tended to be greatly altered, with leaves tending to be spiky in appearance (Figure 3.17) and possessing an erratic vein distribution with vein patterning showing very little symmetry around the midrib.

3.5.2 *alm2* (111-16-1-1G)

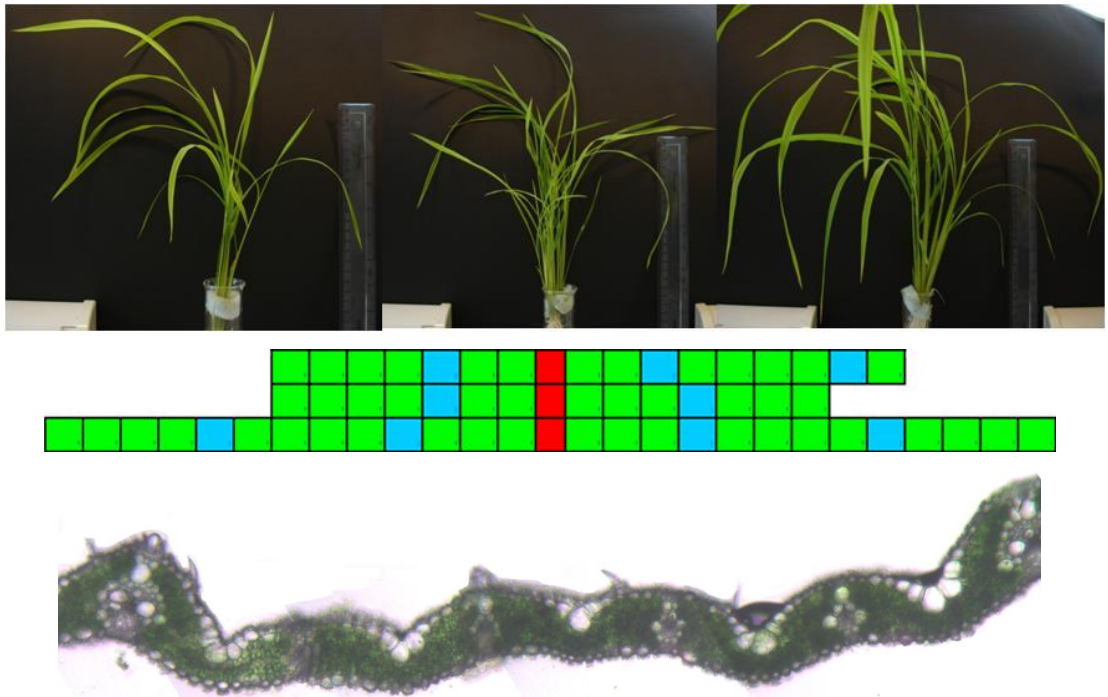


Figure 3.18 Plants of the *alm2* line, along with the relevant section of the vein map for those plants, showing that the leaves display a rough symmetry in vein distribution about the midrib (red denotes the midrib, green a minor vein and blue a major vein). The leaf section shows no major alterations to microscopic anatomy.

Whilst plants of the *alm2* line showed no significant changes in mean values for vein size or spacing, the line was of interest due to the fact that the midrib of the leaf tended to be visibly off-centre. This caused a 'bunching' effect of veins to one side, whilst the other remained relatively well spaced. For this reason, it was believed that it would be useful to accurately visualise and quantify the changes occurring in the 'bunched' portion of the leaf and investigate the effect of this on the plant. The whole plant photographs in Figure 3.18 show that the plants visually appear much healthier than those of other mutant lines.

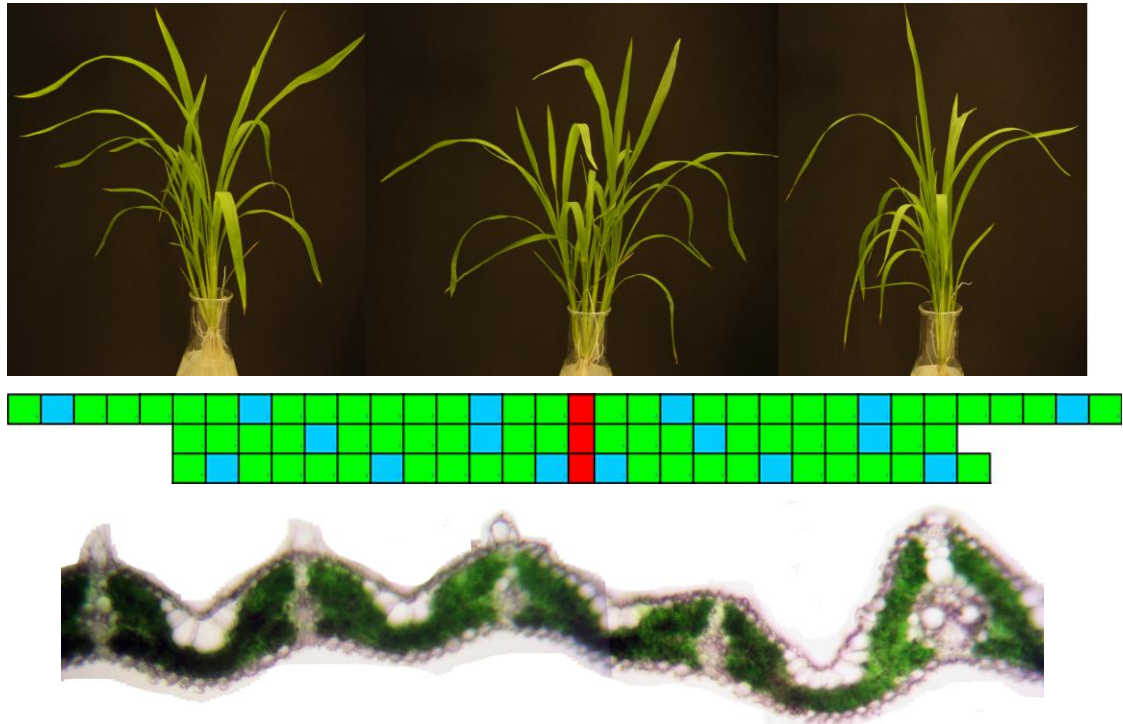
3.5.3 *alm3* (233-7-1-1D)

Figure 3.19 Plants of the *alm3* mutant line of rice, schematic map of vein arrangement and corresponding leaf section taken from the fully expanded leaf 6. In the vein map, red squares denote the midrib, blue the major veins and green the minor veins.

Plants of the *alm3* line demonstrated a significantly ($P < 0.01$) increased thickness at the major vein ($P < 0.01$, $173.7\mu\text{m}$) compared to those of the wild type IR64 ($133.5\mu\text{m}$). Other than this, the gross morphology remained largely unchanged.

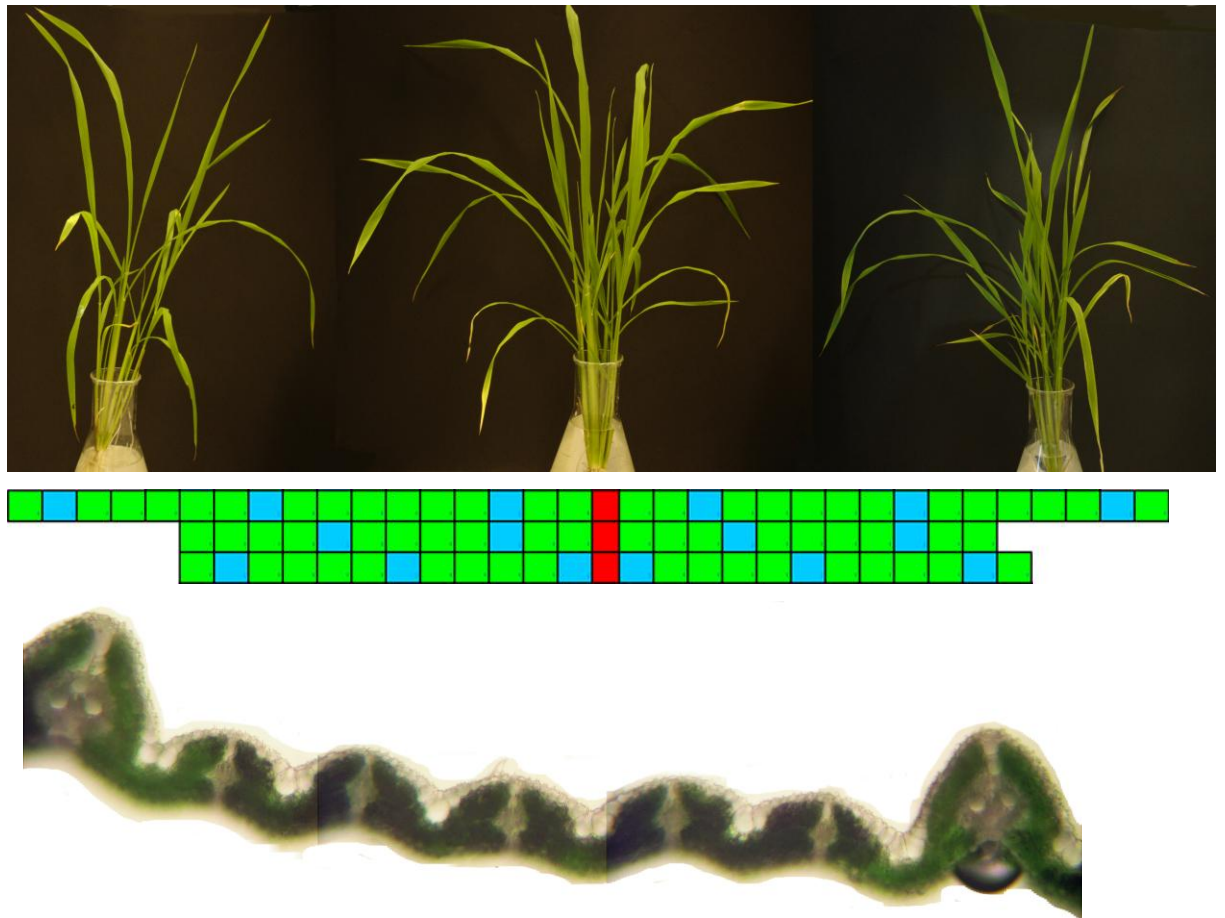
3.5.4 *alm4* (1536-6-1-6D)

Figure 3.20 Plants of the *alm4* mutant line of rice, schematic map of vein arrangement and corresponding leaf section taken from the fully expanded leaf 6. In the vein map, red squares denote the midrib, blue the major veins and green the minor veins.

alm4 plants typically showed very low germination / survival rates (< 9%), but plants which survived to sampling age produced very thick leaves. Average leaf thicknesses of *alm4* plants were 191.5 μ m at the major vein and 108.1 μ m at the minor vein compared with values of 133.3 μ m and 108.1 μ m for the wild type plants respectively. This showed a drastic and significant alteration in vein size.

3.5.5 *alm5* (3965-1-1-6G)

Figure 3.21 Whole plants of the *alm5* mutant line of rice, schematic map of vein arrangement and corresponding leaf section taken from the fully expanded leaf 6. In the vein map, red squares denote the midrib, blue the major veins and green the minor veins.

As seen in the Figure 3.21, *alm5* plants appear very different to those of wild type IR64, generally appearing smaller and having notably 'spiky' leaves. The leaf sections show that 3965-1-1-6G leaves tend to have a very small midrib and far fewer veins than the wild type. 3965-1-1-6G displays a significantly reduced minor to minor vein distance when compared to wild type, with $113.9\mu\text{m}$ versus $152.4\mu\text{m}$ ($P < 0.05$), and minor veins are also significantly wider at $49.4\mu\text{m}$ versus $41.9\mu\text{m}$ ($P < 0.05$).

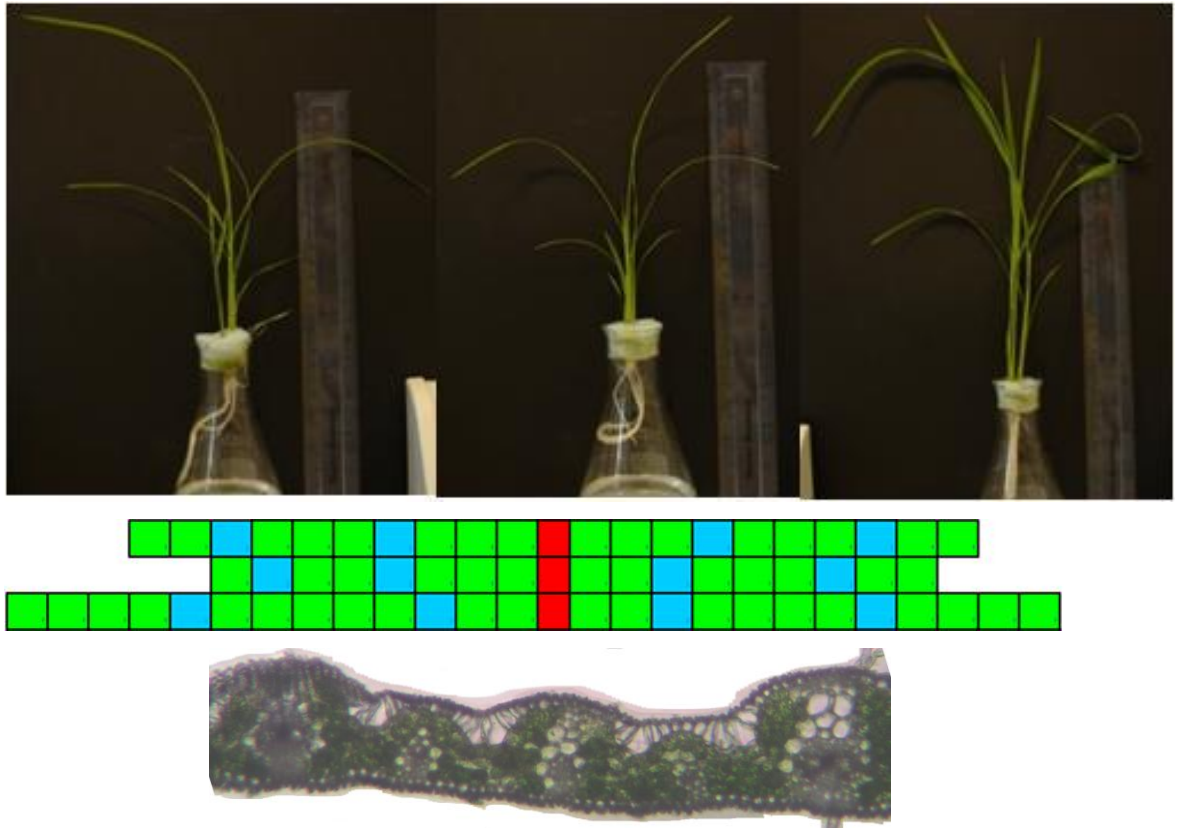
3.5.6 *alm6* (3965-1-1-7G)

Figure 3.22 Plants of the *alm6* mutant line of rice, schematic map of vein arrangement and corresponding leaf section taken from the fully expanded leaf 6. In the vein map, red squares denote the midrib, blue the major veins and green the minor veins.

Plants of the *alm6* line also display a significantly reduced minor to minor vein distance of $91.2\mu\text{m}$ compared with the wild type value of $152.4\mu\text{m}$ ($P < 0.01$). However, unlike those of sister line *alm5*, *alm6* whole plants (Figure 3.22) appear to be relatively healthy and similar in appearance to the wild type plants (Figure 3.3). *alm6* plants also displayed an unaltered number of veins compared to wild type IR64. It is also worth noting that leaf sections possess a far more typical 'C₄-like' appearance, with tightly packed veins of a more regular size rather than the more typical minor / major vein arrangement usually seen in rice.

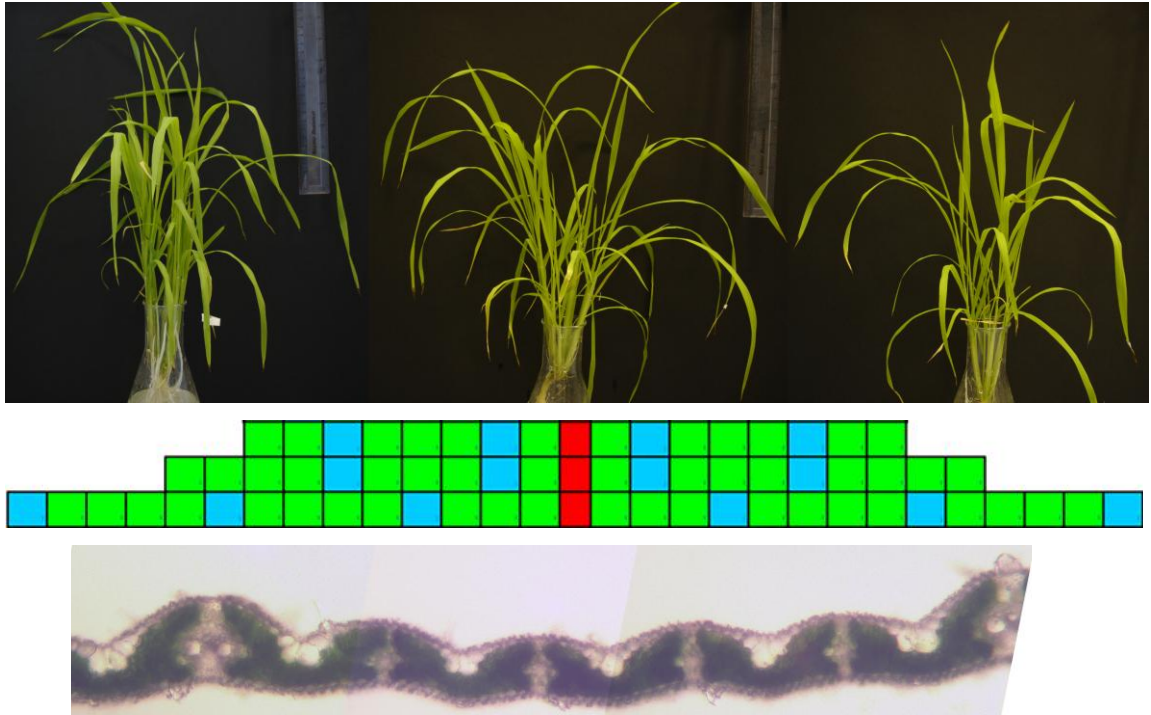
3.5.7 *alm7* (7820-1-1-3G)

Figure 3.23 Plants of the *alm7* mutant line of rice, schematic map of vein arrangement and corresponding leaf section taken from the fully expanded leaf 6. In the vein map, red squares denote the midrib, blue the major veins and green the minor veins.

Whilst whole plants of the *alm7* line do not appear to differ greatly from those of the wild type, they have been shown to produce significantly ($P < 0.05$) thinner leaves when measured at the bulliform cell location ($74.4\mu\text{m}$ versus $82.8\mu\text{m}$ average thickness in wild type), the effect of this is unknown. As seed stocks held at Sutton Bonington aged (approximately 5 years post harvest), germination percentage of *alm7* decreased to such an extent that the entire stock held was deemed to be unviable. Further seed stock was requested from IRRI, but they too were unable to germinate their seed stock so the line is no longer available for study.

3.6 Discussion

This chapter makes use of a forward genetic screen; that is mutations were induced in the population of IR64 rice plants, and the effects were observed. The underlying genetic changes responsible for these changes are unknown.

Mutagenesis by means of chemical agents and ionizing radiation have long been used to induce genetic variation in populations for crop breeding purposes, with over 2200 crop varieties produced during the 20th century by means irradiation mutagenesis (Maluszynski *et al.*, 2000). However mutation in this manner has traditionally not been used as a genetic identification tool as the mutation is not physically tagged, meaning that once an altered phenotype has been identified, identification of the altered gene(s) may take considerable effort. However, more recently the field of high throughput genotyping has improved greatly, allowing the detection of polymorphisms such as point mutations or deletions (Borevitz *et al.*, 2003; Mockler *et al.*, 2005; Arora *et al.*, 2007).

It is in this context that the rice deletion screen is considered. As stated previously, it is thought that anatomical preconditioning of the vascular arrangement and density was essential in the early phases of C₄ evolution (Sage, 2004). This screen has been successful in the identification of a number of mutant lines which potentially altered leaf morphologies which could be exploited in the manipulation of photosynthesis. This is not the first study to demonstrate that rice is amenable to producing an altered vascular arrangement, as a similar effect was also noted by Scarpella *et al.* (2003) in the *radicleless1* (*ral1*) rice mutant. In that case a defect in auxin response was responsible for a reduction in interveinal distance.

However, although significantly altered leaf morphologies have been observed in this screening process, the nature of screening is such that, a compromise must be made between resolution of the screen and the throughput of individuals. It is therefore necessary for the candidate lines outlined here to undergo a detailed characterisation before it is possible

to describe the responses that they display in definite terms, and also to check that the alterations described in this chapter are heritable and repeatedly produced. Therefore detailed characterisation of the mutant lines will allow for a firm understanding of the changes observed in this chapter and allow discussion of potential causes and implications of these changes. Also, the genes responsible for the production of Kranz anatomy are not yet known, and although not part of this project, any lines confirmed as displaying a leaf morphology of significant interest can be returned to IRRI for genetic characterisation (Hei Leung, IRRI, personal communication).

Chapter 4
DETAILED MORPHOLOGY
OF CANDIDATE LINES

Chapter 4: DETAILED MORPHOLOGY OF CANDIDATE LINES

4.1 Introduction

The purpose of the screening process outlined in Chapter 3 was to identify mutant rice lines that produced a significantly altered leaf morphology compared to plants of the wild type. In order to screen a reasonable number of lines within the available time period, a compromise had to be made between resolution of the screen (number of features measured) and throughput (number of plants measured). Hand cut, fresh leaf sections were used as they could be produced quickly enough in order to process a reasonable number of lines, but it was not possible to visualise individual cells using this method. The objective of this Chapter is to present a more detailed anatomical characterisation of the *alm* lines identified in Chapter 3. This was made possible by the higher resolution of the techniques used, allowing a greater range of measurements to be made.

4.2 Methodology

The production and growth conditions of the plants up to the time of sampling are discussed in detail in Chapter 2. Specific methodologies related to the characterisation of the mutant lines are described below.

4.2.1 Fixed and stained leaf sections

Tissue taken from the leaf 5 of each rice mutant was fixed in 4% paraformaldehyde in phosphate buffer solution (PBS, pH 7.2), 0.1% Triton X-100, 0.1% Tween 20. This was done under vacuum infiltration for 30 minutes then left overnight at 4°C on a rotator. Once fixed, the tissue was brought back to room temperature, washed in PBS and moved through an ethanol series to dehydrate the tissue prior to resin embedding. The resin Technovit 7100 was used for embedding. Tissue was pre-infiltrated with an ethanol / resin mixture before infiltration in 100% resin overnight. After infiltration, the tissue sample was placed in a gelatine mould and the resin solution and hardener added and left

overnight to harden. Once set, the sample was attached to a plastic block and cut using a microtome to 5µm thickness to produce a transverse section. This was then stained with 1% toluidine blue for 15 seconds and imaged using a light microscope at x20 magnification.

4.2.2 Confocal microscopy

Tissue was collected from the widest part of fully expanded leaf⁵ of rice plants and cut into sections approximately 15mm in length. These were then fixed overnight in 4% paraformaldehyde (Sigma-Aldrich) at 4°C. Once fixed, tissue was treated with NaEDTA and separated cell preparations were produced as described previously. Once separated, cells were imaged using an argon laser and Leica SP2 confocal microscope (Leica Microsystems, Germany). Excitation was performed at 405nm and fluorescence was detected at wavelengths of 510-525nm and 645-655, to show autofluorescence of the cell wall and chlorophyll respectively (Furbank *et al.*, 2009). Images were captured using the computer program Leica Confocal Software (Leica Microsystems, Germany).

4.2.3 Cleared and stained hand cut sections

In a method adapted from Lux *et al.* (2005), hand cut transverse sections of the leaf 5 of rice were cleared of pigments and stained for imaging with a light microscope at x20 magnification. This was done to allow clear visualisation of the individual mesophyll cells, so that they could be accurately counted and measured in terms of cross sectional area and perimeter. Hand cut sections were cleared in 85% lactic acid solution saturated with chloral hydrate crystals. This was done on a microscope slide at 70°C for 1 hour. The sections were then washed in distilled water to remove any clearing solution still present and stained with 1% toluidine blue containing 1% sodium tetraborate for 10 – 20 seconds depending on the thickness of the section. After staining, the sections were again washed with distilled water to remove excess toluidine blue, before mounting them in distilled water on slides.

4.2.4 Separated cell preparations

Cell separations were produced using a method adapted from Pyke and Leech (1987). Leaf tissue was taken from the widest section of leaf 5 of rice mutant plants, and cut into strips approximately 1cm long. The tissue was then fixed in 4% paraformaldehyde overnight at 4°C. The fixative was removed, 0.1M NaEDTA (pH 9) added and the tissue was heated at 60°C for a minimum of 6 hours in a heating block. To allow comparison of rice mesophyll cells with those of a well categorised species, a reduced time of 2 hours was used for Arabidopsis samples so as not to cause complete disintegration of the tissue. Once heated, the pieces of leaf tissue were placed onto a microscope slide and mounted in the NaEDTA solution. These were then mechanically broken up using a pair of forceps. The tissue was imaged using a Nomarski prism at x40 magnification.

4.2.5 Leaf surface impressions

Impressions were taken of the adaxial and abaxial surfaces of the fully extended leaf 5 of rice mutants at the widest point. This was done by applying Coltene President Plus Jet dental resin, (Colténe Whaledent, Switzerland) onto the leaf surface with a spatula and for it to fully set, approximately 10 minutes at room temperature. Once set the resin was peeled off and no further measurements were taken from the leaf. To visualise the leaf surface, the resin impression was painted with clear nail varnish (Rimmel, UK) and observed under a light microscope at x20 magnification.

4.3 Detailed leaf sections

Several methods were used in order to visualise the arrangement of mesophyll cells within rice leaves.

4.3.1 Fixed and resin-embedded tissue

Initial experiments to produce clear images for detailed characterisation involved fixation of leaf tissue in paraformaldehyde and embedding it in resin. These samples were then cut using a microtome and visualised using a light microscope (Figure 4.1).

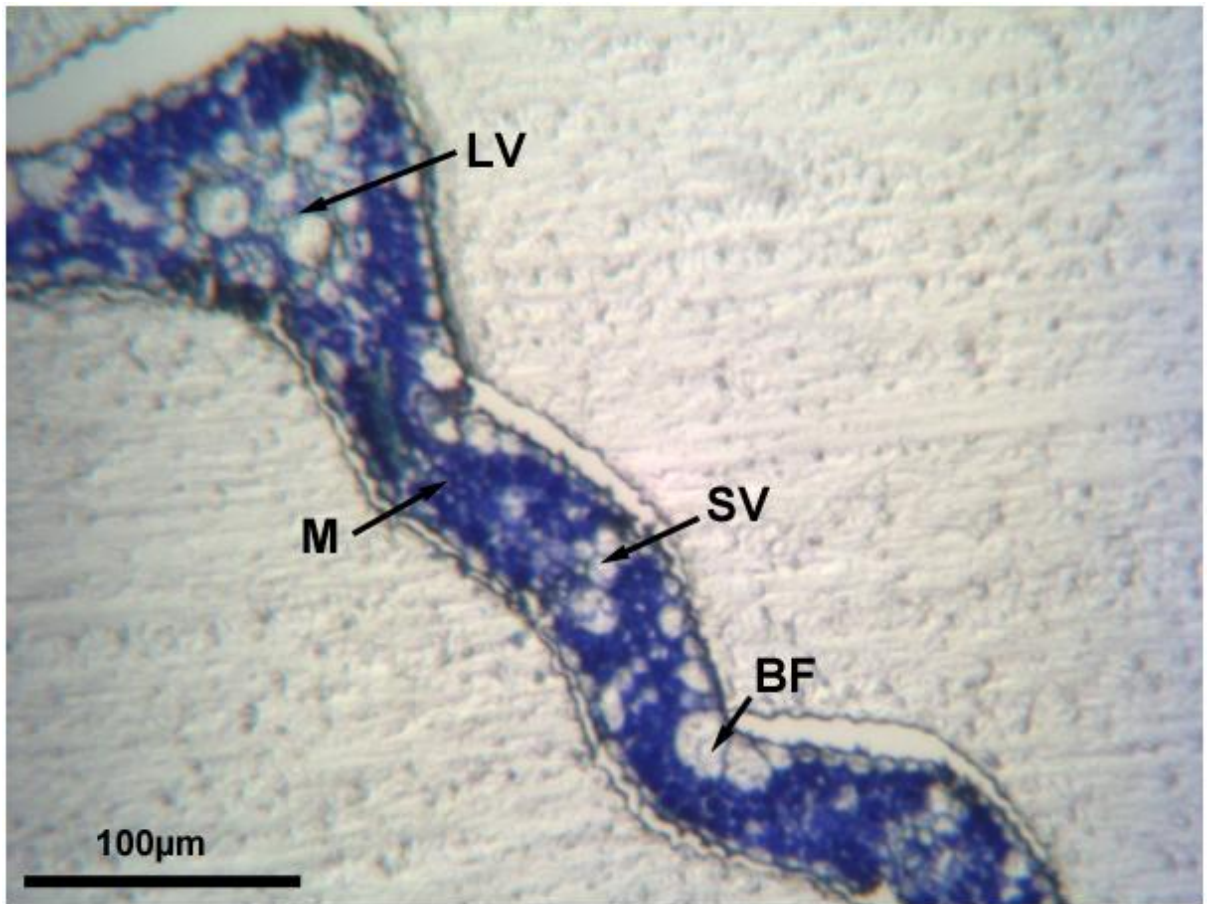


Figure 4.1 Fixed and stained section of leaf 5 of an *alm3* rice mutant, stained with toluidine blue. **LV**, large vascular bundle; **M**, mesophyll; **SV**, small vascular bundle; **BF**, bulliform cells.

Whilst the resin-embedded sections provided more detail than the hand cut sections reported in Chapter 3, it was not possible in all cases to clearly visualise individual mesophyll cells, perhaps because the cells were small and densely packed and extensive lobing caused them to be indistinct in appearance. These features seem to be typical of rice leaves and are discussed later in this chapter. Furthermore, dehydration of the tissue during the embedding process caused it to pull away from the surrounding resin, causing it to no longer be held firmly in place. As it was not possible to take accurate measurements of individual mesophyll

and bundle sheath cells, the technique was not used in detailed characterisation and alternatives were found.

4.3.2 Confocal microscopy

It was hypothesised that by using confocal microscopy, it would be possible to visualise both individual cells and the chloroplasts within them at the same time, thus providing much more information than resin embedded stained sections.

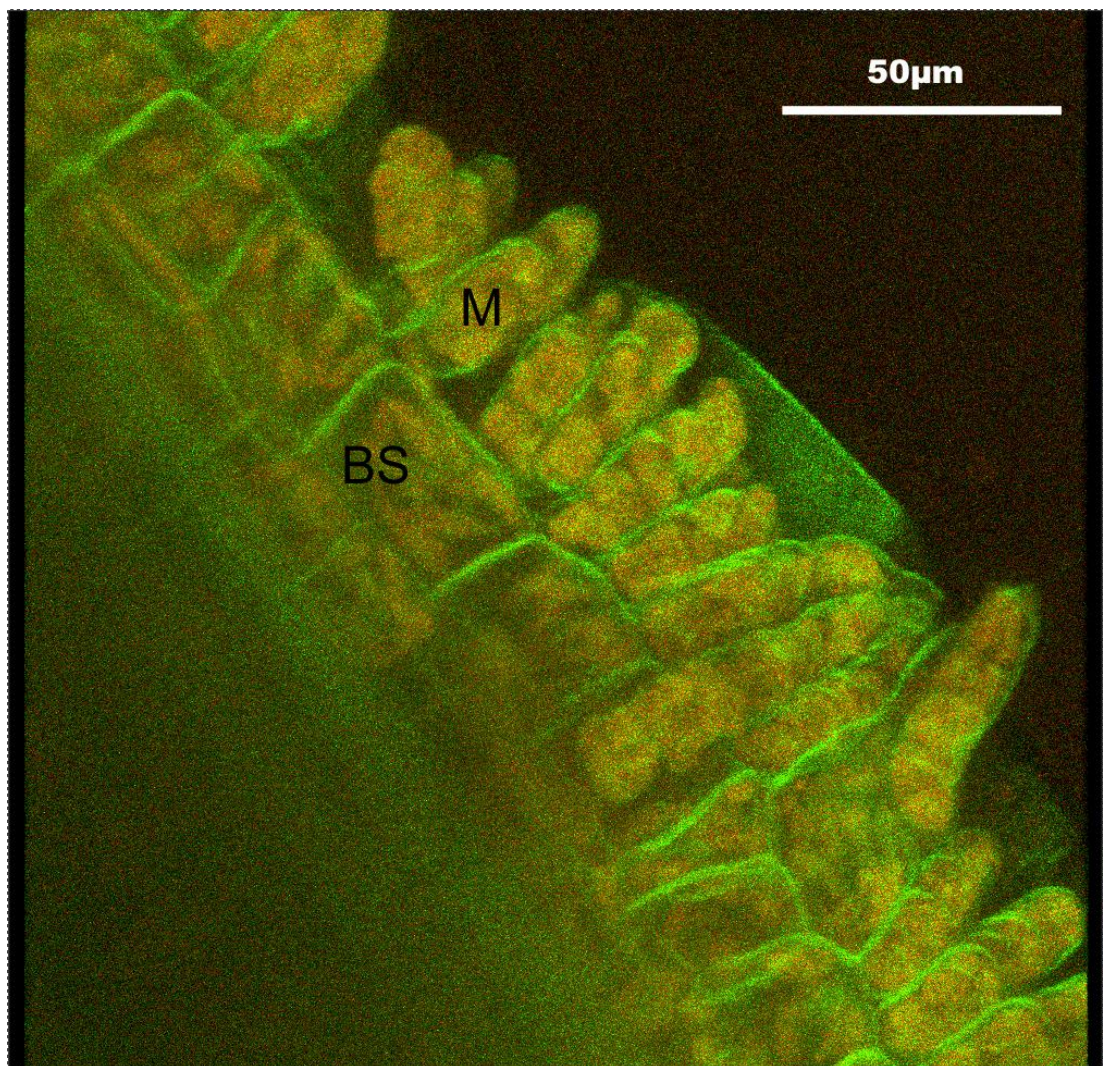


Figure 4.2 Confocal micrograph of tissue taken from leaf 5 of a wild type rice plant. Cell walls are coloured green and chlorophyll is coloured red. **BS**, bundle sheath cell; **M**, mesophyll cell.

The initial results were promising and Figure 4.2 shows adjacent mesophyll and bundle sheath cells attached to the remnants of a vascular bundle, whilst the chloroplasts (shown in red) can also be visualised. This technique was suitable for allowing comparison between the mesophyll and bundle sheath cells and quantification of the chloroplast number present within each cell type. However, because of the high cell density, the tissue needed to be broken up before it could be imaged. As the extent of separation of the cells was highly variable from sample to sample, it was not possible to consistently produce images such as Figure 4.2, with direct comparison between bundle sheath and mesophyll cells. Furthermore, because the tissue had to be broken up, there was a degree of tissue loss, and it was impossible to count the number of cells present or measure the distance between adjacent vascular bundles. For these reasons, the technique was not used in the detailed characterisation of the *alm* lines. However, the few images obtained show some interesting features such as the number and orientation of the mesophyll cells around the bundle sheath, as will be discussed later.

4.3.3 Cleared and stained hand cut sections

A problem with the hand cut sections used in Chapter 3 was that the high cell density and small size of rice mesophyll cells make visualisation of individual cells extremely difficult. To try to overcome this problem, fresh hand cut transverse leaf sections were treated with chloral hydrate to remove leaf pigments in an adaption of the protocol outlined by Lux *et al.* (2005). Following treatment, the cleared leaf sections were stained with toluidine blue (Figure 4.3).

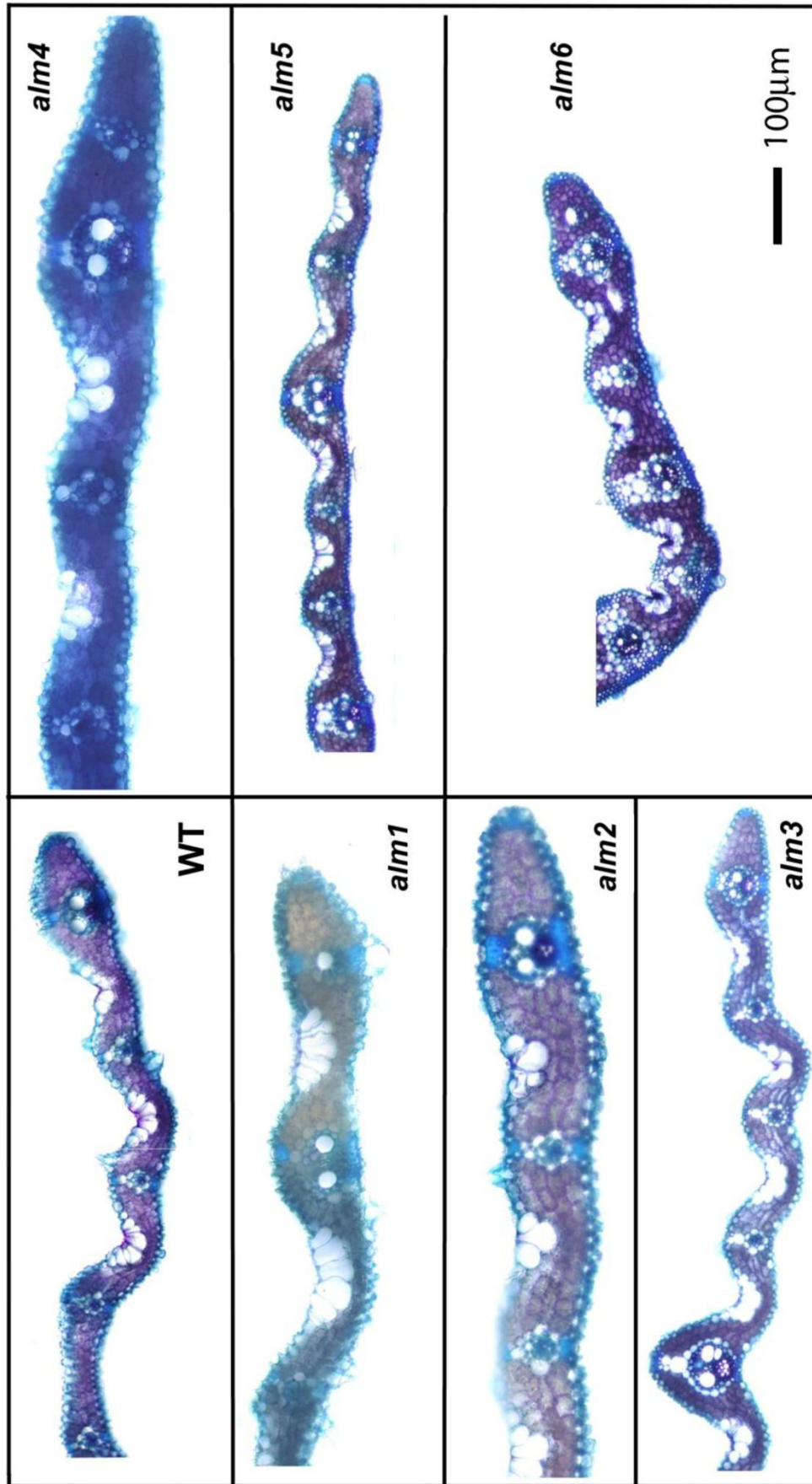


Figure 4.3 Cleared and stained transverse sections of leaf 5 of wild type rice and *alm* lines 1-6.

It became evident that the cleared and stained hand cut fresh leaf sections enabled visualisation of the individual mesophyll cells within the leaf, as these can be seen in Figure 4.3. This technique was therefore used extensively throughout the detailed characterisation process. However, removal of leaf pigments with chloral hydrate, and staining with toluidine blue meant that it was impossible to quantify and measure the chloroplasts within individual mesophyll cells, meaning that another technique was required to characterise these features.

4.3.4 Separated cell preparations

Although the confocal microscopy technique previously outlined was capable of visualising individual chloroplasts, its time-consuming nature meant that the use of separated cell preparations was a preferred option for the identification of chloroplasts.

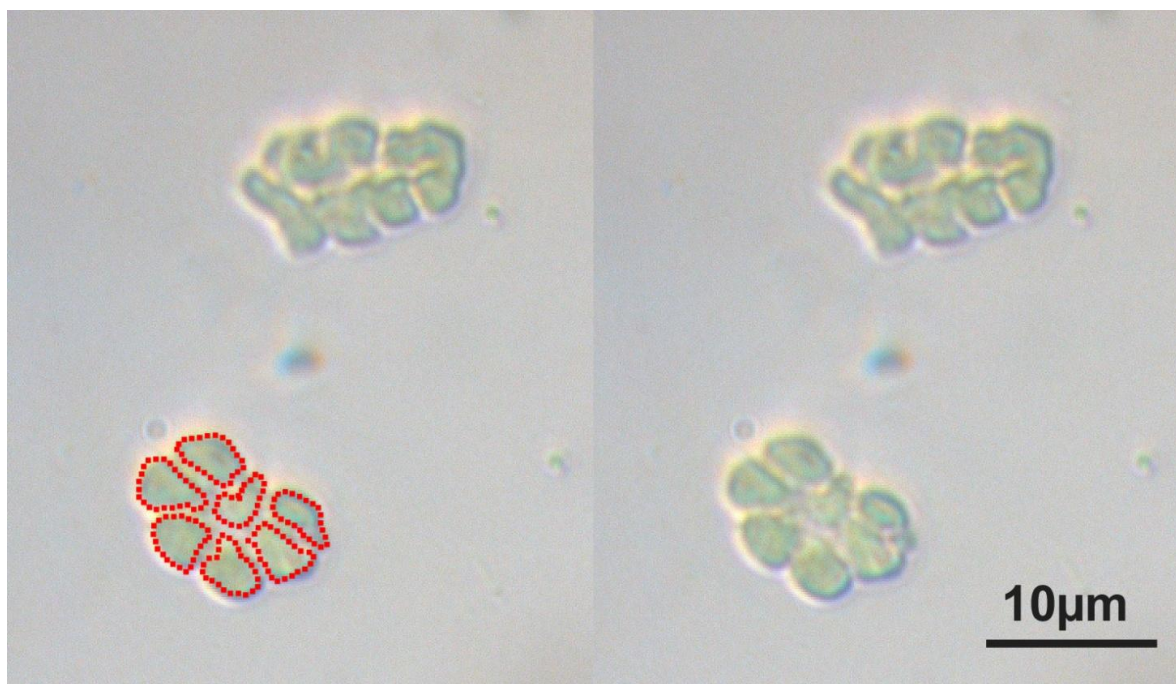


Figure 4.4 Isolated mesophyll cells from leaf 5 of wild type IR64 rice plants. Individual groups of chloroplasts are highlighted with red broken line.

4.4 Interveinal Spacing

Having established working methods for the anatomical analysis of these leaves and cells, detailed analyses of the rice mutants were undertaken.

4.4.1 Distance

Using the cleared and stained transverse leaf sections described in Section 4.2.3, interveinal distance was again measured (Figure 4.5).

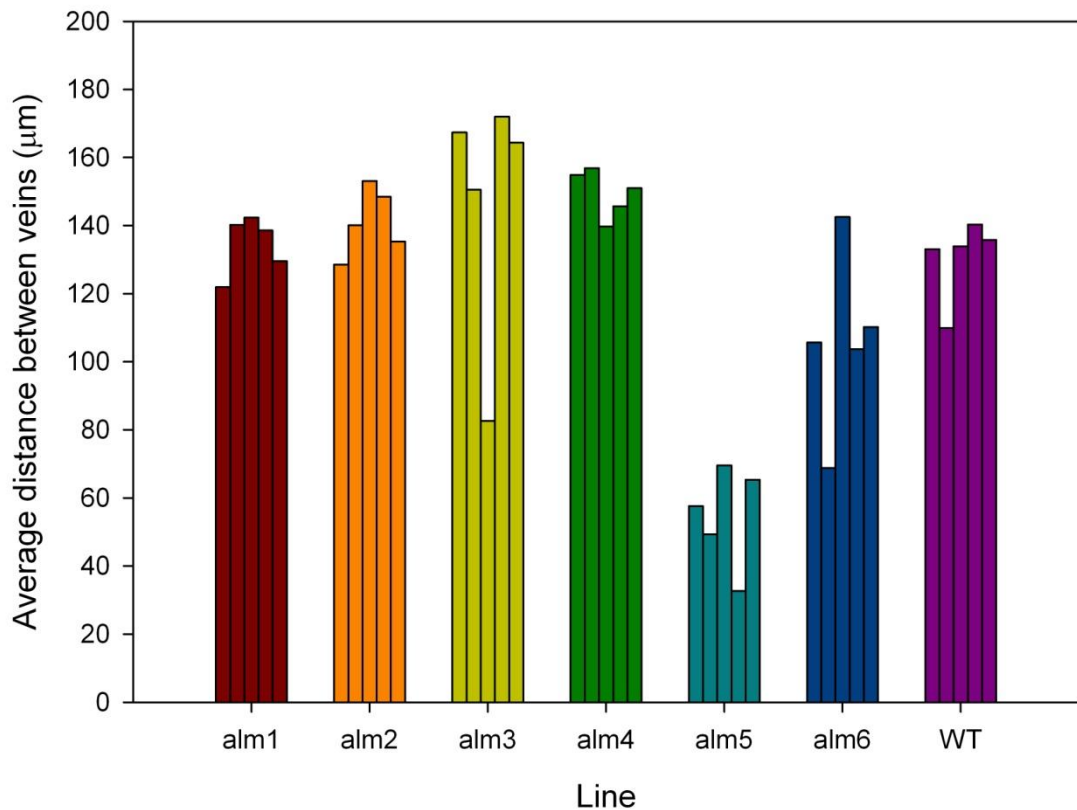


Figure 4.5 Mean distance between two adjacent minor veins in the fully extended fifth leaf. Each histogram represents the mean distance for one plant.

As in Chapter 3, ANOVA tests showed that *alm5* and *alm6* produced minor veins which were significantly closer together than those of wild type plants ($P < 0.05$). As the reduction in interveinal distance was observed in different generations and batches of plants, this suggests that the phenotypes are persistent, and not simply observed in the single generation of plants used in the screening process. A reasonably large variation can again be observed within the lines (for example values for *alm3* ranged from 86.6 to 171.9 µm). Interestingly, *alm3*, *alm5* and *alm6* all produced a single plant which differed greatly in interveinal distance from the others, which were relatively closely clustered together. If interveinal distance had been shown to be consistent between all the individuals within a line, it would be likely that a dominant gene was responsible for the observed phenotype. Speculatively, this is consistent

with a Mendelian pattern of inheritance for interveinal distance, and suggests that a reduced interveinal distance could be the result of expression of a recessive gene. The study was not designed to investigate the presence of Mendelian inheritance, and insufficient plants were sampled to confirm statistically the presence of unique individuals in a 3:1 ratio. It is therefore impossible to confirm or deny the presence of Mendelian ratios of inheritance, this is, however, perhaps unlikely to be present as such a ratio would be expected from a cross between heterozygotes, rather than a selfing line which is assumed to be homozygous. It is also a possibility that the observed variation is an effect of non-Mendelian segregation; however, this is possibly a less likely cause due to the clustering of similar interveinal distances displayed by the majority of the individuals sampled. If segregation were the primary cause, potentially more variation between all of the individuals would be expected.

4.4.2 Cell number

As mentioned in Section 1.6.2, although Kranz-anatomy C_4 plants often display a reduced interveinal distance compared to C_3 species, an important factor in Kranz anatomy is the number of cells present between neighbouring vascular bundles. This feature is designed to maximise the rate of diffusion of C_4 metabolites between mesophyll and bundle sheath cells by reducing the number of membranes which have to be crossed. For this reason, interveinal cell number is an important factor to consider when looking for C_4 -like characteristics (Figure 4.6).

The number of individual mesophyll cells in a single row was counted between the adjacent vascular bundles. Bundle sheath cells were considered to be part of the vascular bundle and not included in the count.

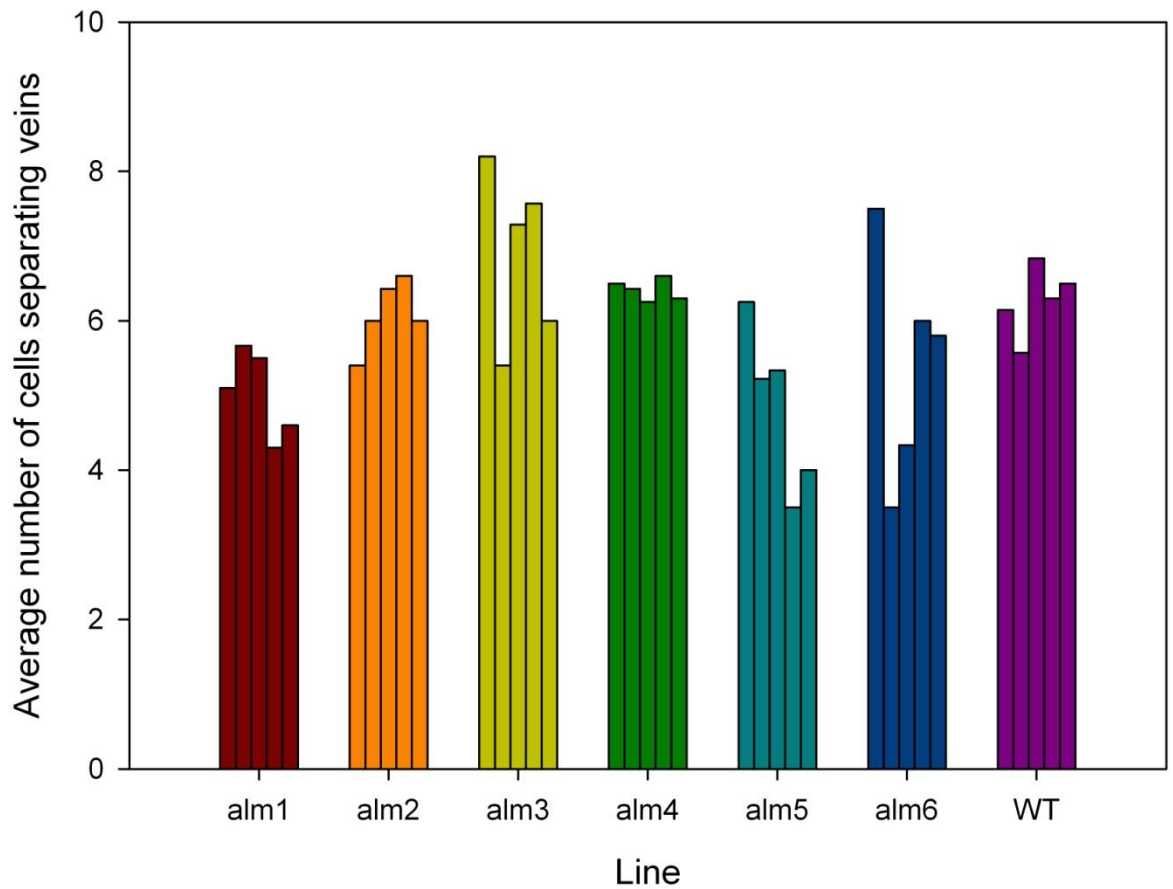


Figure 4.6 Mean number of mesophyll cells present between two adjacent minor veins in the fully extended leaf 5. Each histogram represents the mean number for one plant.

As for interveinal distance, Figure 4.6 shows that there was large intra-line variation, and some individual plants appear to have demonstrated a reduced number of mesophyll cells between adjacent vascular bundles (for example plants 4 and 5 of the *alm5* line compared to plants 1-3). However ANOVA tests showed that no *alm* line had produced a significantly altered interveinal cell number when compared with the wild type. The variation in cell number within each *alm* line was greater than that for interveinal distance, although *alm1*, *alm2* and *alm4* displayed relatively well conserved interveinal cell numbers. *alm3* and *alm5* both produced two groups of individual plants with a similar interveinal cell numbers, with three and two plants within each group. As with

interveinal distance, this may indicate that interveinal cell number is not under the control of a single dominant gene. Again it is impossible to confirm or deny the presence of Mendelian ratios of phenotypes with this experiment, but it remains a possibility.

The variation demonstrated by the *alm6* line appears to differ slightly from the others in that there two individuals showed a mean interveinal cell number of approximately six cells, two individuals with approximately four cells and one individual with seven cells. The presence of three different observed cell numbers again suggests that alteration in mean cell number is not due to change in a single dominant gene. It is again possible that this effect resulted from a single recessive gene, but it is impossible to confirm or deny the presence of a Mendelian ratio using homozygous lines.

The airspaces within leaves were primarily observed to follow a longitudinal orientation (Figure 4.7), and the lines demonstrated minimal variation in the volume of air space seen in transverse sections. It can therefore be said that the interveinal region in transverse section consists primarily of mesophyll cells, and thus an alteration of the size of this region should demonstrate an alteration in either the number, or the size of these cells.

As two of the lines have shown a reduced interveinal distance but no reduction in cell number, mesophyll cell size was studied in order to establish whether significant variation could be observed.

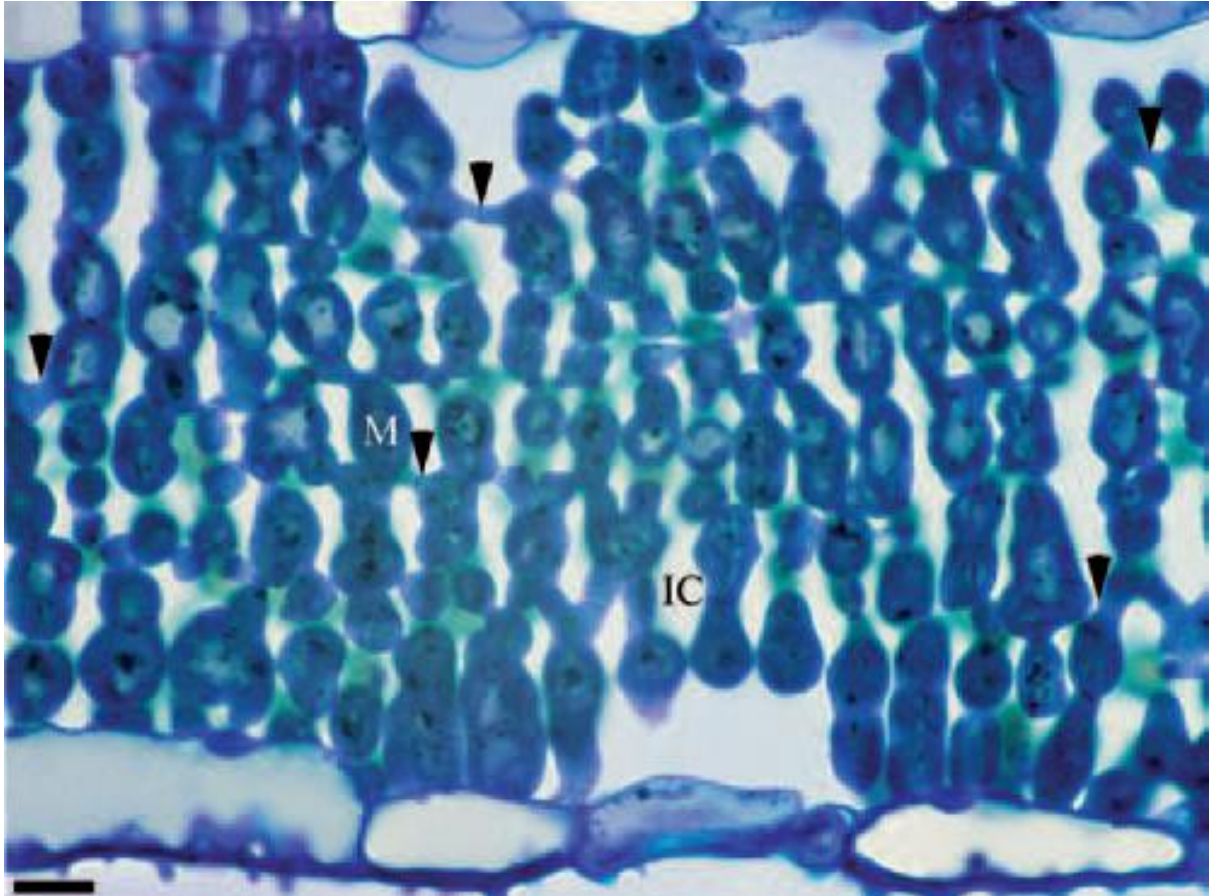


Figure 4.7 Longitudinal section of wild type rice leaf showing intercellular airspaces (IC); mesophyll cells (M) and the junctions between mesophyll cells (arrowheads). Bar = 10 μ m. Taken from Sage and Sage (2009).

4.4.3 Cell size

Although individual mesophyll cells can be visualised and counted using the cleared and stained sections discussed previously, the combination of the high density and extensive lobing of the cells can make it difficult to accurately determine where one ends and the next begins. The small size of the mesophyll cells also contributes to this problem (Figure 4.8). For this reason, the plan area of isolated mesophyll cells produced using the cell separation method outlined in Section 4.2.4 was used to determine mesophyll cell size (Figure 4.9, Figure 4.15). Once cells had been separated and imaged, plan area was measured by tracing the individual cell outline in the computer software package Infinity Analyze and using this information to calculate the enclosed area of the outline.

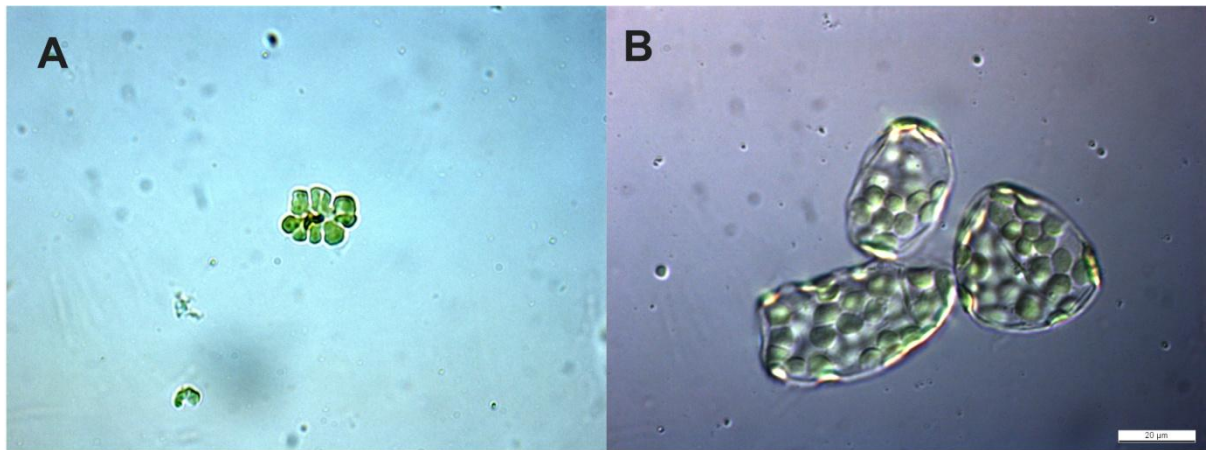


Figure 4.8 Comparison of **A** wild type IR64 rice mesophyll cell and **B** *Arabidopsis thaliana*. Note that plan area of rice mesophyll cells is typically 20 -30% of that for *Arabidopsis*. The extensive lobing displayed by the rice mesophyll cells is also apparent.

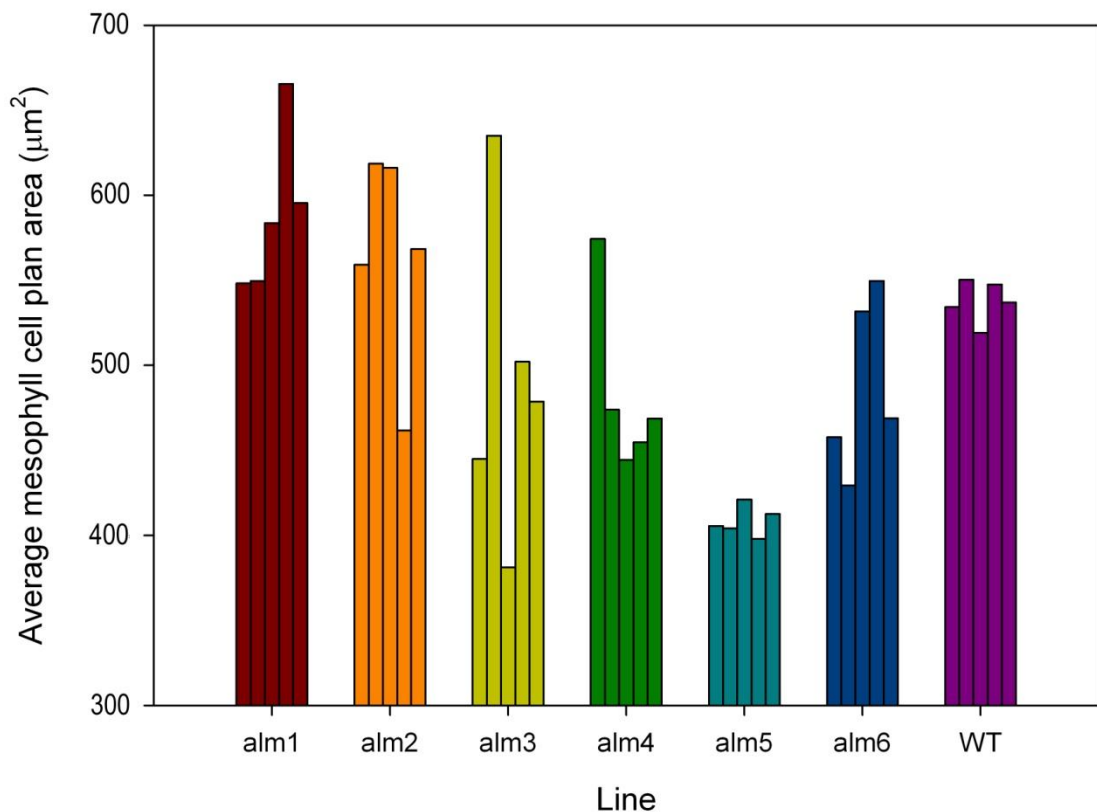


Figure 4.9 Average plan area of mesophyll cells present between two adjacent minor veins in the fully extended leaf 5. Each histogram represents the mean plan area of cells of one plant.

ANOVA testing showed that plants of the *alm5* line produced mesophyll cells which were significantly smaller than those of the wild type ($P < 0.01$).

As the *alm5* line displayed both a reduced interveinal distance and a reduced mesophyll cell size, it is considered that there is a link between these two factors.

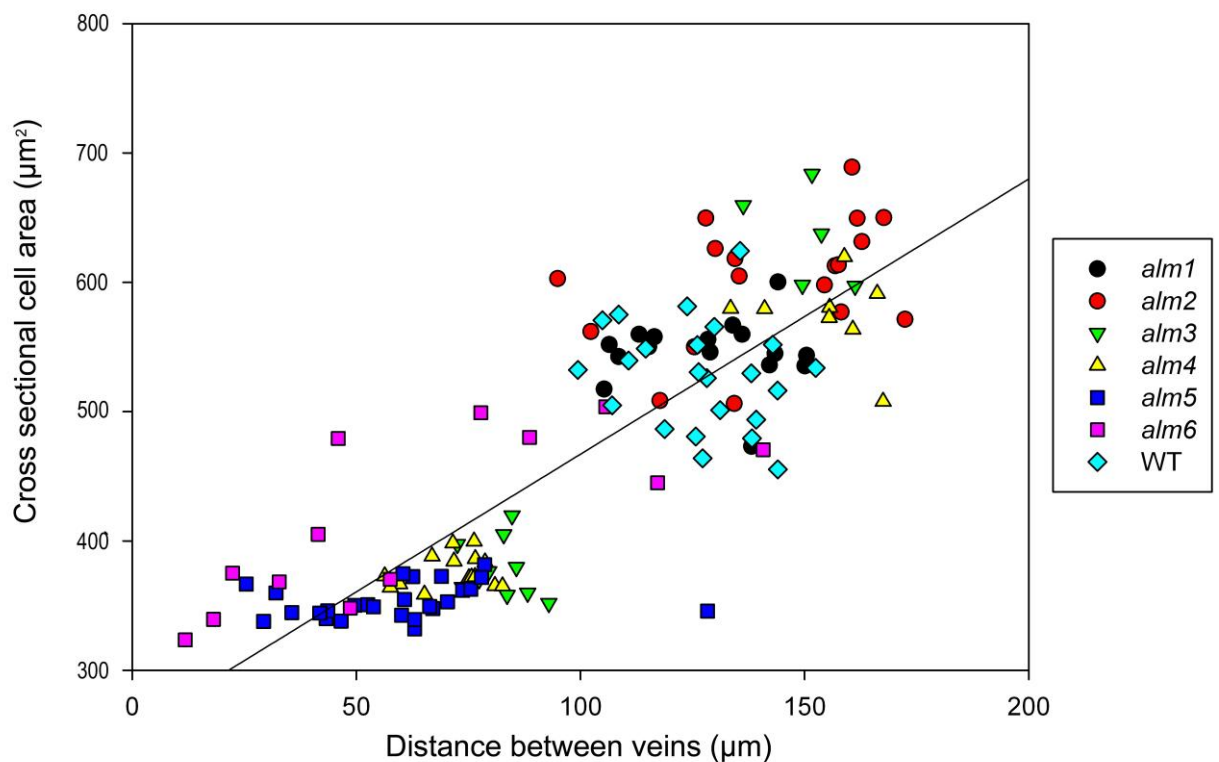


Figure 4.10 The relationship between mesophyll cell area and mean interveinal distance in the fully expanded leaf 5 of rice plants.

Figure 4.10 shows that there is a strong correlation between interveinal distance and cell size ($R^2 = 0.70$, $P < 0.001$), suggesting that the size of the mesophyll cells is an important determinant of interveinal distance. Given that the 'typical' Kranz anatomy states that interveinal distance should be small, with few, large mesophyll cells separating the vascular bundles, it would be expected that any potentially 'C₄ like' plants would

predominantly fall above the line of best fit in Figure 4.10. The lines *alm2* and *alm6* predominantly fall above this line suggesting that, in terms of cell size and interveinal distance, these lines may have a closer similarity to C_4 plants than the others. The lines *alm1*, *alm3* and *alm4* are broadly evenly spread either side of the line, and *alm5* lies predominantly below it, thus suggesting that these lines possess a leaf morphology which is the least similar to a typical Kranz anatomy. However, as previously mentioned, the number of mesophyll cells present between adjacent vascular bundles is also a key feature of the Kranz anatomy, and it has been shown in Figure 4.6 that no *alm* line produced a significantly reduced interveinal mesophyll cell number.

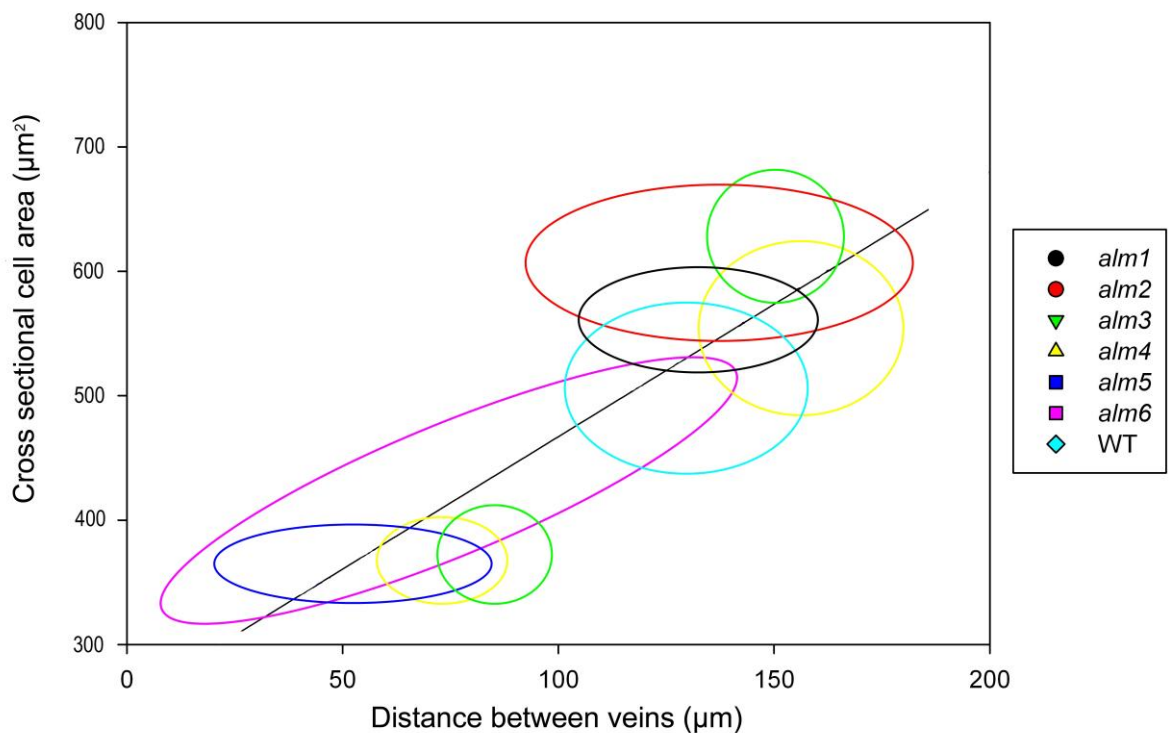


Figure 4.11 Schematic diagram showing the position of the major groups of individual plants for mean cross-sectional cell area versus interveinal distance for each *alm* line.

When considering the groupings of positions for each line in terms of cross sectional area and interveinal distance (Figure 4.11), the spread of

data for most lines is relatively small. However, it is worth noting that the lines *alm3* and *alm4* each appear to form two separate groups of points. This indicates that these plants are displaying two separate responses to interveinal distance, possibly resulting from the segregation effects discussed previously.

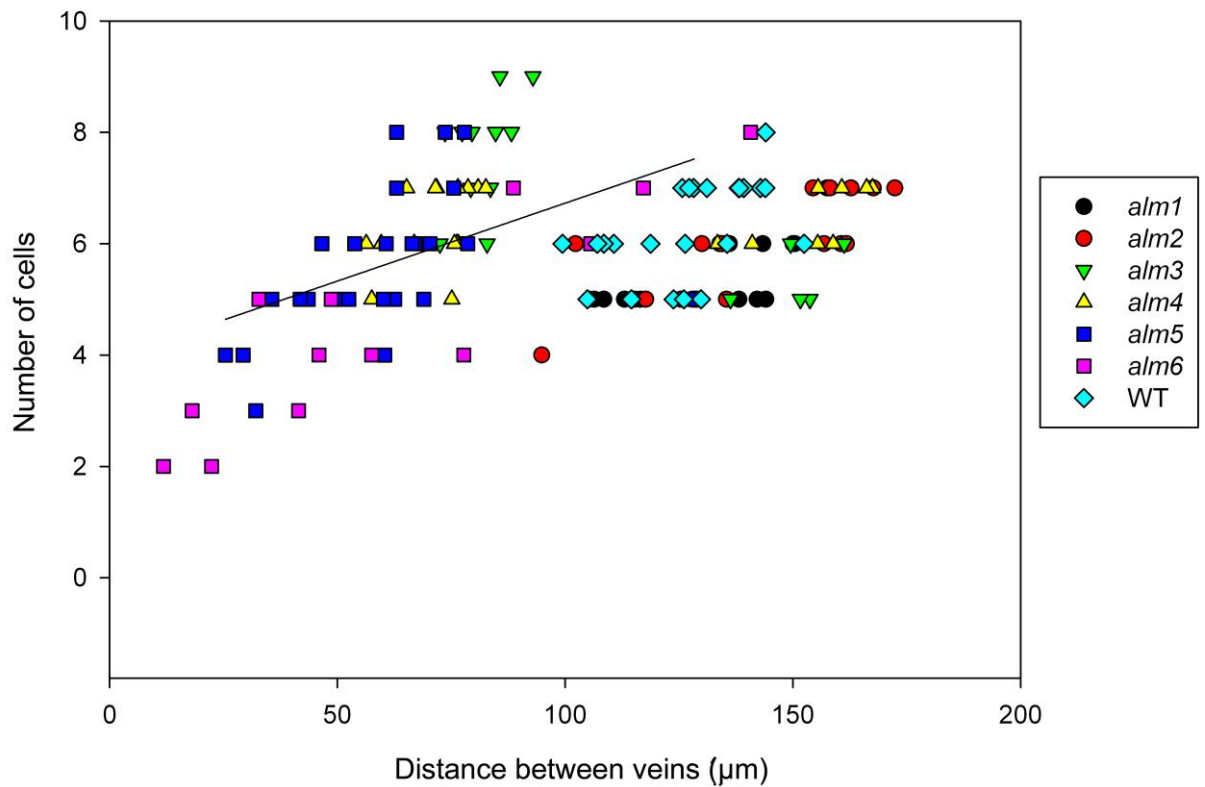


Figure 4.12 Relationship between the number of cells present and the interveinal distance in the fully expanded leaf 5 of rice plants.

Figure 4.12 shows that when examining all of the mutant lines, there was a very weak correlation between cell number and interveinal distance ($R^2 = 0.07$). This is perhaps unsurprising as Figure 4.9 suggests there is a strong relationship between cell size and interveinal distance rather than the number of cells present.

Looking at the spread of data, there may be two responses, with a strong linear correlation between cell number and interveinal distance up to an interveinal distance of approximately $90\mu\text{m}$, and very little correlation beyond this point (Figures 4.12, 4.13). The fact that two *alm*

lines demonstrated two distinct responses to interveinal distance (Figure 4.11) provides further evidence that the relationship between interveinal distance and cell number may be biphasic.

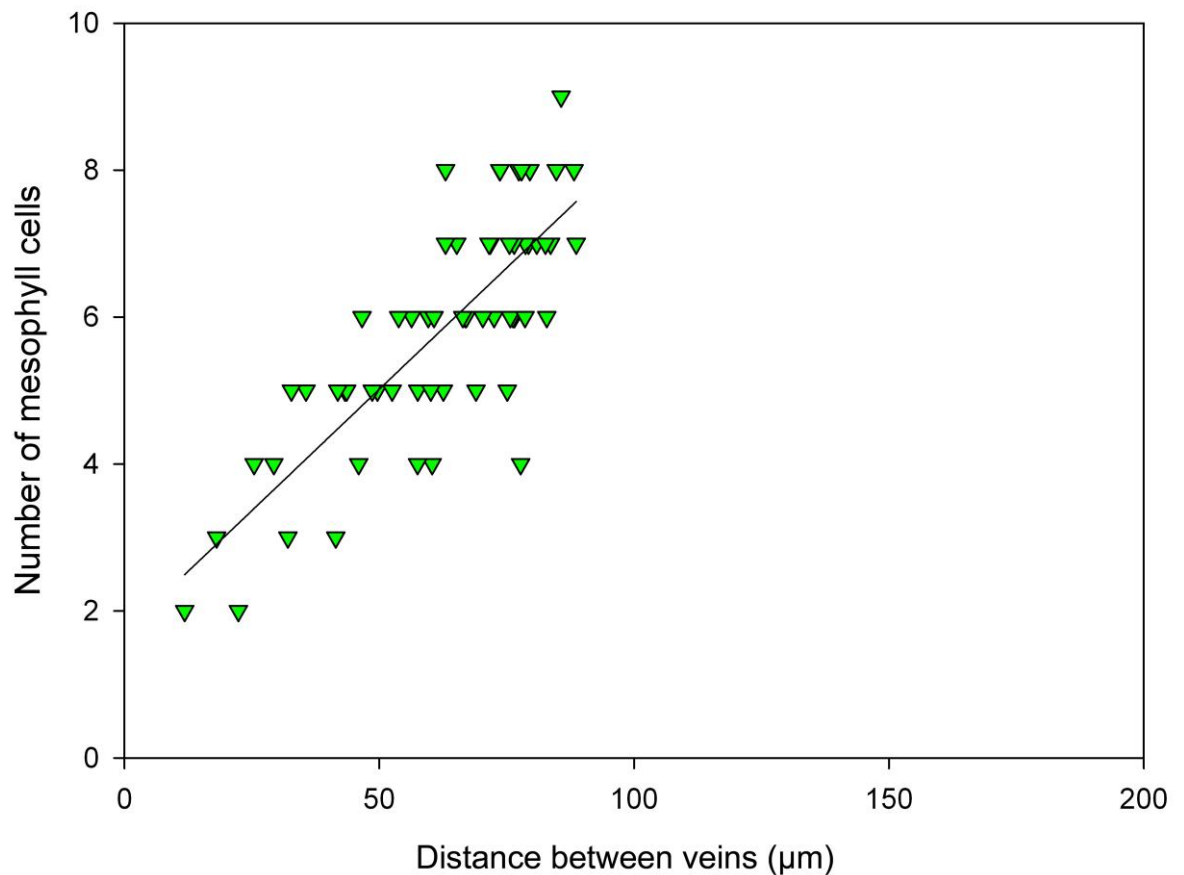


Figure 4.13 Relationship between interveinal cell number and interveinal distance in individual plants demonstrating interveinal distances of 90µm or less. $R^2 = 0.64$, $P < 0.01$.

One explanation for this may be that cell size is normally an important determinant of interveinal distance, but at extremely small interveinal distances the mesophyll cells have become as small as they possibly can whilst still remaining functional. This physical constraint means that, as the cells have reached their minimum size, any further reduction in interveinal distance would have to be due to a reduction in cell number.

If this theory is correct, mesophyll cell size should remain broadly static for interveinal distances up to approximately 90 μm .

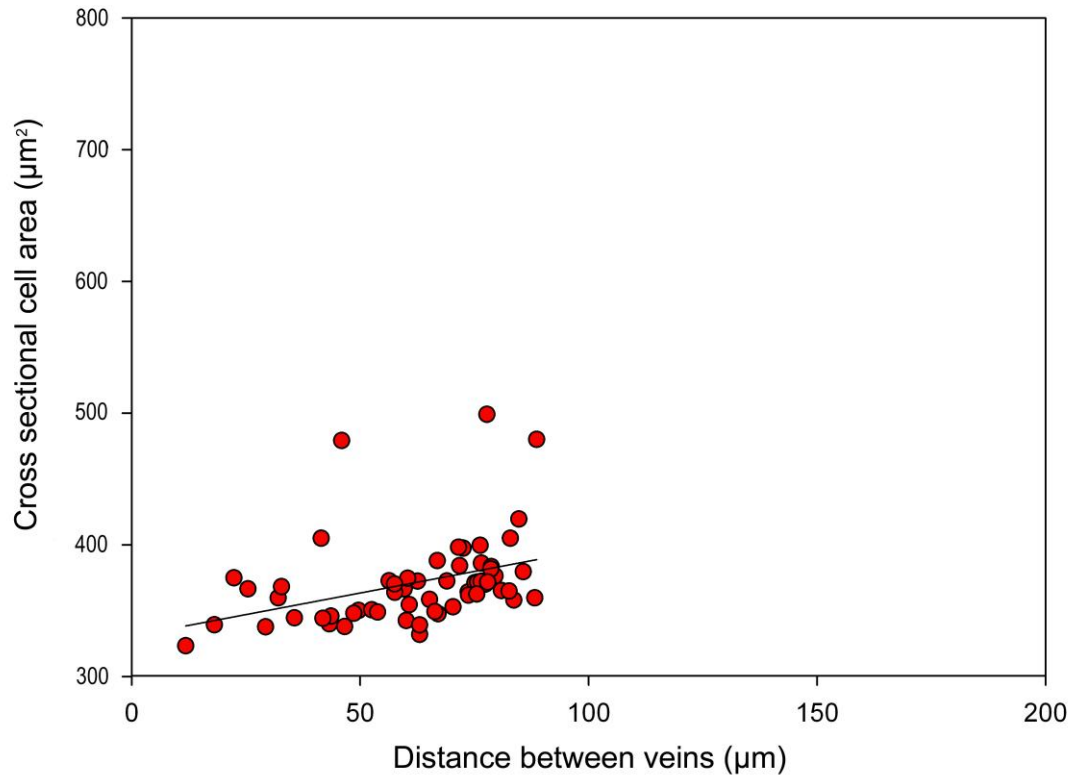


Figure 4.14 Relationship between cross-sectional cell area and interveinal distance in individual plants demonstrating an interveinal distance of <90 μm . $R^2 = 0.14$, $P = >0.1$.

Figure 4.14 shows that there was no significant linear correlation between cross sectional cell area and interveinal distance when the interveinal distance was less than 90 μm , providing further evidence that the minimum mesophyll cell size is determined by a factor other than interveinal distance.

Physical constraint, however, is not the only possible explanation for the potentially biphasic relationship between interveinal distance and mesophyll cell size. An alternative explanation is that there is a developmental advantage in producing small mesophyll cells at low

interveinal cell numbers, or that the production of large numbers of interveinal mesophyll cells somehow promotes cell expansion. If this is correct, signalling would be required during leaf development in order to promote mesophyll cell expansion in response to an increased interveinal distance.

4.4.4 Mesophyll cell morphology and chloroplast distribution

So far it has been shown that some of the *alm* lines produce leaves with a reduced mean interveinal distance. It has also been shown that this reduction is primarily due to a reduction in mesophyll cell size. To investigate the effects on photosynthesis resulting from altered mesophyll cell morphology, it is necessary to characterise the mesophyll cells in terms of their shape and how this impacts on chloroplast distribution. Apart from their small size, one striking feature of the rice mesophyll cells is the degree to which they are lobed (Figure 4.15).

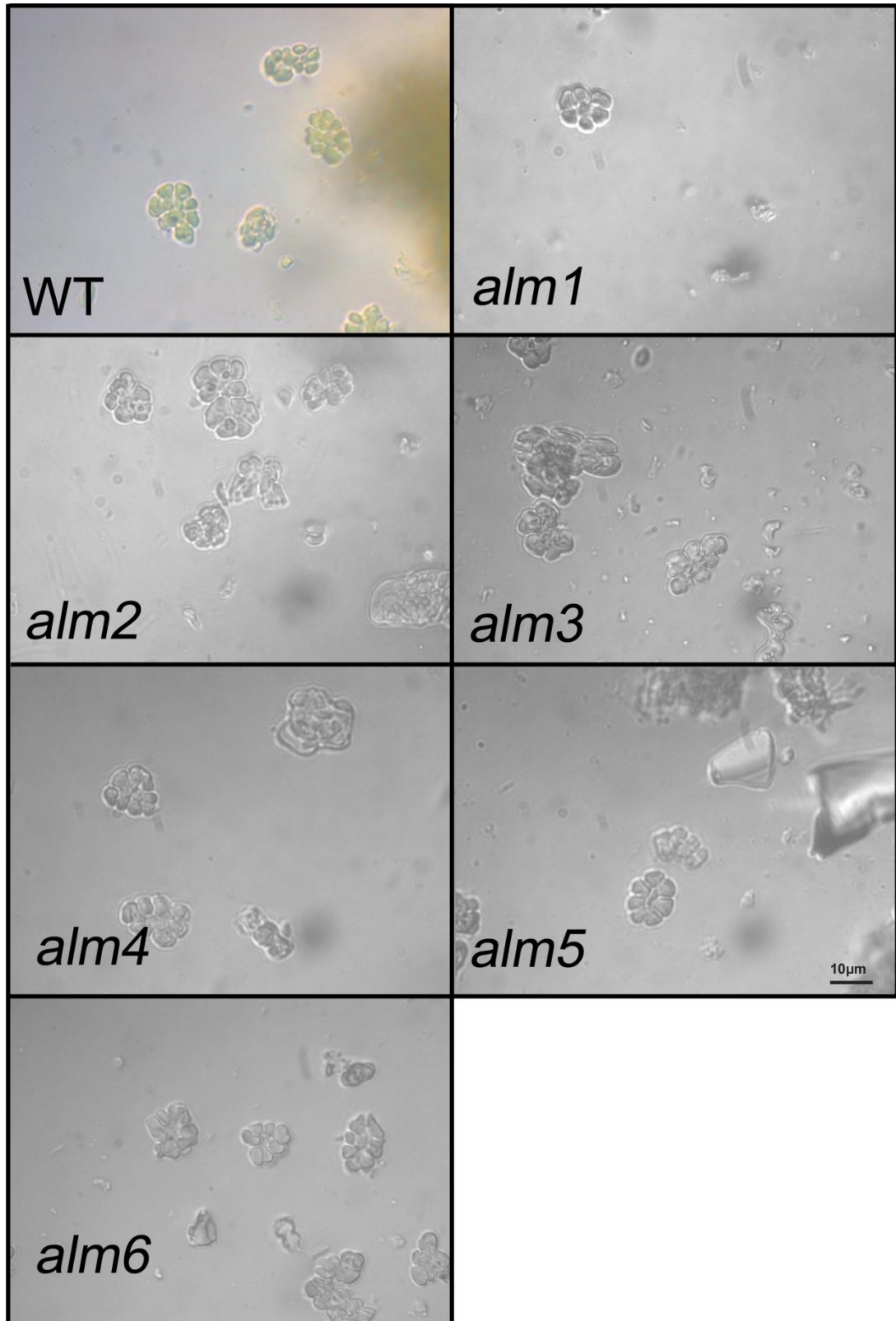


Figure 4.15 Comparison of separated mesophyll cells of the *alm* mutant lines and wild type (WT) rice plants. Note the consistent degree of lobing displayed by each line.

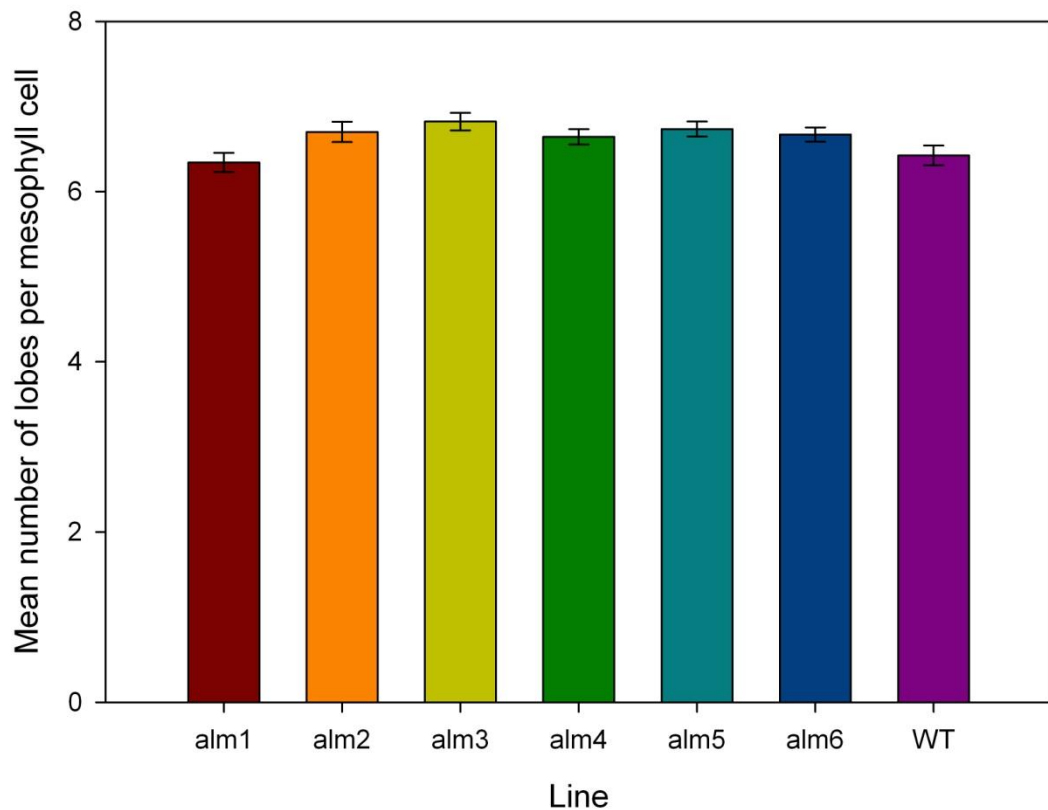


Figure 4.16 The mean number of lobes per mesophyll cell. Bars denote single standard error of the means.

Typically the number of lobes per cell ranged from 6 to 8, with as many as 10 lobes not being uncommon, although most of the cells observed were towards the lower end of this range. The maximum number of lobes observed was 12, although this was rare. Figure 4.16 shows that there was very little variation in the extent of mesophyll cell lobing either within or between lines, suggesting that this feature of the cells in these mutant lines is highly conserved.

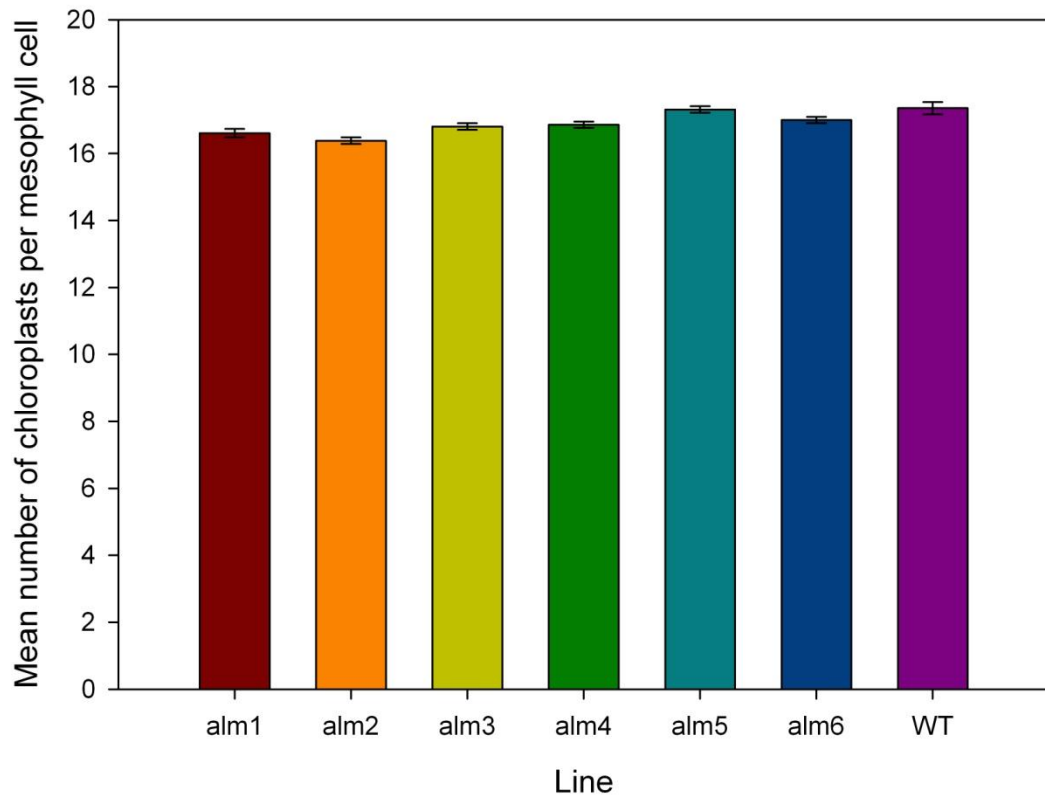


Figure 4.17 Mean number of chloroplasts per mesophyll cell. Bars denote single standard error of the means.

Chloroplasts were identified as green areas within each lobe, visualised as outlined in Section 4.2.4. As with the number of lobes per cell, Figure 4.17 shows that the number of chloroplasts per cell was well conserved. Residual plots showed that the number of chloroplasts per cell was not normally distributed, following a poisson distribution instead. Regression analysis and Dunnett's test showed that none of the *alm* lines differed significantly compared with wild type plants.

When compared to other species, the number of chloroplasts observed appears to be low (Figure 4.8). However, Figure 4.8 also shows that the mesophyll cells are also extremely small in comparison to *Arabidopsis* and it is possible that the maximum number of chloroplasts present cannot be increased due to physical constraints.

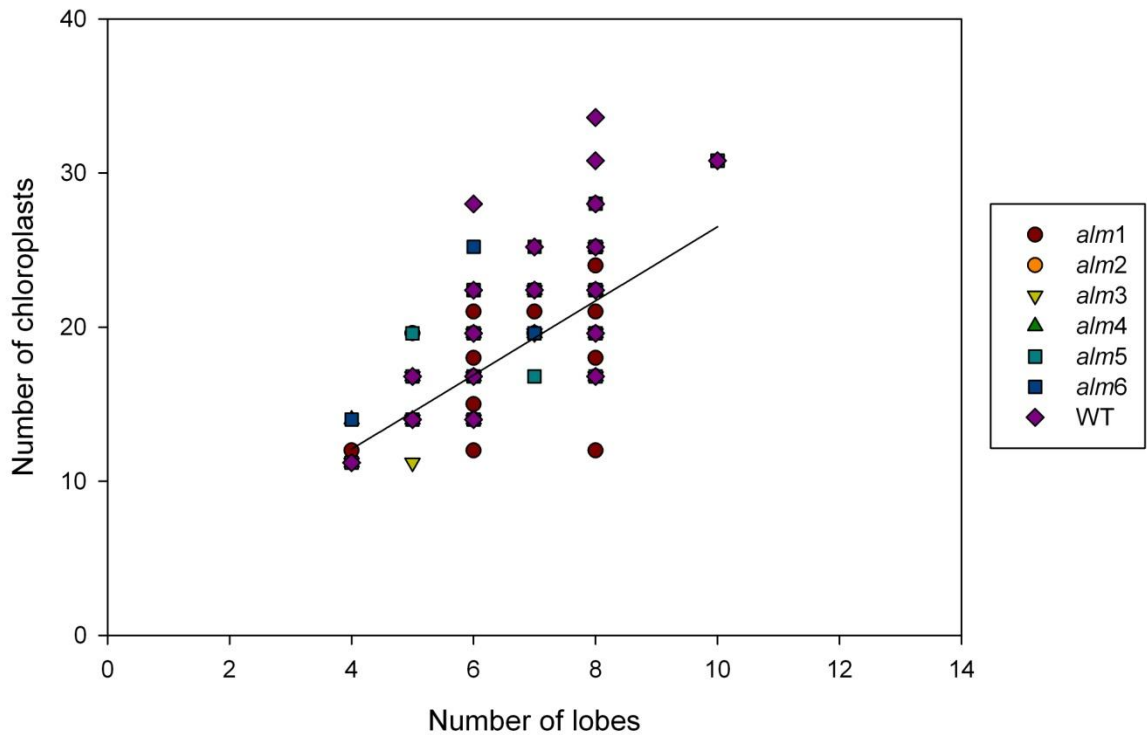


Figure 4.18 Relationship between the mean number of chloroplasts per mesophyll cell and the mean number of lobes per mesophyll cell in the fully expanded leaf 5 of rice plants.

There was a strong correlation between the mean number of chloroplasts per mesophyll cell and the mean number of lobes ($R^2=0.50$, $P < 0.0001$). Figure 4.18 shows that the ratio of chloroplasts to lobes was approximately 2.8:1. Although correlation may initially appear to be weak, a huge number of values fall directly on top of one another due to the discrete nature of number of chloroplasts and number of lobes as characteristics and the very small range of values shown in Figures 4.16 and 4.17.

This strong correlation between chloroplast number and mesophyll cell size indicates that there is a very strong and conserved link between chloroplast number and the number of lobes present within mesophyll cells. One possible explanation for this would be that during cell initiation, mesophyll cells contain very few proplastids. Due to the small size of the

mesophyll cells, these proplastids had insufficient space to divide repeatedly, preventing an increase in plastid number. As the plastids enlarge, the only space available within the cell is in the lobes, causing the chloroplasts to be closely associated with the lobes, with the result that lobe number has a large effect in determining chloroplast number.

4.4.5 Stomata

The final feature of leaf anatomy studied was the stomata. The reason for this was that the stomata often form rows between the vascular bundles, and therefore an alteration in vascular positioning could have an effect on the stomata (Figure 4.19).

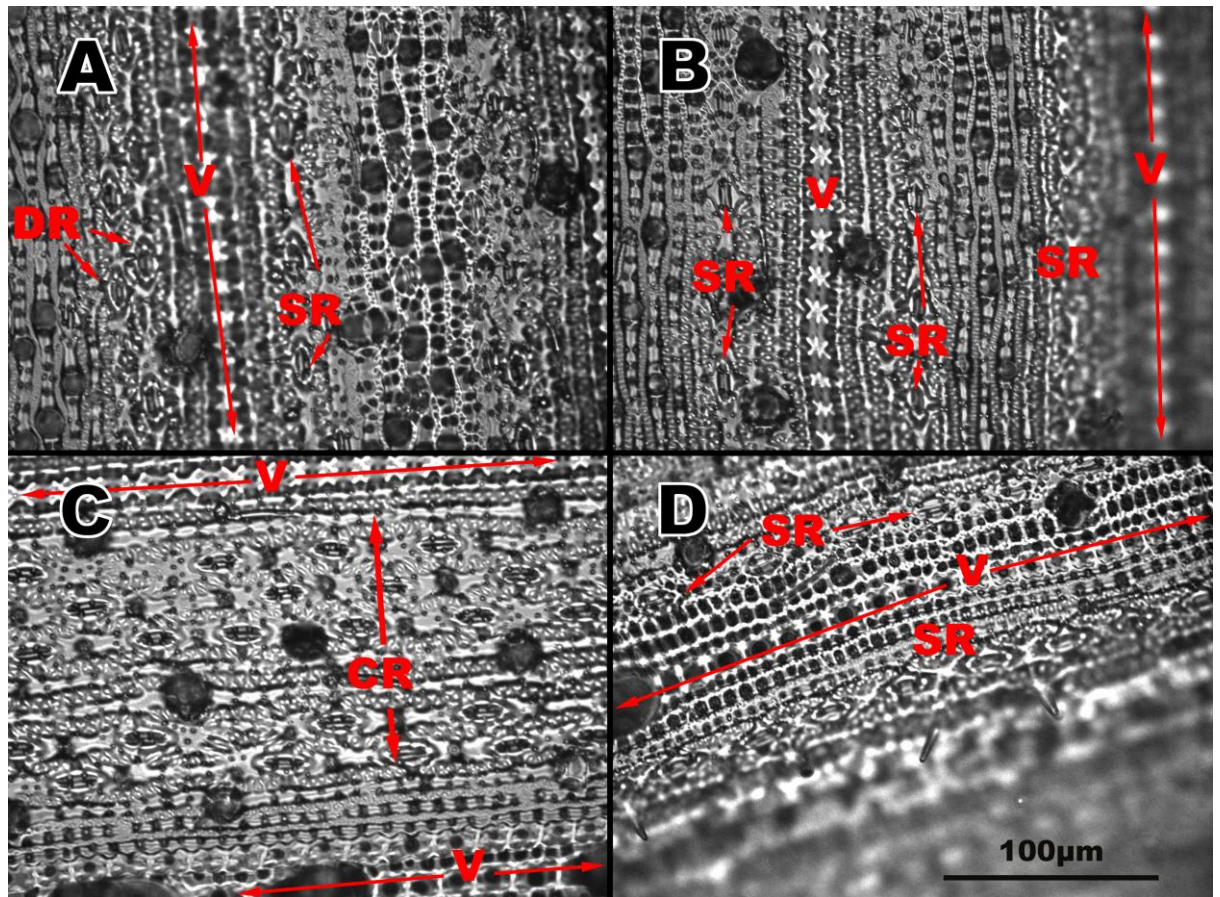


Figure 4.19 Leaf surface impressions for **A)** *alm3* adaxial surface, **B)** wild type rice adaxial surface, **C)** *alm3* abaxial surface and **D)** wild type rice abaxial surface. V, vascular bundle; SR, single row of stomata; DR, double row of stomata; CR, continuous rows of stomata.

In wild type rice plants, stomata were generally present in either single or double rows or files of stomata, on either side of the vascular bundle. No significant alteration in the number of stomatal rows per mm (stomatal row density) was found for any of the *alm* lines, although one interesting individual of the *alm3* line produced continuous rows of stomata between the first three veins out from the midrib (Figure 4.19 C). This effect was not shown at the leaf margins. This suggests that the tethering of stomatal rows to the vascular bundle has somehow become broken in this individual.

Stomatal distribution between the adaxial and abaxial surfaces was broadly even in all cases. Most lines displayed a slight bias to the abaxial surface but no significant differences between the two were found.

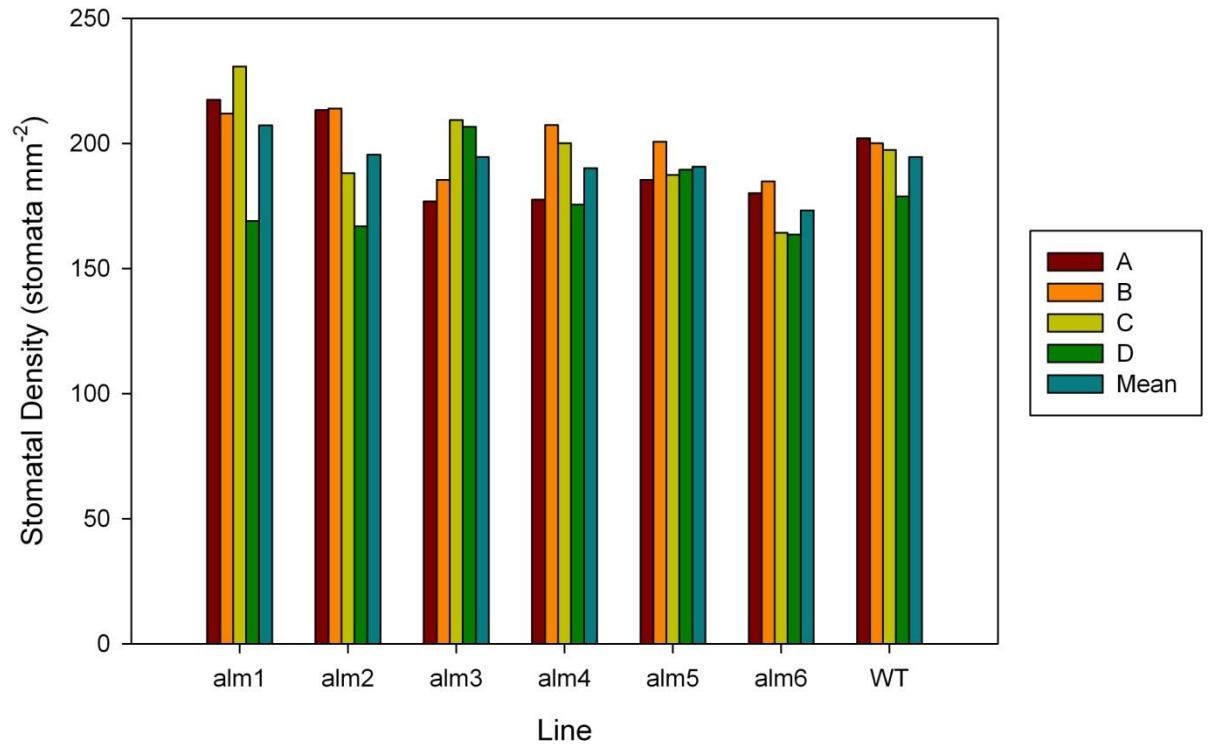


Figure 4.20 Relative stomatal density across different sections of the abaxial surface of leaf 5 of rice plants. A represents the field of view nearest to the midrib, moving through successive fields of view to D at the leaf margin.

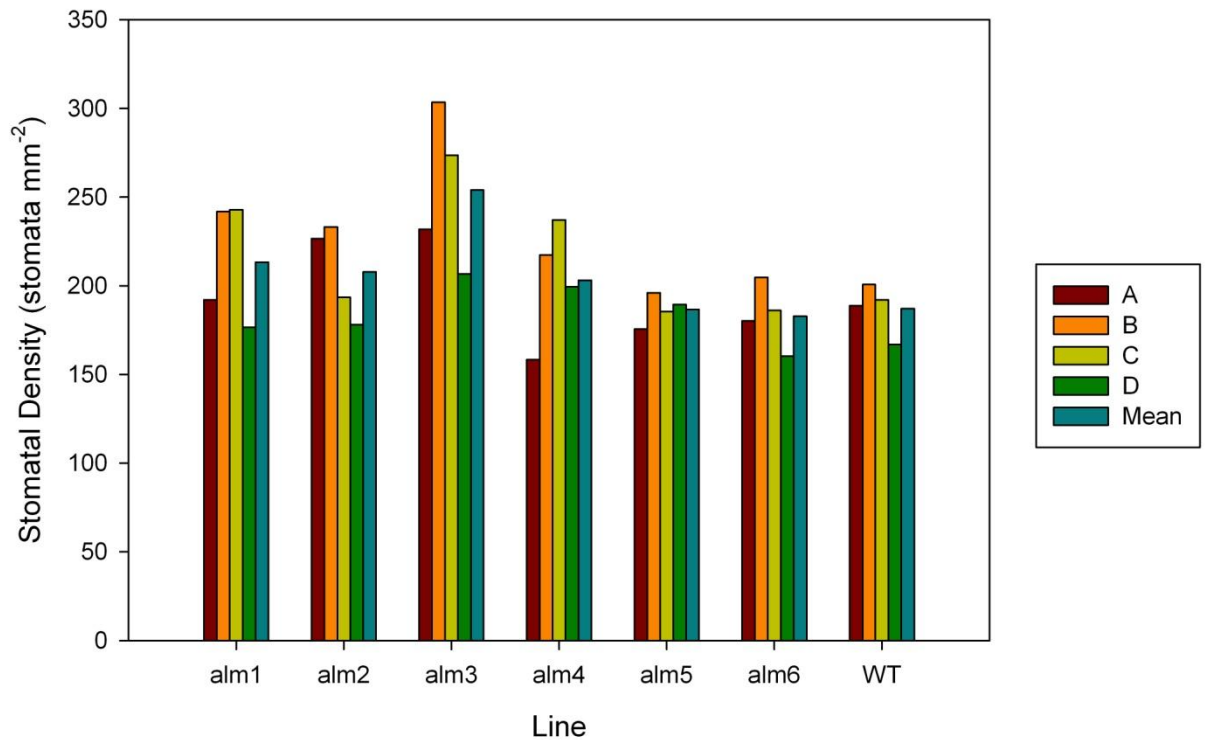


Figure 4.21 The relative stomatal density across different sections of the adaxial surface of 5th leaf of rice plants. A represents the field of view nearest to the midrib, moving out through successive fields of view out to D at the leaf margin.

4.5 Discussion

4.5.1 Interveinal distance and cell number

During the screening process outlined in Chapter 3, interveinal distance was used in an attempt to identify mutant lines which were displaying a slight shift towards a C_4 -like leaf anatomy. This was done to provide a rapid screening process under the assumption that interveinal distance would be a good indicator of interveinal cell number, and was chosen because a key feature of the Kranz anatomy is a reduced number of mesophyll cells between vascular bundles. However, Figures 4.10 and 4.12 show that in the majority of cases this assumption was not correct,

and alterations in interveinal distance were instead coupled with alterations in mesophyll cell size rather cell number. In spite of this, however, Figure 4.13 shows that there was a good correlation between cell number and interveinal distance at very small interveinal distances. This observation suggests that, although not accurate in many cases, screening for a reduced interveinal distance may be an appropriate method for identifying plants which possess a reduced interveinal cell number, providing that the reduction in interveinal distance is large enough.

4.5.2 Genetics

As the lines were from selfed M4 seed, it was expected that the lines would be broadly homozygous and that the variation which was apparent within individual lines would not be observed. For this reason, the focus of the experimental design was to study a larger number of lines with fewer replicates than would be required for a genetic assessment of the lines. For this reason, although it is possible to suggest the presence of Mendelian ratios of inheritance, it is not possible to prove their existence within this study.

However, if Mendelian ratios of inheritance were to be demonstrated, this would require the inactivation of a dominant gene involved in determining interveinal spacing during the mutagenesis process, allowing expression of a recessive gene. If this were the case, it would not be the first example of mutation resulting in the loss of function, providing a potentially useful new phenotype from a crop improvement perspective. In studies involving disease resistance in *Arabidopsis*, it was shown by Zhang *et al.* (2003) that point mutation of the dominant *SNC1* gene resulted in the production of an inactive repressor molecule. The removal of this repressor results in the constituent expression of *R* (resistance) genes and ultimately causes the activation of both salicylic acid (SA) dependent and independent disease resistance pathways.

4.5.3 Chloroplast number and cell size

Plastids develop from proplastids, which are present in meristematic cells and divide prior to meristem cell division (Pyke, 1994). Owing to their

small size and colourless appearance, it was not within the scope of this investigation to investigate the numbers of proplastids present within cells. However, other studies have shown that meristematic cells typically contain between 10 and 20 proplastids in a variety of monocotyledonous and dicotyledonous species (Juniper and Clowes, 1965; Cran and Possingham, 1972; Lyndon and Robertson, 1976).

Figure 4.16 shows that the number of chloroplasts per mesophyll cell is typically less than 17, and is strongly correlated with cell size and the number of lobes present. Numerous other studies of various species have also shown that mesophyll cell size is a primary determinant in chloroplast number, suggesting that available space within the mesophyll cell may be one of the key limiting factors in determining chloroplast number (Ellis and Leech, 1985; Pyke and Leech, 1992, Pyke, 1999). Assuming that the above estimate of 10 to 20 proplastids per meristematic cell also applies to rice, this would suggest that newly formed rice mesophyll cells already contain all of the proplastids required for chloroplast production when they are created. This would mean that any proplastid division within the cell is minimal, if it occurs at all. An orthologue of the *ARC3* gene identified in *Arabidopsis thaliana* as being involved in the initiation of chloroplast division has been identified in rice (Miyagishima, 2005), but little appears to be known about its role in rice. It is also possible that, if larger rice mesophyll cells were produced, a corresponding increase in the number of chloroplasts may be observed, which would therefore require an increase in proplastid division to provide the greater chloroplast numbers.

4.5.4 Stomata

It has been shown here, and was noted also by Hoshikawa (1989) that the stomata of the wild type rice plant form in either single or double rows adjacent to the vascular bundles. The presence of continuous rows of stomata between adjacent veins suggests that stomatal development had been disrupted in plants of the *alm3* line.

The *SCARECROW* (*SCR*) gene was reported to regulate asymmetric division in cells of *Arabidopsis* roots (Di Laurenzio *et al.*, 1996). An

orthologue of this gene has been identified in rice, *OsSCR*, which is believed to play an important role in the determination of stomatal formation (Kamiya *et al.*, 2003). It is believed that the position of rows where stomata are to be formed is determined before any stomata-specific cells are produced as cells in this region uniformly express *OsSCR*. *OsSCR* expression is then down-regulated as guard cell mother cells are formed. The means by which *OsSCR* expression is limited only to the regions flanking the vascular bundles is unknown, although it may be hypothesised that the formation of additional rows of stomata is an effect of *OsSCR* expression outside of this region.

Chapter 5
PHYSIOLOGICAL
RESPONSES OF THE
CANDIDATE LINES

Chapter 5: PHYSIOLOGICAL RESPONSES OF CANDIDATE LINES

5.1 Introduction

Having identified mutant rice lines which are significantly altered compared to wild type plants (Chapter 3) and then carried out a more detailed morphological and anatomical characterisation of the mutants (Chapter 4), the next step was to investigate the effects of mutation from a physiological standpoint to allow correlations to be established between the observed anatomical features and the resulting physiologies. Of particular interest were (a) the effects of alterations in cell size on photosynthesis and (b) the impact of changes in vein density on the physiological responses of the plants.

5.1.1 Response to carbon dioxide

The photosynthetic response to carbon dioxide concentration provides information regarding a variety of parameters important to leaf physiology. The availability of carbon dioxide is a key factor in determining the net rate of assimilation of CO₂ (*A*) during photosynthesis, although the relationship between CO₂ concentration and *A* is not linear and can be limited by a number of different factors. Farquhar, von Caemmerer and Berry (1980) stated that increasing [CO₂] will initially result in an increase in *A* because CO₂ is the substrate for this reaction, and the competitive exclusion of O₂ from the active sites of Rubisco gives a reduction in levels of photorespiration (see Section 1.4 for details). The initial linear increase in the rate of *A* is limited by the quantity of active Rubisco to fix more CO₂ and photosynthesis is then said to be in a Rubisco-limited state.

As [CO₂] increases, all of the available Rubisco active sites become saturated with CO₂, and *A* is then limited by the regeneration of the substrate RuBP. *A* can no longer increase until RuBP is regenerated within the Calvin cycle. Photosynthesis is said to be in the RuBP – regeneration limited state.

At very high $[\text{CO}_2]$, a third state may be observed whereby no further increase in A may be observed because the leaf is unable to utilise the products of photosynthesis (primarily triose phosphate) as fast as the chloroplasts can supply them. This is called the triose phosphate use (TPU) limitation, and often represents the maximum possible A (A_{max}) (Sharkey *et al.*, 2007).

Each of the three states outlined above displays a recognisable response of A to an alteration in $[\text{CO}_2]$ which can be visualised by plotting these parameters against one another. Using the curve fitting model produced by Sharkey *et al.* (2007) and based upon the original model of Farquhar *et al.* (1980), it is possible to calculate the various biochemical capacities of photosynthesis.

5.1.2 Light response

For photosynthesis to occur, light must be absorbed by chlorophyll. The light harvesting complexes of photosystem II and photosystem I (PSII and PSI) are located on within the thylakoid membrane of chloroplasts. The quanta of energy absorbed by chlorophyll cause excitation of the chlorophyll molecule, and this energy is passed into the PSII and PSI reaction centres where electron transport is initiated from the photolysis of water. Electron transport is then used in the reduction of NADP^+ as well as enabling ATP synthesis. Both NADPH and ATP are then consumed in the Calvin cycle (see Chapter 1: Introduction for more details).

Light is therefore a potentially limiting factor to photosynthesis and an increase in absorbed light may increase photosynthetic activity. However, there are many other factors which may also limit photosynthesis, including environmental factors such as temperature, water or nutrient deficiency, or genetic. In some situations, light is provided in excess of what is required for photosynthesis (Murchie and Niyogi, 2011). In the presence of excess light, singlet oxygen evolution can occur, which is potentially damaging to membranes. For this reason, plants have evolved methods of photoprotection, i.e. methods of dissipating excess energy absorbed by chlorophyll (photochemical quenching, q_p), or preventing it from being absorbed in the first place (non-photochemical quenching,

NPQ). As photoprotection involves reduction of quantum yield, it can be considered that there is a compromise between photoprotection and maximum photosynthetic rate. It has been shown that there can be a level of 'over-protection' displayed in some cases, and that a reduction in the level of photoprotection is predicted to result in an increase in maximum productivity without causing harm to the plant (Murchie *et al.*, 2009).

5.1.3 Fluorescence

As light is absorbed by chlorophyll within the chloroplasts, the energy of the absorbed light is used to raise electrons within the chlorophyll molecule to an excited state. As electrons are restored to their ground state, energy is released into one of three pathways; the electron transport chain, heat loss or fluorescence (Figure 5.1).

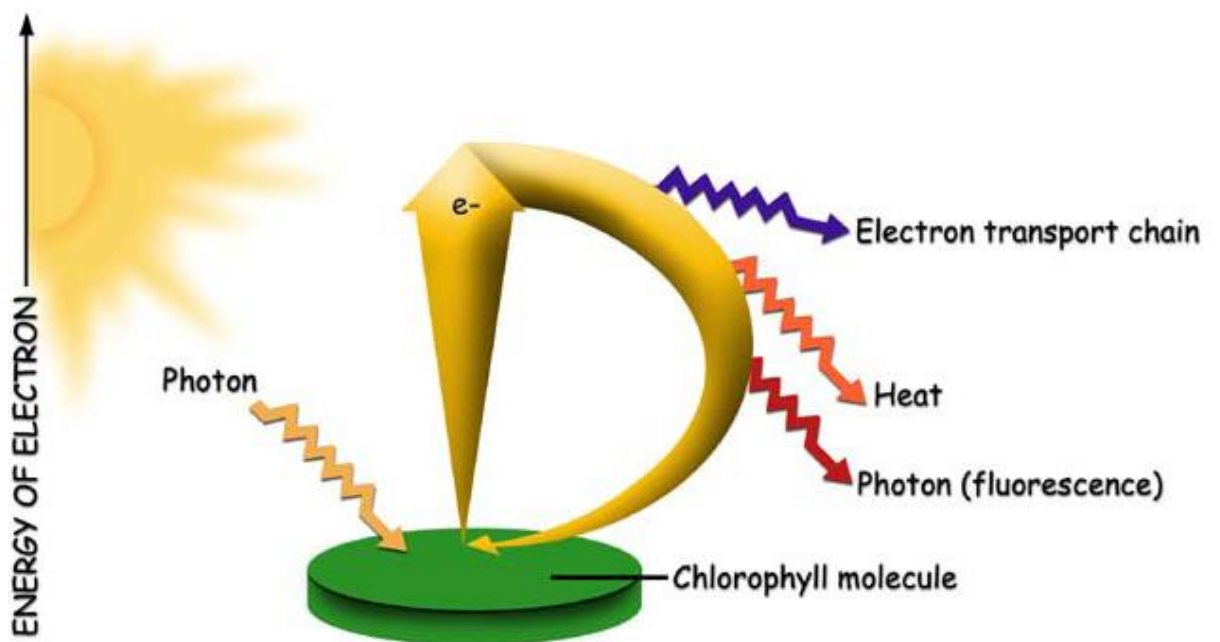


Figure 5.1 Schematic showing the pathways of energy release from the excited chlorophyll molecule following capture of a photon of light. (LiCor 6400 XT user manual v6.4).

The relationship between these three pathways can be expressed as:

Equation 5.1
$$F + H + P = 1$$

where fluorescence (F), heat (H) and photochemistry (P) are given as a proportion of the total absorbed quanta of light. P can therefore be considered as a measure of efficiency, as it is the proportion of absorbed light which is used within photosynthesis, and is termed quantum yield. Healthy plants usually display a quantum yield of 0.75 to 0.85 (Maxwell and Johnson, 2000).

5.2 Methods

5.2.1 CO₂ response measurement

The effects of alteration in atmospheric [CO₂] on rice leaf photosynthesis were measured using a LiCor 6400 XT Infra Red Gas Analyser (IRGA) (LiCor Biosciences, Illinois, USA). Details of the conditions used for this measurement are given in Section 2.5.1.

Using the atmospheric CO₂ concentrations outlined in Table 5.1, values of A and C_i were entered into the $A C_i$ curve fitting tool written in Microsoft Excel (Microsoft, USA) produced by Sharkey *et al.* (2007) in order to calculate parameters relating to photosynthesis. This tool is available from: <http://www.blackwellpublishing.com/plantsci/pcecalculation/>

Table 5.1 Range and order of CO₂ concentrations used in the production of CO₂ response curves.

Observation Number	[CO ₂] (μmol)
1	400
2	400
3	50
4	60
5	80
6	100
7	160
8	200
9	300
10	400
11	600
12	800
13	1200

Once the data had been collected, A was plotted against the CO₂ partial pressure within the intercellular airspaces (C_i) to produce A/C_i curves (see Section 4.3 for calculation of C_i). The C_i values were then converted to the CO₂ partial pressure within the chloroplasts (C_c) and analysed using the previously mentioned curve fitting tool developed by Sharkey *et al.* (2007).

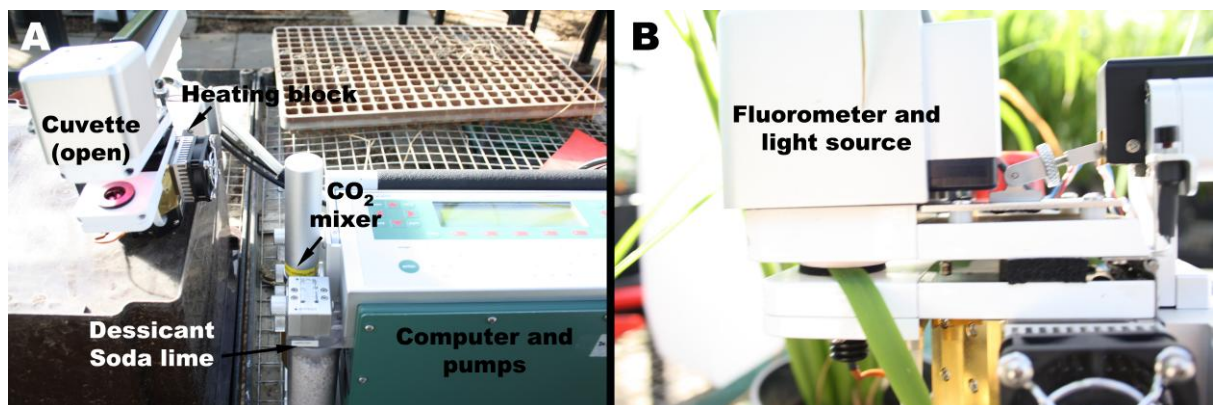


Figure 5.2 **A)** LiCor 6400 XT IRGA with cuvette open. **B)** Rice leaf in LiCor cuvette for gas analysis.

5.2.2 Light response measurements

Measurements were taken using the LiCor 6400 XT IRGA and details of the atmospheric conditions used in this experiment are outlined in Section 2.5.2. The range of PPFD values used in this experiment are given in table 5.2.

Table 5.2 Range and order of light intensities used in the determination of light CO₂ responses

Observation Number	PAR ($\mu\text{mol m}^{-2}$)
1	0
2	100
3	200
4	300
5	400
6	600
7	800
8	1000
9	1200
10	1500
11	2000

5.3 Plant response to CO₂

As outlined in Section 5.2.1, IRGA measurements were made to determine the response of the mutant lines to varying levels of atmospheric CO₂. However, whilst atmospheric CO₂ concentration is important, the concentration of CO₂ within the leaf (C_i) has a greater bearing on photosynthesis. C_i is calculated as follows:

Equation 5.2

$$C_i = \frac{(g_{tc} - \frac{E}{2})C_s - A}{g_{tc} + \frac{E}{2}}$$

where g_{tc} is the total conductance to CO₂, E is transpiration rate, C_s is the atmospheric concentration of CO₂ and A is net photosynthesis (von Caemmerer and Farquhar, 1981). When an A/C_i curve (net

photosynthesis vs. substomatal [CO₂]) is plotted (Figure 5.3), three phases can be visualised, the Rubisco limited phase, the RuBP-regeneration phase, and the triose phosphate utilisation (TPU) limited phase (see Section 5.1.1 for more details).

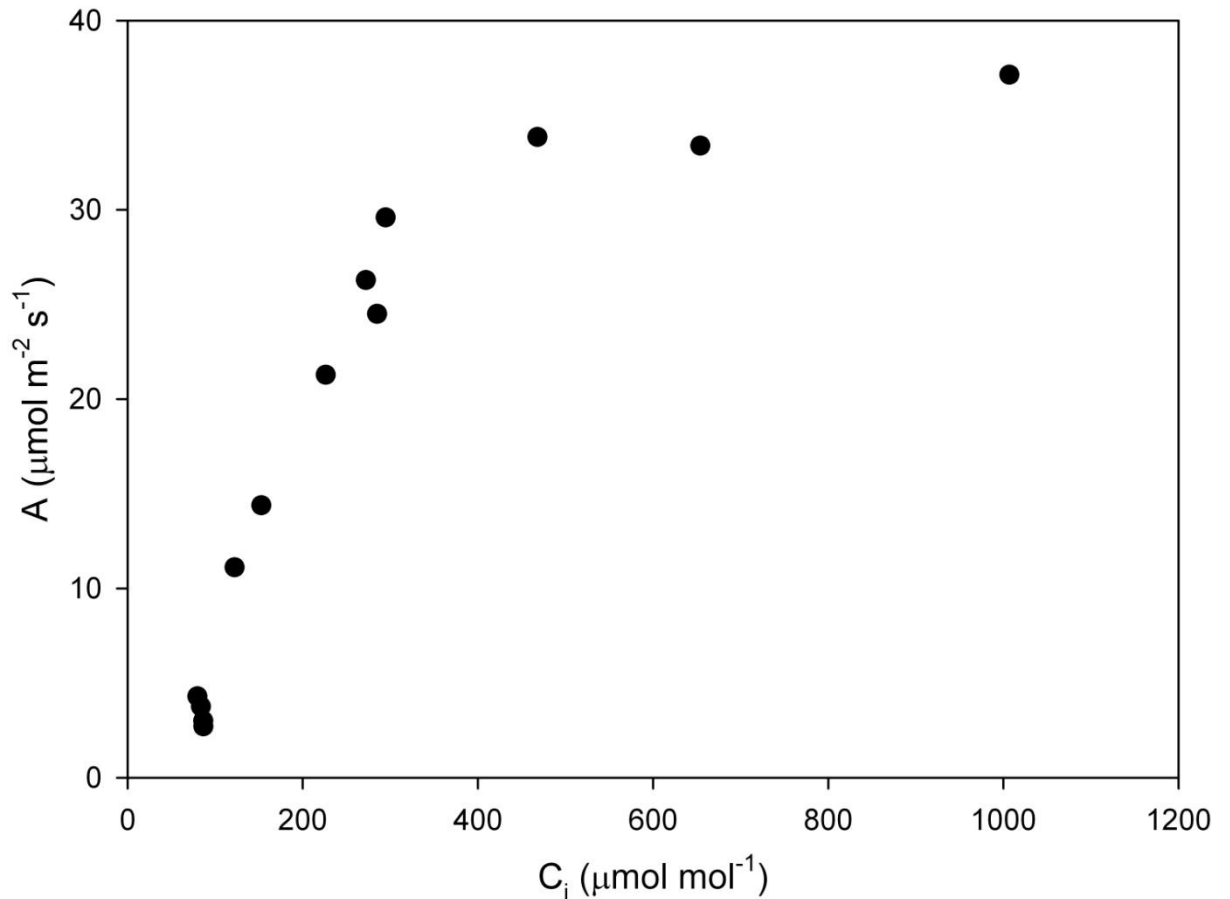


Figure 5.3 Example A/C_i curve demonstrating the relationship between net assimilation (A) and substomatal carbon dioxide concentration (C_i) for a wild type IR64 rice plant.

In order to fit the A/C_i curves for analysis, C_i is converted to C_c (chloroplast [CO₂]) using the following equation:

Equation 5.3
$$C_c = C_i - \frac{A}{g_m}$$

where g_m is the conductivity of the mesophyll cells to CO₂. Also the portion of the curve represented by each phase is determined (Figure 5.4).

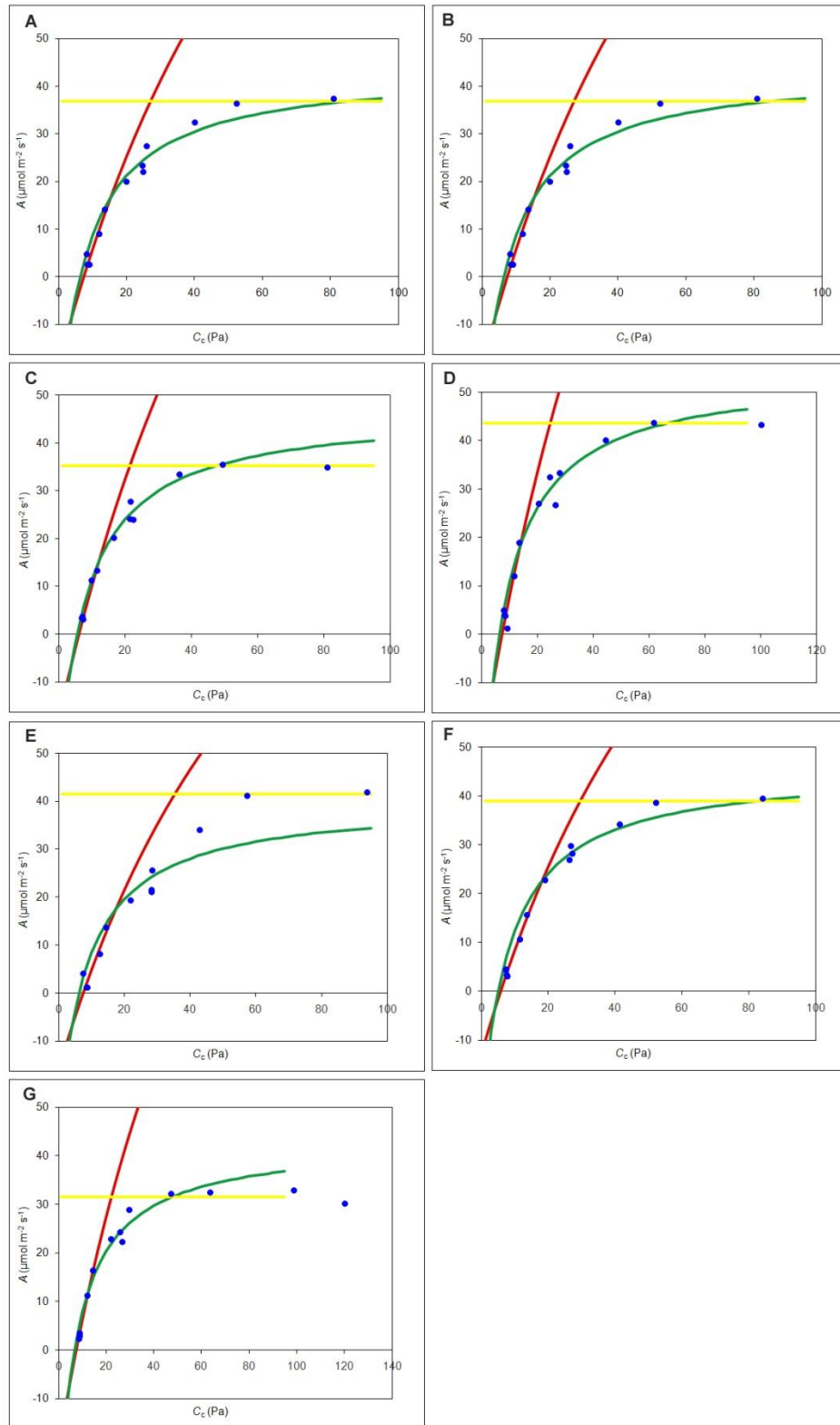


Figure 5.4 Sample output from the curve fitting tool. Blue circles (A_{obs}) denote the observed values of A at a known C_c . The red line represents the portion of photosynthesis described by the Rubisco-limited state, the green line the RuBP-regeneration state and the yellow line the TPU state. **A**, WT; **B**, *alm1*; **C**, *alm2*; **D**, *alm3*; **E**, *alm4*; **F**, *alm5*; **G**, *alm6*.

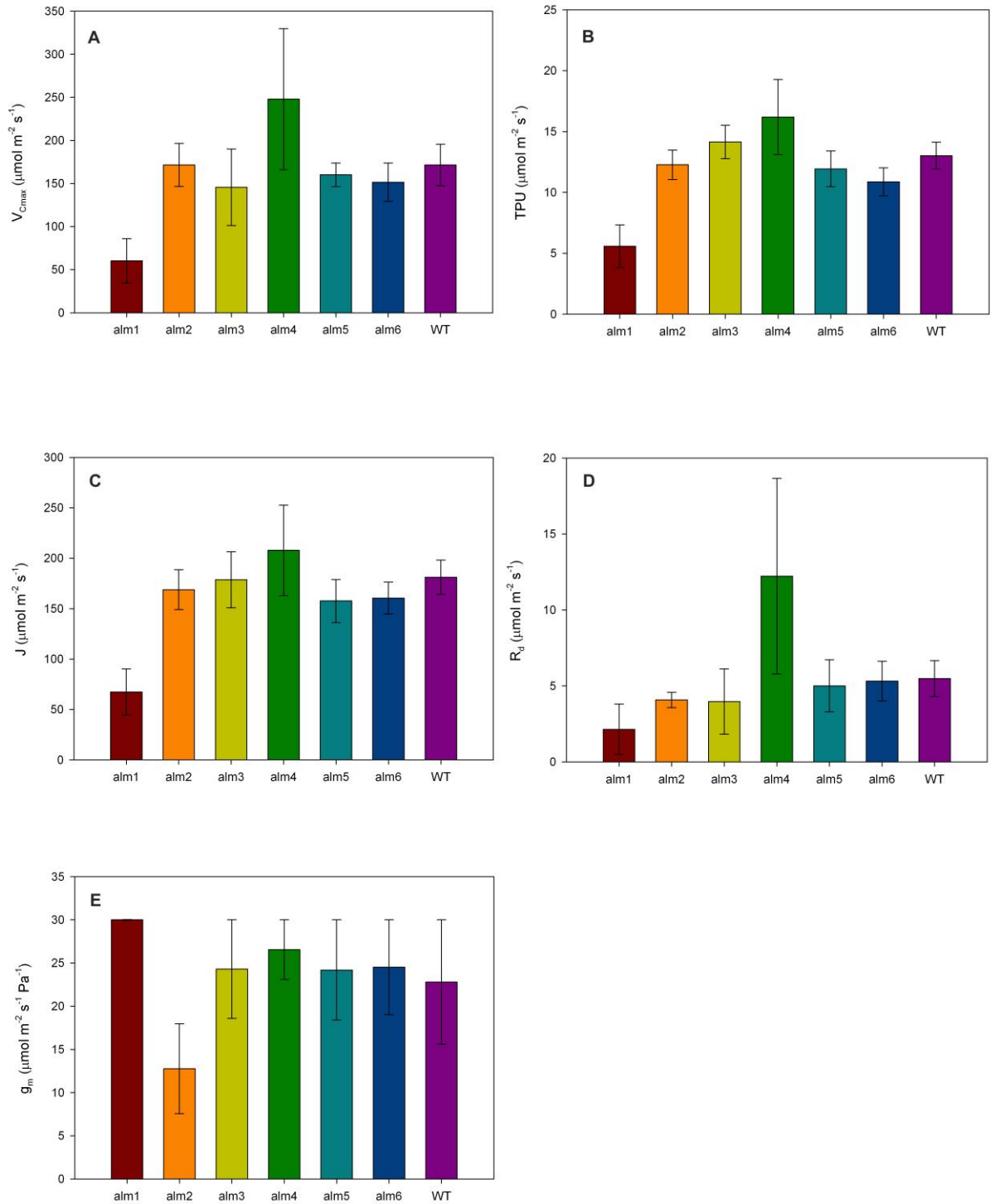


Figure 5.5 Values determined from fitted A/C_i curves measured at leaf temperature (T_{leaf}). **A**, Maximum rate of carboxylation ($V_{C_{max}}$); **B**, Triose phosphate utilisation (TPU); **C**, Rate of electron transport (J); **D**, Dark respiration rate (R_d); **E**, Mesophyll cell conductance (g_m). Bars denote single standard error of the mean ($n=5$).

Figure 5.5 shows that the *alm* lines displayed a variety of different responses to CO₂ in terms of maximum rate of carboxylation by Rubisco (VC_{max}), triose phosphate utilisation (TPU), rate of electron transport (J) dark respiration rate (R_d) and mesophyll cell conductance. However, these observations are based on the measured values at leaf temperature. As all measurements were taken in the controlled environment room the variation in leaf temperature was small (29.0°C – 30.2°C); however it was still necessary to normalise these values to an equal temperature, within the curve fitting model to account for temperature dependant differences in enzyme kinetics and allow accurate direct comparison between the lines (Figure 5.6).

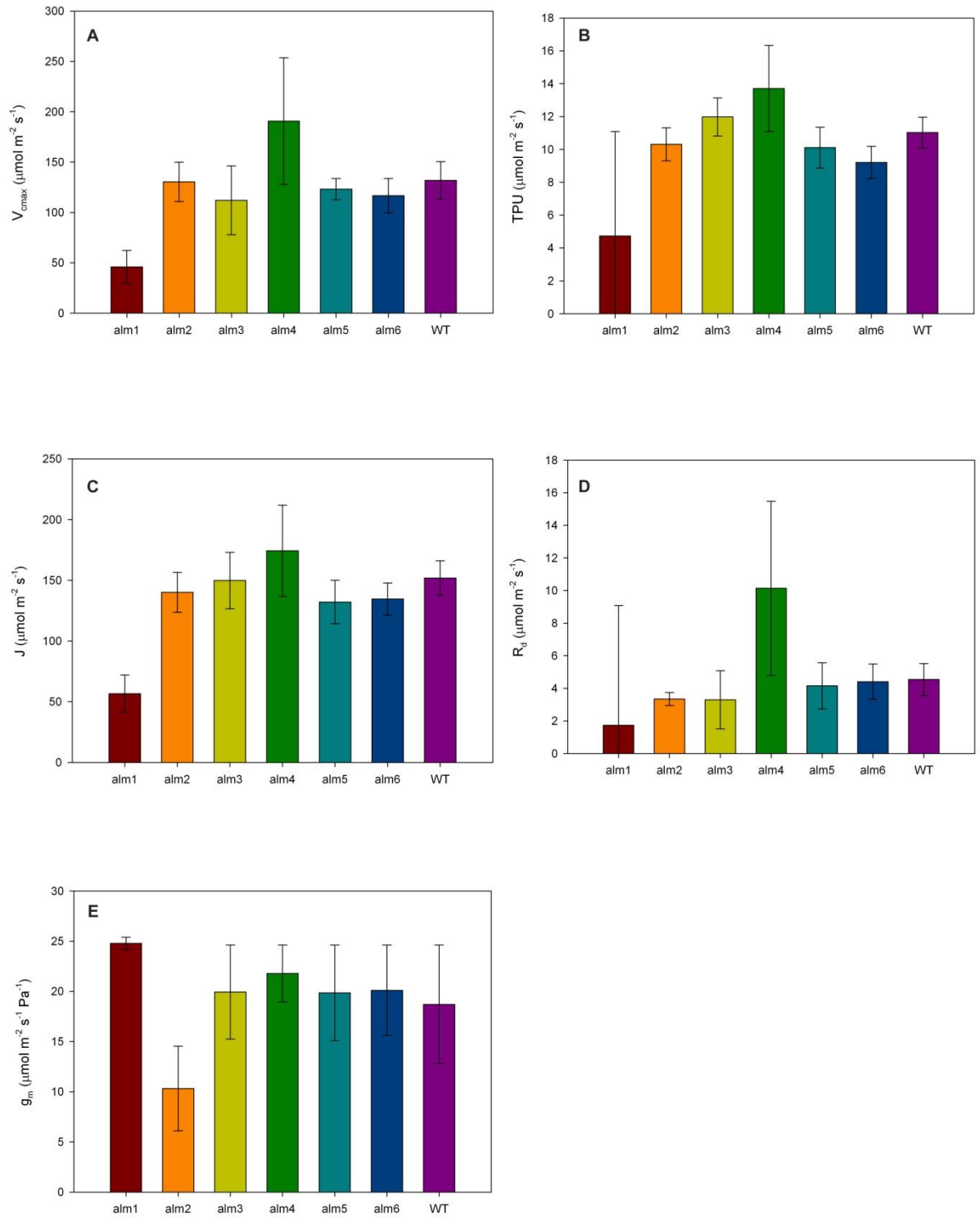


Figure 5.6 Values determined from fitted A/C_i curves, normalised to a leaf temperature of 25°C. **A**, Maximum rate of carboxylation ($V_{C_{max}}$); **B**, Triose phosphate utilisation (TPU); **C**, Rate of electron transport (J); **D**, Dark respiration rate (R_d); **E**, Mesophyll conductance (g_m). Bars denote single standard error of the mean ($n=5$).

Figure 5.6 shows that although variation was present, there were few significant differences detected when the *alm* lines were compared to wild type plants. ANOVA testing showed that plants of the *alm1* line displayed a significantly reduced maximum rate of carboxylation (VC_{\max}) compared with wild type rice plants ($P < 0.05$, Figure 5.6 A). No other *alm* line displayed a significant alteration. Carboxylation is carried out by Rubisco and the observed reduction in VC_{\max} could be due to a number of factors including a reduction in the quantity of Rubisco present within the leaf, reduced specificity of Rubisco to CO_2 , or an increased affinity for O_2 . As the kinetic properties of Rubisco such as O_2 and CO_2 affinity are highly conserved between higher plant species, the most likely explanations are a reduced amount of Rubisco protein, or an inhibition of its activity. This could potentially be caused by reduced Rubisco activase activity or inhibition through abiotic stress, which is itself unlikely under the controlled growth conditions.

Figure 5.6B shows that *alm1* plants demonstrated a low triose phosphate utilisation (TPU) compared to wild type IR64 rice plants. Despite the large standard error demonstrated, ANOVA showed that TPU was lower in *alm1* plants than in wild type plants ($P < 0.05$). TPU in the other *alm* lines was not significantly altered compared to wild type plants.

alm1 plants also demonstrated a lower rate of electron transport (J) than those of the wild type (Figure 5.6 C) when compared using ANOVA ($P < 0.01$). Although variation in J was observed in the other *alm* lines, this was not significant ($P > 0.05$ in all cases).

Although *alm3* plants displayed a large elevation in dark respiration rate (R_d) compared to wild type plants and *alm1* plants a slightly reduced rate, ANOVA testing showed neither to be significantly altered ($P = 0.60$ and 0.16 respectively). R_d specifically relates to the dark respiratory release of CO_2 and does not include photorespiration. This would suggest that no *alm* line displayed a significant alteration in terms of mitochondrial activity or number.

No *alm* line showed significant alteration in mesophyll conductance (g_m) compared to wild type plants.

5.4 Response to PAR

As stated in Section 5.1.3, quantum yield can be considered as the fraction of absorbed PAR which is consumed in photochemistry, and is a measure of photosynthetic efficiency. Quantum yield of photosynthesis can be derived from the light-limited, linear, portion of light response curves. However, quantum yield can also be calculated using fluorescence measurements from dark adapted plants.

Equation 5.1 states that the energy from PAR wavelengths absorbed by chlorophyll may be released as heat (H), fluorescence (F) or in the photochemical reactions (P). At saturating PPFD levels no further increase in P is possible with increasing PPFD, so P becomes zero and de-excitation of electrons is assumed to be due to H and F , which are at their maximal values (H_m and F_m) respectively. This gives the equations:

Equation 5.4
$$F_m + H_m + 0 = 1$$

so

Equation 5.5
$$H_m = 1 - F_m$$

It is assumed that the ratio of heat to fluorescence does not change during a short pulse of saturating light, therefore:

Equation 5.6
$$\frac{H}{F} = \frac{H_m}{F_m}$$

By substitution of Equation 5.5, this can be re-written as

Equation 5.7
$$H = \frac{F(1 - F_m)}{F_m}$$

As the equation for H has been determined and fluorescence was measured, quantum yield (P) is calculated by substitution of Equation 5.7 into Equation 5.1 to give:

Equation 5.8
$$P = \frac{F_m - F_o}{F_m} = \frac{F_v}{F_m}$$

where F_o is the minimal fluorescence measured in dark adapted plants, and F_v is the variable fluorescence ($F_m - F_o$).

Equation 5.8 therefore shows that the ratio of variable to maximal fluorescence (F_v/F_m) in dark adapted leaves can be used to calculate quantum efficiency (Figure 5.7).

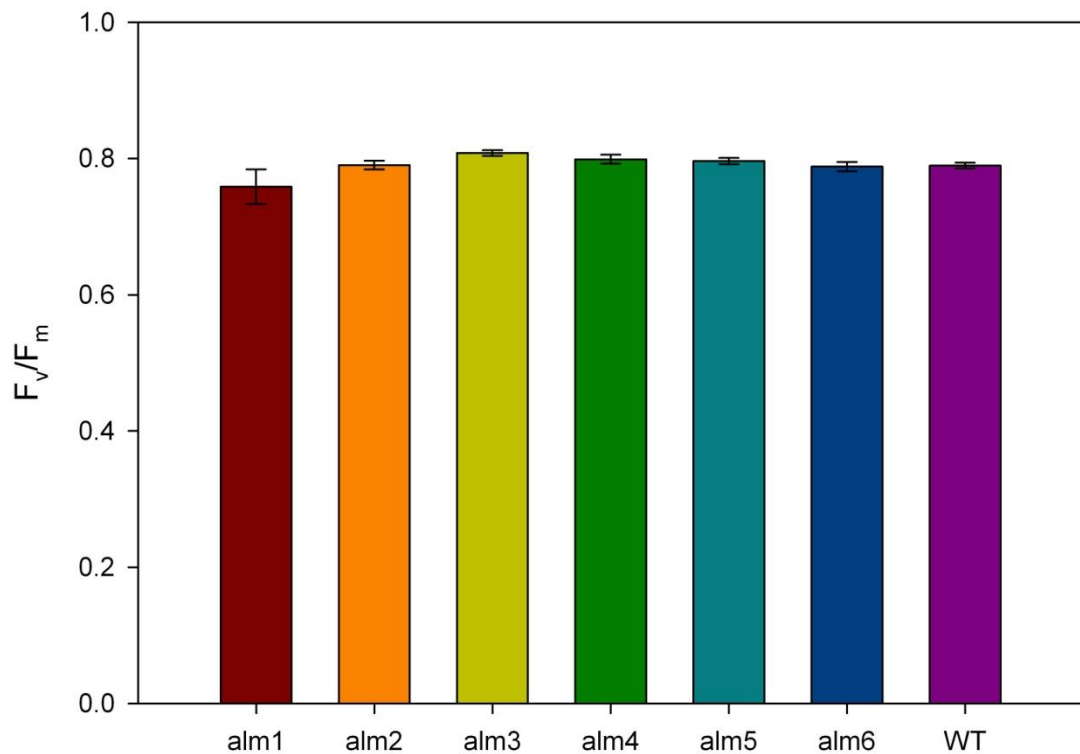


Figure 5.7 Quantum yield (F_v/F_m) of WT and *alm* mutant lines of rice. Bars denote single standard error of the mean ($n=5$).

As a measure of the efficiency of absorption of energy obtained from solar radiation into the photosynthetic pathway, quantum yield can be considered to be the major limiting factor in the net photosynthetic

response to PPFD. As is clearly shown by Figure 5.7, there was no significant difference between the *alm* lines in terms of the initial gradient of the slope (the apparent quantum yield of CO₂ assimilation). *alm1* had a slightly lower initial gradient of the CO₂ assimilation response, and a slightly reduced quantum yield, but neither was significantly reduced.

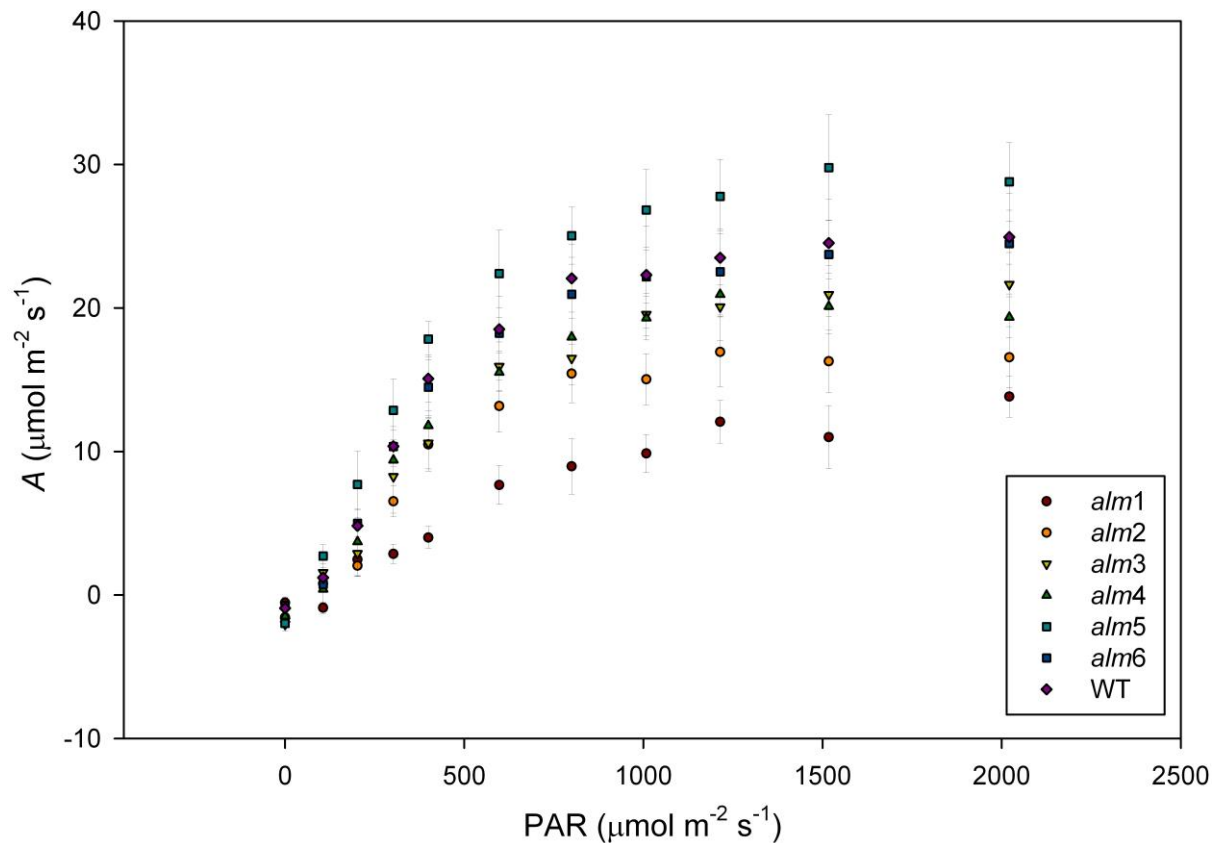


Figure 5.8 Response of net photosynthesis (A) to varying photosynthetically active radiation (PAR). Bars denote single standard error of the mean ($n=5$).

Plants belonging to the lines *alm1*, *alm2* and *alm4* all displayed a significantly lower maximum A when compared to wild type plants ($P < 0.001$, $P < 0.05$ and $P < 0.05$ respectively). There are several possible causes for the observed reduction in A_{\max} . Figure 5.6B showed that *alm1* plants displayed a significantly reduced TPU, an important limiting factor for A_{\max} (see Section 5.5). Lines *alm2* and *alm4* did not display any significant reduction in the CO₂ response-specific factors outlined in Section 5.3, perhaps suggesting that a light dependent factor or process was responsible for limiting A_{\max} in these plants.

Curves fitted to the light response graphs using the statistical program Photosyn Assistant (Dundee Scientific, Scotland) showed that A at light respiration (mitochondrial respiration plus photorespiration) was in the range -2.15 to $-2.39 \mu\text{mol m}^{-2} \text{s}^{-1}$ in plants of the *alm2-6* lines and the wild type. Assimilation under light respiration conditions in *alm1* plants was much higher at $-1.30 \mu\text{mol m}^{-2} \text{s}^{-1}$. Dark respiration was unchanged in plants of the *alm1* line (Figure 5.6D), suggesting that *alm1* plants displayed a reduction in photorespiration compared to the other *alm* lines.

Curve fitting also showed variation in the light compensation point (the PPFD at which net assimilation is 0). The light compensation point was reasonably well conserved in lines *alm5* and *alm6* and wild type plants, at $45 - 50 \mu\text{mol m}^{-2} \text{s}^{-1}$, but was much greater in the *alm4*, *alm3*, *alm2* and *alm1* lines, at 65.4 , 68.0 , 76.9 and $82.4 \mu\text{mol m}^{-2} \text{s}^{-1}$ respectively. This suggests that plants of these lines displayed an increasingly compromised photosynthetic response to light, as is reflected by the lower values for A_{max} displayed in Figure 5.8.

5.4.1 Gas exchange response to varying PAR

As the rate of photosynthesis (A) increases, it is expected that the rate of transpiration will also increase due to the increase in stomatal aperture which is required in plants which do not possess the crassulacean acid metabolic (CAM) pathway in order to increase CO_2 supplies to support the increasing rate of photosynthesis. However, transpiration is often limited by partial or complete stomatal closure when water supply is restricted, as an increasing rate of water loss causes the risk of water stress. Therefore photosynthetic rates are closely linked to stomatal aperture to prevent unwanted water loss by transpiration (Figure 5.9).

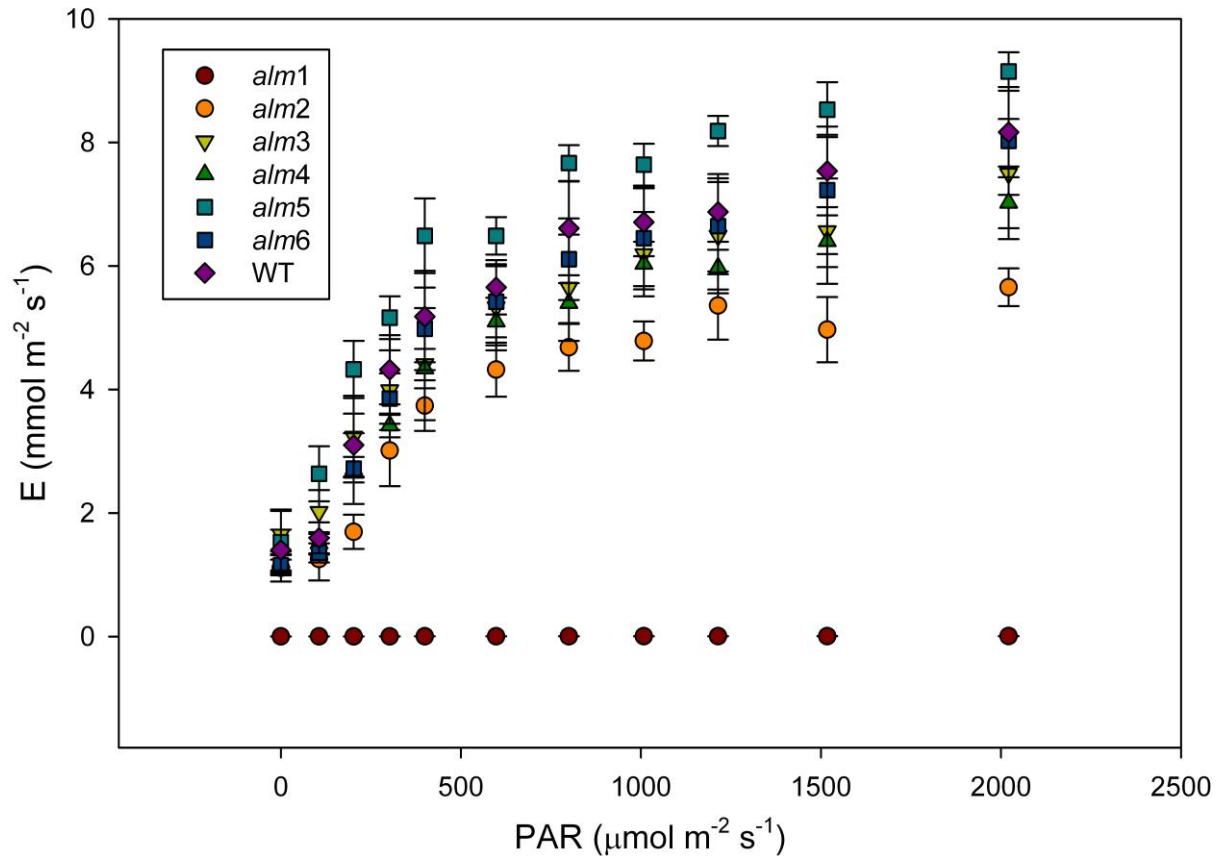


Figure 5.9 Response of transpiration rate (E), to varying PAR. Bars denote single standard error of the mean (n=5).

Figure 5.9 shows that the majority of the *alm* lines displayed no significant difference in levels of transpiration when compared to wild type plants. *alm1* displayed almost zero transpiration, this would suggest that plants of the *alm1* line either do not produce stomata, or produce stomata which are predominantly closed. As it was shown in Chapter 4 that plants of the *alm1* line possessed a stomatal density which was not significantly different to wild type plants, this suggests that although stomata are present, they remain closed to give an extremely low stomatal conductance. This would also explain the relatively low levels of net photosynthesis displayed even at high light intensities shown by *alm1* plants in Figure 5.8. *alm2* did not display a statistically altered transpiration rate until very high PPFD levels were reached. Transpiration in *alm2* plants was significantly lower than in the wild type at a PPFD of $2000 \mu\text{mol m}^{-2}$ suggesting either that *alm2* plants produced a reduced

number of stomata or stomatal conductance is being limited at high PPFD levels. As with *alm1*, *alm2* plants displayed no significant reduction in stomatal density (Chapter 4), suggesting that stomatal conductance was limited. It is possible that the stomata of *alm2* plants were smaller than those of the wild type, giving a reduced maximum stomatal aperture and in turn a reduced stomatal conductance, or stomatal size may be unchanged but signalling within the plant could be causing their partial closure. Alternatively, water uptake may have been limited in *alm1* and *alm2* plants, which would have reduced transpiration even if stomata were fully open. Drought conditions would have also given this effect, although this was not the case in the present study as the plants were grown in a hydroponic system with ample available water (see Chapter 2 for methods relating to plant production).

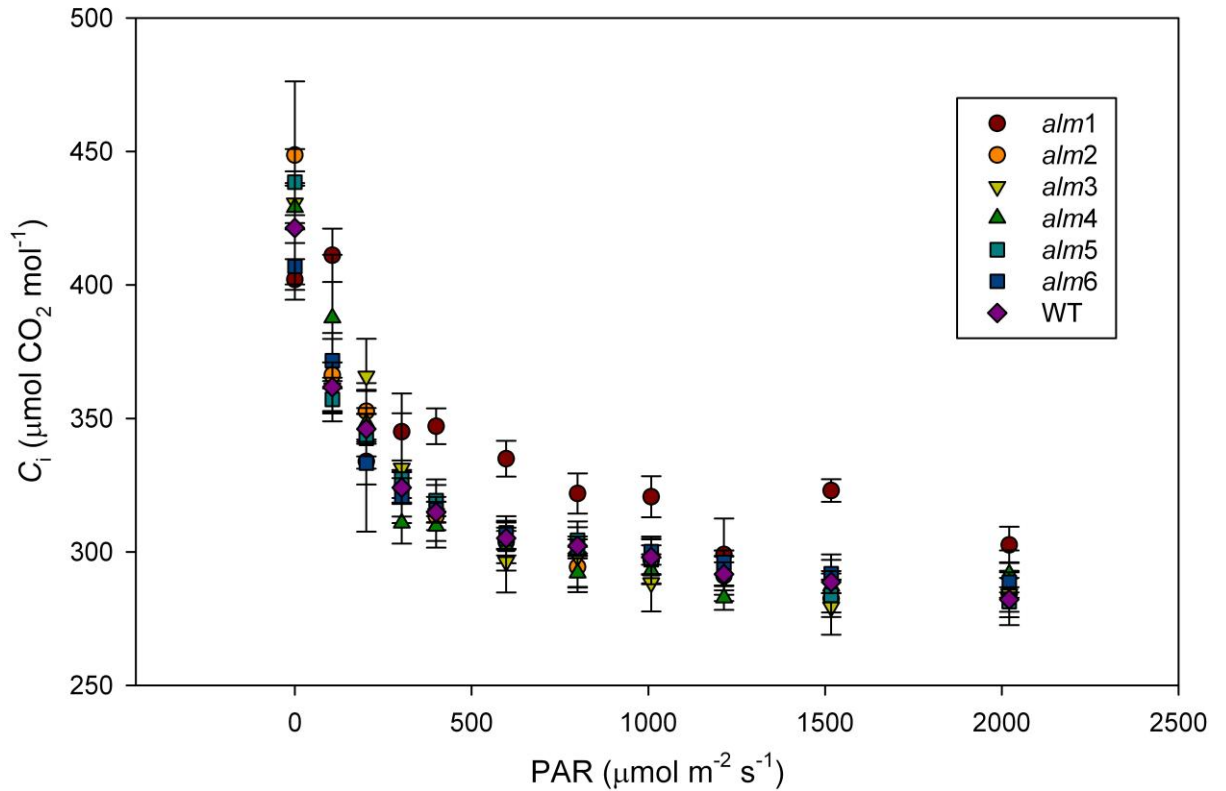


Figure 5.10 Response of substomatal CO_2 concentration (C_i) to PAR flux. Bars denote single standard error of the mean ($n=5$).

The shape of the curves shown in Figure 5.10 can be explained as follows. As the rate of photosynthesis increases, the demand for CO_2 also increases. As PPFD is increased and high rates of photosynthesis are reached CO_2 cannot diffuse into the leaf as fast as it is consumed even when the stomata are fully open and this causes C_i to decrease. If C_i becomes limited to such an extent that photosynthesis is inhibited, a slight rise in C_i may be observed as CO_2 is released by respiration.

ANOVA testing showed that *alm1* plants displayed a significantly higher C_i at the PPFD values $>400 \mu\text{mol m}^{-2} \text{s}^{-1}$ compared to the wild type plants ($P < 0.01$). This would suggest either that photosynthesis was consuming less carbon dioxide than wild type plants, or that CO_2 was able to diffuse into the leaf to maintain higher levels of C_i . The previously mentioned limitations on TPU and A_{max} displayed by plants of the *alm1* line suggest that photosynthesis was limited and did not consume CO_2 at the same rate as wild type plants.

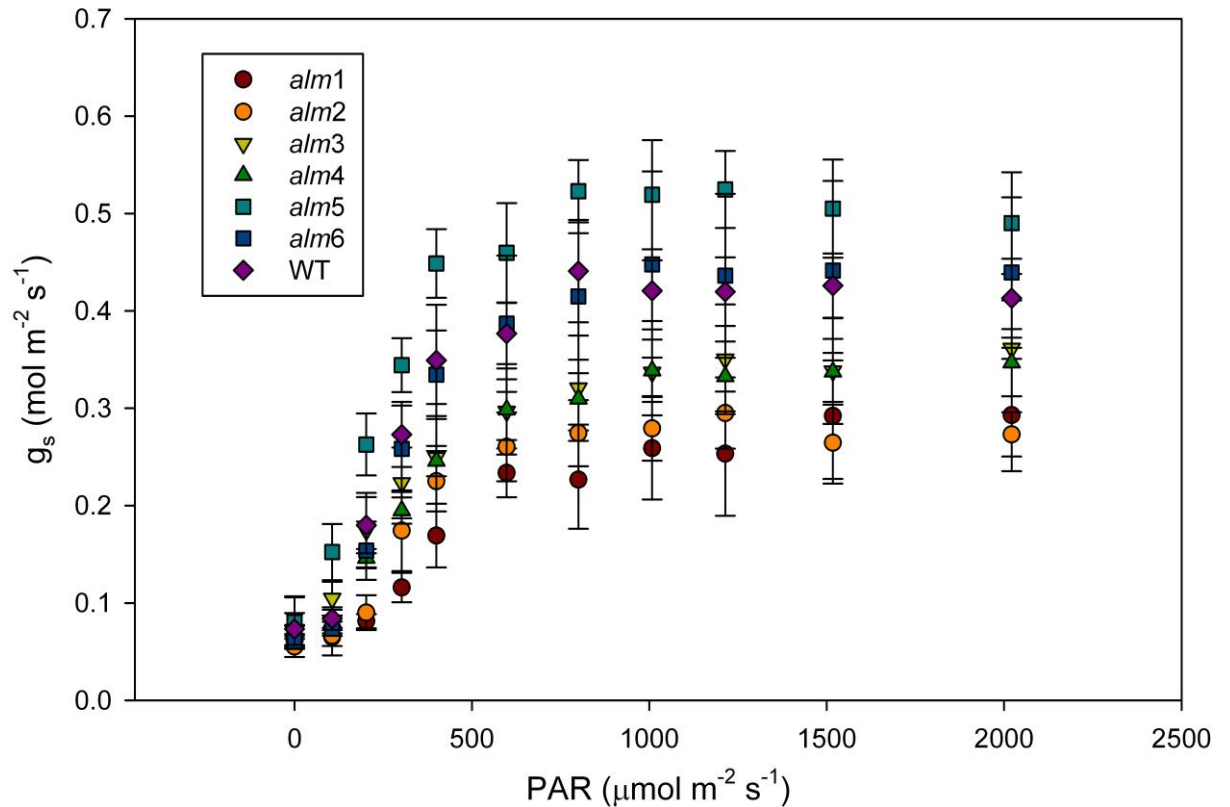


Figure 5.11 Response of stomatal conductance (g_s) to PAR flux. Bars denote single standard error of the mean ($n=5$).

The initial response of stomatal conductance to increasing PPFD was well conserved between the *alm* lines and wild type plants (Figure 5.11), although significant variation in the maximum stomatal conductance was observed. Plants of the *alm2* line had the lowest stomatal conductance ($P < 0.01$). As it was reported in Section 4.3.5 that none of the *alm* lines displayed changes in stomatal density, this does not explain the observed differences in stomatal conductance. Stomatal conductance is, however, under the control of hormones such as ABA (abscisic acid), and differing hormonal levels or sensitivities may have been responsible for these differences in observed stomatal conductance.

5.4.2 Electron transport in photosynthesis

The majority of rice *alm* lines displayed no significant alteration in the quantum yield of photosystem II (Φ_{PSII}) compared with wild type plants. However, plants of the *alm1* line displayed a significantly reduced ETR ($P < 0.001$) at all PPFD levels except darkness.

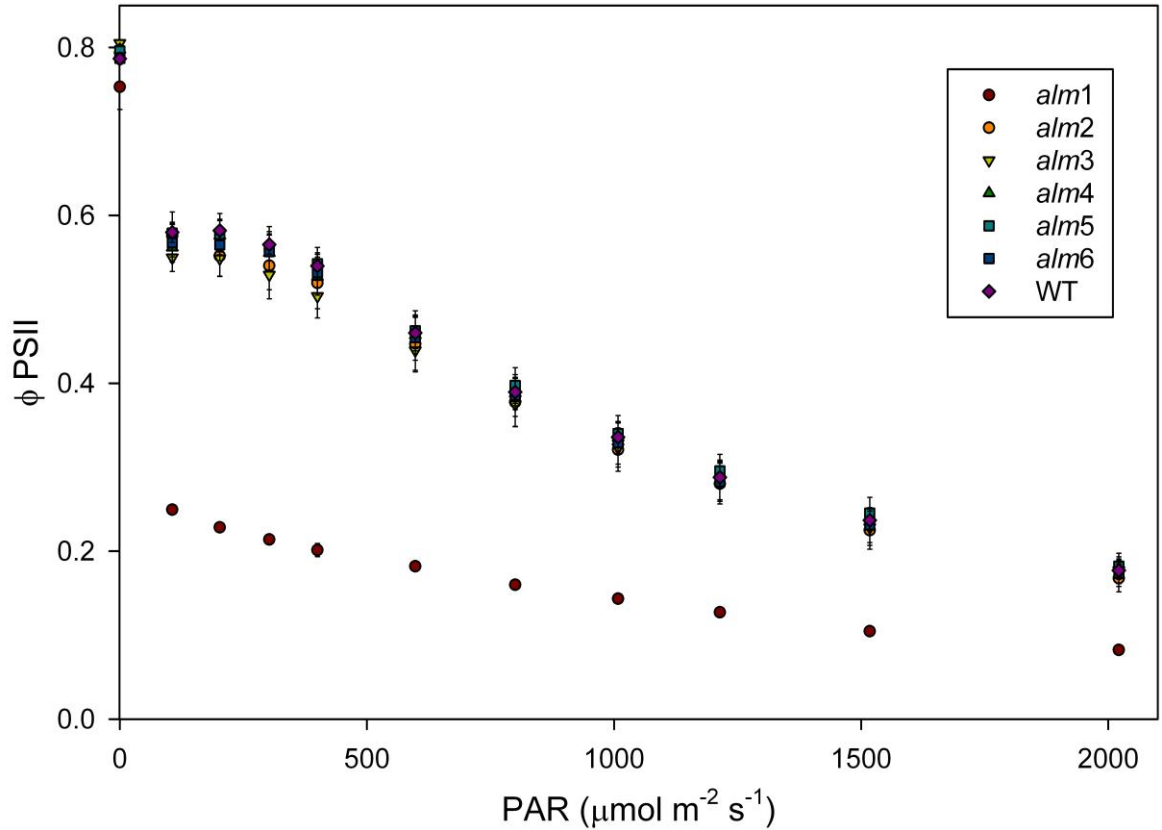


Figure 5.12 Response of quantum yield of photosystem II (Φ_{PSII}) to varying PAR flux. Bars denote single standard error of the mean.

Electron transport rate is a function of Φ_{PSII} and can be described by the following equation:

Equation 5.9
$$ETR = \left(\frac{F_m' - F_s}{F_m'} \right) fI\alpha_{leaf}$$

where $\left(\frac{F_m' - F_s}{F_m'}\right)$ represents ΦPSII in a light-adapted leaf at steady state photosynthesis, f is the fraction of absorbed quanta used by PSII, I is the incident photon flux density and α_{leaf} is leaf absorptance. Therefore, it can be said that:

Equation 5.10 $\text{ETR} = \Phi\text{PSII} \times \text{leaf absorptance} \times \text{electron requirement}$

Changes in any of these characteristics will influence ETR.

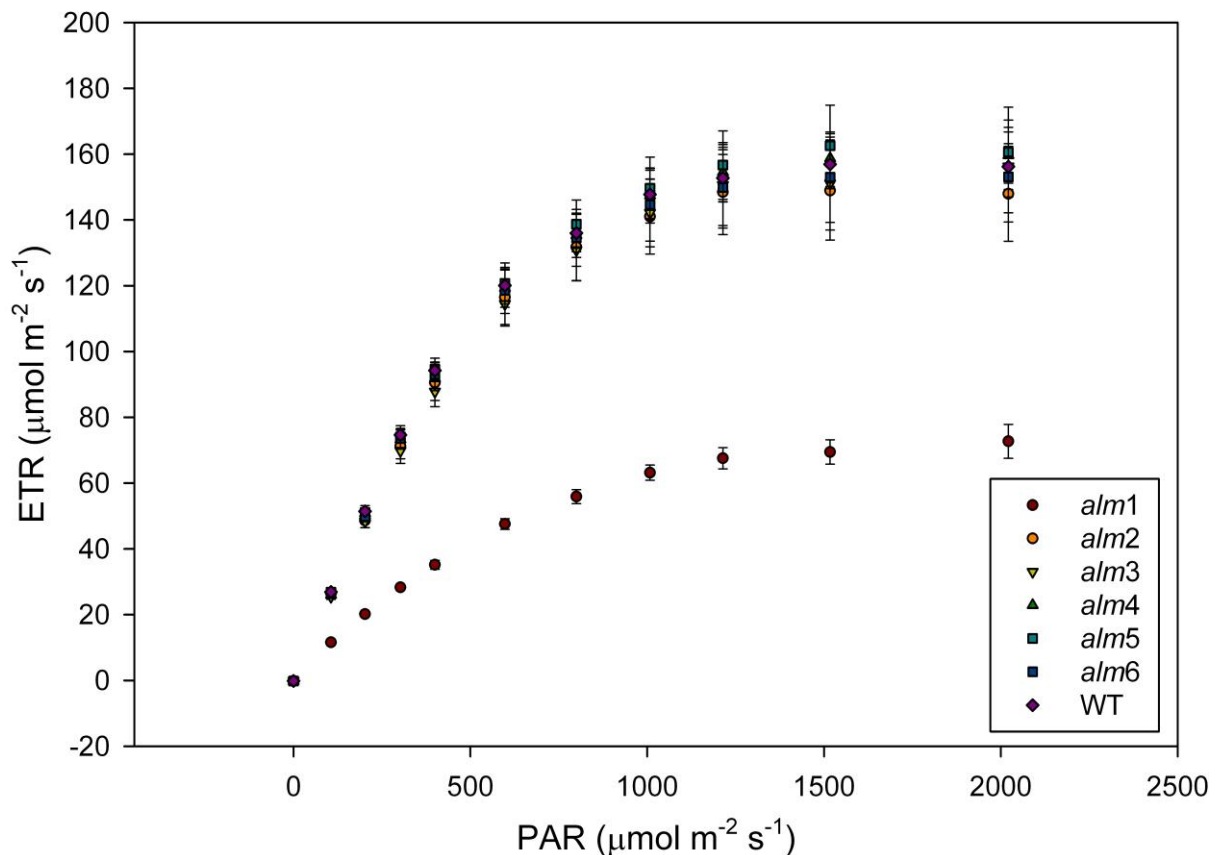


Figure 5.13 Response of electron transport rate (ETR) to PAR flux. Bars denote single standard error of the mean (n=5).

The majority of lines displayed no significant alteration in ETR compared to wild type plants. However, ANOVA showed that plants of the *alm1* line displayed a reduced ETR ($P < 0.001$) at all PPFD levels examined except darkness. This was expected as Figure 5.12 showed that ΦPSII was reduced in *alm1* rice plants compared to wild type plants.

As none of the other *alm* lines demonstrated an alteration in Φ_{PSII} or ETR, it can be assumed that absorptance of the leaf and the electron requirement of photosynthesis also remain unchanged in these lines.

5.4.3 Photoprotection

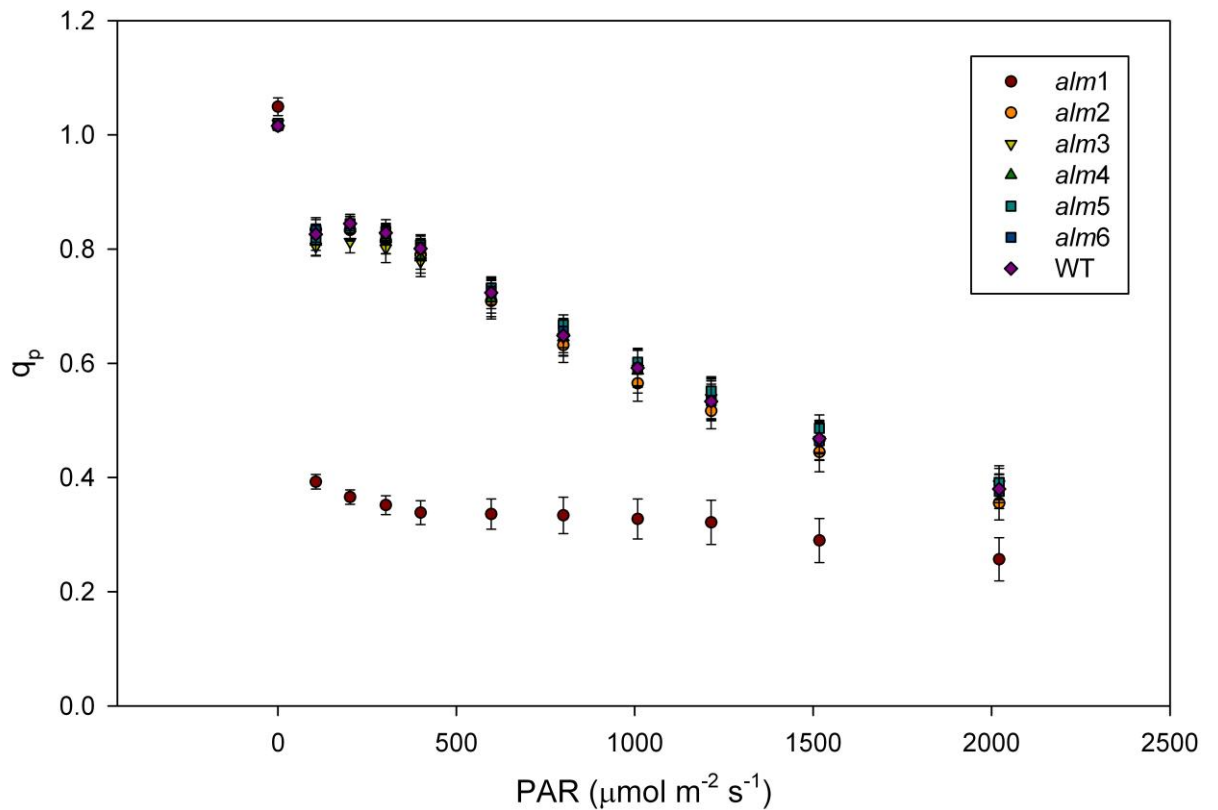


Figure 5.14 Response of photochemical quenching (q_p) to PAR flux. Bars denote single standard error of the mean ($n=5$).

alm1 demonstrated extremely low levels of photochemical quenching (q_p), with values of less than 0.4 even at low PPFD levels (Figure 5.14). ANOVA testing showed this was lower than wild type rice plants ($P<0.001$). This observation suggests that *alm1* plants were very highly photoinhibited at PPFD levels which were not saturating to wild type plants. Given the observed lack of activity at low PPFD levels demonstrated by plants of the *alm1* line, it can be assumed that PSII electron transport was greatly inhibited. This theory also explains the

observed low ETR displayed by *alm1* plants (Figure 5.13) and the reduction in assimilation (Figure 5.8) compared to wild type rice plants.

Non-photochemical quenching (NPQ) in the *alm* lines was largely unchanged compared to wild type plants (Figure 5.15).

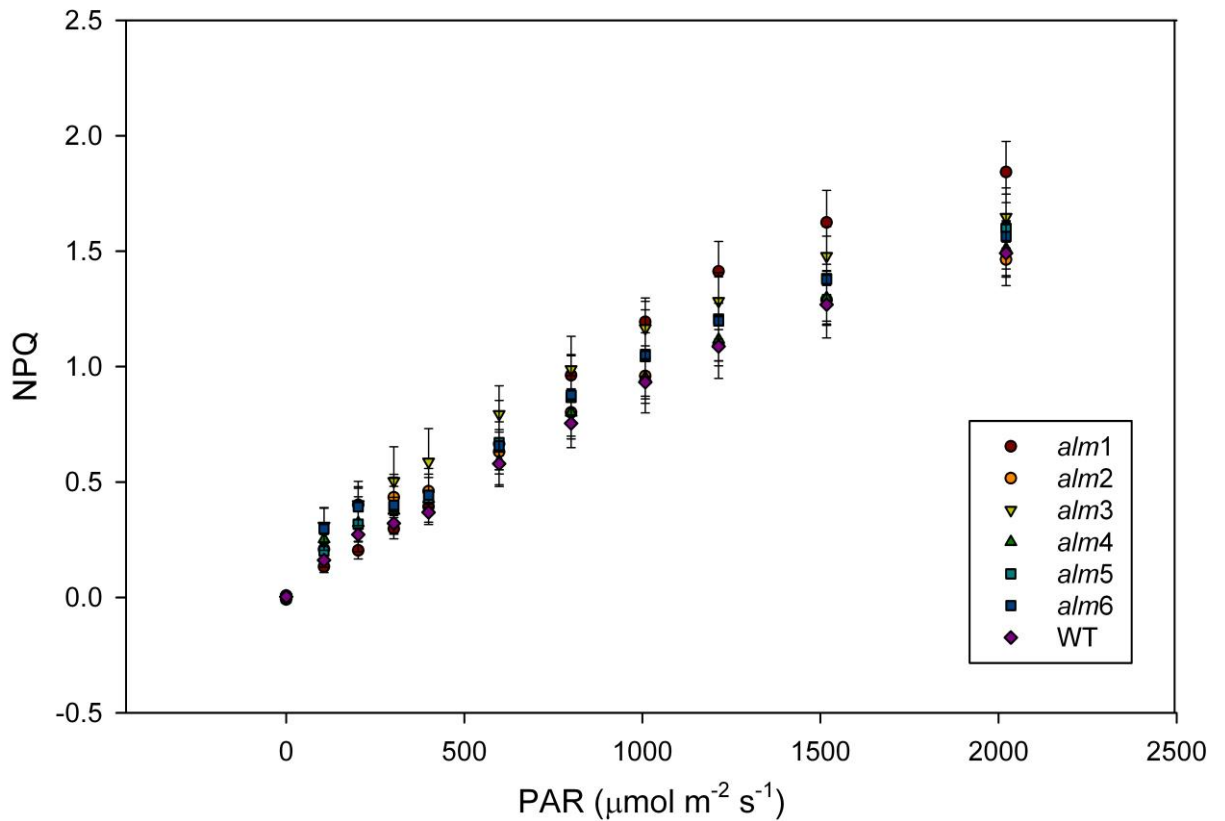


Figure 5.15 Response of non-photochemical quenching (NPQ) to PAR flux. Bars denote single standard error of the mean (n=5).

At low PPFD levels NPQ was initially present at lower levels in plants of the *alm1* line than in wild type rice plants, however NPQ became more extensive at higher light intensities in *alm1* than the wild type. However, ANOVA testing did not show the difference in levels of NPQ to be significant ($P = 0.08$ at $2000 \mu\text{mol m}^{-2} \text{s}^{-1}$ PAR). The low levels of assimilation demonstrated by *alm1* plants (Figure 5.8) suggest that much of the quanta absorbed by the leaf is not used to drive photosynthesis, and would therefore require elevated levels of NPQ to dissipate excess energy and prevent damage to the leaf.

5.5 Discussion

It was hypothesised that the anatomical responses described previously may influence the physiological responses displayed in this chapter for a number of reasons. It was shown in Chapter 4 that several of the *alm* lines produced mesophyll cells which were significantly smaller than in wild type rice. Dunstone and Evans (1974) noted that the mesophyll cells of diploid wheat species were significantly smaller than the more commonly grown hexaploid species and it was shown that photosynthetic rate in the *Triticum* species was negatively correlated with mesophyll cell size. This phenomenon was also observed in *Lolium perenne* (Wilson and Cooper, 1969), and was shown to exist in fifteen species including sorghum, cotton, soybean, sunflower and maize by El-Shakawy and Hesketh (1965). The observed increase in *A* may be the result of an increased mesophyll conductance to CO₂ due to the increased surface area to volume ratio of smaller mesophyll cells, although this is speculation. It was therefore hypothesised that *alm* lines producing mesophyll cells with a significantly reduced plan area compared to wild type plants may display an improved photosynthetic response.

A number of *alm* lines also displayed a significantly reduced interveinal distance, i.e. vein density was increased. It was hypothesised that increased vein density may increase hydraulic conductance, with which *A* is known to be positively correlated. It was stated by Roth-Nebelsick *et al.* (2001) that the arrangement and density of vascular architecture affect the transport of water and carbohydrates by influencing hydraulic conductance. Furthermore, it was shown by Brodribb *et al.* (2007) that vein density, leaf thickness and cell shape were strongly correlated with hydraulic conductance and maximum photosynthetic rate. It was later stated by Brodribb and Feild (2010) that increasing hydraulic conductance allowed the evolution of increased photosynthetic capacity. The reasoning for this was that increased hydraulic conductance allows more rapid transport of water throughout the plant, meaning that stomatal aperture can increase without risking water stress through increased transpiration, providing water is available to the root system. Increases in stomatal aperture cause an increase

stomatal conductance, thereby enhancing diffusion of CO₂ into the leaf and providing necessary substrate to support an increase in *A*.

However, although these factors would potentially allow an increase in *A*, no *alm* line showed any increase in photosynthetic capacity. Figure 5.6D shows that dark respiration remained unchanged in the *alm* lines, which shows that these lines displayed a reduction in *A* compared to wild type rice plants.

Plants belonging to the *alm1* line especially were highly stressed, as is clearly shown by the extreme reduction in q_p compared to the wild type (Figure 5.14). Physically, *alm1* plants were smaller than wild-type plants at sampling age and were also wilted in appearance. When growth is restricted, large levels of excess excitation energy may occur (Demmig-Adams and Adams, 2006), which can cause the formation of reactive oxygen species (ROS) which are potentially harmful to the leaf (Ledford and Niyogi, 2005). This effect is avoided by the slightly elevated levels of NPQ displayed by *alm1* (Figure 5.15). However, plants of the *alm2* and *alm4* lines also demonstrated a significant reduction in photosynthetic rate. Possible explanations for the physiological responses displayed by each of the *alm* lines in relation to their displayed anatomy are considered in the General Discussion. However, as previously mentioned, photosynthesis is a substantial and intricate process. Figure 5.16 shows a schematic diagram of the major protein complexes found in the thylakoid membrane. Modification of these as a result of mutation can cause their inactivation and ultimately inhibit photosynthesis, making it impossible to suggest what may cause a reduction in photosynthetic activity from physiological and anatomical data alone.

Yamori *et al.* (2011) showed that reductions in either the cytochrome (Cyt) *b₆f* complex or ATP synthase reduced electron transport rate and acted as a limiting factor to photosynthesis in transgenic tobacco leaves. This study was carried out using antisense constructs designed to target the Rieske iron-sulphur protein of the Cyt *b₆f* complex or the δ -subunit of chloroplast ATP synthase. It was shown that reduction of the Cyt *b₆f* complex gave a larger decrease in ETR than a reduction in ATP synthase,

suggesting that Cyt b_6f is a more likely limiting factor for photosynthesis than ATP synthase.

The effects of damage to the photosystem II complex were discussed by Takahashi and Badger (2011), who stated that, as PSII absorbs light, it is in a constant flux of damage and repair, with photoinhibition only occurring if damage is greater than repair. It was shown that photodamage occurred primarily in the oxygen-evolving complex of PSII, suggesting that this area of the molecule is particularly sensitive to disruption, either through photodamage or possibly through mutation. Inhibition of the repair process of PSII can also result in the observation of reduced q_p values.

Inhibition of any of the sensitive processes outlined above may result in the reductions in A displayed by plants of the *alm1*, *alm2* and *alm4* lines, or limit any expected gains resulting from the potentially favourable morphologies of plants of the *alm3*, *alm5* or *alm6* lines.

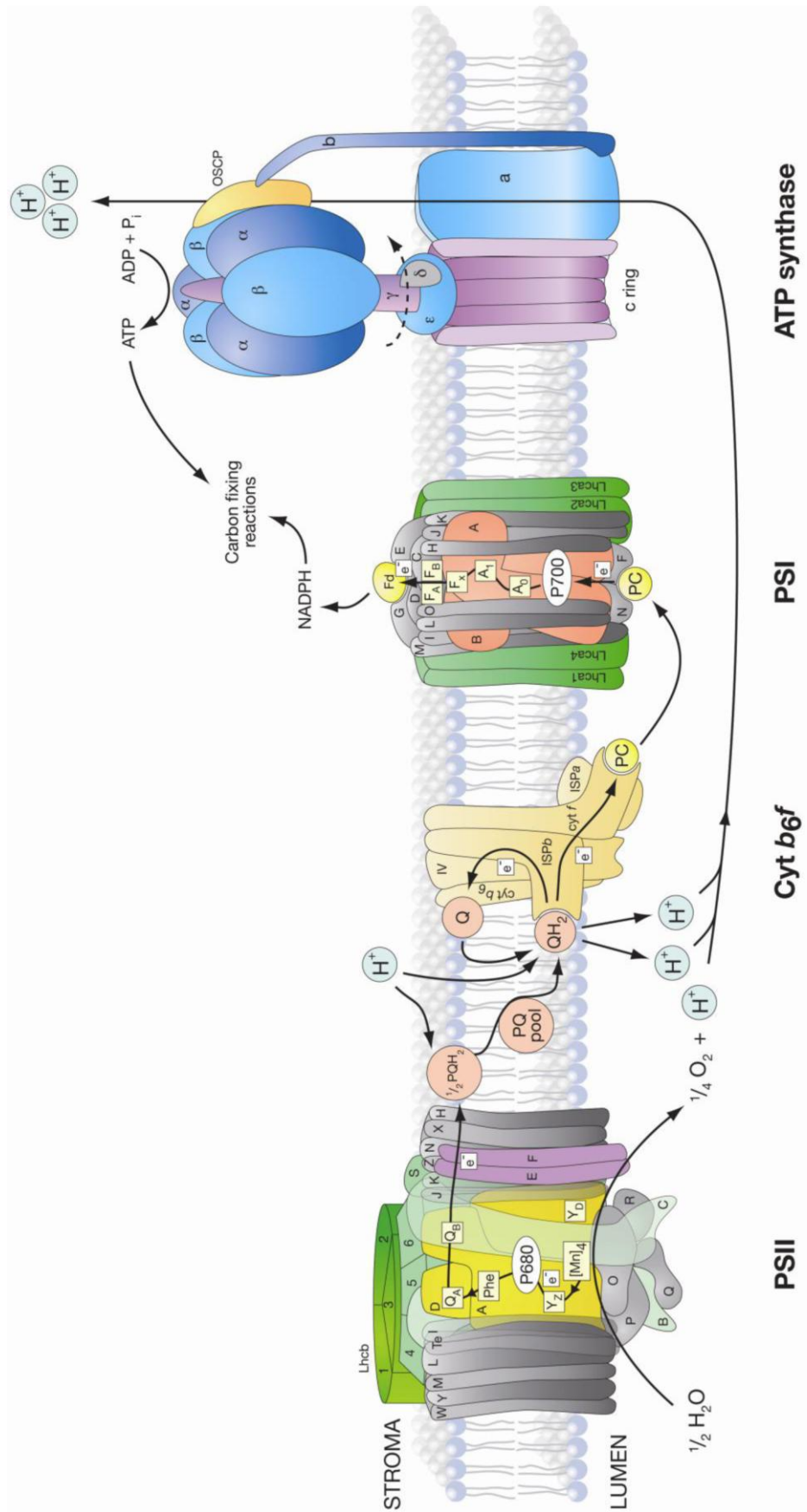


Figure 5.16 Schematic diagram of the major protein complexes of the thylakoid membrane. Taken from Pyke (2009)

Chapter 6

GENERAL DISCUSSION

Chapter 6: GENERAL DISCUSSION

6.1 Introduction

Chapter 3 introduced the mutant screen, which was responsible for the identification of interesting mutagenised lines of IR64 rice plants. In total, 100 lines were screened to identify alterations in leaf morphological traits compared to wild type plants. Of the 100 lines screened, seven were found to be of interest and termed altered leaf morphology (*alm*) mutants. Six of these lines were retained for further study.

The screen outlined in Chapter 3 was designed to have a high-throughput (lines screened / unit time) and, as such, required a compromise in terms of resolution, even though this was several-fold higher than in ongoing morphology screens at IRRI, which measured only vein density. An even higher resolution characterisation of the anatomy of the *alm* lines was discussed in Chapter 4 to provide a better understanding of the anatomical changes displayed by each mutant line. Chapter 5 was concerned with the physiological characterisation of the *alm* lines, primarily in terms of photosynthetic response.

This chapter considers the consequences of producing altered leaf morphologies in rice plants in terms of leaf function, and aims to evaluate the prospects for the production of rice plants capable of C₄ photosynthesis.

6.2 Conserved anatomical features of the rice leaf

It was shown in Chapter 3 that the mesophyll cells of the rice leaves were consistently small and highly lobed compared to those of other species. It has also been noted by Burundukova *et al.* (2003) and Chonan (1970) that rice mesophyll cells are amongst the smallest in crop plants. The combination of these factors causes the chloroplasts to be pushed to the cell periphery, resulting in a cell peripheral cover by chloroplasts of over 97% (Sage and Sage, 2009). It is thought that this high level of

peripheral cover has evolved in rice as a response to the high photorespiratory potential it is typically subject to as a result of high irradiance, high temperatures and high photosynthetic capacity. This is thought to aid photorespiratory CO₂ scavenging and / or maximisation of CO₂ diffusion into the chloroplast stroma.

6.2.1 Photorespiratory scavenging

It has been shown in C₃-C₄ intermediate plants that the oxygenation of RuBP in photorespiration results in the production of P-glycollate which is converted to glycine in the peroxisome (Monson, 1999), as in C₃ photorespiration. However, this is then allowed to diffuse from the mesophyll cells into the bundle sheath, where decarboxylation takes place within the mitochondria. The resulting release of CO₂ within the enlarged, organelle-rich bundle sheath has the effect of increasing CO₂ concentration within the bundle sheath chloroplasts (von Caemmerer, 1989).

It was suggested by Sage and Sage (2009) that rice makes use of a similar, single celled photorespiratory CO₂ scavenging system. Mitochondria are located within the centre of the mesophyll cells and are closely associated with the chloroplasts as a lack of available space ensures that all of the organelles are closely associated. This ensures that photorespiratory metabolites are easily able to diffuse into the mitochondria. The positioning of chloroplasts along the cell periphery and the extent to which it is covered ensures that, for photorespired CO₂ to leave the mesophyll cell, it must first pass through the chloroplast stroma. This should therefore result in an increase in stromal CO₂ concentration and improvement of the carboxylation capacity of Rubisco, depending on the rate of photorespiration. It has been shown that the C₃ species *Flaveria cronquistii* employs a similar system of photorespiratory scavenging, and refixes 48% of photorespired CO₂ at 28°C (Bauwe *et al.* 1987).

6.2.2 Mesophyll conductance to CO₂

For photosynthesis to occur, CO₂ must diffuse from the atmosphere (C_a), through the substomatal airspaces (C_i) to the chloroplast (C_c). The latter

step is determined by the mesophyll conductance to CO₂ (g_m), which is large enough to represent a limiting factor for photosynthesis (Flexas *et al.*, 2008). Under high light conditions it was estimated that g_m was responsible for a 30% reduction in C_c (Evans and von Caemmerer, 1996). Mesophyll conductance is primarily limited by the permeability of the membranes to CO₂ and the likelihood of CO₂ to reach the chloroplast (Evans and Loreto, 2000). The latter is greatly increased by the enlarged surface area of chloroplasts exposed to intercellular airspaces provided by the small mesophyll cell size, increased mesophyll cell surface area and localisation of chloroplasts to the cell periphery.

6.2.3 Implications of the conserved nature of cell size, lobing and chloroplast distribution

None of the lines observed during the mutant screen displayed obviously enlarged mesophyll cells, and the fact that the small mesophyll cell size compared to other species, deep lobing and chloroplast localisation to the periphery of the cells occurred in all of the *alm* lines and the wild type rice plants suggests that these characteristics are highly conserved. Sections 6.2.1 and 6.2.2 suggest possible evolutionary reasons for this to be the case and provide suggestions as to why these characteristics are desirable. Although introduction of a Kranz anatomy system of C₄ photosynthesis would represent a potential area for improvement in photosynthetic efficiency for rice under tropical conditions (Mitchell and Sheehy, 2006), this strong adaptation to minimisation of and recovery from photorespiration potentially explains why the C₄ photosynthetic pathway has never evolved in the *Oryza* genus of grasses.

This high degree of specialisation in minimising the impact of photorespiration may complicate any attempt to introduce the C₄ pathway into rice. The small mesophyll cell size and high degree of lobing in rice are inconsistent with C₄ grasses (Chonan, 1970), in which mesophyll cells exhibiting the typical Kranz anatomy are much larger than those of rice. If Kranz anatomy was to be introduced into rice with a typical interveinal mesophyll cell number of two and mesophyll cell size

remained as small as it currently is then either vein density would actually be higher than a typical C₄ leaf or if vein number were maintained, the leaf width would be very small.

The potential implications of the introduction of single celled C₄ photosynthesis into rice are more difficult. In recently discovered terrestrial single celled C₄ species such as *Bienertia cycloptera* and *Borszczowia aralocaspica*, Rubisco is spatially separated from intercellular airspaces to minimise its exposure to oxygen, whilst PEP carboxylation occurs in the cytosol at the cell periphery (Edwards *et al.*, 2004). This has been achieved in such species by the evolution of large, columnar cells to permit spatial separation of the different reactions and processes. In rice the inverse is true, with chloroplasts located at the cell periphery whilst any PEP carboxylase would be located in the central cytosol and only have access to CO₂ released from photorespiration or that which had succeeded in bypassing the chloroplast barrier (Sage and Sage, 2009). Any attempt to introduce single celled C₄ photosynthesis into rice would require the inversion of the chloroplast and cytosol arrangement within the mesophyll cell, which in turn would require a significant alteration in mesophyll cell size and shape to accommodate the chloroplasts (Figure 6.1).

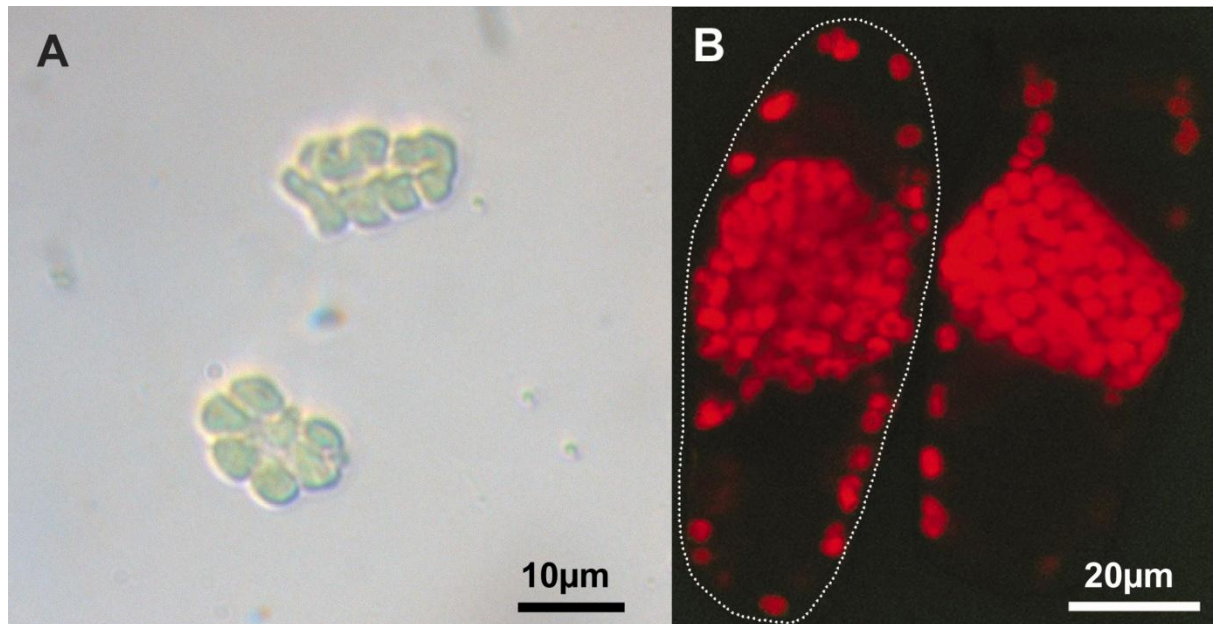


Figure 6.1 Comparison of **A)** rice mesophyll cell with **B)** mesophyll cell of *Borszczowia aralocaspica* which employs single celled C_4 photosynthesis. In **B)** the chloroplasts are coloured red and the cell outline is shown by the broken white line. Note the scale differs between images, and the *Borszczowia aralocaspica* mesophyll cell is significantly larger than that of rice. *Borszczowia aralocaspica* confocal image reproduced from Edwards *et al.* (2004).

6.3 Alterations displayed by the *alm* lines

6.3.1 *alm1*

Table 6.1 shows that plants of the *alm1* mutant line of rice demonstrated significant differences in anatomical and physiological characteristics compared to wild type plants. *alm1* plants were shown to display extensive and significant photoinhibition and an underdeveloped morphology.

Table 6.1 Significantly altered physiological and anatomical characteristics displayed by plants of the *alm1* mutant line of rice compared to wild type rice plants.

Anatomical	Physiological
Slightly reduced interveinal distance	Reduced maximum rate of carboxylation by Rubisco (VC_{max})
Small minor veins	Reduced triose phosphate utilisation (TPU)
Short, narrow, pale leaves	Reduced electron transport rate (ETR)
Erratic vascular distribution	Reduced net assimilation (A) response to photosynthetically active radiation (PAR)
	Reduced light compensation point
	Reduced photorespiration
	Reduced substomatal CO_2 concentration (C_i)
	Reduced quantum yield of photosystem II (Φ_{PSII})
	Reduced photochemical quenching (q_p)
	Slightly increased non-photochemical quenching (NPQ)
	Transpiration (E) almost zero

It is hypothesised that the weak establishment of *alm1* plants is the result of their significantly reduced A , which in turn is an effect of the inhibition of PSII. This is coupled with a presumed extremely low hydraulic conductance in *alm1* plants.

6.3.1.1 Possible limitations in hydraulic conductance in *alm1* plants

the physiological data presented in Chapter 5 showed that transpiration was reduced almost to zero in plants of the *alm1* line, but g_s was maintained. As the anatomical data in presented Chapter 4 indicated that stomatal density was unaltered it is clear that stomata were present and functional. As stomata were open and gas exchange was presumably unimpaired, it is suggested that water supply was highly limited and insufficient to supply transpiration. This theory is also supported by the observation of a wilted phenotype in plants of the *alm1* line (Chapter 3).

Table 6.1 shows that plants of the *alm1* line showed a significant reduction in the size of the minor vascular bundles compared to the wild type. This situation closely resembles that described by Koizumi *et al.* (2007) when studying the CM2088 mutant of rice. In their study a reduction in the diameter of xylem vessels in large vascular bundles of leaves gave a significantly increased resistance to water transport. There was also an increased number of narrowed or scalariform plates present compared to wild type plants and many xylem vessels were occluded. This effect was not noted in the roots or stems of the CM2088 population. Similarly, the roots and stems of *alm1* plants appeared to be healthy, if somewhat smaller than those of the wild type. The additive effects of the decreased diameter of xylem vessels displaying poor hydraulic conductivity and increased cavitation in the CM2088 population were such that transpiration was almost eliminated, despite the fact that stomata were able to function as normal. Due to the similarities in both anatomical (reduced vascular bundle size) and physiological (minimal transpiration, maintained stomatal conductance) responses, and the fact that, despite serious functional impairment, neither *alm1* nor the CM2088 mutations are lethal, it is hypothesised that a similar reduction in hydraulic conductivity following xylem disruption causes the observed lack of transpiration in *alm1* plants.

Hydraulic conductance through the vascular system does not represent the only potential resistance to water transport through the plant however. Aquaporins are the proteins primarily responsible for

facilitating water transport across cell membranes. It has been shown in tobacco that a defect in the NtAQP1 gene caused inactivation of a root aquaporin and resulted in a decreased root hydraulic conductivity (Siefritz *et al.* 2002). However, this is not thought to be the case for the *alm1* line, as its roots appeared to be healthy rather than water stressed. In anycase, water flow through the roots of rice plants is dominated by the apoplastic pathway (Ranathunge *et al.* 2003), reducing reliance on root aquaporins. It has been shown that the *OsPIP2;7* gene is predominantly expressed in the mesophyll cells of rice and encodes an aquaporin protein. It has been shown that upregulation of the *OsPIP2;7* gene results in an increased rate of transpiration (Li *et al.*, 2008); and downregulation or inactivation of such genes may therefore result in an impaired transpiration rate such as that displayed by the *alm1* line. However, whilst this scenario is possible, it is thought that a response similar to that described by Koizumi *et al.* (2007) is the more likely cause of the physiological effects displayed by the *alm1* line, due to the similarity in both observed anatomy and physiology with the *alm1* and CM2088 mutants.

6.3.1.2 Possible inhibitors of PSII in *alm1* rice plants

Although transport of water within the *alm1* plants appears to be highly limited, it is considered impossible for water to be so limited that there is insufficient present to permit photolysis. Because the water requirement of photolysis is extremely small relative to the quantity required to maintain cell turgidity, it is unfeasible that water supplies could be limited to such an extent without severe tissue dehydration. As the chloroplast stroma is predominantly composed of water, the chloroplasts would appear visibly shrunken, if not desiccated to the point where they were no longer visible, if water supplies were so limited as to prevent photolysis. This suggests that the observations of reduced activity of PSII and reduced transpiration were not linked and raises the question of what is causing the inhibition of PSII in *alm1* plants.

As stated, transpiration in *alm1* plants was almost completely eliminated, which could have had the effect of raising leaf temperature due to the reduction in transpirational cooling. High temperatures could potentially cause denaturation of the PSII protein complex. However, no significant increase in leaf temperature was observed in *alm1* plants compared to wild type plants (LiCor cuvette data), so inhibition of PSII cannot be considered to be an effect of increased leaf temperature in this case.

Photochemical quenching (q_p) was consistently reduced in *alm1* plants compared to those of the other lines. It is known that the NPQ response is regulated by the pH gradient across the thylakoid membrane (ΔpH) which arises when net efflux of hydrogen ions from the thylakoid lumen in photolysis, exceeds the influx of H^+ powering ATP synthesis (Figure 6.2) (Rees and Horton, 1990; Horton *et al.* 1996; Li *et al.* 2000; Demmig-Adams and Adams, 2006). As the levels of NPQ were unchanged in the *alm1* line compared to wild type rice, it is concluded that a pH gradient was able to form and PSII was active. This conclusion is supported by the unchanged F_v/F_m value in *alm1* plants compared to wild type plants.

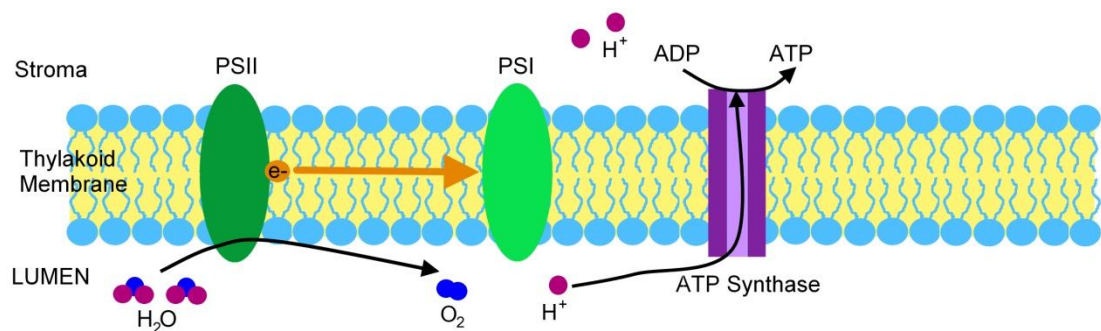


Figure 6.2 Schematic of the thylakoid membrane proteins.

The low value of q_p observed in the *alm1* line indicated that a high proportion of the reaction centres of PSII were closed, that is they have accepted extra electrons, but are unable to pass them on and centres are therefore reduced. However, it is known that PSII was functional as ΔpH was established (shown by NPQ induction); and if this were not the case,

a complete blockage of PSII would result in plant death, as shown by the application of the herbicide diuron (Matoo *et al.*, 1981). A reduction in the number of electron carriers between PSII and PSI would be expected to result in a severely impaired NPQ and is therefore inconsistent with the results obtained. It is therefore suggested that a reduction in the number of PSII reaction centres relative to the number of light harvesting complexes might be the cause of greater reduction of PSII and low observed q_p in *alm1* plants, as electrons would be passed to PSII reaction centres faster than they could enter the electron transport chain. This reduction in the number of active PSII reaction centres would therefore result in a reduction of net output of electrons into the electron transport chain.

Reduced activity of PSII in *alm1* plants also explains many of the other observed physiological deficiencies. With reduced electron transport from PSII, it is expected that ATP synthesis would be limited, which in turn limits activity of the Calvin cycle reactions, reducing A and even photorespiration. Although the effects of mutation in the *alm1* line are detrimental to the productivity of the plants, if it were shown definitively that the physiological response displayed was resulted from a reduction in the number of PSII complexes present, this line may be of use in the introduction of the C_4 pathway into rice. This is because chloroplasts deficient in PSII has been noted before, primarily in the bundle sheath cells of C_4 plants. If the hypotheses outlined here were shown to be correct, this would suggest that the production of C_4 -like chloroplasts in rice is indeed possible. The next challenge would be to target their localisation to the bundle sheath.

It may seem an unsatisfactory explanation that two separate mutations are responsible for the appearance of two significant inhibitions in the same mutant line. However as stated in Chapter 3, *alm1* is a mutant produced by gamma ray irradiation, which is expected to cause numerous large deletions within the genome (Wu *et al.* 2005). These, in turn might conceivably cause multiple effects such as those demonstrated by plants of the *alm1* line.

6.3.2 *alm2*

Table 6.2 shows that plants of the *alm2* line displayed moderate anatomical and physiological disruption compared to wild type plants. It was shown that stomatal conductance was significantly reduced in the *alm2* population and it is likely that this had the effect of limiting transpiration. It is also possible that an alteration in vascular arrangement could limit hydraulic conductance and therefore transpiration as with plants of the *alm1* line. However, as *alm2* rice plants displayed no net reduction in vascular size this is considered unlikely.

Beyond this, it is difficult to infer too much about the responses displayed by plants of the *alm2* line, as the anatomical alterations displayed were somewhat unspecific and the number of potential inhibitors to processes as complicated as photosynthesis is substantial (see Chapter 5).

Table 6.2 Significantly altered physiological and anatomical characteristics displayed by plants of the *alm2* mutant line of rice compared to wild type plants.

Anatomical	Physiological
Altered vascular arrangement	Reduced (A) response to PAR
Visibly off centre mid-rib	Reduced light compensation point
	Reduced E
	Reduced stomatal conductance (g_s)

6.3.3 *alm3* and *alm4*

Tables 6.3 and 6.4 show that leaf 5 of plants of lines *alm3* and *alm4* was significantly thicker than in wild type plants. It has been shown previously that there is a direct correlation between leaf thickness and Rubisco content in rice leaves (Murchie *et al.*, 2005). As A is expressed as a function of leaf area, it was hypothesised that an increase in leaf thickness increase Rubisco content per unit leaf area, thereby causing an

increase in A . However, Tables 6.3 and 6.4 show that, despite an increase in leaf thickness, plants of the *alm3* line showed no increase in A , while *alm4* displayed a reduction in A , suggesting that this hypothesis may not be correct.

Table 6.3 Significantly altered physiological and anatomical characteristics displayed by plants of the *alm3* mutant line of rice compared to wild type rice plants.

Anatomical	Physiological
Increased leaf thickness	No physiological alteration displayed
Separate responses to cell size	

Table 6.4 Significantly altered physiological and anatomical characteristics displayed by plants of the *alm4* mutant line of rice compared to wild type rice plants.

Anatomical	Physiological
Increased leaf thickness	Reduced A
Separate response to cell size	Reduced light compensation point
	Reduced germination rate

It has been shown that A is positively correlated with leaf thickness, providing that there is a proportional increase in Rubisco content per unit leaf area (Evans, 1996, Terashima *et al.* 2001, Terashima *et al.* 2011). If Rubisco content per unit leaf area is constant, A_{\max} is limited by the internal resistance of the leaf to CO_2 diffusion (Evans and von Caemmerer, 1996) and an optimal leaf thickness can be calculated.

Beyond this optimal thickness, no net gain to A is observed but construction and maintenance costs of to the leaf are increased (Terashima *et al.*, 2001). Although it may be unusual to observe an increase in leaf thickness without a corresponding increase in Rubisco content, then this would potentially explain why no increase in A was noted in plants of the *alm3* and *alm4* lines. The reduced g_s and increased resistance to internal CO_2 diffusion (i.e. mesophyll conductance) resulting from the increased leaf thickness in *alm3* plants would help to compound this problem. The LiCor data do not suggest that there was an increase in mesophyll conductance in *alm3* and *alm4* plants.

Whilst the above scenario outlined is possible, it is impossible to establish its likelihood given the genetic background of the mutants. As with the *alm2* line, A may in fact be limited by a range of potential inhibitors of photosynthesis, cancelling out any potential gains resulting from an increase in leaf thickness.

Although the mutant lines which displayed an increased leaf thickness in this study did not exhibit an increase in A , leaf thickness mutants may still represent an area of interest for the improvement of A in rice. It was noted by Terashima *et al.* (2001) that leaves containing high concentrations of Rubisco required a high mesophyll cell and chloroplast surface area to be exposed to intercellular airspaces to avoid limitation of the diffusion of CO_2 and realise high values of A . To satisfy these conditions, not only is an increase in leaf thickness required, but also small mesophyll cells. As outlined previously, rice mesophyll cells are consistently small and have a high conductivity to CO_2 , suggesting that rice may be amenable to an increase in photosynthetic capacity in this way. Whilst potential increases to photosynthetic capacity would be welcomed, it is important to note that such increases represent an increase in capacity rather than efficiency. Increasing leaf thickness in the absence of any alteration in Rubisco to chlorophyll ratios may lead to a high level of intra-leaf shading, reducing photosynthetic rate per of unit Rubisco. Furthermore, increasing leaf thickness in the absence of reduction in leaf area index has a clear resource cost in terms of nitrogen and carbon allocation (Mediavilla *et al.*, 2001; Terashima *et al.*, 2001).

Internal leaf anatomy is important in determining resource use efficiency, meaning that potential yield gains from exploiting leaf thickness may not be available to the large numbers of subsistence farmers who lack the resources to apply significant quantities of fertilisers to crops (Sheehy *et al.*, 2008)

6.3.4 *alm5* and *alm6*

alm5 and *alm6* were unique in that they were the only lines to demonstrate a significantly altered leaf architecture and no significant physiological impairment.

Table 6.5 Significantly altered physiological and anatomical characteristics displayed by plants of the *alm5* mutant line of rice compared to wild type rice plants.

Anatomical	Physiological
Small midrib	None
Increased vascular size	
Reduced interveinal distance	
Reduced mesophyll cell size	

Table 6.6 Significantly altered physiological and anatomical characteristics displayed by plants of the *alm6* mutant line of rice compared to wild type rice plants.

Anatomical	Physiological
Reduced interveinal distance	None
Little distinction between major and minor veins	

The *alm5* and *alm6* lines provide some encouragement for the prospects of introducing the C₄ photosynthetic pathway into rice utilising a Kranz anatomy as they lines demonstrate that vascular density can be

increased without any intrinsic physiological cost to the plants. However, as discussed in Chapter 4, the reduction in interveinal distance was shown to be a function of cell size rather than a reduction in cell number. It is possible that a bi-phasic relationship exists between mesophyll cell number, mesophyll cell size and interveinal distance, and that other lines may demonstrate a reduction in interveinal distance so extensive as to also give a reduction in interveinal cell number, however to date this has not been observed.

Screening of wild relatives of rice at IRRI has revealed species with an interveinal mesophyll cell number of as little as five. Lines with increased vein densities and a reduced interveinal mesophyll cell number have also been observed for both activation-tagged lines (unpublished data, C₄ rice project, IRRI) and EMS deletion mutants (unpublished data, Aryo Feldman, IRRI / University of Nottingham). Whilst an interveinal mesophyll cell number of five is still greater than the two cells typically displayed in Kranz anatomy plants such as maize or sorghum, it would provide a potentially important opportunity to identify genes controlling vein density. There is also ongoing work at IRRI using deletion mutants of sorghum which aims to identify lines which have lost their C₄ mesophyll cell arrangements; these may also potentially provide information about vein density genes which could be used in C₄ engineering.

Rice lines displaying a reduction in interveinal mesophyll cell number also draw comparison with species of the *Flaveria* genus, which is known to contain seven C₄ species, four C₃ species and several C₃-C₄ intermediates (McKown *et al.*, 2005). It was noted that *F. robusta*, the closest relative to the C₄ *Flaveria* species, possesses a closer vein spacing than is typically observed in C₃ plants. The same was also true of the C₃ plant *Cleome sparsifolia*, a close relative of the C₄ species *Cleome gynandra* (Sanchez-Acebo, 2005). It was therefore suggested by Sage and Sage (2008) that an initial increase in vein density plays an essential role in C₄ preconditioning, even if it is not a typical Kranz anatomy.

However, the narrow range of interveinal mesophyll cell numbers observed in screened populations to date suggests that reorganisation of the vascular and mesophyll cell arrangement in rice to resemble that of

C₄ plants with Kranz anatomy will pose a significant challenge. To date, none of the genes controlling C₄ leaf anatomy have been identified (Kajala *et al.*, 2011), although it is hoped that the previously mentioned activation-tagged rice lines and sorghum deletion mutants may provide valuable information regarding this.

6.4 Potential alterations in leaf development

The process of rice leaf development was described by Itoh *et al.* (2005) and summarised in Chapter 1. It was shown that vascular arrangement was determined during early leaf development and differentiation of vascular tissue may first be observed in the P2 leaf primordium, which suggests that the altered morphologies displayed by plants of the *alm1*, *alm5* and *alm6* lines are the result of changes during this stage of development. It was noted by Nishimura *et al.* (2002) that the expression of *OsPNH1* always preceded the morphological development of vascular tissue by approximately one plastochron (the interval of time between which two leaves are produced from the shoot apical meristem, SAM), and was strongly expressed in the pro-vascular regions. It was also noted expression of an antisense transcript of *OsPNH1* caused incomplete vascular development and disordered arrangement of vascular bundles within the leaf primordium, providing strong evidence that *OsPNH1* plays a significant role in leaf vascular development. Furthermore, it was also noted that antisense plants displayed vascular defects only in the leaves and not in the stem or root tissue, suggesting that *OsPNH1* functions only in leaves. The molecular function of *OsPNH1* is not known.

Interveinal spacing in the *alm* lines was shown to be correlated with mesophyll cell size, suggesting that the reductions observed in the present study were not due to changes in *OsPNH1* expression as the relative position of the vascular bundles had not changed, although the size of the cells separating them had. However, it is possible that production of a Kranz type anatomy displaying a low interveinal

mesophyll cell number will require alteration in the localisation of *OsPNH1* expression during production of the P1 leaf primordium.

6.5 Implications for the integration of C₄ pathway into rice

It is not thought that rice lacks any genes associated with the C₄ pathway (Kajala *et al.*, 2011), as all enzymes of the C₄ cycle are found in C₃ plants, albeit at low levels in many cases. In fact it was shown by Bräutigam *et al.* (2011) that there is as little as 3% difference in the transcriptome of mature leaves of the closely related C₃ plant *Cleome spinosa* and its C₄ relative *Cleome gynandra*. Brown *et al.*, (2011) showed that a small cis-element of the *CgNAD-ME* of *C. gynandra* (a C₄ relative of the model plant species *Arabidopsis thaliana*) is essential in conferring cell-specific expression of the enzyme NAD-ME, and that the removal of this region causes NAD-ME to be expressed in both mesophyll and bundle sheath cells. It was hypothesised that modification of transcription factors to recognise the pre-existing cis-elements of the *Oryza sativa* NAD-ME gene in rice would limit NAD-ME expression solely to the bundle sheath cells. This would therefore allow the cell-specific accumulation of proteins such as the enzyme NAD-ME to be generated without alteration of the genes which encode them. These discoveries provide grounds for cautious optimism for the prospects of the introduction of a C₄-like pathway into rice.

However, as previously mentioned, rice plants display a highly conserved mesophyll cell size, degree of lobing of the mesophyll cells and a strong relationship between interveinal distance and mesophyll cell size. It may prove that the highly adapted anatomy of rice to cope with the photorespiratory pressures that it faces may pose a significant obstacle in the introduction of Kranz anatomy. Without reduction of the interveinal mesophyll cell number, it is hard to see how diffusion of C₄ metabolites can occur sufficiently rapidly to power C₄ photosynthesis. The effects of deep lobing on potential C₄ mesophyll cells are also unknown; however, C₄ grasses do not exhibit lobing to the extent displayed by rice (Chonan, 1978). This suggests that some of the specificity in rice mesophyll cell morphology may need to be undone to allow the

introduction of C₄ photosynthesis, the feasibility of which is unknown. however it is likely that creating a leaf anatomy in rice amenable to C₄ photosynthesis will be difficult.

Discoveries of the type made by Brown *et al.* (2011) provide great encouragement that a Kranz anatomy-like system can be introduced into rice, and were made possible because many of the genes relating to the biochemical pathways of C₄ photosynthesis are known. However, this is not the case for the genes controlling the C₄ leaf anatomy and, without knowledge of these, it may be impossible to engineer the anatomical changes required to utilise the C₄ biochemistry. The outcomes of the tagged activation line and sorghum deletion revertant mutant screening being carried out at IRRI may well prove crucial in the search for these genes. If screening techniques such as these are unable to identify essential genes relating to leaf anatomy, the endeavour to engineer C₄ rice will remain extremely challenging; however, if they were to be discovered, this would certainly suggest that there is potential for success.

6.6 Future Work

The effects of deep lobing on a C₄ system are unknown, although C₄ plants typically do not produce mesophyll cells which are lobed to the same degree as rice. For this reason, it has been suggested that the deeply lobed cells of rice may be incompatible with a C₄ system. Whilst the evolutionary benefits of lobing have been outlined in this chapter, the genetic causes of this trait remain unknown. The actual mechanism by which lobing is achieved in both mesophyll and pavement epidermal cells is thought to involve the control of microtubule and / or actin filament organisation within the cell wall, causing localised inhibition of cell growth and the formation of lobes and constrictions (Panteris and Galatis, 2005). However the exact methods for intercellular signalling, perception and localisation within the cell remain unknown. The identification of rice lobing mutants could potentially prove very useful in understanding these functions, as well as the potential benefit of being more amenable to inclusion in a C₄ system. Several genes have been identified which

influence the cytoskeleton for lobed cell morphogenesis, although work is primarily based on pavement epidermal cells rather than mesophyll cells, and rice orthologues have not been identified. In maize, the BRICK protein is required for pavement cell waviness and defective plants lack radial microtubule arrays resulting in a lack of waviness in the pavement cells (Frank *et al.*, 2003). The *Arabidopsis* mutants *spike1*, *quasimodo1* and *scd1* display 'gaps' in the epidermis where the lobes of adjacent mesophyll cells do not match together (Qiu *et al.*, 2002; Bouton *et al.*, 2002; Falbel *et al.*, 2003), and it has been suggested that the *SPIKE1* gene in particular is involved in the alteration of cytoskeletal organisation in response to the perception of as yet unknown extracellular signals. It may be useful to aim to elucidate rice orthologues of the above genes in order to identify potential mechanisms for cytoskeletal organisation before any attempt to reduce the degree of mesophyll cell lobing is made.

The present study has shown that the other major feature of rice mesophyll cells that is incongruous to C₄ anatomy is cell size. The small size and orientation of the mesophyll cells and comparatively large size of the bundle sheath cells provides limited contact through which C₄ metabolites could be exchanged in a C₄ system (Figure 6.3).

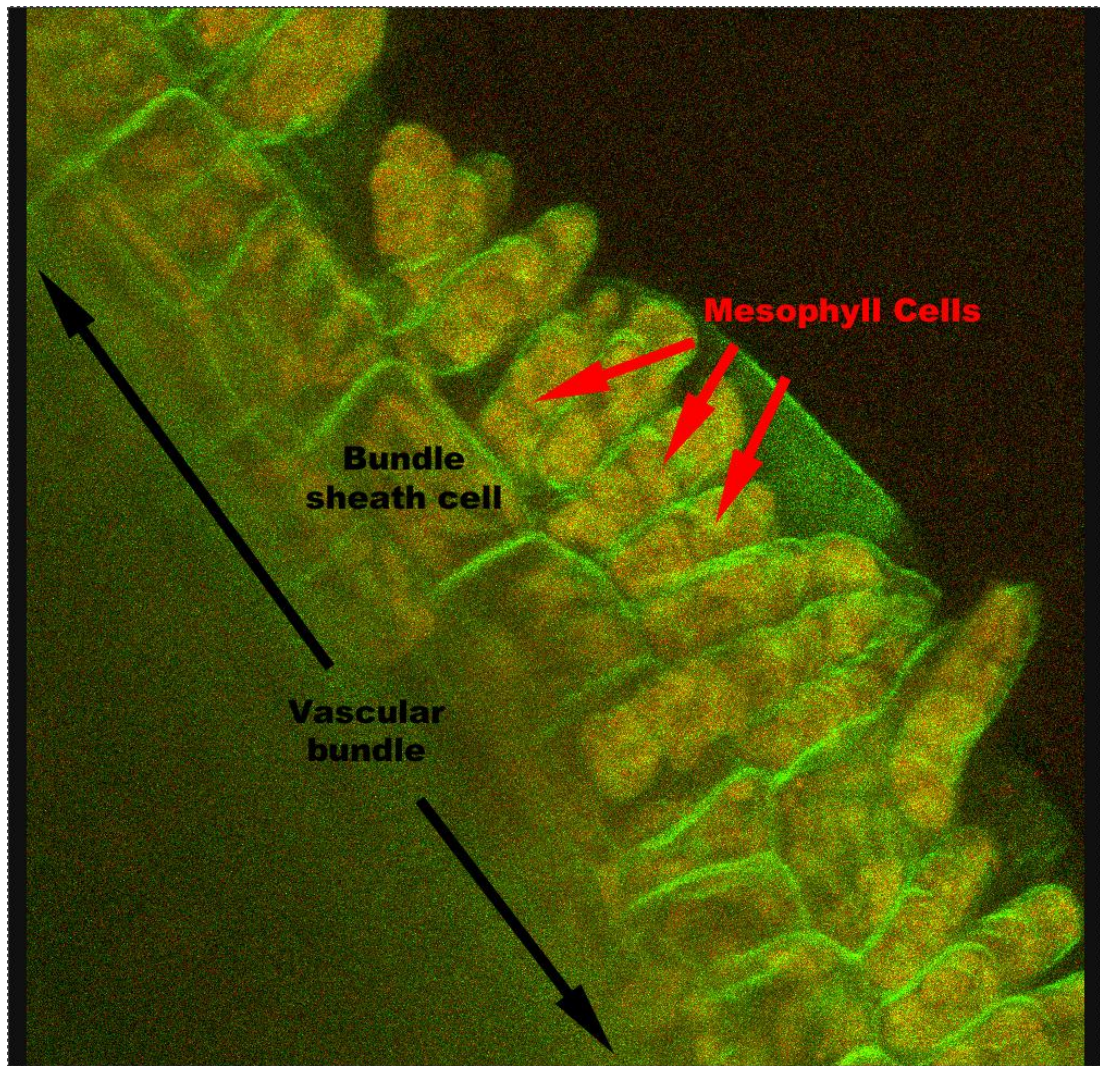


Figure 6.3 Partially separated tissue from the fully expanded leaf 6 of wild type rice showing mesophyll cells arranged perpendicularly to the bundle sheath.

Although, as previously suggested, there is a likely evolutionary benefit to the small mesophyll cell size displayed by rice, the method by which it is achieved is unknown. It has been shown that colchicine treatment of rice seedlings can induce mixoploidy, which gives an increase in mesophyll cell size, although the physiological effects of this are unknown (Hassan and Wazuddin, 2000). It was also shown by Murchie *et al.* (2005) that the mesophyll cells of rice plants grown under high PPFD were larger than those grown under low PPFD. It was not established how this response was mediated; however, this does suggest that there is plasticity in the variation of mesophyll cell size which may be exploited.

The limitation on cell size due to the extent of lobing is also unknown. As lobing appears to be produced by the inhibition of growth within large sections of the cell wall, it would seem possible that an increase in cell size may be induced if the degree of lobing could be inhibited.

It is therefore suggested that the control of mesophyll cell size and the degree of mesophyll cell lobing are key areas where our understanding needs to be improved if the C₄ photosynthetic pathway is to be successfully integrated into rice. These two features are highly conserved amongst the rice mutant lines examined here as part of successful adaptation in coping with photorespiratory stress, although there is reason to believe that this specialisation can be undone. Current screening projects of rice and sorghum populations at IRRI may well yield information regarding genes involved in the production of Kranz type anatomy. However, if the specificity in mesophyll cell size and lobing are not overcome, it is questionable whether C₄ rice plants would be able to utilise Kranz anatomy efficiently.

Chapter 7

BIBLIOGRAPHY

Chapter 7: BIBLIOGRAPHY

- Arora, R., Agarwal, P., Ray, S., Kumar Singh, A., Pal Singh, V., Tyagi, A.K., Kapoor, S.** 2007. MADS-box gene family in rice: genome-wide identification, organization and expression profiling during reproductive and developmental stress. *BMC Genomics* **8**, 242-263.
- Bauwe, H., Keerberg, O., Bassüner, R., Pärnik, T., Bassüner, B.** 1987. Reassimilation of carbon dioxide by *Flaveria* (Asteraceae) species representing different types of photosynthesis. *Planta* **172**, 214-218.
- Borevitz, J., Liang, D., Plouffe, D., Chang, H., Zhu, T., Weigel, D., Berry, CC., Winzeler, E., Chory, J.** 2003. Large-scale identification of single-feature polymorphisms in complex genomes. *Genome Research* **13** 513-523.
- Bouton, S., Leboeuf, E., Mouille, G., Leydecker, M.T., Talbotec, J., Granier, F., Lahaye, M., Höfte, H., Truong, H.** 2002. *QUASIMODO 1* encodes a putative membrane-bound glycotransferase required for normal pectin synthesis and cell adhesion in *Arabidopsis*. *The Plant Cell* **14**, 2577-2590.
- Bräutigam, A., Kajala, K., Wullenweber, J., Sommer, M., Gagneul, D., Weber, K.L., Carr, K.M., Gowik, U., Maß, J., Lercher, M.J., Westhoff, P., Hibberd, J.M., Weber, A.P.M.** 2011. An mRNA blueprint for C₄ photosynthesis derived from comparative transcriptomics of closely related C₃ and C₄ species. *Plant Physiology* **155**, 142-156.

- Brodribb, T.J., Feild, T.S.** 2010. Leaf hydraulic evolution led a surge in leaf photosynthetic capacity during early angiosperm diversification. *Ecology Letters* **13**, 175-183.
- Brodribb, T.J., Feild, T.S., Jordan, G.J.** 2007. Leaf maximum photosynthetic rate and venation are linked by hydraulics. *Plant Physiology* **144**, 1890-1898.
- Brown, N.J., Newell, C.A., Stanley, S., Chen, J.E., Perrin, A.J., Kajala, K., Hibberd, J.M.** 2011. Independent and parallel recruitment of preexisting mechanisms underlying C₄ photosynthesis. *Science* **331**, 1436-1439.
- Burundukova, O.L., Zhuravlev, Y.N., Solopov, N.V., P'yankov, V.I.** 2003. A method for calculating the volume and surface area in rice mesophyll cells. *Russian Journal of Plant Physiology* **50**, 133-139.
- Cantrell, R.** 2000. Foreward in *Redesigning Rice Photosynthesis to Increase Yield*, eds. Sheehy, J., Mitchell, P.L., Hardy, B. Elsevier Science publishing, Amsterdam. pp. 5-6.
- Casati, P., Lara, M.V., Andreo, C.S.** 2000. Induction of a C₄-like mechanism of CO₂ fixation in *Egeria densa*, a submersed aquatic species. *Plant Physiology* **123**, 1611-1621.
- Chonan, N.** 1970. Studies on the photosynthetic tissues in the leaves of cereal crops. V. Comparison of the mesophyll structure among seedling leaves of cereal crops. *Proceedings of the Crop Science Society of Japan* **39**, 418 – 425.
- Chonan, N.** 1978. Comparative anatomy of mesophyll among the leaves of gramineous crops. *Japan Agricultural Research Quarterly* **12**, 128 – 131.

- Cran, D.G., Possingham, J.V.** 1972. Variation of plastid types in spinach. *Protoplasma* **74**, 197-213.
- Dawe, D.** 2000. The contribution of rice research to poverty alleviation in *Redesigning Rice Photosynthesis to Increase Yield*, eds. Sheehy, J., Mitchell, P.L., Hardy, B. Elsevier Science Publishing, Amsterdam. pp.3-12.
- Demmig-Adams, B., Adams, W.W.** 2006. Photoprotection in an ecological context: the remarkable complexity of thermal energy dissipation. *New Phytologist* **172**, 11-21.
- Dengler, N.G., Dengler, R.E., Donnelly, P.M., Hattersley, P.W.** 1994. Quantitative leaf anatomy of C₃ and C₄ grasses (Poaceae): Bundle sheath and mesophyll surface area relationships. *Annals of Botany* **73**, 241 – 255.
- Dengler, N.G., Taylor, W.C.** 2000. Developmental aspects of C₄ photosynthesis in *Photosynthesis: Physiology and Metabolism*, eds. Leegood, R., Sharkey, T., von Caemmerer, S. Kluwer Academic Publishing, Netherlands pp. 471-491.
- Di Lorenzo, L., Wysocka-Diller, J., Malamy, J.E., Pysh, L., Helariutta, Y., Freshour, G., Hahn, M.G., Feldmann, K.A., Benfey, P.N.** 1996. The *SCARECROW* gene regulates an asymmetric cell division that is essential for generating the radial organisation of the *Arabidopsis* root. *Cell* **86**, 423-433.
- Dingkuhn, M., Farquhar, G.D., De Datta, S.K., O'Toole, J.C.** 1991. Discrimination of ¹³C among upland rices having different water use efficiencies. *Australian Journal of Agricultural Research* **42**, 1123-1131.

- Downton, W.J.S., Tregunna, E.B.** 1968. Carbon dioxide compensation – its relation to photosynthesis carboxylation reactions, systematic of the Graminae and leaf anatomy. *Canadian Journal of Botany* **46**, 207 – 215.
- Dunstone, R.L., Evans, L.T.** 1974. Role of changes in cell size in the evolution of wheat. *Australian Journal of Plant Physiology* **1**, 157-165.
- Edwards, G.E., Franceschi, V.R., Voznesenskaya, E.V.** 2004. Single – cell C₄ photosynthesis versus the dual-cell (Kranz) paradigm. *Annual Review of Plant Biology* **55**, 173-196.
- Edwards, G.E., Walker, D.A.** 1983. *C₃, C₄: Mechanism and Cellular and Environmental Regulation of Photosynthesis*. Blackwell Scientific Publications, Oxford.
- Ellis, J.R., Leech, R.M.** 1985. Cell size and chloroplast size in relation to chloroplast replication in light-grown wheat leaves. *Planta* **165**, 120-125.
- El-Sharkawy, M., Hesketh, J.** 1965. Photosynthesis among species in relation to characteristics of leaf anatomy and CO₂ diffusion resistance. *Crop Science* **5**, 517-521.
- Esau, K.** 1965. *Plant Anatomy* 2nd edn. Wiley, New York.
- Evans, J.R.** 1996. Developmental constraints on photosynthesis: effects of light and nutrition. In *Photosynthesis and the Environment*. ed. Baker, N. Kluwer Academic, Dordrecht. pp. 281-304.
- Evans, J.R., Loreto, F.** 2000. Acquisition and diffusion of CO₂ in higher plant leaves. In *Photosynthesis: Physiology and Metabolism*. eds. Leegood, R.C., Sharkey, T.D., von Caemmerer, S. Kluwer Academic, Dordrecht. pp 321–351.

- Evans, J.R., von Caemmerer, S.** 1996. Carbon dioxide diffusion inside leaves. *Plant Physiology* **110**, 339-346.
- Evans, J.R., von Caemmerer, S.** 2000. Would C₄ rice produce more biomass than C₃ rice in *Redesigning Rice Photosynthesis to Increase Yield*, eds. Sheehy, J., Mitchell, P.L., Hardy, B. Elsevier Science publishing, Amsterdam. pp. 53-73.
- Evans, L.T.** 1998. *Feeding the Ten Billion: Plants and population growth*. Cambridge University Press, Cambridge. pp. 196 – 227.
- Falbel, T.C., Koch, L.M., Nadeau, J.A., Swgui-Simarro, J.M., Sack, F.D., Bednarek, S.Y.** 2003. SCD1 is required for cytokinesis and polarized cell expansion in *Arabidopsis thaliana*. *Development* **130**, 4011-4024.
- FAOSTAT**, Food and Agriculture Organisation of the United Nations. Crop production statistics 2009.
<http://faostat.fao.org/site/567/default.aspx#ancor>
- Farquhar, G.D., von Caemmerer S., Berry, J.A.** 1980. A biochemical-model of photosynthetic CO₂ assimilation in leaves of C₃ species. *Planta* **149**, 78-900.
- Fladung, M.** 1994. Genetic variants of *Panicum maximum* (Jacq.) in C₄ photosynthetic traits. *Journal of Plant Physiology* **143**, 165-172.
- Fleming, A.J.** 2005. The control of leaf development. *New Phytologist* **166**, 9-20.
- Flexas, J., Ribas-Carbo, M., Diaz-Espejo, A., Galmés, J., Medrano, H.** 2008. Mesophyll conductance to CO₂ current knowledge and future prospects. *Plant, Cell and Environment* **31**, 602-621.

- Frank, M.J., Cartwright, H.N., Smith, L.G.** 2003. Three Brick genes have distinct functions in a common pathway promoting polarized cell division and cell morphogenesis in the maize leaf epidermis. *Development* **130**, 753-762.
- Furbank, R.T., von Caemmerer, S., Sheehy, J., Edwards, G.** 2009. C₄ rice: a challenge for plant phenomics. *Functional Plant Biology* **36**, 845-856.
- Garris, A.J., Tai, T.H., Coburn, J., Kresovich, S., McCouch, S.** 2005. Genetic structure and diversity in *Oryza Sativa* L. *Genetics* **169**, 1631-1638.
- Hassan, L., Wazuddin, M.** 2000. Colchicine-induced variation of cell size and chloroplast number in leaf mesophyll of rice. *Plant Breeding* **119**, 531-533.
- Hatch, M.D.** 1987. C₄ photosynthesis: A unique blend of modified biochemistry, anatomy and ultrastructure. *Biochimica et Biophysica Acta* **895**, 81-106.
- Henikoff, S., Comai, L.** 2003. Single-nucleotide mutations for plant functional genomics. *Annual Review of Plant Biology* **54**, 375-401.
- Hibberd, J.M., Sheehy, J.E., Langdale, J.A.** 2008. Using C₄ photosynthesis to increase the yield of rice – rationale and feasibility. *Current Opinion in Plant Biology* **11**, 228-231.
- Hirochika, H., Guiderdoni, E., An, G., Hsing, Y., Young Eun, M., Han, C., Upadhyaya, N., Ramachandran, S., Zhang, Q., Pereira, A., Sundaresan, V., Leung, H.** 2004. Rice mutant resources for gene discovery. *Plant Molecular Biology* **54**, 325-334.

- Hirochika, H., Guideroni, E., An, G., Hsing, Y., Eun, M.Y., Han, C., Upadhyaya, N., Ramachandran, S., Zhang, Q., Pereira, A., Sundaresan, V., Leung, H.** Rice mutant genes for discovery. *Plant Molecular Biology* **54**, 325-334.
- Horton, P., Ruban, A.V., Walters, R.G.** 1996. Regulation of light harvesting in green plants. *Annual Review of Plant Physiology and Plant Molecular Biology* **47**, 655-684.
- Hoshikawa, K.** 1989. *The Growing Rice Plant*. Nosan Gyoson Bunka Kyokai (Nobunkyo), Tokyo.
- Itoh, J., Nonomura, K., Ikeda, K., Yamaki, S., Inukai, Y., Yamagishi, H., Kitano, H., Nagato, Y.** 2005. Rice plant development: from zygote to spikelet. *Plant Cell Physiology* **46**, 23-47.
- Izawa, T., Shimamoto, K.** 1996. Becoming a model plant: the importance of rice to plant science. *Trends in plant science* **1**, 95-99.
- Jellings, A.J., Leech, R.M.** 1982. The importance of quantitative anatomy in the interpretation of whole leaf biochemistry in species of *Triticum*, *Hordeum* and *Avena*. *New Phytologist* **92**, 39-48.
- Jin, S., Hong, J., Li, X., Jiang, D.** 2006. Antisense inhibition of Rubisco activase increases Rubisco content and alters the proportion of Rubisco activase in stroma and thylakoids in chloroplasts of rice leaves. *Annals of Botany* **97**, 739-744.
- Juniper, B.E., Clowes, F.A.L.** 1965. Cytoplasmic organelles and cell growth in root caps. *Nature* **208**, 864-865.

- Kajala, K., Covshoff, S., Karki, S., Woodfield, H., Tolley, B.J., Dionora, M.J.A., Mogul, R.T., Mabilangan, A.E., Danila, F.R., Hibberd, J.M., Quick, W.P.** 2011. Strategies for engineering a two-celled C₄ photosynthetic pathway into rice. *Journal of Experimental Botany* **62**, 3001-3010.
- Kamiya, N., Itoh, J., Morikami, A., Nagato, Y., Matsuoka, M.** 2003. The *SCARECROW* gene's role in asymmetric cell divisions in plants. *The Plant Journal* **36**, 45-54.
- Kiniry, J.R., Jones, C.A., O'Toole, J.C., Blanchet, R., Cabelguenne, M., Spanel, D.A.** 1989. Radiation-use efficiency in biomass accumulation prior to grain-filling for five grain-crop species. *Field Crops Research* **20**, 51-64.
- Kinsaman, E.A., Pyke, K.A.** 1998. Bundle sheath cells and cell-specific plastid development in *Arabidopsis* leaves. *Development* **125**, 1815-1822.
- Kobayashi, H., Yamada, M., Taniguchi, M., Kawasaki, M., Sugiyama, T., Miyake, H.** 2009. Differential positioning of C₄ mesophyll and bundle sheath chloroplasts: recovery of chloroplast positioning requires the actomyosin system. *Plant Cell Physiology* **50**, 129-140.
- Koizumi, K., Ookawa, T., Satoh, H., Hirasawa, T.** 2007. A wilted mutant of rice has impaired hydraulic conductance. *Plant and Cell Physiology* **48**, 1219-1228.
- Kropff, M.J., Cassman, K.G., Peng, S., Matthews, R.B., Setter, T.L.** 1994a. Quantitative understanding of yield potential. In *Breaking the yield barrier. Proceedings of a workshop on rice yield potential in favourable environments*, ed. Cassman, K.G. International Rice Research Institute, Manila. pp. 21-38.

- Kropff, M.J., van Laar, H.H., Matthews, R.B.** 1994b. *ORYZA1: an ecophysiological model for irrigated rice production*. SARP Research Proceedings, Wageningen (The Netherlands).
- Ledford, H.K., Niyogi, K.K.** 2005. Singlet oxygen and photo-oxidative stress management in plants and algae. *Plant, Cell and Environment* **28**, 1037–1045.
- Leegood, R.C.** 2008. Roles of bundle sheath cells in C₃ plants. *Journal of Experimental Botany* **59**, 1663-1673.
- Leegood, R.C., Sharkey, T., von Caemmerer, S.** 2000. *Photosynthesis: Physiology and Metabolism*. Elsevier Science Publishing, Amsterdam.
- Li, G., Zhang, M., Cai, W., Sun, W., Su, W.** 2008. Characterization of OsPIP2;7, a water channel protein in rice. *Plant and Cell Physiology* **49**, 1851-1858.
- Li, X., Björkman, O., Shih, C., Grossman, A.R., Rosenquist, M., Jansson, S., Niyogi, K.K.** 2000. A pigment-binding protein essential for regulation of photosynthetic light harvesting. *Nature* **403**, 391-395.
- Lux, A., Morita, S., Abe, J., Ito, K.** 2005. An improved method for clearing and staining free-hand sections and whole-mount samples. *Annals of Botany* **96**, 989-996.
- Lyndon, R.F., Robertson, E.S.** 1976. The quantitative ultrastructure of the pea shoot apex in relation to leaf initiation. *Protoplasma* **87**, 387-402.
- Maluszynski, M., Nichterlein, K., van Zanten, L., Ahloowalia, B.S.** 2000. Officially released mutant varieties-the FAO/IAEA Database. *Mutation Breeding Review* **12**, 1-84

- Matoo, A.K., Pick, U., Hoffman-Falk, H., Edelman, M.** 1981. The rapidly metabolised 32,000-dalton polypeptide of the chloroplast is the "proteinaceous shield" regulating photosystem II electron transport and mediating diuron herbicide sensitivity. *Proceedings of the National Academy of Science* **78**, 1572-1576.
- Maxwell, K., Johnson, G.** 2000. Chlorophyll fluorescence – a practical guide. *Journal of Experimental Botany* **51**, 659-668.
- McKown, A.D., Moncalvo, J.M., Dengler, N.G.** 2005. Phylogeny of Flaveria (Asteraceae) and inference of C₄ photosynthesis evolution. *American Journal of Botany* **92**, 1911-1928.
- Mediavilla, S., Escudero, A., Heilmeyer, H.** 2001. Internal leaf anatomy and photosynthetic resource-use efficiency: interspecific and intraspecific comparisons. *Tree Physiology* **21**, 251-259.
- Mitchell, P.L., Sheehy, J.E.** 2006. Supercharging rice photosynthesis to increase yield. *New Phytologist* **171**, 688-693.
- Mitchell, P.L., Sheehy, J.E.** 2007. pp. 27-37 in *Charting New Pathways to C₄ Rice*. eds. Sheehy, J., Mitchell, P.L., Hardy, B. World Scientific Publishing, Singapore.
- Miyagishima, S.** 2005. Origin of the chloroplast division machinery. *Journal of Plant Research* **118**, 295-306.
- Miyao, B., Fukayama, H.** 2003. Metabolic consequences of overproduction of phosphoenolpyruvate carboxylase in C₃ plants. *Archives of Biochemistry and Biophysics* **414**, 197-203.
- Mockler, T.C., Chan, S., Sundaresan, A., Chen, H., Jacobsen, S.E., Ecker, J.R.** 2005. Applications of DNA tiling arrays for whole genome analysis. *Genomics* **85**, 1-15.

- Monson, R.K.** 1999. The origins of C₄ genes and evolutionary pattern in the C₄ metabolic phenotype. In *C₄ Plant Biology*. eds. Sage, R.F., Monson, R.K. Academic Press , San Diego. pp. 377 – 410.
- Monteith, J.L.** 1977. Climate and the efficiency of crop production in Britain. *Philosophical Transactions of the Royal Society* **281**, 277-294.
- Muhaidat, R., Sage, R.F., Dengler, N.G.** 2007. Diversity of Kranz Anatomy and Biochemistry in C₄ Eudicots. *American Journal of Botany* **94**, 362-381.
- Murchie, E.H., Hubbart, S., Peng, S., Horton, P.** 2005. Acclimation of photosynthesis to high irradiance in rice: gene expression and interactions with leaf development. *Journal of Experimental Botany* **56**, 449-460.
- Murchie, E.H., Niyogi, K.K.** 2011. Manipulation of photoprotection to improve plant photosynthesis. *Plant Physiology* **155**, 86-92.
- Murchie, E.H., Pinto, M. Horton, P.** 2009. Agriculture and the new challenges for photosynthesis research. *New Phytologist* **181**, 532-552.
- Nelson, T., Dengler, N.G.** 1992. Photosynthetic differentiation in C₄ plants. *International Journal of Plant Science* **153**, 93-105.
- Nishimura, A., Ito, M., Kamiya, N., Sato, Y., Matsuoka, M.** 2002. *OsPNH1* regulates leaf development and maintenance of the shoot apical meristem in rice. *The Plant Journal* **30**, 189-201.
- Ogren, W.L.** 1984. Photorespiration: pathways, regulation and modification. *Annual Review of Plant Physiology* **35**, 415-442.

- Panteris, E., Galatis, B.** 2005. The morphogenesis of plant cells in the mesophyll and epidermis: organisation and distinct roles of cortical microtubules and actin filaments. *New Phytologist* **167**, 721-732.
- Pyke, K.A.** 1994. *Arabidopsis* – its use in the genetic and molecular analysis of plant morphology. *New Phytologist* **128**, 19-37.
- Pyke, K.A.** 1999. Plastid division and development. *The Plant Cell* **11**, 549-556.
- Pyke, K.A.** 2009. *Plastid Biology* p. 64. Cambridge University Press, Cambridge.
- Pyke, K.A., Leech, R.M.** 1987. The control of chloroplast number in wheat mesophyll cells. *Planta* **170**, 416-420.
- Pyke, K.A., Leech, R.M.** 1992. Nuclear mutations radically alter chloroplast division and expansion in *Arabidopsis thaliana*. *Plant Physiology* **99**, 1005-1008.
- Qiu, J.L., Jilk, R., Marks, M.D., Szymanski, D.B.** 2003. The *Arabidopsis* SPIKE1 gene is required for normal cell shape control and tissue development. *The Plant Cell* **14**, 101-118.
- Ranathunge, K., Steudle, E., Lafitte, R.** 2003. Control of water uptake by rice (*Oryza sativa* L.): role of the outer part of the root. *Planta* **217**, 193-205.
- Rees, D., Horton, P.** 1990. The mechanism of changes in photosystem II efficiency in spinach thylakoids. *Biochemica et Biophysica Acta* **1016**, 219-227.

- Reiskind, J.B., Madsen, T.V., van Ginkel, L.C., Bowes, G.** 1997. Evidence that inducible c_4 -type photosynthesis is a chloroplastic CO_2 -concentrating mechanism in *Hydrilla*, a submersed monocot. *Plant, Cell and Environment* **20**, 211-220.
- Ren-Yong, C., Zhuge, G., Wan, S.** 1990. pp. 370-392 Loss assessments and factor-finding analysis of grain post-production systems in China. In *Proceedings of the Thirteenth ASIAN Seminar on Grain Postharvest Technology, Brunei Darussalam, 4-7 Sept. 1990*. ed. Naewbanij, J.O. ASIAN grain post-harvest programme, Bangkok.
- Roth-Nebelsick, A., Uhl, D., Mosbrugger, V., Kerp, H.** 2001. Evolution and function of leaf venation architecture: a review. *Annals of Botany* **87**, 553-566.
- Sage, R.** 2004. The Evolution of C_4 photosynthesis. *New Phytologist* **161**, 341-370.
- Sage, R., Pearcy, R.** 2000. pp. 497-532 In *Photosynthesis: Physiology and Metabolism*, eds. Leegood, R., Sharkey, T., von Caemmerer, S. Kluwer Academic Publishing, Netherlands.
- Sage, R., Sage, T.L.** 2008. Learning from nature to develop strategies for the directed evolution of C_4 rice. In *Charting Pathways to C_4 Rice*. eds. Sheehy, J.E., Mitchell, P.L., Hardy, B. World Scientific, Singapore. pp. 195-216.
- Sage, T.L., Sage, R.** 2009. The functional anatomy of rice leaves: implications for refixation of photorespiratory CO_2 and efforts to engineer C_4 photosynthesis into rice. *Plant Cell Physiology* **50**, 756-772.

- Sage, R., Sharkey, T., Percy, R.** 1990. The effect of leaf nitrogen and temperature on the CO₂ response of photosynthesis in the C₃ dicot *Chenopodium album*. *Australian Journal of Plant Physiology* **17**, 135-148.
- Sánchez-Acebo, L.** 2005. A phylogenetic study of the New World *Cleome* (Brassicaceae, Cleomoideae). *Annals of the Missouri Botanical Garden* **92**, 179-201.
- Scarpella, E., Rueb, S., Meijer, A.** 2003. The *RADICLELESS1* gene is required for vascular pattern formation in rice. *Development* **130**, 645-658.
- Scarpella, F., Meijer, A.** 2004. Pattern formation in the vascular system of monocot and dicot plant species. *New Phytologist* **164**, 209-242.
- Sharkey, T.D., Bernacchi, C.J., Farquhar, G.D., Singaas, E.L.** 2007. Fitting photosynthetic carbon dioxide response curves for C₃ leaves. *Plant, Cell and Environment* **30**, 1035-1040.
- Curve fitting tool produced by Sharkey *et al.* can be found at <http://www.blackwellpublishing.com/plantsci/pcecalculation/>
- Sheehy, J.E., Ferrer, A.B., Mitchell, P.L., Elmido-Mabilangan, A., Pablico, P., Dionora, M.J.A.** 2008. How the rice crop works and why it needs a new engine. In *Charting Pathways to C₄ Rice*. eds. Sheehy, J.E., Mitchell, P.L., Hardy, B. World Scientific, Singapore. pp. 3-26.
- Sheehy, J.E., Dionora, M.J.A., Mitchell, P.L.** 2001. Spikelet numbers, sink size and potential yield in rice. *Field Crops Research* **71**, 77-85.
- Siefritz, F., Tyree, M.T., Lovisolo, C., Schubert, A., Kaldenhoff, R.** 2002. PIP1 plasma membrane aquaporins in tobacco: from cellular effects to function in plants. *The Plant Cell* **14**, 869-876.

- Smith, L.G., Hake, S., Sylvester, A.W.** 1996. The *tangled-1* mutation alters cell division orientations throughout maize leaf development without altering leaf shape. *Development* **122**, 481-489.
- Stockhaus, J., Schlue, U., Koczor, M., Chitty, J., Taylor, W., Westhoff, P.** 1997. The promoter of the gene encoding the C₄ form of phosphoenolpyruvate carboxylase directs mesophyll-specific expression in transgenic C₄ *Flaveria* spp. *The Plant Cell* **9**, 479-489.
- Takahasi, S., Badger, M.R.** 2011. Photoprotection in plants: a new light on photosystem II damage. *Trends in Plant Science* **16**, 53-60.
- Terashima, I., Hanba, Y.T., Tholen, D., Niinemets, Ü.** 2011. Leaf functional anatomy in relation to photosynthesis. *Plant Physiology* **155**, 108-116.
- Terashima, I., Miyazawa, S.I., Hanba, Y.T.** 2001. Why are sun leaves thicker than shade leaves? Consideration based on analyses of CO₂ diffusion in the leaf. *Journal of Plant Research* **114**, 93-105.
- The Arabidopsis Genome Initiative.** 2000. Analysis of the genome sequence of the flowering plant *Arabidopsis thaliana*. *Nature* **408**, 796-815.
- United Nations** – Department of Economic and Social Affairs Population Division. 2005. World Population Prospects, The 2004 revision. www.un.org/esa/population/publications/WPP2004/2004Highlights_finfinal.pdf
- Veit, B.** 2004. Determination of cell fate in apical meristems. *Current Opinion in Plant Biology* **7**, 57-64.
- von Caemmerer, S.** 1989. A model of photosynthetic CO₂ assimilation and carbon-isotope discrimination in leaves of certain C₃-C₄ intermediates. *Planta* **178**, 463-474.

- von Caemmerer, S.** 2003. C₄ Photosynthesis in a single C₃ cell is theoretically inefficient but may ameliorate internal CO₂ diffusion limitations of C₃ Leaves. *Plant, Cell and Environment* **26**, 1191-1197.
- Von Caemmerer, S., Evans, J.R.** 2010. Enhancing C₃ photosynthesis. *Plant Physiology* **154**, 589-592.
- von Caemmerer, S., Furbank, R.** 1999. Modelling C₄ photosynthesis. In *C₄ Plant Biology*. eds. Sage, R., Monson, R. Academic Press, San Diego. pp. 89-131.
- von Caemmerer, S., Farquhar, G.D.** 1981. Some relationships between the biochemistry of photosynthesis and the gas-exchange of leaves. *Planta* **153**, 376–387.
- Voznesenskaya, E.V., Franceschi, V.R., Kiirats, O., Freitag, H., Edwards, G.E.** 2001. Kranz anatomy is not essential for terrestrial C₄ plant photosynthesis. *Nature* **414**, 543-546.
- Wilson, D., Cooper, J.P.** 1969. Effect of temperature during growth on leaf anatomy and subsequent light-saturated photosynthesis among contrasting *Lolium* genotypes. *New Phytologist* **68**, 1115-1123.
- Winzeler, E.A., Castillo-Davis, C.I., Oshiro, G., Liang, D., Richards, D.R., Zhou, Y., Hartl, D.L.** 2003. Genetic diversity in yeast assessed with whole-genome oligonucleotide arrays. *Genetics* **163**, 79-89.
- Wu, J.L., Wu, C., Lei, C., Baraoidan, M., Bordeos, A., Suzette, M.R., Madamba, Ramos-Pamplona, M., Mauleon, R., Portugal, A., Jun Ulat, V., Bruskiwich, R., Wang, G., Leach, J., Khush, G., Leung, H.** 2005. Chemical and irradiation induced mutants of *indica* rice IR64 for forward and reverse genetics. *Plant Molecular Biology* **59**, 85 – 97.

- Yamori, W., Takahashi, S., Makino, A., Price, G.D., Badger, M.R., von Caemmerer, S.** 2011. The roles of ATP synthase and the cytochrome *B₆/f* complexes in limiting chloroplast electron transport and determining photosynthetic capacity. *Plant Physiology* **155**, 956-962.
- Yu, J., Hu, S., Wang, J., Wong, G.K., Li, S., Liu, B., Deng, Y., Dai, L., Zhou, Y., Zhang, X., Cao, M., Liu, J., Sun, J., Tang, J., Chen, Y., Huang, X., Lin, W., Ye, C., Tong, W., Cong, L., Geng, J., Han, Y., Li, L., Li, W., Hu, G., Huang, X., Li, W., Li, J., Liu, Z., Li, L., Liu, J, Qi, Q., Liu, J., Li, L., Li, T., Wang, X., Lu, H., Wu, T., Zhu, M., Ni, P., Han, H., Dong, W., Ren, X., Feng, X., Cui, P., Li, X., Wang, H., Xu, X., Zhai, W., Xu, Z., Zhang, J., He, S., Zhang, J., Xu, J., Zhang, K., Zheng, X., Dong, J., Zeng, W., Tao, L., Ye, J., Tan, J., Ren, X., Chen, X., He, J., Liu, D., Tian, W., Tian, C., Xia, H., Bao, Q., Li, G., Gao, H., Cao, T., Wang, J., Zhao, W., Li, P., Chen, W., Wang, X., Zhang, Y., Hu, J., Wang, J., Liu, S., Yang, J., Zhang, G, Xiong, Y., Li, Z., Mao, L., Zhou, C., Zhu, Z., Chen, R., Hao, B., Zheng, W., Chen, S., Guo, W., Li, G., Liu, S., Tao, M., Wang, J., Zhu, L., Yuan, L., Yang, H.** 2002. A draft sequence of the rice genome (*Oryza sativa* L. ssp. *Indica*). *Science* **296**, 79-92.
- Zhang, C., Halsey, L.E., Szymanski, D.B.** 2011. The development and geometry of shape change in *Arabidopsis thaliana* cotyledon pavement cells. *BMC Plant Biology* **11**, 27-40.
- Zhang, Y., Goritschnig, S., Dong, X., Li, X.** A gain-of-function mutation in a plant disease resistance gene leads to constitutive activation of downstream signal transduction pathways in *suppressor of npr1-1, constitutive 1*. *The Plant Cell* **15**, 2636-3646.
- Zhu, X.G., Portis JR, A.R., Long, S.P.** 2004. Would transformation of *C₃* crop plants with foreign Rubisco increase productivity? A computational analysis extrapolating from kinetic properties to canopy photosynthesis. *Plant, Cell and Environment* **27**, 155-165.